# Detection, Classification and Control of Power Quality Disturbances Based on Complementary Ensemble Empirical Mode Decomposition and Artificial Neural Networks

A thesis submitted in partial fulfilment of the requirements for the degree of Doctor of Philosophy (PhD)

by

**Saeed Sultan Alshahrani**

Electronic and Computer Engineering

College of Engineering, Design and Physical Sciences

Brunel University London

United Kingdom

June 2017

# Abstract

Power quality has become a vital concern recently due to the expansion of the consumption of electrical load and the growth in the use of sensitive devices connected to power systems. Nevertheless, complexity in modern daily life and the increased usage of semiconductors make non-linear load a real threat to power quality level. The modern power supply, based on developing renewable sources such solar, wind and nuclear energy, has increased power quality disturbances to significant levels. In order to maintain power quality and to ensure its reliability, power quality disturbances must be detected and identified correctly and precisely. Thus, detection algorithms assist decision makers to solve and mitigate the disturbance, and protect the power network from a high level of financial loss.

In this thesis, a new approach of a detection algorithm and classification technique is proposed for power quality disturbances based on the methodology of an advanced signal processing algorithm and artificial neural networks. First, an investigation process covering the most important and common power quality disturbances is analysed and discussed. Thereafter, most of the powerful signal processing algorithms in addition to artificial intelligence techniques are investigated and their results are discussed. Since power quality disturbances are non-stationary signals, a characterisation process is built by simulating 10 power quality disturbances in power systems. This stage is based on the international standards in the field of power quality. As a result, a validation methodology is conducted based on discrete wavelet transform and the extracted features are recorded. Artificial Intelligence techniques can classify complex data and enhancing the evaluation process. Therefore, these extracted features are fed to artificial neural networks to train the database of the generated power quality disturbances. This method achieved a sufficient detection algorithm which overcame the Fourier transform limitation and resulted in an accuracy of 91%. Thereafter, a new method of detection algorithm and classification technique is proposed based on Complementary Ensemble Empirical Mode Decomposition and artificial neural networks. This resulted in a significant improvement in terms of accuracy, with more than 98%. In this thesis, a comparison analysis for both detection algorithms combined with the artificial neural networks classifier is presented and this shows the robustness and the effectiveness of the proposed methodology.

The next stage is presenting a recognising system to detect and identify these disturbances using on-line power system faults. This stage is achieved by introducing faults into the power transmission system and recording the system response through the resulting waveforms. These waveforms are analysed by applying them to the hybrid detection and classification approach.

The final stage is control and decision making, where a bank of hybrid filters is connected to the power transmission system. Three factors of these filters are investigated: the magnitude of the transient, and the time and reduction in the total harmonics distortion. The results show better performance in the system response, as harmonics were reduced by more than half compared to the normal case. Furthermore, a tuning process is conducted to optimise the controller and reduce the transient in the system. The results show a stable system in terms of overshoot and recovery time.

# Publications Based on this Research

1) S. Alshahrani, M. Abbod and G. Taylor, "Detection and classification of power quality disturbances based on Hilbert-Huang transform and feed forward neural networks," *2016 51st International Universities Power Engineering Conference (UPEC)*, Coimbra, Portugal, 2016, pp. 1-6.

2) S. Alshahrani, M. Abbod and B. Alamri, "Detection and classification of power quality events based on wavelet transform and artificial neural networks for smart grids," *2015 Saudi Arabia Smart Grid (SASG)*, Jeddah, 2015, pp. 1-6.

3) S. Alshahrani, M. Abbod, B. Alamri and G. Taylor, "Evaluation and classification of power quality disturbances based on discrete Wavelet Transform and artificial neural networks," *2015 50th International Universities Power Engineering Conference (UPEC)*, Stoke on Trent, 2015, pp. 1-5.

4) S. Alshahrani, M. Abbod, "Feature Extraction and Classification of Power Quality Disturbances Based on Empirical Mode Decomposition and Artificial Neural Networks," *The 9th Saudi Student Conference (SSC 9)*, Birmingham, 2016.

5) S. Alshahrani, M. Abbod, "Measurement of Power Quantities at Non-Sinusoidal Conditions based on Wavelet Transform," *Brunel University Research Student Conference 2015*, London, 2015.

6) S. Alshahrani, M. Abbod, "Measurement of Power Quality at Non-Sinusoidal Conditions using Artificial Neural Networks," *The Eighth Saudi Student Conference (SSC 8)*, King's College London, 2015.

7) S. Alshahrani, A. Zobaa, "Analysis of Power Quality Measurement at Non-sinusoidal Conditions," *the 7th Annual SED Research Student Conference (SED 07)*, Brunel University, London, 2014.

# Declaration

It is hereby declared that the thesis in focus is the author's own work and is submitted for the first time to the Post Graduate Research Office. The study was originated, composed and reviewed by the mentioned author in the Department of Electronic and Computer Engineering, College of Engineering, Design and Physical Sciences, Brunel University London, UK. All the information derived from other works has been properly referenced and acknowledged.

Saeed S. Alshahrani
June 2017
London, UK

# Acknowledgements

In the name of Allah, the Most Gracious and the Most Merciful. Above all, I am grateful to Allah for the strengths, patience and guidance to complete this thesis. Thereafter, without whose incalculable blessings and prayers of parents and family, none of this would be possible. It is my pleasure to attribute credit to the many people who have contributed to this research.

First of all, I would like to express my sincere appreciation and gratitude to Dr Maysam Abbod for his invaluable guidance, continuous encouragement and strong motivation during this research and preparation of the thesis.

Secondly, I want to express my sincere thanks to all my teachers, and all those from whom I have learnt and gained knowledge. I would also like to thank my colleagues and friends at Brunel University London who joined me in creative discussions and productive ideas led towards my goal.

Thirdly, I would also like to thank the Saudi Standards, Metrology and Quality Organisation and the Ministry of Education for their financial support.

Lastly, I would like express my sincere thanks to my parents and family for their support, love and encouragement throughout this period where they have played an important role in helping me to reach this stage.

# Thesis Contents

# List of Figures

# List of Tables

# List of Abbreviations

| | |
|---|---|
| AI | Artificial Intelligence |
| ANN | Artificial Neural Network |
| ANSI | American National Standards Institute |
| BSI | British Standards Institute |
| CEEMD | Complementary Ensemble Empirical Mode Decomposition |
| CWT | Continuous Wavelet Transform |
| DFT | Discrete Fourier Transform |
| DVR | Dynamic Voltage Restorer |
| DWT | Discrete Wavelet Transform |
| EEMD | Ensemble Empirical Mode Decomposition |
| EMD | Empirical Mode Decomposition |
| EPRI | Electric Power Research Institute |
| FES | Fuzzy Expert System |
| FFNN | Feed Forward Neural Network |
| FFT | Fast Fourier Transform |

| | |
|---|---|
| FT | Fourier Transform |
| GA | Genetic Algorithm |
| HHT | Hilbert-Huang Transform |
| HSA | Hilbert Spectral Analysis |
| HTG | Hydraulic Turbine And Governor |
| IEC | International Electrotechnical Commission |
| IEEE | Electrical And Electronics Engineering |
| IMFs | Intrinsic Mode Functions |
| ISO | International Organization For Standardization |
| LG Fault | Line-To-Ground |
| LL Fault | Line-To-Line Fault |
| LLG Fault | Double Line-To-Ground Fault |
| MB-PSS | Multi-Band Stabiliser |
| MRA | Multi-Resolution Analysis |
| PCA | Principal Component Analysis |
| PCC | Point Of Common Coupling |
| PI Controller | Proportional Integral Controller |

| | |
|---|---|
| PQ | Power Quality |
| PQDs | Power Quality Disturbances |
| PSS | Power System Stabiliser |
| PSS2B | Generic Stabiliser |
| PSS4B | Multi-Band Stabiliser |
| PWM | Pulse Width Modulation |
| RLC filter | Passive Filters |
| RMS | Root Mean Square |
| RNN | Recurrent Neural Network |
| SASO | Saudi Standards, Metrology And Quality Org. |
| SI units | International Systems Of Units |
| SMES | Superconducting Magnetic Energy Storage |
| SSTS | Solid State Transfer Switch |
| ST | Stockwell Transform |
| STFT | Short Time Fourier Transform |
| SVM | Support Vector Machine |
| SWT | Stationary Wavelet Transform |

| | |
|---|---|
| THD | Total Harmonic Distortion |
| UPS | Uninterruptible Power Supply |
| WPT | Wavelet Packet Transform |
| WT | Wavelet Transform |

# Chapter 1 – Introduction

## 1.1 Introduction

Power quality (PQ) holds an important role nowadays for modern electric power utilities and their customers, especially with regard to power quality disturbances. The significant increase in nonlinear load and the increase usage of sensitive electronic devices have made the power quality problems a more critical issue than ever [1]. The necessity of implementing green power worldwide, with the increase of applications towards renewable energy, consequently caused major sources of disturbance in electrical power systems [2]. The increased levels of use of semiconductor devices, lighting controls, solid-state switching devices, inverters, and protection and relaying equipment are causing nonlinear loads, interruption and other disturbances. Such problems have formed one of the major challenges facing engineers and decision makers, where these events are responsible for a large economic loss to power utilities.

Moreover, the global demand for electricity is growing, which presents many challenges to the reliability of any electrical power system. Energy efficiency programmes are also becoming more important in order to cope with such changes and the large capacities of electric power systems. Due to such growth, electrical power utilities are becoming more complex than in the past. They are not centralised as they were before, where plants supplying new areas are planned on multiple micro grids distributed locally. These grids are not traditional grids anymore, considering their integration with renewable energy sources such as solar, wind and nuclear plants. Moreover, distributed generation is going to be utilised by electronic devices and controllers, which indeed cause more PQ issues in electric power systems. Unfortunately, reliability in such modern power plants is lower than that of traditional power sources [3]. Therefore, it is essential to improve the power quality to protect power utilities and reduce the cost due to economical losses in UK and worldwide.

## 1.2 The Economic Impact of Power Quality

Economic impact can be defined as the summation of financial losses due to disturbances which affect the power supply. The economic impact on power systems due to power quality disturbances is also called ‘PQ cost’ in many publications.

Power networks at all stages seek to sustain power quality at the highest level possible, since losing it would lead to major economic loss. Poor quality of power delivery is still very challenging from a financial perspective. According to a report conducted by the Institute of Electrical and Electronics Engineering (IEEE), the cost of power quality problems has reached up to $10 Billion in the USA over just one year [4]. Transient power disturbances come from lightning, switching in transmission or distribution systems, or from sudden breakdown in the system. Such failures can cause a serious trip in the protection device and lead to damage to supported equipment in the system. Another report, presented by the European Cooper Institute, gave an estimation of economic loss by type of power quality disturbance: semiconductor production – €3,800,000, financial trading – €6,000,000 per hour, computer centre – €750,000, and telecommunications – €30,000 per minute, as presented in [5]. Moreover, such disturbances cost a lot technically when it is occurred from 3 to 120 per kVA per event, as reported in [6]. In further investigation, Figure 1-1 shows a summary of economic loss in the US (by customer type) caused by interruption in both its types: short and sustained interruptions, as reported in [7]. Figure 1-2 shows the overall loss based on interruption types.

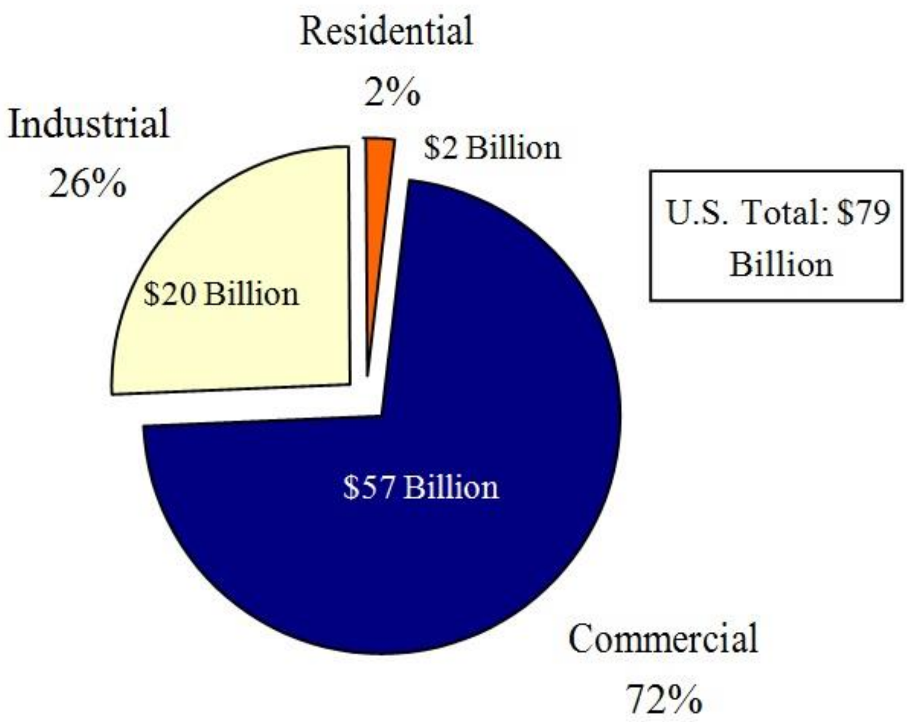


**Figure 1-1 The economic impact of interruptions based on customer type [7]**

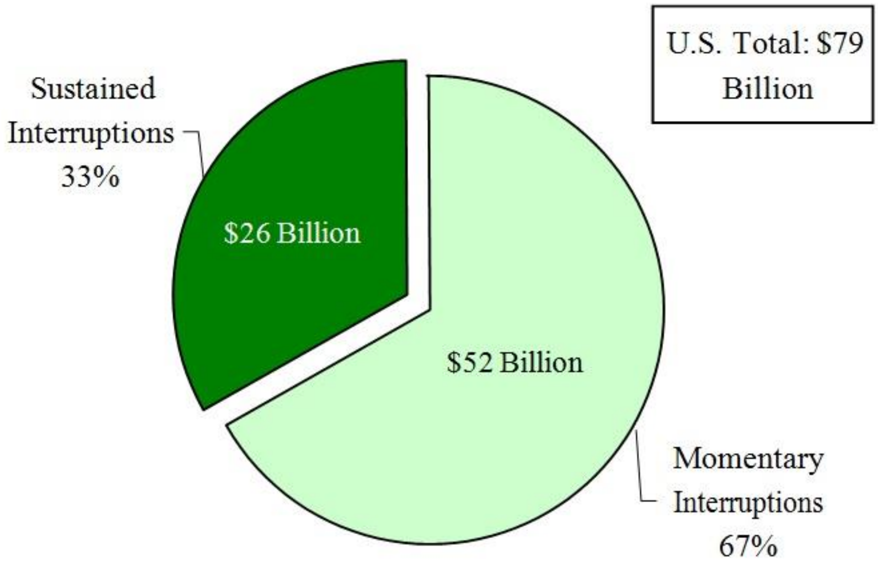


**Figure 1-2 The economic impact of interruptions based on interruption type [7]**

Another report, published by the Electric Power Research Institute (EPRI), presented the cost of power quality disturbances based on their time duration [8]. Figure 1-3 summarises the results of this study around interruptions from comprehensive analysis. The EPRI divided interruption disturbance into four sets, which are 1 sec, Re-closer (1 min), 3 minutes and 1 hour. Thereafter, groups of customers are assembled according to their consumption of energy, with the relation of disturbance duration versus cost presented below.

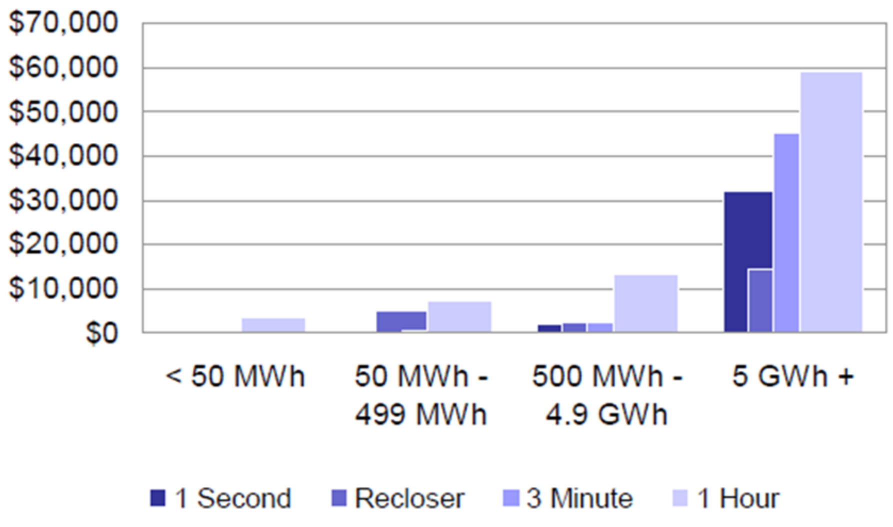


**Figure 1-3: Cost of interruption disturbance in annual kWh consumption [8]**

Such economic impact and data are not accessible for scientists and engineers in UK as USA.

## 1.3 Motivation of the Research

Detecting power quality problems is crucial to enhancing power quality level in electric power systems, and leads to effective decision making in handling these disturbances in the network. There are several ways to identify and classify power disturbances such as engineers capturing waveforms in the field. Unfortunately, manual capturing is almost impossible due to the data required to be sampled in modern power systems. Moreover, power quality is one of the main factors in meeting the demands of power utilities and customers. The growth in transformation to renewable energy and the increased usage of nonlinear applications, including microelectronic processors, caused more equipment failure in power systems and damage to its sensitive controllers. Consequently, the cost of repairing these problems is severe in financial terms, and also leads to losses in load and time. Therefore, it is essential to investigate and study the waveforms of power quality disturbances, so they can be precisely detected and classified.

Signal processing algorithms such as Fourier Transform, Stockwell Transform and Wavelet Transform have provided powerful mathematical algorithms for detecting power quality problems in electrical power systems, where they show significant successes in this field. Classification techniques support the detecting algorithm by testing, validating and training large amounts of power signals to ensure the effectiveness and efficiency of the chosen algorithm.

## 1.4 Aim and Objectives

This research study aims to develop a novel detection algorithm and classification technique of power quality disturbances in electrical power systems.

The objectives of this project are:

- To characterise the main power quality problems in electrical power systems according to their definitions, and based on international approved power quality standards such as IEEE 1159 and IEC 61000-4-30. This objective shall ensure the representation of each of these disturbances within waveform specifications and their limits.

- To investigate and develop a novel detection algorithm and classification technique of power quality disturbances based on signal processing technique.

- To validate, test and train the proposed methodology based on comparison analysis with recent and powerful detection methods.

- To analyse and model on-line power faults in the electrical power transmission system model and apply the resulting responses to the proposed methodology to examine the robustness of the developed approach of the detecting algorithm and classification technique.

- To investigate and study control strategies in response to the presence of power quality disturbances, and propose solutions to mitigate these effects and retrain power operations at normal conditions within the lowest time achievable.

## 1.5 Contributions to Knowledge

The following summarises the original contributions achieved in this research study:

1. A characterisation of power quality issues in electrical power systems (Chapter 3).

2. A novel detection algorithm and classification technique of power quality disturbances (Chapter 4).

3. A recognition system of power quality problems using on-line power system faults in transmission power system (Chapter 5).

4. A proposed bank of harmonics filters with optimisation to the MB-PSS controller in transmission power systems (Chapter 6).

## 1.6 Thesis Outline

Based on findings of the research and the objectives achieved, there are seven chapters in this thesis:

Chapter 2 reviews, with a detailed background, the existing algorithms related to detection methods of power quality problems, as well as artificial intelligence techniques in the field. Firstly, four powerful detection methods are highlighted: Fourier transform, Wavelet transform, Stockwell Transform and Hilbert-Huang Transform. Furthermore, the role of classification techniques using artificial intelligence is introduced, which includes: artificial neural networks, support vector machine, fuzzy expert system and genetic algorithm.

The chapter concludes with issues related to the mentioned methods, and challenges facing each one of them.

Chapter 3 analyses and models the character of each of power quality disturbances, which starts from the concept of power quality and what it involves. Following this is a focused view on international power quality standards related to these phenomena. Each one of these waveform signals is then described by its definition, and its formulas and limitations.

Chapter 4 presents a novel approach in terms of a detection method and classification technique of power quality disturbances, based on the hybrid methodology of complementary ensemble empirical mode decomposition and feed forward neural networks. Furthermore, the research in this section shows a validation methodology, in the beginning, the detection of these disturbances are based on discrete wavelet transform with feed forward neural networks. Moreover, the proposed algorithm is constructed with the same classifier. The chapter concludes with the results obtained, and compares these with the previous method, which shows the efficiency of the proposed methodology.

Chapter 5 presents and illustrates modelling of on-line power disturbances in a specific transmission power system. These disturbances are due to its faults, which are analysed and recorded. The results are then detected by the proposed approach and the outputs are analysed

Chapter 6 investigates and evaluates control strategies to handle such power problems. This section begins with an explanation of the principle of power quality control and important strategies in this field. Thereafter, research focuses on the stability efforts for transmission power systems experiencing power quality disturbances. An investigation is conducted on system performance with its controllers. Following this, a proposed method to enhance and improve system stability is introduced, with comprehensive analysis of its results with previous solutions. A tuning process is then followed to ensure the optimum performance of the system and results achieved.

Chapter 7 summarises the research main conclusions and significant contributions. It also highlights future work in this field and provides suggestions of further areas for study.

# Chapter 2 – Literature Review

## 2.1 Introduction

To analyse power quality and its disturbances, it is necessary to detect and identify these disturbances in time, precisely and correctly. Furthermore, it is crucial to categorise them according to their standards, in order to act and solve these disturbances. Power quality disturbances depend on the magnitude and frequency of their signal. Direct measurement can be obtained from the root mean square (RMS Values) of the signal, which can provide the required information and features, but unfortunately it does not provide the beginning point of the waveform detected, and does not provide data about the phase angle [9].

In complex power systems and during operations, a huge number of PQ disturbances are reported, which makes any ordinary analysis of such data difficult for monitoring programmes and analysts. Thus, an advanced algorithm is essential for detection, feature extraction and classification of this data in order to ensure an understanding of these events [10]. Signal processing algorithms provide the mathematical solution to handle signals, especially in the electrical power system. In this literature, several methodologies of signal processing algorithms and their capabilities, in terms of detection and feature extraction, are investigated and discussed to detect, recognise and identify power quality disturbances.

## 2.2 Detection Algorithms

To discuss signal processing algorithms effectively, it is important to understand advantages and disadvantages for each signal processing algorithm in power quality studies. The features extraction process is the core stage of a detection algorithm, where each signal waveform has unique features, as will be discussed in detail in this thesis. Features which can be obtained directly from the root mean square measurements (RMS values), as well as through the detection algorithm, should be available to meet the event characterisation and report the disturbance signal efficiently [11]. The feature extraction process involves finding unique features from the obtained mathematical coefficients which represent the original signals. In this literature, a set of effective signal processing algorithms is discussed, including Fourier Transform, Wavelet Transform, Stockwell Transform and Hilbert-Huang

Transform, as shown in Figure 2-1. The extracted features of PQDs are then used for the classification technique system in order to achieve the highest level of accuracy [12].

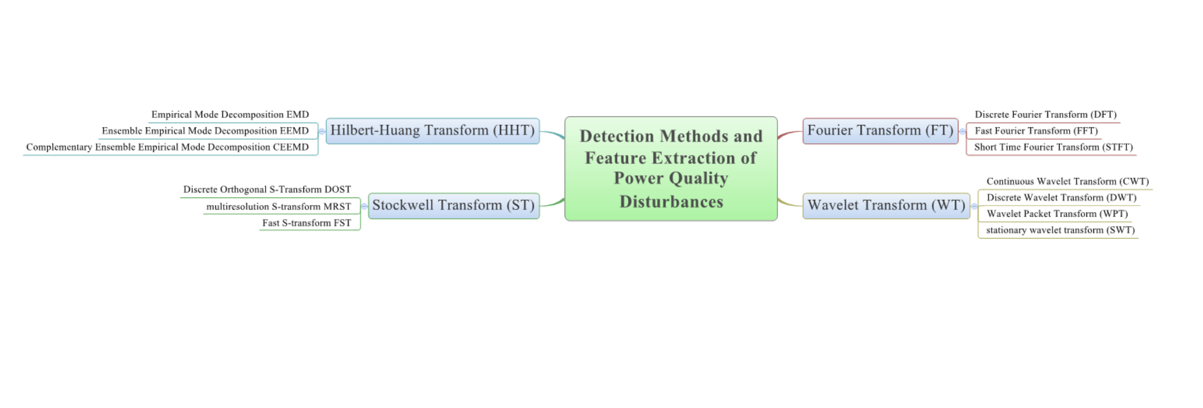


**Figure 2-1 Detection algorithms discussed in this thesis**

### 2.2.1 Fourier Transform

Fourier Transform (FT) is considered the basic algorithm to analyse signals in the frequency domain in many areas, such as engineering and physical sciences [13]. FT is the base analysis method for the definition of power quantities in IEEE standard 1459-2010 [14]. FT stands on decomposing the signal into a summation of sinusoidal functions at specific frequencies. Fourier Transform can be divided into three main derivatives working in the power quality field: Discrete Fourier Transform (DFT), Short Time Fourier Transform (STFT) and Fast Fourier Transform (FFT).

FT is broadly used for stationary signals, where it divides the signal into a sum of frequencies [15]. However, FT faces difficulty in collecting time information when the signal fluctuates [16]. Therefore, developments to FT were conducted, which led to derivatives of FT, mentioned earlier. One of these derivatives is Discrete Fourier Transform (DFT), which is involved in detecting disturbances in power systems [17]. DFT is unable to handle changes in power quality disturbances; it is a suitable algorithm for stationary PQDs only.

Another derivative of FT, named Short Time Fourier Transform (STFT), has a role in detecting PQDs, where it has the ability to split the disturbed signal into small segments, and each of these segments is considered as a stationary signal, as in [18]. Authors introduced a relationship between the signal frequency and time [19], but it is still difficult to detect non-stationary signals using STFT, as proved in [20]. Fast Fourier Transform (FFT) is sufficient for analysing harmonics, as it is one of the steady state events [21], where it has the same results that can be achieved by DFT, but in less time. A developed version used windowed FFT to analyse power quality for harmonics only [22]. However, the signal factors (amplitudes, frequencies and phases) could not be achieved precisely due to leakage reached by FFT [23].

### 2.2.2 Wavelet Transform

Wavelet Transform (WT) is an advanced signal progressing algorithm that has a role in power quality studies. WT gains its power from the ability to detect and represent power signals in the time and frequency domain. WT can also decompose the signal in the frequency domain and find the wave coefficients, which is the key to recognising the disturbance in the signal [24].

Although WT was initially an interesting algorithm for researchers in the medical field, it became an interesting algorithm in power quality research [25]. WT offers a powerful feature extraction process for distorted power signals, which has been proven in harmonic cases, as in [26]. In detail, signals are preceded through a decomposition procedure, which decomposes the signal into several sums of short-term waveforms, called the mother wavelet. The main difference between WT and FT is that WT provides the signal information in the time–frequency domain, which gives WT an advantage in analysing power quality disturbances. Moreover, WT has a mathematical coefficient which is able to hold characteristics of the signal at different frequency bands. These coefficients hold more information about signals, such as the amplitude, energy level and standard deviation [27]. In terms of detecting power quality disturbances, WT is able to detect non-stationary disturbances in short time periods, as in [28]. WT was classified originally into two main categories, Continuous Wavelet Transform (CWT) and Discrete Wavelet Transform (DWT) [29]. Authors introduced WT as a detection algorithm for power quality disturbances based on the multiresolution method [30]. CWT is introduced to measure power quality disturbances, as in [31]. DWT is a powerful algorithm in detecting PQ disturbances, as can be seen in what is proposed to determine the magnitude of single event which is voltage sag in [32]. Furthermore, authors applied a hybrid approach based on DWT with FFT to detect PQ disturbances [33], where DWT is responsible for detecting distorted signals and gaining the benefit of the process of features extraction. Based on the feature extraction process, DWT shows its ability to decompose the 10 cases of stationary and non-stationary power quality disturbances into 8 different levels of resolution in the time domain, as shown in [34]. Other derivatives of WT have effects in the field of power quality as well. Authors in [35] introduced a combined algorithm to analyse power disturbance information using DWT and wavelet packet transform (WPT). Authors' proposal in [36] is produced based on WPT for power quality indices for balanced and unbalanced systems under operating conditions. The authors in [37] proposed a perspective for the IEEE standard 1459-2000 dentitions using the stationary wavelet transform (SWT) to define power components.

### 2.2.3 Stockwell Transform

The Stockwell Transform (ST) is a time–frequency signal processing algorithm introduced by Stockwell et al. [38], which is considered a hybrid combination of WT and STFT, giving a time and frequency representation. ST tracks the signal dynamics accurately, where it combines the real and imaginary spectra.

ST becomes part of power quality detection algorithms once it is implemented to detect power waveforms, as proposed in [39]. ST uses a window to localise the complex Fourier sinusoidal signal, similarly to STFT, but the width and height of the window scale with frequency is similarly to wavelets. Such description can be seen in detecting voltage sag and swell in [40]. Authors proposed the detection and classification of complex and single power quality disturbances using ST and a probabilistic neural network with overall accuracy of 89% [41]. Furthermore, a real-time approach to detect and classify distorted power signals was presented recently [42]. A derivative algorithm of ST named Discrete Orthogonal S-Transform is involved in five single disturbances, as mentioned in [43]. Authors in [44] present another approach for detecting power quality disturbances based on multiresolution S-transform for seven cases, with accuracy close to 97%.

### 2.2.4 Hilbert-Huang Transform

Hilbert-Huang Transform (HHT) is a recent and advanced algorithm in signal processing, which is designed to analyse non-stationary signals when time is important. HHT was proposed in 1998 by Dr. Huang [45]. HHT consists of two major processes: the decomposition process, which is known as the empirical mode decomposition (EMD), and

Hilbert Spectral Analysis (HSA). The EMD procedure is capable of decomposing any non-stationary power signal with its information in the time domain into an array of sub-signals. Thereafter, each of these sub-signals has a particular frequency and, depending on their frequency, EMD extracts sub-signals into more specific categories named intrinsic mode functions (IMFs). The first IMF collected belongs to the highest frequency component of the extracted signal, where the lowest frequency component comes as the lower one [46]. Thereafter, Hilbert Spectral Analysis (HSA) determines the instantaneous magnitude and instantaneous frequency with a time curve. This combination in signal processing algorithms of EMD and HSA is known as the HHT [47]. The main advantage for HHT over other algorithms in PQ studies, such as FT or WT, is that the EMD process derives its basic functions from the signal itself, so it is acting according to nature.

HHT is initially implemented for voltage sag only which established the bath in power quality studies [48]. Thereafter, authors implemented HHT intensively with eight power quality disturbances, where they concluded an accuracy of 97.22% for the HHT detection method, as published in [49], with a compression with WT. Another hybrid methodology was conducted to analyse power quality based on wavelet and Hilbert Transform, as introduced in [50]. Authors present two classification attempts, based on the HHT algorithm, to detect seven power quality events, which reach significant accuracy with 94.57% using support vector machine (SVM), as in [51].

HHT has no clear categories or derivatives, since it is a very recent algorithm and has been implemented for power quality in only a few publications. In this literature, it is assumed that HHT has categories based on the improvements to the EMD process. Where most mentioned studies are based on the EMD approach, authors have proposed a new derivative of HHT named ensemble empirical mode decomposition (EEMD), where the accuracy in the study is not provided clearly. The newest derivative of HHT is proposed in the data analysis, named complementary ensemble empirical mode decomposition (CEEMD) in the mechanical field [52].

## 2.3 Classification Techniques Based on Artificial Intelligence

Artificial intelligence (AI) techniques can be identified as the automation of human thinking and actions such as learning, problem solving, estimation and decision making. With such a powerful mathematical base, AI techniques became powerful tools to diagnose power quality disturbances correctly.

Power quality suffers similarity in their shape, and each one of these distorted signals needs to be handled within a short time. Therefore, AIs are required in the classification of power quality disturbances. AI has proven its importance and ability to classify power signal disturbances, and handle data extracted from detection algorithms [53]. Figure 2-2 shows AIs discussed in this study.

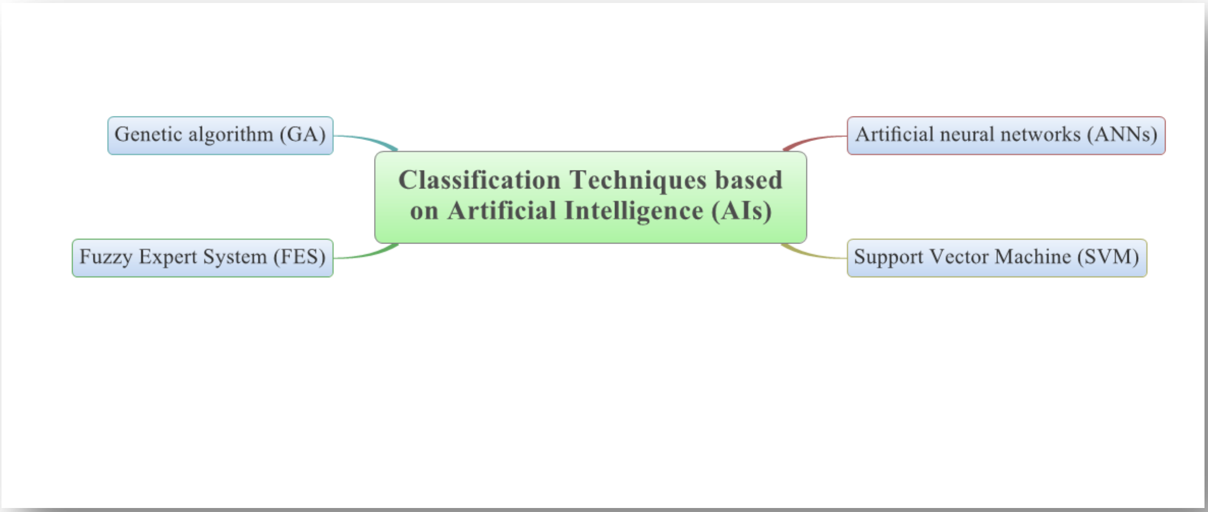


**Figure 2-2 Classification techniques using artificial intelligence (AI)**

### 2.3.1 Artificial Neural Networks

Artificial neural network is one of the main, robust AI techniques used in power systems as well as classification for PQDs [54]. Authors in [55] proposed an early implementation of the neural network approach to classify distorted power waveforms. An approach to recognise the harmonics source is proposed, based on a neural network [56]. Moreover, artificial neural network (ANN) is proposed to identify four cases of disturbances according to the faults in a transmission lines system [57]. Authors presented a robust ANN classifier for data extracted of power quality events in smart grids based on DWT algorithm [58]. Authors in [59] presented a detector based on WT, with a classification system using neural networks for real-time PQ disturbances configured by an Electrical Power Generator.

### 2.3.2 Support Vector Machine

The principle of a support vector machine (SVM) was introduced by Vapnik [60]. An SVM is a supervised learning machine technique, which is applied for pattern recognition in many areas of sciences and classification systems techniques. Regarding power quality, SVM was used to identify voltage disturbances as a classifier in [61].

Pattern recognition is one of the approaches that relies on statistical learning theory and is applied to solve problems, and for forecasting and estimation. Five different power quality disturbances were detected by S-transform and classified by SVM, as presented in [62]. Authors in [63] presented a WT-based deletion algorithm to recognise distorted events with an SVM classifier. Five single power quality disturbances were detected by DWT and classified based on SVM in [64].

### 2.3.3 Fuzzy Expert System

The fuzzy expert system (FES) is one of the classical Al techniques, which is based on two decision choices for uncertain situations. It is driven by the calculation that human intellectual can apply models that do not have fixed boundaries [65]. A fuzzy system is a task that plans objects at specified domain to their membership values, which is called the membership function [66].

In power quality studies, an early approach to evaluate and quantify power quality based on fuzzy logic is proposed in [67]. Authors presented a fuzzy expert system using a group of fuzzy sets and rules as a replacement for Boolean sets to classify PQDs [68]. Another fuzzy classifier is implemented based on four levels of the decomposition process of WT, as in [69].

Another approach to classify power disturbances is based on a combination of FES and ANN, which is named the Neuro-Fuzzy system, as introduced by authors in [70]. The study has focused on the recognition learning process for these disturbances, with an overall accuracy of 96%. Moreover, a classification system is proposed for PQ disturbances using 3-D space referential representation, and Principal Component Analysis (PCA) is based on the neuro-fuzzy approach [71].

### 2.3.4 Genetic Algorithm

The Genetic Algorithm (GA) is an evolutionary search technique based on the evolutionary concepts of natural range. GA is used in the fields of finding problems, optimisation, machine learning and solutions; it is discussed deeply in [72]. An approach to assess power quality for a single case in the simulation environment is conducted based on the GA, and presented in [73]. A novel analytic method of power quality events is proposed based on wavelet transform and GA in [74].

## 2.4 Summary

A significant number of studies are involved in enhancing power quality. In terms of detection algorithms, it can be concluded that FT, WT, ST and HHT are the potential detection methods used in this field.

It is clear, as mentioned earlier, that FT is the base of detection algorithms used in this power quality analysis, but it is proven that FT suffers from representing PQDs in time, especially when the disturbance fluctuates, where FT is unable to provide information needed due to the limitation of the fixed window width [75]. Moreover, STFT is still a successful algorithm to analyse stationary PQDs, but it is difficult to detect and analyse non-stationary signals, which are the major ones causing problems for power utilities [76].

WT is a useful algorithm which has the ability to characterise PQDs in both the time and frequency domain. Therefore, it is sufficient in time–frequency resolution and analysis. WT is experimentally proven to be better than STFT [76]. However, it is still important to choose a suitable wavelet branch, where the computational cost increases with the increase in filter length. Nevertheless, WT is often utilised when there is no requirement of the exact frequency, but it is still hard to extract features in low frequency components of the distorted power signal, as in [77].

HHT is a powerful algorithm based on its capabilities in analysing power quality disturbances, and its magnificent feature extraction through the empirical mode decomposition process (EMD), which is able to have the instantaneous magnitude and frequency information, and eventually precise signal detection is determined. However, as it is a very recent algorithm in the PQ field, it is necessary to have a well-proved analysis for the HHT algorithm in comparison with other powerful algorithms under the same environment and conditions. Through suitable indicators, and with a robust comparison analysis, questions regarding which is the better detection and measurement algorithm for power quality can be answered.

This literature features many studies focused on detecting and classifying power quality disturbances. However, it is obvious that many of these studies were conducted for one or two disturbances such sag or swell, and a few others are conducted for five cases under research and results presented. It can also be noticed that the majority of these studies were conducted for single cases, but not multiple cases. The average of detecting accuracies using AI classifiers was in the range of 90.0% to 96%. Nevertheless, there is a clear shortage in the research of comparison analysis with on-line disturbances occurring in power lines due to faults in power systems.

In this thesis, and according to the literature conducted, WT and HHT are the two promising yet questionable algorithms in detecting power quality disturbances precisely. A suitable approach for this thesis is to investigate both of these algorithms in the same conditions and for specific formulas of power disturbances. For a greater understanding, ANN is also investigated to classify PQDs; for both approaches, results are presented and analysed.

# Chapter 3 – Characterisation of Power Quality Disturbances

## 3.1 Introduction

The term ‘power quality’ is one of the major buzzwords of providers and customers in the power industry [78]. Authors in [79] have studied power quality issues according to their causes, and how signal processing algorithms can handle and represent them. Another context is presenting an investigation of electrical power quality disturbances which describe signals variation [2], and the impact of these problems in electrical machines in power systems [80]. This chapter will discuss the concept of power quality and international standards related to the subject. Moreover, various power quality disturbances will be discussed in detail. Disturbance definitions, waveform phenomena and mathematical equations are also provided. Nevertheless, causes and possible effects to power systems, when such disturbances occur, are introduced, along with remedies and solutions presented for each case.

## 3.2 Power Quality

Several definitions for power quality were introduced, due to its importance. Early in the eighties, power quality had two main factors to be identified: quality of voltage and continuity of supply [81]. Nowadays, the term ‘power quality’ became attached to voltage disturbances in power systems. Researchers in the technical field prefer to use the term ‘voltage quality’ where most of the power quality disturbances are actually based on voltage, representing the majority of such events in the field [82], [83].

Current quality is considered complementary to voltage quality, containing the deviation of current in power systems. Although it was introduced recently, it is rarely used term as in [84] and [85], it is still related to what can be provided to customers by utilities. Therefore, power quality is considered to represent voltage and current quality even if the voltage events still reflect the meaning of the phenomena, where it is broadly approved and suitable as a representation of the signal phenomenon. The definition of PQ produced by the IEEE (Institute of Electrical and Electronic Engineers) is: “the concept of powering and grounding sensitive equipment in a matter that is suitable to the operation of that equipment and compatible with the premise wiring system and other connected equipment.” [86]

Once a high power quality is achieved, power systems’ equipment will run effectively and power system conditions reach satisfaction. Otherwise, with poor quality, the power devices might be destroyed, or a reduction of its efficiency is highly likely to occur. The power system will run in the affected conditions, and the cost of repairing and protection will be extremely high [87].

## 3.3 International Standards of Power Quality

Standards organisations, whether they are national, such as the American National Standards Institute (ANSI), British Standards Institute (BSI), Saudi Standards, Metrology and Quality Org. (SASO), or international, such as the International Organization for Standardization (ISO), are the authorised bodies who are responsible for delivering or adopting standards to a country or region. Power quality has many standards which exist to frame a full description for PQ issues and their electromagnetic phenomena. Moreover, such standards have nominal operational conditions for voltage, and acceptable variation within the power networks. Moreover, in these standards, the selection of the appropriate monitoring instruments is described along with their limitations, while measurement methods and terminologies of results are also demonstrated.

The goal of producing power quality standards is to protect power utilities, providers and the end user or customer from any failure, dropdown or misoperation when a voltage disturbance occurs [88]. Power quality standards provide limits, measurements and settings for voltage, current and frequency values when they deviate from nominal conditions [89]. Such standards draw lines and provide guidance regarding acceptable and unacceptable levels in the service provided for both providers and customers. It is important to provide customers with an acceptable level of disturbance events and variations where it is impossible to gain a healthy supply [90].

One of the essential standards in the power quality field is the IEEE 1159 standard which was introduced by the Institute of Electrical and Electronics Engineers (IEEE). According to this standard [91], power quality disturbances have specific categories: transient (oscillatory and impulsive), short duration variations (sag, swell and interruption), long duration variations (under voltages and over voltages), steady state variations (harmonics, notch and flickers) and frequency variations. These categories include a time scale for each event. Before this standard, many studies on PQ were fundamentally building descriptions of the disturbance waveforms on IEEE Std. 1459-2010, which includes definitions for the measurement of electric power quantities under sinusoidal, non-sinusoidal, balanced and unbalanced conditions [92]. Furthermore, the European standard EN 50160 specifies root mean square (RMS) measurements for voltages where disturbances occur [93]. One of the most important standards is the International Electrotechnical Commission, IEC 61000-4-30, which provides the guide and roles used by power experts and engineers to test and measure techniques related to power quality [94].

## 3.4 Power Quality Disturbances

Power quality is principally attached to any deviations or changes in voltage or current waveforms from the ideal signal at a designated frequency and magnitude. Therefore, any deviation in power signal is called power quality disturbance in general terms [9]. In reality, it is almost impossible to maintain voltage values in nominal sinusoidal conditions, where there is usually some sort of disturbance in the system.

It is important to group power quality disturbances into groups, or further subgroups, as each one of these disturbances has a special wave shape. From a power electronics perspective, power quality disturbances are broadly divided into events and variations. An event is a sudden change in the voltage waveform which has a beginning point and ending point, such as sag, swell and interruption. A variation is a steady state waveform that requires a continuous measurement such as harmonics and notching [79], as shown in Figure 3-1. Such terminology is found in research publications presented in the power quality field.

From a signal progressing perspective, the signal performance and wave shape are critical, and power quality disturbance can also be broadly categorised into two main cases: stationary or non-stationary signals, based on signal progressing terminology. In reality, almost all power quality disturbances are non-stationary signals.

In this study, several voltage power quality disturbances are discussed in terms of their characteristics, mentioned in IEEE Std [95] and IEC [96], and how they are really represented in power networks, as shown in

Table 3-1.

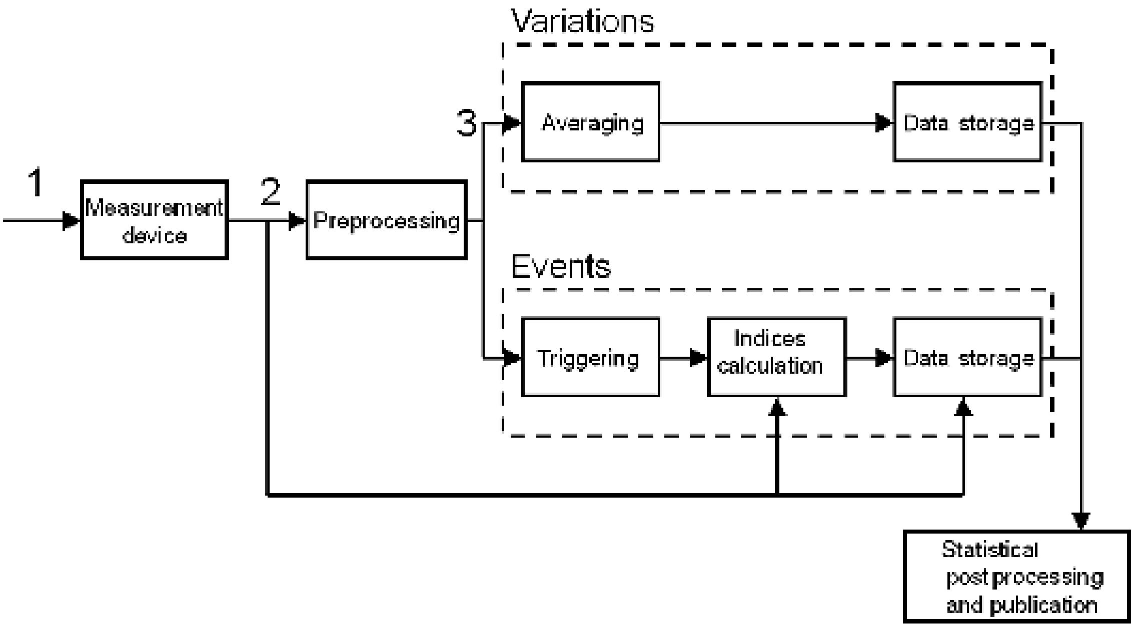


**Figure 3-1 Power quality measurements for voltage and current for variations and events [75]**

### 3.4.1 Pure Sine Signal

Before describing in detail each power quality disturbance in this thesis, it is vital to reference pure voltage signals for a better understanding of disturbance wave shape. The pure sine waveform signal is the ideal waveform for voltage or current, which can also be named as a healthy signal in some publications.

According to the standard IEEE 1159, the voltage signal has a known frequency of 50 or 60 Hz, as shown in Figure 3-2. A pure voltage signal can be modelled by Equation 3.1:

$$f(t) = A\sin(\omega t) \qquad (3.1)$$

where the parameters for this equation include the amplitude (A) of the signal, along with the frequency, and they have the conditions: A = 1.0 f = 50 Hz, $\omega = 2\pi\ 50$ rad/sec.

**Table 3-1 Categories of typical characteristics of power quality disturbances [95]**

| Categories | Typical spectral content | Typical duration | Typical voltage magnitude |
|---|---|---|---|
| **1.0** Transients | | | |
| **1.1** Impulsive | | | |
| **1.1.1** Nanosecond | 5 ns rise | < 50 ns | |
| **1.1.2** Microsecond | 1 µs rise | 50 ns – 1 ms | |
| **1.1.3** Millisecond | 0.1 ms rise | > 1 ms | |
| **1.2** Oscillatory | | | |
| **1.2.1** Low frequency | < 5 kHz | 0.3–50 ms | 0–4 pu |
| **1.2.2** Medium frequency | 5–500 kHz | 20 µs | 0–8 pu |
| 1.2.3 High frequency | 0.5–5 MHz | 5 µs | 0–4 pu |
| 2.0 Short-duration root-mean-square (rms) variations | | | |
| 2.1 Instantaneous | | | |
| 2.1.1 Sag | | 0.5–30 cycles | 0.1–0.9 pu |
| 2.1.2 Swell | | 0.5–30 cycles | 1.1–1.8 pu |
| 2.2 Momentary | | | |
| 2.2.1 Interruption | | 0.5 cycles – 3 s | < 0.1 pu |
| 2.2.2 Sag | | 30 cycles – 3 s | 0.1–0.9 pu |
| 2.2.3 Swell | | 30 cycles – 3 s | 1.1–1.4 pu |
| 2.3 Temporary | | | |
| 2.3.1 Interruption | | >3 s – 1 min | < 0.1 pu |
| 2.3.2 Sag | | >3 s – 1 min | 0.1–0.9 pu |
| 2.3.3 Swell | | >3 s – 1 min | 1.1–1.2 pu |
| 3.0 Long-duration rms variations | | | |
| 3.1 Interruption, sustained | | > 1 min | 0.0 pu |
| 3.2 Undervoltages | | > 1 min | 0.8–0.9 pu |
| 3.3 Overvoltages | | > 1 min | 1.1–1.2 pu |
| 3.4 Current overload | | > 1 min | |
| 4.0 Imbalance | | | |
| 4.1 Voltage | | steady state | 0.5–2% |
| 4.2 Current | | steady state | 1.0–30% |
| 5.0 Waveform distortion | | | |
| 5.1 DC offset | | steady state | 0–0.1% |
| 5.2 Harmonics | 0–9 kHz | steady state | 0–20% |
| 5.3 Interharmonics | 0–9 kHz | steady state | 0–2% |
| 5.4 Notching | | steady state | |
| 5.5 Noise | broadband | steady state | 0–1% |
| 6.0 Voltage fluctuations | < 25 Hz | intermittent | 0.1–7%<br>0.2–2 $P_{st}$ |
| 7.0 Power frequency variations | | < 10 s | ± 0.10 Hz |

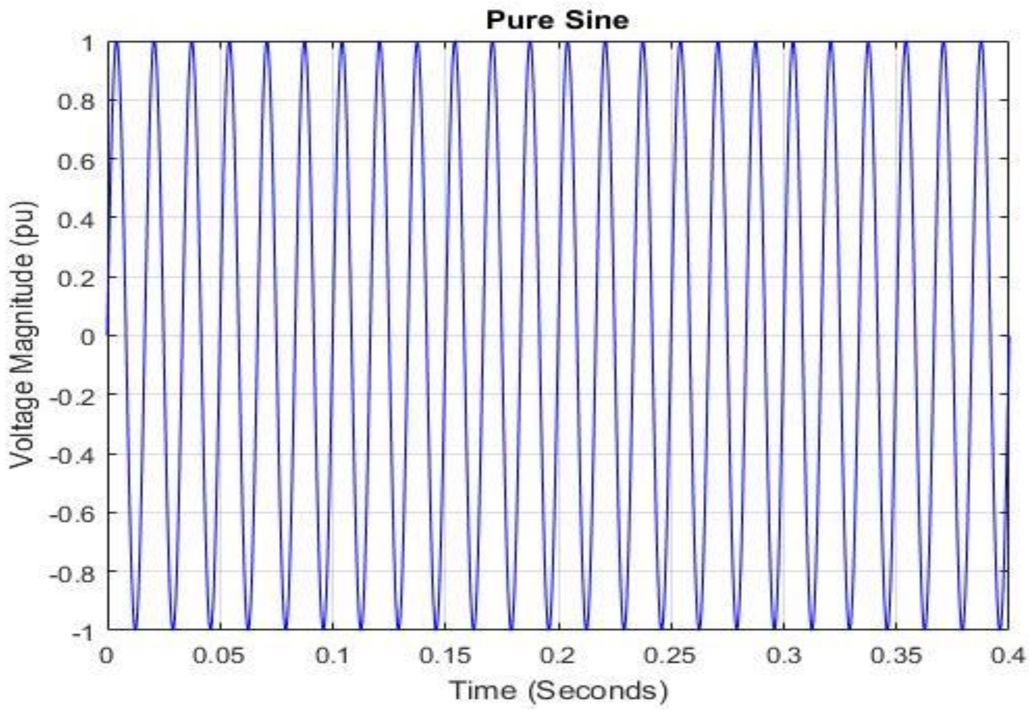


**Figure 3-2 Pure Voltage Signal**

### 3.4.2 Sag

Sag, as a major PQD in electrical power systems, is known as a momentary decrease of RMS voltage magnitude (between 0.1 and 0.9 Pu) at a power frequency that lasts for a short period of time (from 0.1 to 1 min), which is typically from 0.5 to 30 cycles. Short sags are usually from 2 to 5 seconds, mainly from clear faults. Sustain sags lasting for 1 minute are mainly caused by permanent faults. Figure 3-3 shows a typical sag magnitude and its duration.

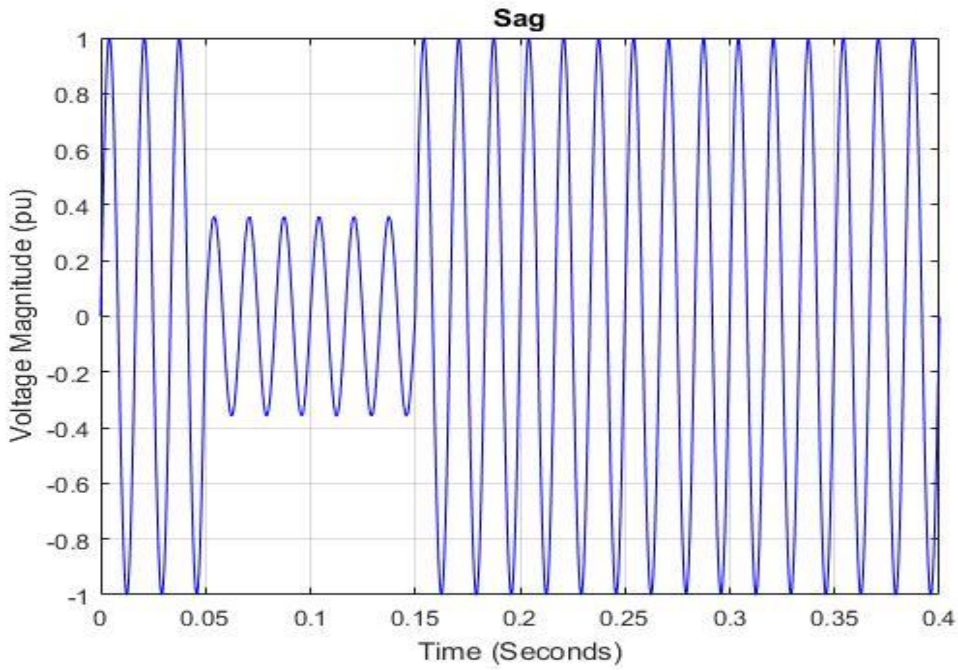


**Figure 3-3 The sag phenomenon caused by single phase fault**

Based on the description of the sag phenomenon, and to model this disturbance, the signal specification of sag disturbance is given by Equation 3.2:

$$f(t) = A(1 - \alpha(u(t - t_1) - u(t - t_2)))\sin(\omega t) \qquad (3.2)$$

where the sag phenomenon described in the above equation shall be within the range of the following parameter limitations: $0.1 < \alpha < 0.9$ and $T \leq t_2 - t_1 \leq 9T$.

Sag courses include starting large motors, cleared faults and initial faults. A feeder fault can result in a voltage sag in the substation bus. Large load changes can cause sags in the system. Sag can occur with the starting of an induction motor when it produces a slight change in the speed. The sag phenomenon is named by the IEC as ‘dip’, which is more European terminology, whereas the term ‘sag’ is chosen in the North American power quality community.

Voltage sag can result in damage to electronic devices, especially sensitive ones, and it might cause the loss of synchronised data or even stability. Sag is identified by controllers provided with fault detection sensors, which start the shutdown of the load [97]. During the sag event, it might be noticed that there is a reduction in lighting.

Remedies for sag include replacing faulty breakers, and repairing or adding large wiring. Additionally, installing a voltage regulator for initial cases and supporting the electronic devices with battery backups to handle short sag in the system. There are other solutions for sag as well, such as adding uninterruptible power supply (UPS) or transformers. Moreover, there are effective approaches to prevent sag, such as tree trimming, improving pole grounding and modification of conductor spacing [98].

### 3.4.3 Swell

Swell disturbance is the opposite phenomenon to sag, where a swell is an increase of RMS voltage of between 1.1 to 1.8 pu at the power frequency for a duration of time (from 0.1 to 1 min) which is typically from 0.5 to 30 cycles. Figure 3-4 shows typical swell and its duration. The magnitude of swell in many research publications is defined whenever its line's voltage is greater than 1.0 pu.

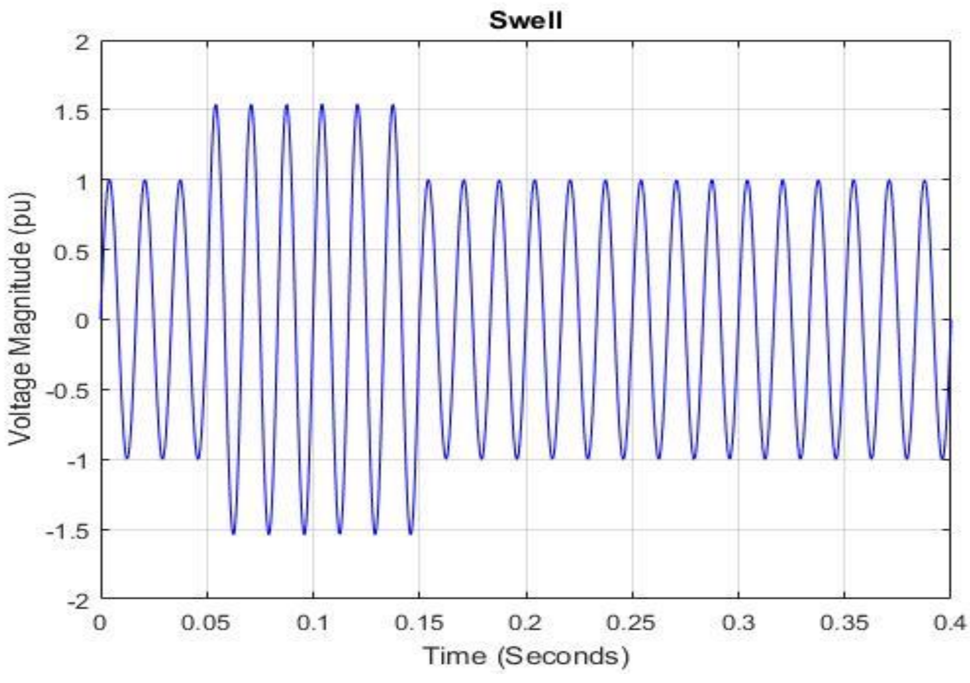


**Figure 3-4 Swell phenomenon**

Swell can be caused by single line to ground faults, but appears much less frequently than sags in power systems. In addition, swell can be caused by sudden load dropping or switching off a heavy load, and loose wiring as well. Switching on a large capacitor bank is considered the most common cause for such a disturbance [95].

Swell's signal formula is provided by Equation 3.3:

$$f(t) = A(1 + \alpha(u(t - t_1) - u(t - t_2))) \sin(\omega t) \qquad (3.3)$$

where the signal parameters are at the following limits: $0.1 < \alpha < 0.8$ , $T \leq t_2 - t_1 \leq 9T$.

The two main factors in swell characteristics are the magnitude (RMS values) and duration of time. The recognised description of swell in IEEE Std C62.41in [99] is "A momentary increase in the power-frequency voltage delivered by the mains, outside of the normal tolerances, with a duration of more than one cycle and less than a few seconds".

Swell impact on electrical power systems includes: failure in electronic devices, computers and controllers, which might go further and result in a complete blackout for the system. Power grid components normally have protection from swell, with switchgears in the bus bars, but they may suffer for a short time if live. However, regular swells on the capacitor bank result in an individual bulge. There are several possible solutions to handle voltage swell, such as utilising voltage regulators or motor generators set to mitigate voltage swells, before resulting overvoltage to equipment can occur.

### 3.4.4 Interruption

An interruption is defined as the reduction of RMS voltage to less than 0.1 pu for a time duration of less than 1 minute. When an interruption occurs, it is often after the voltage sag and can be a consequence of a system fault. The interruption disturbance is a result of losing connection, control failures, lightning stroke, severe faults that do not clear, equipment failures and reclosing of the circuit breaker. Interruptions are measured by their duration and magnitude. The voltages are at a minimum magnitude, which is less than 10% or almost zero for most cases, where there is no more power in the system. Figure 3-5 shows typical interruption.

In many cases an interruption event occurs following the presence of sag in the system, or it could be the scenario between the sag event and the protective device operation. This means that resolution of the interruption depends on operating a protective device. For most cases, the remedy process is less than 30 cycles.

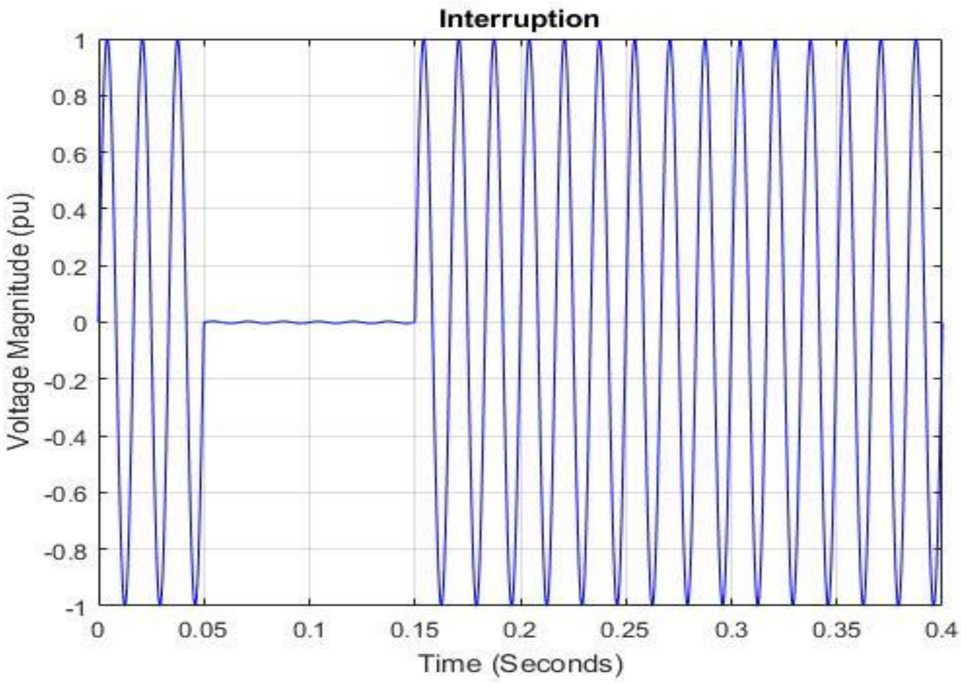


**Figure 3-5 Interruption disturbance**

In this work, momentary interruption is the case selected which is belongs to short duration of power quality disturbances, but there are other two types of interruptions in the field of power quality. The first is temporary interruption, which has the same specifications of momentary interruption, but with duration from 3 to 60 seconds, and the second is long term, which exceeds a 1 minute time duration, as can be seen in Figure 3-5. Therefore, interruption can be represented according to Equation 3.4 [95]:

$$f(t) = A(1 - \alpha(u(t - t_1) - u(t - t_2))) \sin(\omega t) \quad (3.4)$$

where interruption disturbance is represented by the above equation and its limits are: $0.9 < \alpha < 1.0$ , $T \leq t_2 - t_1 \leq 9T$.

Interruption impact on power systems includes operation interruption, revenue losses and production losses. In detail, instantaneous interruptions would disturb lighting and electronic equipment, and result in a shutdown or misoperation. Electronic equipment includes controllers, computers and any related controls for rotating machines. In temporary saturations or manometry of interruptions, it is usually a result of stop operating or a drop-out to the induction motor.

Interruption remedy scenarios include the UPS and static switches to help the system restore to its normal conditions.

### 3.4.5 Harmonics

Harmonics can be defined as sinusoidal voltages (or currents) having frequencies that are integer multiples of the frequency at which the supply system is designed to operate, according to both IEEE and IEC definitions [91], [94]. The ideal voltage waveform is a sinusoidal wave at a precise fundamental frequency, where the term fundamental frequency is either 50 Hz or 60 Hz, but this case would not exist on a daily basis, due to nonlinear load in power systems, as shown in Figure 3-6.

As one of the main disturbances appearing in power networks, harmonics can be represented by Equation 3.5:

$$f(t) = A(\alpha_1 \sin(\omega t) + \alpha_3 \sin(3\omega t) + \alpha_5 \sin(5\omega t) \qquad (3.5)$$

where the conditions for this complicated equation are: $0.05 \leq \alpha_3, \alpha_5, \alpha_7 \leq 0.15$, $\sum \alpha_i{}^2 = 1$.

There are many sources that can create harmonics, and unfortunately they are increasing, but the major source of harmonics in power systems is the usage of electronic devices. This equipment acts as a source of harmonics, and consequently a nonlinear voltage is accrued. These electronic devices with loads act as current sources that insert harmonic currents in power systems. Thereafter, voltage disturbance occurs where these currents are the source of nonlinear voltage drops in system impedance. Nowadays, modern lifestyles and the enormous usage of semiconductor devices have become rising concerns in many applications.

Any of these harmonics distortion levels has a specific category in the complete harmonic spectrum, with the magnitudes and phase angle of each harmonic element. It is known in the scientific communities as the total harmonic distortion (THD) as the magnitude of harmonic distortion [100].

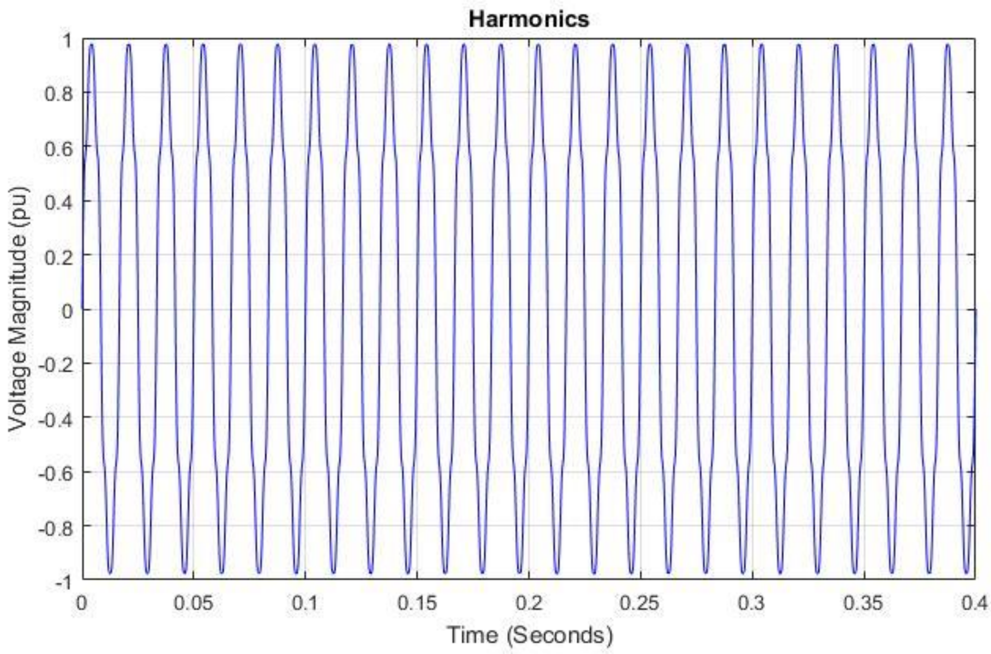


**Figure 3-6 Harmonics in power systems**

In terms of the harmonics impact on the electrical power supply, this starts from the injection of the harmonics currents produced by customers' load, which leads to harmonic voltage appearance in power systems. Voltage harmonics result in overshooting in rotating machines, transformers and misoperation to the system. These problems can cause a breakdown to the customer process. Limits of harmonic voltage and current are presented in the IEEE std 519 to voltage supply [101]. This standard gives harmonics control to the electrical power utilities and customers as well, which helps to minimise such a disturbance and its effects.

### 3.4.6 Flicker

Flicker is a regular variation of the voltage waveform, and it can be described as a series of random voltage changes. Voltage flicker magnitude is between 0.9 to 1.1 pu of the input nominal voltage, which represents a variation of ±10% of voltage magnitude, as mentioned in [102]. Flicker is a type of voltage variation located at the end of distribution load, or it can be detected just by the input to the customer's building [103]. Moreover, the most used definition in this field is still the one introduced by IEEE std 1159: Flicker is an impression of unsteadiness of visual sensation induced by a light stimulus whose luminance or spectral distribution fluctuates with time [104].

International recognised standards such as IEC 61000-3-3 have described Flicker types [105] (along with IEEE Std 1453 [106]) which enhance and determine the IEC methodology for these measurements. However, there are mainly two types of flicker phenomenon, short-time flicker and long-time flicker, where they are categorised by their durations. A special standard was introduced for flicker events [107].

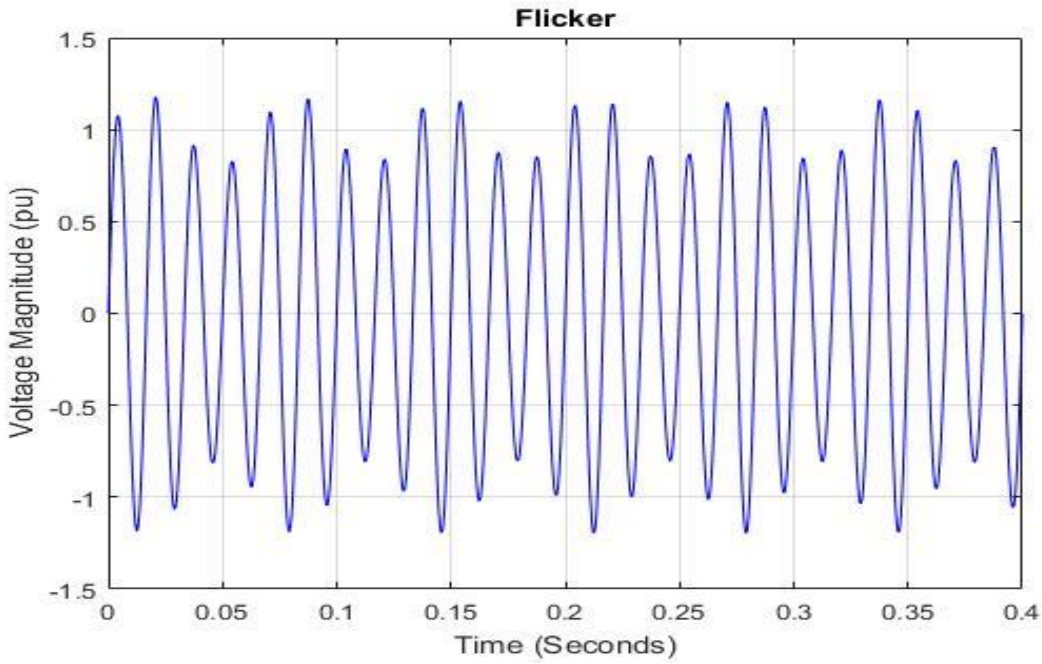


**Figure 3-7 Voltage flicker caused by arc furnace [95]**

One of the main sources of voltage flickers in the transmission and distribution systems is arc furnace. An example of a voltage flicker waveform caused by arc furnace is shown in Figure 3-7 [104]. However, there are many courses leading to flicker disturbances; for example, any load that has significant repeated variations coming from reactive components. A sudden variation in the current load can lead to voltage flicker.

Flicker disturbance is a unique variation in the wave shape of its signal and given by Equation 3.6:

$$f(t) = A + \alpha_f \sin(\omega t)\,(1 + \beta \sin(\gamma \omega t)) \qquad (3.6)$$

The formula's two components have the following signal progressing limits:

$$0.1 < \alpha_f < 0.2\ ,\ 0.1 \leq \beta \leq 0.2\ ,\ 0.1 \leq \gamma \leq 0.2\ .$$

Voltage flicker performing as a waveform has a modification of the fundamental frequency, where it is determined by RMS measurements of the voltage magnitude. This process is achieved by splitting the waveform frequencies by removing the fundamental frequency and calculating the magnitude of the variation components. Flicker disturbance can cause loss of lighting in the networks and misoperation of sensitive loads. These effects, along with others, are based on equipment tolerance, as mentioned in IEEE 141 standard [108].

### 3.4.7 Transient

The transient term is one of the most common descriptions for any disturbance occurring in power systems. It represents any variation in power signals which leads to confusion and, finally, making inappropriate decisions. It belongs to the indication of a disturbance that is unwanted, but a limitation in its effect. The transient definition was attached to the word ‘rapid’, as presented in the Authoritative Dictionary of IEEE standards [109]. Transient is widely defined as a voltage (or current) deviation with a short duration in the frequency of a power system [110]. According to standardisation authorities such as IEEE, transients are categorised into two main types, as an impulse transient or oscillatory transient, based on their different wave shapes, which will be discussed in this chapter.

#### 3.4.7.1 *Impulsive Transient*

An impulsive transient event is defined as a sudden change in nominal conditions for voltage or current, without affecting the power signal frequency. Impulsive transient has one polarity, which would be either positive or negative. An impulsive transient is categorised by its rise and decay times. This disturbance can be designated by its spectral content, as described in the IEEE Std C62.41 [99]. The main cause of an impulsive transient is lightning. Figure 3-8 shows a typical impulsive transient caused by lightning, and usually such a disturbance leads to oscillatory transient in the power signal [95].

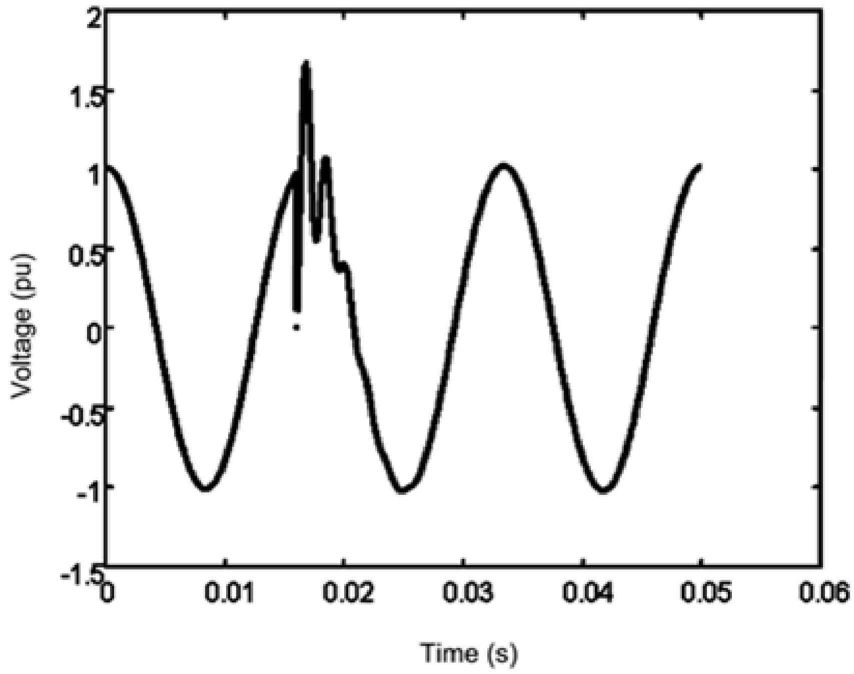


**Figure 3-8 Impulsive transient [95]**

#### 3.4.7.2 *Oscillatory Transient*

An oscillatory transient disturbance is defined as a sudden change in the steady state conditions of voltage or current, without changing power signal frequency. Such a disturbance usually oscillates in both polarities in positive and negative sides. As an oscillatory phenomenon, it consists of rapid changes in values of voltage. Figure 3-8 shows a typical oscillatory transient in power systems. Oscillatory transients are described by their duration, magnitude and spectral content, and have three main subcategories: low frequency oscillatory, medium frequency oscillatory and high frequency oscillatory, based on their spectral content [95].

Low frequency oscillatory transient is normally less than 500 Hz, with a duration less than 30 cycles, and the main cause for this event is capacitor switching. Low frequency oscillatory transient has an impact on power systems, including tripping sensitive equipment, as shown in Figure 3.9.

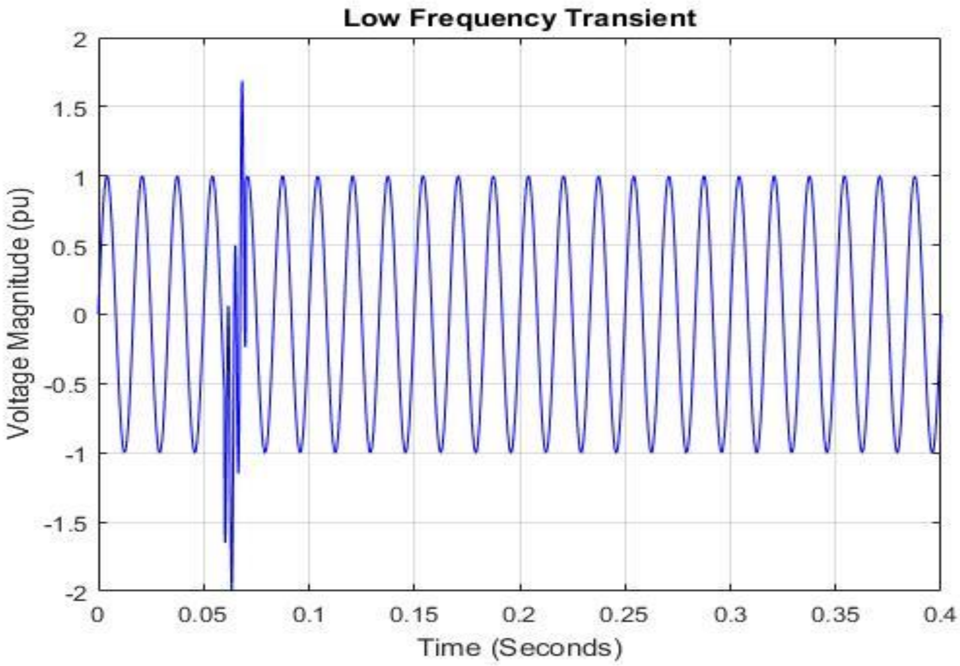


**Figure 3-9 Low Frequency Transient**

Medium frequency oscillatory transient is usually in the range between 500 Hz and 2 kHz with duration of 3 cycles. Medium frequency oscillatory transient can occur as a result of travelling waves from lightning impulses or circuit switching. This event would harm customer equipment.

High frequency oscillatory transient usually starts from 2 Hz, with duration of 0.5 cycles. High frequency oscillatory transient causes include switching on secondary systems, lightning or local Ferro resonance. As with others, this type of oscillation can disrupt sensitive electronic equipment and might cause a low voltage power supply to fail .

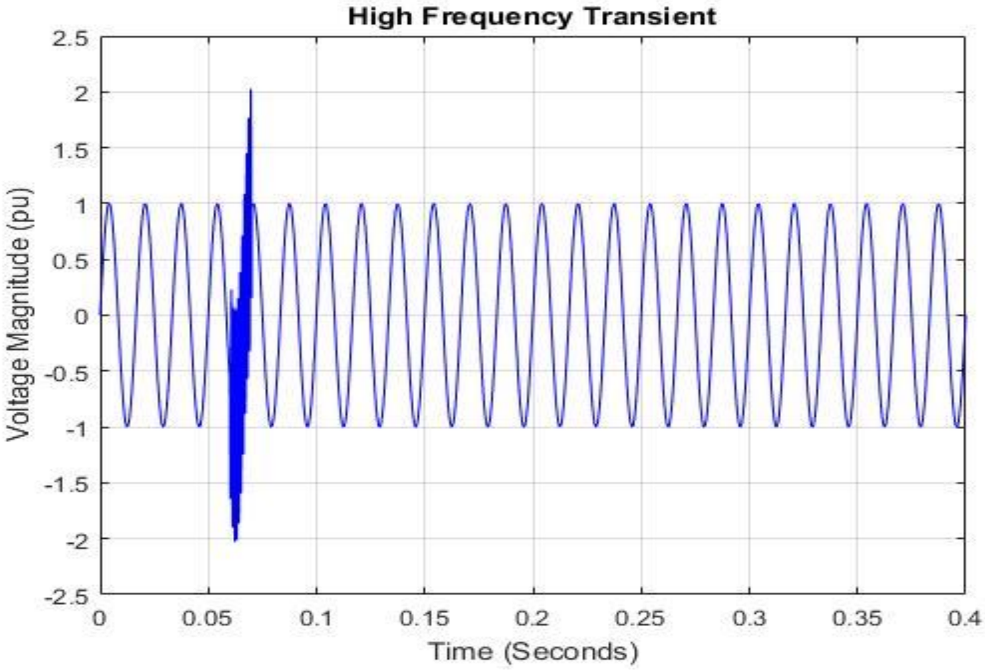


**Figure 3-10 High Frequency Transient**

In this research, it is recognised that low frequency transient and high frequency transient are the two most common disturbances in transient phenomena. Therefore, a deep study will focus on both of them [95].

As high frequency transient is considered as one of the disturbances to be represented in this study, the following formula is provided:

$$f(t) = A\,(\sin(\omega t) + \alpha e^{-t/\lambda} \sin(b\omega t)) \qquad (3.7)$$

where factors control the representation of this phenomenon are: $20 \leq b \leq 80$ , $0.1 \leq \lambda \leq 0.2$ , $0.1 \leq \alpha \leq 0.9$ , $T \leq t2 - t1 \leq 3T$, $1500\ Hz < f_n < 2000\ Hz$.

In low frequency oscillatory transient, the case is also represented in the signal processing environment by Equation 3.8:

$$f(t) = A \sin(\omega t) + \alpha e^{-t/\lambda} \sin(b\omega t)) \qquad (3.8)$$

where similarity to the high transient equation can be noticed, the parameter limits are: $5 \leq b \leq 20$ , $0.1 \leq \lambda \leq 0.2$ , $0.1 \leq \alpha \leq 0.9$ , $T \leq t_2 - t_1 \leq 9T$ , and $300\ Hz < f_n < 1000\ Hz$.

### 3.4.8 Multiple Power Quality Disturbances

As mentioned in the literature, it is clear that most of the detection algorithm research and publications are focused on detecting single disturbances occurring in power systems. The term 'single disturbance' in this study means that modelling disturbances such as sag, swell, interruption and harmonics can be represented in research work as individual phenomena, separately from each other. But in reality, it is common to have two disturbances at the same time. In this work, two of the main, most reported disturbances together are adopted: sag with harmonics and swell with harmonics [95].

### 3.4.9 Sag with Harmonics

Many cases in the real operation of power systems involve more than one disturbance at the same time. Such phenomenon is rarely discussed in terms of representation as signals. Sag and harmonics are different power quality disturbances which can occur at the same time, considered as a multiple disturbance in power systems. The phenomena of sag and harmonics occur simultaneously at the same time. Figure 3-11 shows the modelling of multiple disturbance sag with harmonics [95].

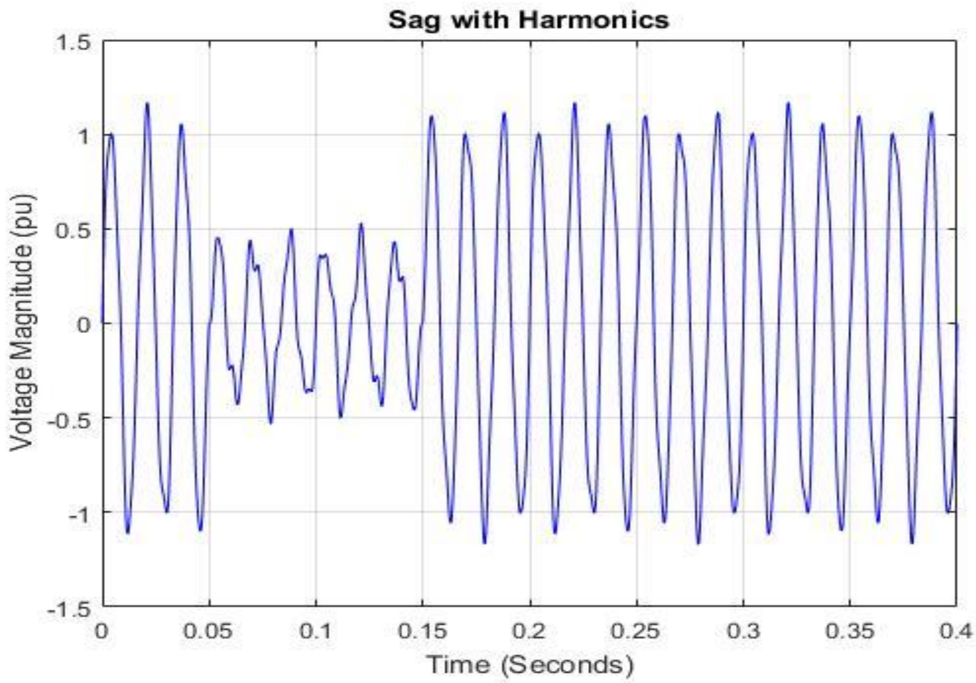


**Figure 3-11 Sag with harmonics**

The above phenomenon for sag and harmonics which is represented mathematically by the Equation 3.9:

$$f(t) = A(1 - \alpha(u(t - t_1) - u(t - t_2))) \, (\sin(\omega t) + \alpha_3 \sin(3\omega t) + \alpha_5 \sin(5\omega t))) \quad (3.9)$$

where factors in the above mathematical model have the parameters:

$0.1 < \alpha < 0.9$ , $0.05 < \alpha_3 < 0.15$ , $0.05 < \alpha_5 < 0.15$ , $T \leq t_2 - t_1 \leq 9T$ , $\sum \alpha_i{}^2 = 1$.

### 3.4.10 Swell with Harmonics

Another common multiple disturbance is swell and harmonics disturbance. This is swell and harmonics combined as a multiple disturbance, which occurs in power systems secondary to sag and harmonics. Figure 3-12 shows a typical example of swell with harmonics [95].

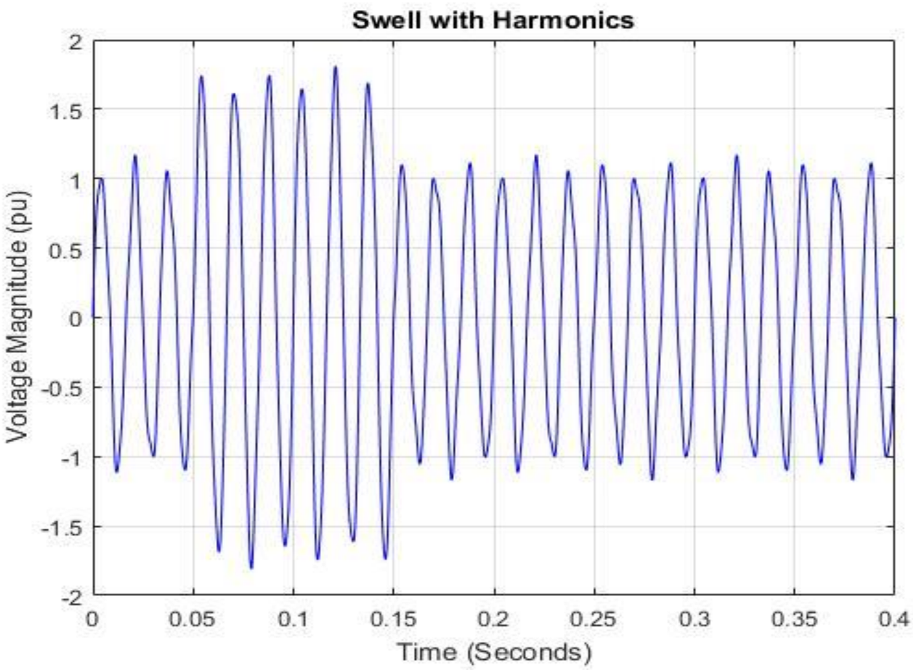


**Figure 3-12 Swell with harmonics disturbances**

In modelling this phenomenon, it is given by Equation 3.10 in signal processing as:

$$f(t) = A(1 + \alpha(u(t - t_1) - u(t - t_2))) \, (\sin(\omega t) + \alpha_3 \sin(3\omega t) + \alpha_5 \sin(5\omega t))) \quad (3.10)$$

where each of the above parameters in the equation has value limitations:

$0.1 < \alpha < 0.8$ , $0.05 < \alpha_3 < 0.15$ , $0.05 < \alpha_5 < 0.15$ , $T \leq t_2 - t_1 \leq 9T$ , $\sum \alpha_i{}^2 = 1$.

## 3.5 Summary

In this chapter, ten power quality disturbances including the pure signal were discussed in detail. Each of these disturbances has a unique definition in scientific, engineering and standards research, all of which were outlined and discussed clearly in this chapter. The waveform of each disturbance is presented and, thereafter, a precise mathematical expression for PQDs is introduced based on the signal processing environment. Causes of each disturbance were discussed deeply in terms of time duration and magnitude. Moreover, remedies and possible solutions for PQDs were also outlined. International standards authorised and accredited by international committees, designated to cover power quality, are discussed, which are the basis of the detecting algorithm analysis and further development.

# Chapter 4 - Detection Algorithms and Classification Techniques

## 4.1 Introduction

The main objective of power quality research is to provide the most appropriate algorithm, which accurately and precisely detects and identifies power quality disturbances. To achieve this, well-known procedures need to be followed. In general, the procedure starts with modelling and expressing power quality issues facing power grids.

In this chapter, power quality disturbances are modelled according to their parametrical equations. These equations, introduced in the previous chapter, have limits and barriers, according to recognised international standards. Thereafter, a signal processing algorithm is implemented to extract signal features from the system. In this stage, two of the promising signal processing algorithms are utilised. The first algorithm in this research is named the discrete wavelet transform, and the results of detecting these disturbances, with their features, are presented and discussed. Thereafter, the new algorithm is proposed, named complementary empirical model decomposition, and it is implemented to detect disturbances. The results of its features are then presented, analysed and discussed. For the results of each approach, a classifier technique is built, which is also trained and tested. Finally, the accuracy of each detection algorithm is calculated for each disturbance, for single or multiple cases, and for overall accuracy. Moreover, a comparison analysis for both algorithms is studied and analysed based on the obtained results and overall accuracy. All the experiments and simulations of this thesis are performed using MATLAB 2014b and 2016b versions, on a PC with 3.70 GHz, Intel CORE i7 and 16.0 GB RAM and 64 bit operating system, using Microsoft Windows 7 operating system. MATLAB has plenty of tools such as ANN, WT, and EEMD which can be used in assessing the power quality.

## 4.2 Wavelet Transform

### 4.2.1 Introduction

Wavelet Transform (WT) is a powerful signal processing algorithm, and a popular mathematical tool used in power engineering applications [111]. The word "wavelet" means a small wave representation with oscillations. The main difference between WT and FT is that WT can localise signals in the time and frequency domain simultaneously, with the ability to automatically adjust window widths based on its frequency. Figure 4-1 shows the principle dynamics of wavelet representation, where the signal (a) is a pure sinusoidal wave, (b) is the Gauss function and the summation is the wavelet signal in (c) [112].

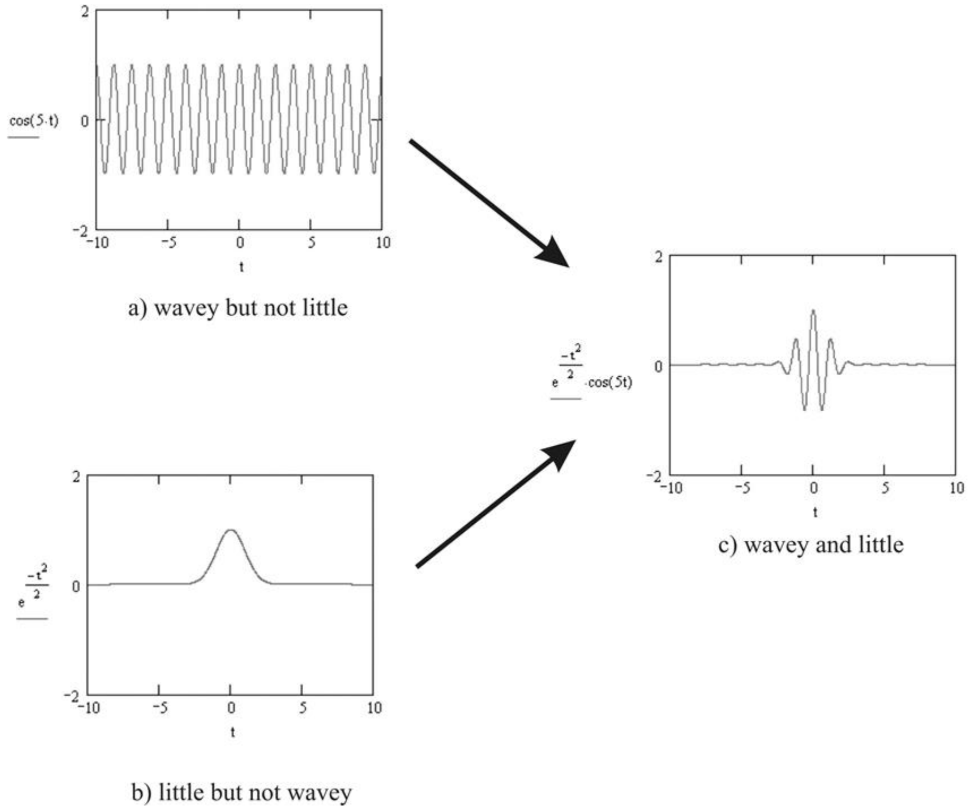


**Figure 4-1 The basic principle of wavelet** [112]

The WT algorithm is able to decompose signal data into various components with different frequency bands. WT was proposed by Morlet for use in image processing in 1982 [112]. It was then developed mathematically by many researchers such as Meyer and Daubechies. It was used to smoothly analyse distorted signals [113]. With these characteristics, it has been broadly implemented in many studies, such as those pertaining to data compression and computing, and provides solutions for complex differential equations

[114]. However, professionally, WT was initially used in power systems to measure power quantities and provide robust assessments, as conducted in [115].

WT is considered a time-frequency algorithm, as it is able to evaluate signals in the time and frequency domains, which is promoted with limited energy to each group of these small waves and zero average [116].

$$\int_{-\infty}^{+\infty} \psi(t)dt = 0 \tag{4.1}$$

where functions are normalised by knowing that $||\psi|| = 1$ concentrated in the neighbourhood of $t = 0$. Such an equivalent represents the same representations of the sine and cosine roles in Fourier transform. At the beginning, a certain wavelet type is chosen from the base of wavelets, which is known as the mother of wavelet. Thereafter, expanded and converted forms of the mother wavelet are generated where the scale parameter is named ($a$) and the time form is named ($b$), as in [111].

$$\psi_{a,b}(t) = \frac{1}{\sqrt{a}} \psi \left(\frac{t-b}{a}\right) \tag{4.2}$$

where both $a$ and $b$ are positive and real numbers. The wavelet equivalent of the signal f (t) at (a) and (b) is the dot multiplication output of the signal f (t), and the specific choice of mother wavelet $\psi_{a,b}(t)$. Therefore, the relationship between the signal and the wavelet function can be expressed by Equation 4.3:

$$W\{f(a,b)\} = \langle f, \psi_{a,b} \rangle = \int_{-\infty}^{+\infty} f(t) \cdot \frac{1}{\sqrt{a}} \psi^* \left(\frac{t-b}{a}\right) dt \tag{4.3}$$

The selected version for the mother of wavelet is attached to high frequency and used time analysis, and a detailed version is attached to lower frequency and used in frequency analysis.

In wavelet function, information of scale $a < 1$, which is attached to high frequencies, is achievable. But to determine information of the scale $a > 1$, which is attached to low frequencies, and to complete the representation of the original signal, it is important to introduce another scaling factor named $\phi(t)$, which considers the aggregation of the mother wavelet $\psi(t)$ for scales of $a > 1$. The scaling function $\phi(t)$ will take the translated formula as in Equation 4.4:

$$\phi_{a,b}(t) = \frac{1}{\sqrt{a}} \phi \left(\frac{t-b}{a}\right) \quad (4.4)$$

The scaling function is introduced – the lower frequency components of *f(t)* at the scale (a) are clearly the dot product for the signal and its specific scaling function; therefore, it can be computed with the convolution Equation 4.5:

$$\mathcal{L}\{f(a,b)\} = \langle f, \phi_{a,b} \rangle = \int_{-\infty}^{+\infty} f(t) \cdot \frac{1}{\sqrt{a}} \phi^{*} \left(\frac{t-b}{a}\right) dt \quad (4.5)$$

Implementing Equations 4.3 and 4.5 can be achieved easily in wavelet transform derivatives either with Continuous Wavelet Transform (CWT) or Discrete Wavelet Transform (DWT). One of the important attributes of WT is that its non-uniform time and frequency spreads through the frequency plane. To explain this, it is possible to compare the way that both the derivatives of Fourier and wavelet can handle the signal with the scale (a), as presented in Figure 4-2 for Short-Time Fourier Transform (STFT) and discrete wavelet transform (DWT). With STFT, the relationship between time and frequency in terms of resolutions (Δt and Δf) is constant by the fixed square measures. However, the resolution's relationship with DWT varies through both execs. The variation is gentle at a lower frequency, where the time resolution is rough, while the frequency resolution is fine.

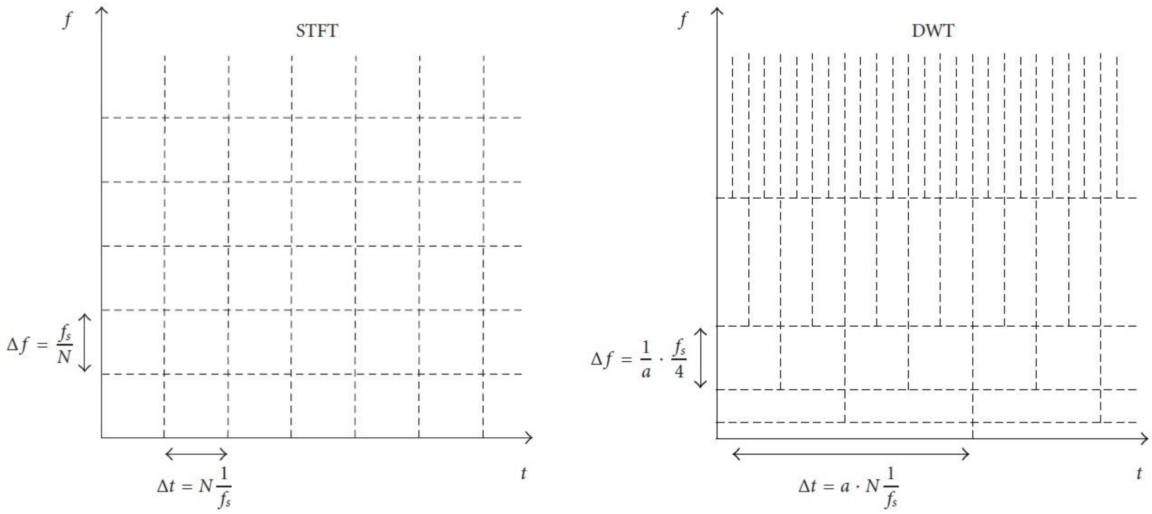


**Figure 4-2 Time and frequency resolutions for STFT and DWT**, **where *fs* is the sampling frequency and N is the number of sample points per window** [116]

DWT enables precise tracking of the frequency, along with allowing satisfactory time for the slow parts to be known before analysis. Moreover, the higher frequency range is extracted when fast variations occur. The time resolution is then small, but the frequency resolution will compromise that.

### 4.2.2 Discrete Wavelet Transform

As wavelet transform is described earlier regarding its ability in being effective in analysing signals in the time-frequency domain [117], it is also important to investigate its performance with transient signals. Several attempts to implement wavelet transform for the detection and identification of power quality disturbances indicate its performance as an appropriate algorithm to handle non-stationary signals, as earlier studied in [30], [118]. These studies were for three single disturbances, sag, swell and transient only, or according to line faults for five cases without any classification techniques or taking into account multiple events.

In this research, DWT is chosen to detect and analyse PQDs, where it uses the wavelet function $\psi$ and scaling function $\phi$ to promote multiresolution analysis and reconstruct signals at the same time. The procedure in this stage begins mathematically, as in [33], [54], which are based on Multiresolution Analysis (MRA) as follows:

$$f(x) = \sum_{ij} a_{i,j}\psi_{i,j}(x) \tag{4.6}$$

where *i* and *j* characterise the integer values, $\psi_{i,j}(x)$ is the wavelet expansion function and $a_{ij}$ stands for the two coefficients of DWT for the signal $f(x)$. These coefficients have the formula:

$$a_{i,j} = \int_{-\infty}^{+\infty} f(x)\psi_{i,j}(x) \tag{4.7}$$

where $\psi_{i,j}(x)$ is the mother of wavelet and can achieve its scaling parameters through Equation 4.8:

$$\psi_{i,j}(x) = 2^{-i/2}\psi(2^{-j}x - j) \tag{4.8}$$

where $i$ represents the scaling parameter and j the translation parameter. For multiresolution condition fulfilment, the two-scale differential equation is given as:

$$\phi(x) = \sqrt{2}\sum_{k} h(k)\phi(2x - k) \tag{4.9}$$

where $h(k)$ must give a unique and orthogonal value to satisfy wavelet conditions. Thereafter, the scaling function $\phi$(x) is related to the mother of wavelet $\psi_{i,j}(x)$ by Equation 4.10:

$$\psi(x) = \sqrt{2}\sum_{k} g(k)\phi(2x - k) \tag{4.10}$$

where $h$ in Equation 4.9 and $g$ in Equation 4.10 are considered the filter coefficients of half band, as the low pass filter and high pass filter, respectively. From all the above equations, the wavelet decomposition in DWT of J-level can be determined, as in Equation 4.11:

$$f_0(x) = \sum_{k} a_{0,k}\phi_{0,k}(k) = \sum_{k} a_{J+1,k}\phi_{J+1,k}(x) + \sum_{j=0}^{J} d_{j+1,k}\psi_{j+1,k}(x) \tag{4.11}$$

where $a_{0,k}$, $a_{J+1,k}$, $d_{j+1,k}$ are the coefficients at scale *j+1* and can be determined under the condition of the availability of scale *j*, as in Equations 4.12 and 4.13:

$$a_{j+1,n} = \sum_{k} a_{j,k}h(k - 2n) \tag{4.12}$$

$$d_{j+1,n} = \sum_{k} a_{j,k}g(k - 2n) \tag{4.13}$$

where $a_{j+1,n}$ is the set of approximation coefficients and $d_{j+1,n}$ the detailed coefficients at scale *j+1*.

Feature extraction is the internal process for transforming the original distorted signal into the DWT domain before collecting and building the database, which can be used as an input to any classification system technique. DWT coefficients are achieved with the assistance of multiresolution analysis for power quality disturbances. Since PQDs are non-stationary signals, each distorted signal has a unique frequency component and, consequently, a unique energy distribution.

Figure 4-3 shows the MRA of the four-level decomposition process for each selected signal [54]. The parameter (a4) is the approximation level, and considered the parameter with the lowest frequency band. On the other hand, approximation levels from (d1) to (d4) are high frequency bands. Each one of these bands is examined separately and, thereafter, they can be reconstructed in a new signal.

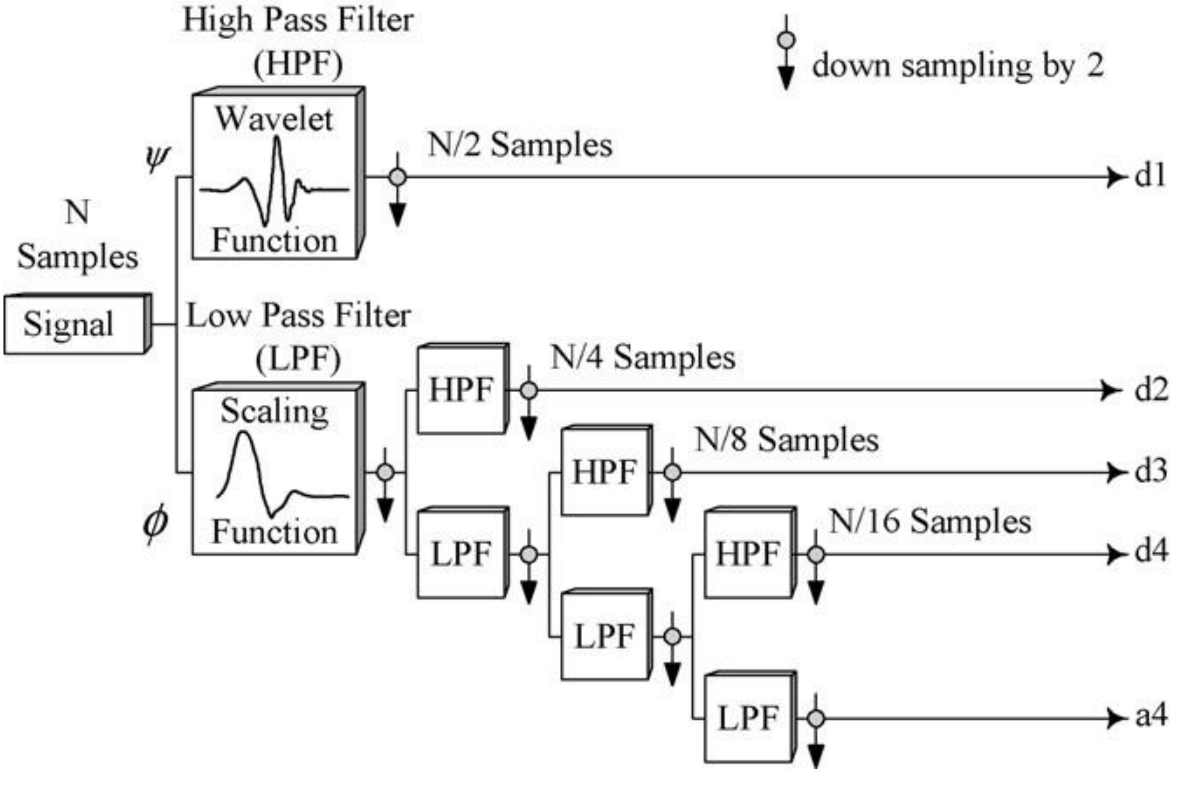


**Figure 4-3 Typical example of the four-level decomposition process for a signal based on DWT** [54]

## 4.3 Hilbert-Huang Transform

Hilbert-Huang Transform (HHT) is a very recent algorithm and an effective signal processing algorithm in time-frequency analysis. HHT promotes the detection and analysis of non-stationary and non-linear signals. It contains a powerful feature extraction process named Empirical Mode Decomposition (EMD), combined with Hilbert Spectral Analysis (HSA). The HHT algorithm decomposes the signal using the EMD process and HSA into intrinsic mode functions (IMFs), where each of these IMFs has its own instantaneous amplitude and instantaneous frequency, as described and explained in [45] and [47].

### 4.3.1 Empirical Mode Decomposition

Empirical mode decomposition is a process which has the ability to decompose non-stationary signals in a time series into a group of sub-signals, where each one of these sub-signals has a unique frequency. The EMD processes the distorted signal and decomposes it into an IMF for each sub-signal. Furthermore, each IMF has a specific order, where the first IMF goes to the highest frequency content of the extracted signal, and the lower IMF belongs to the lowest frequency content [119].

The starting point in the decomposition process for the distorted signal is to find the cubic spline lines by searching all extreme points of the disturbance separately, as an upper envelope and lower envelope. These two envelopes are derived from the original disturbance to produce a resultant signal, which will be subtracted into IMFs according to its frequency. By repeating this process *n* times, the original signal is decomposed into *n* empirical modes. The sum of IMFs is equivalent to the original disturbance signal, as mathematically expressed in [120], which can be characterised as:

$$x\,(t\,) = \sum_{j=1}^{n} C_i + r_n \tag{4.14}$$

where *cj* represents IMFs from *j* = 1 to *n*. Thereafter, HHT begins with a significant step, by transforming the disturbance signal from a real signal to an analytical signal as:

$$y\,(t\,) = \int_{-\infty}^{\infty} \frac{x\,(t\,)}{t-\tau}\, dt \tag{4.15}$$

where $y(t)$ is the convolution of *x(t)* in with *1/t*. then, the analytical signal can be achieved from the HHT analytical signal as:

$$z(t) = x(t) + iy(t) = a(t)e^{i\theta(t)} \tag{4.16}$$

where *a(t)* represents the instantaneous amplitude and *θ(t)* represents the instantaneous phase, and they are specified as:

$$a(t) = \sqrt{x^2(t) + y^2(t)} \tag{4.17}$$

$$\theta(t) = arctan\,(y(t)/x(t)) \tag{4.18}$$

then, after, the frequency IF named $\omega(t)$ is given by:

$$\omega(t) = \frac{d\theta(t)}{dt} \tag{4.19}$$

As a result, components of time dependent on amplitude and frequency are extracted for each IMF in HHT. But when it comes to the time-frequency domain, the amplitude can be expressed as in Equation 4.20:

$$H(\omega, t\,) = real\ value \sum_{i=1}^{n} a(t)e^{i\theta(t)} \tag{4.20}$$

Finally, the signal marginal spectrum delivers the value of the total amplitude calculated from each frequency and time. This marginal spectrum is defined in Equation 4.21:

$$h\ (\omega, t\,) = \int_0^{\mathrm{T}} H(\omega, t\,)dt \tag{4.21}$$

where *T* is the signal information length, which is obtained by extracting the vectors of the instantaneous amplitude and the instantaneous frequency of each IMF. Each instantaneous amplitude result provides the magnitude of the signal at a specific frequency with time variation from 0 to N–1 samples. Feature extraction involves all the information determined from instantaneous amplitude, the instantaneous phase and instantaneous frequency.

### 4.3.2 Ensemble Empirical Mode Decomposition

One of the main developments in Hilbert transform is Ensemble Empirical Mode Decomposition (EEMD), as proposed by Wu and Huang [121]. In this proposal, the intrinsic local oscillations have a natural filter band, which has been fitted adaptively for EMD with white noise, which is the random signal having deferent frequencies with equal intensity [122]. The result is a decrease in white noises and the rule will be:

$$\varepsilon_n = \frac{\varepsilon}{\sqrt{N}} \tag{4.22}$$

where $N$ represents the trials implemented to gain the ensample IMFs, $\varepsilon_n$ is the standard deviation of error and $\varepsilon$ is the amplitude root mean square (RMS) of noises added.

### 4.3.3 Complementary Ensemble Empirical Mode Decomposition

Complementary Ensemble Empirical Mode Decomposition (CEEMD) is the new approach in Hilbert transform, which has never been involved in detecting power quality disturbances. In this approach, white noise is added to the original distorted signal in pairs to generate double sets of IMFs, one on the positive side and the other one on the negative side. Thus, the two combinations composed of original signal data with the added noise will be:

$$\begin{bmatrix} M_1 \\ M_2 \end{bmatrix} = \begin{bmatrix} 1 & 1 \\ 1 & -1 \end{bmatrix} \begin{bmatrix} S \\ N \end{bmatrix} \tag{4.22}$$

where $S$ is representing the original data of the signal, $N$ is the added white noise in the signal, $M_1$ is the summation of the original data with positive noise in the signal, and $M_2$ is the total sum of the original data in the signal with the negative noise.

Additionally, Figure 4-4 shows the original signal with its intermittent sections. The sinusoidal waveform and the intermittent instability of the simulated signals can be seen from Figure 4-5, It is found that many components of the first IMF were changed by the intermittent signal.

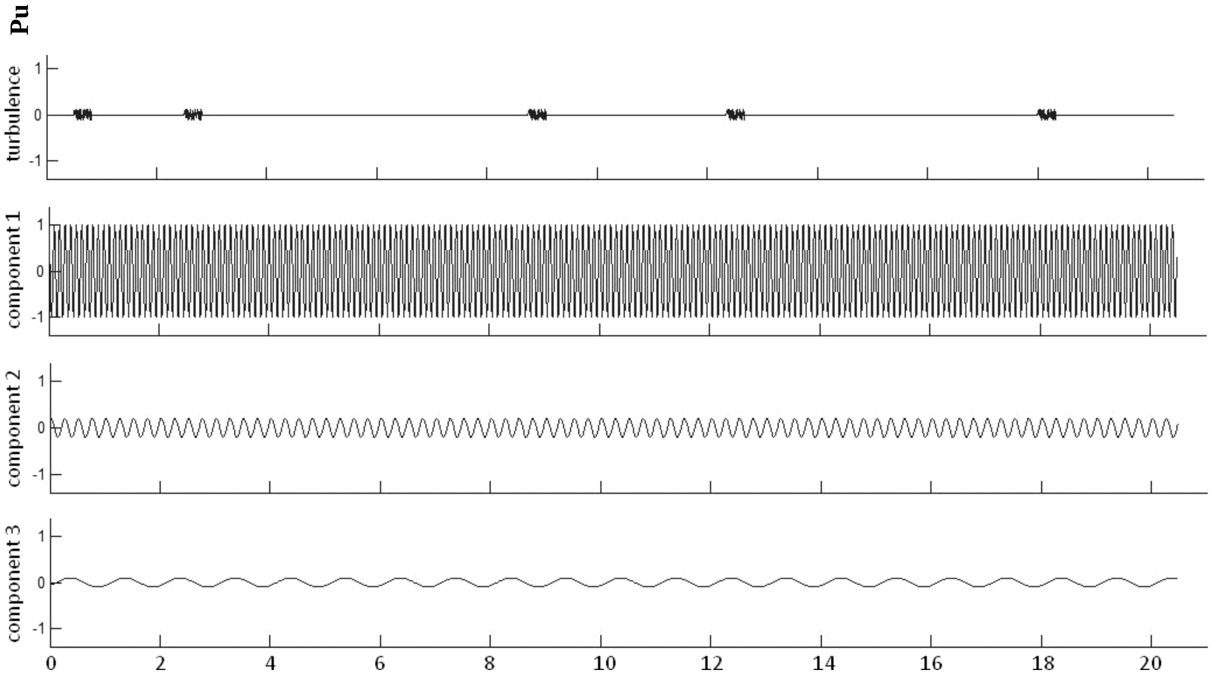


**Figure 4-4 The simulated signal with decomposed components by EMD [123]**

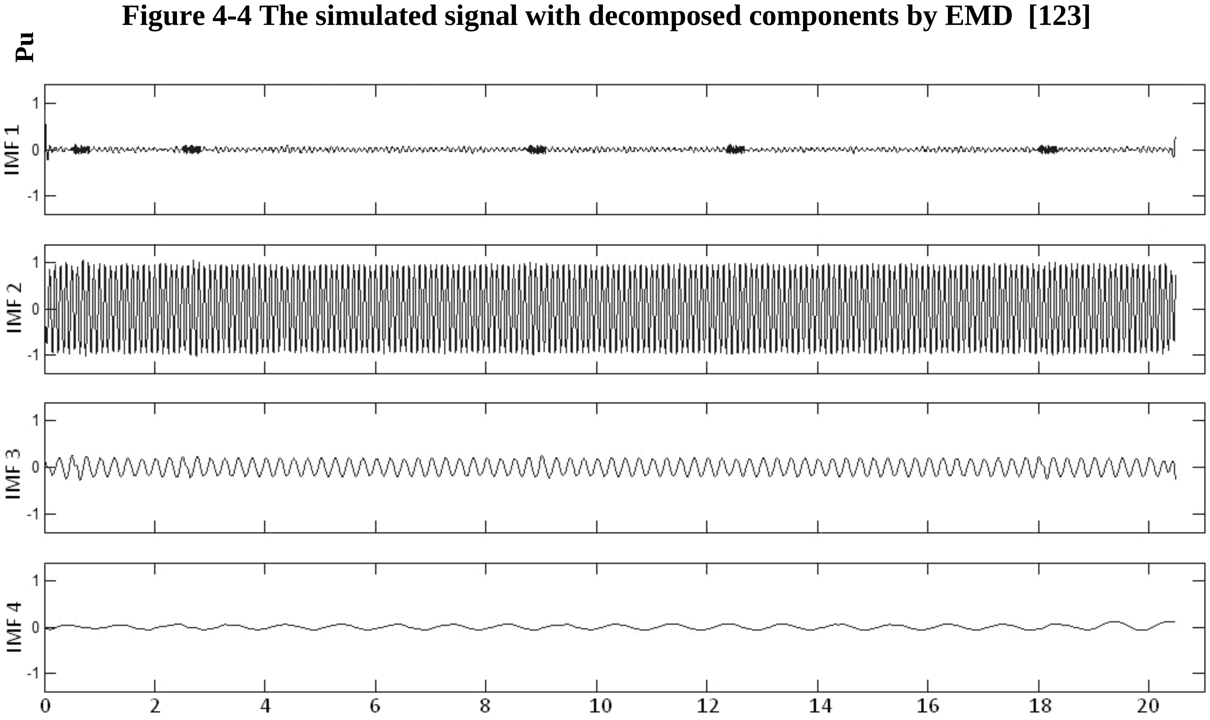


**Figure 4-5 The signal and the decomposed IMFs by EEMD [123]**

The IMFs achieved by the EEMD process from positive combinations which participate to a set of IMFs with positive residues of inserted white noises and likewise with The IMFs achieved by the EEMD process from negative combinations. Figure 4-6 shows IMFs achieved from the signal decomposed using 20 pairs of inserted white noises to the signal by the CEEMD process which similar to those IMFs made by EEMD. A comparison of the IMFs of the signals results from EEMD and CEEMD shows no obvious difference.

Nevertheless, there is an obvious difference between the reconstructed signals through the IMFs and the original signal as it can be seen from Figure 4-7.

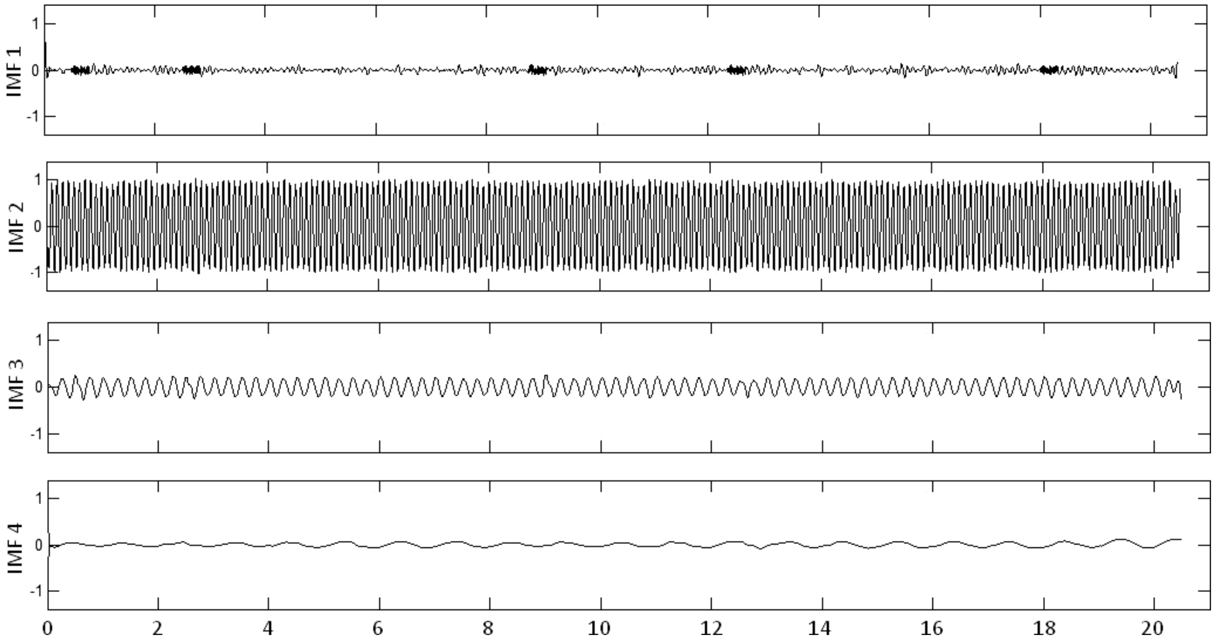


**Figure 4-6 The signal with the decomposed IMFs using CEEMD [123]**

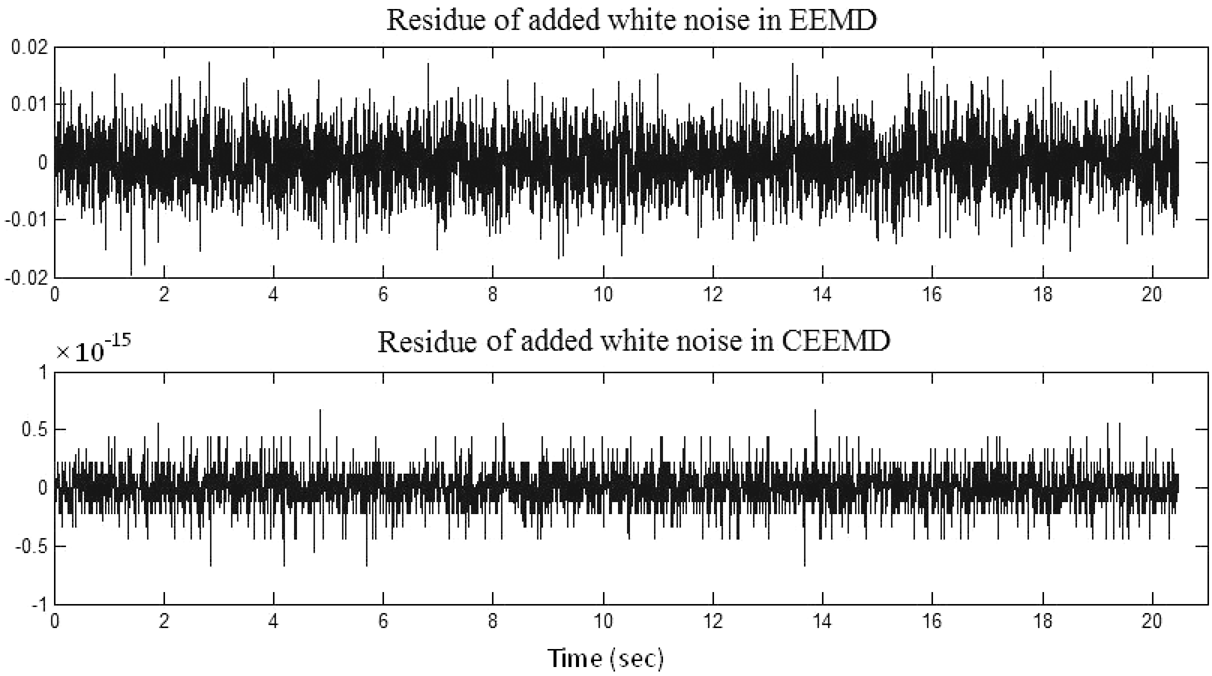


**Figure 4-7 Residues of inserted white noises resulting by EEMD and CEEMD processes [123]**

The advantage of CEEMD is simply saving the computational time to reconstruct a distorted signal, due to its ability to pair noises, successfully decreasing the final white noise residue. Thus, CEEMD is able to improve the process results of decomposition by removing the residue of the inserted white noise which enhances low frequency components [123].

## 4.4 Classification Technique Using Artificial Neural Networks

### 4.4.1 Introduction

Artificial Intelligence (AI) is a term that indicates the ability of a machine to perform functions similar to human thinking, and also refers to computer programmes capable of executing complex tasks. AI can be categorised into two main branches: expert systems and artificial neural networks. Expert systems are allowed to make decisions based on interpreting roles and selecting a rule or a process among choices, which is known as a logic programme, which has a technique called rule-based inference.

An Artificial Neural Network (ANN) is one of the broadly accepted techniques which offer an alternative means to solve complex and challenging problems. ANN can learn from samples and is able to handle a noisy environment. It can process incomplete data and non-linear problems, as with most of the cases in power systems. The training stage can achieve prediction and estimation. Particularly in system modelling, ANN is useful in realising complex mappings and parameter identification.

ANN is a platform of individual processing units. Signal representation or formulas are passed to these units as inputs. Each one of these inputs has two characters: an input value and a weight. Thereafter, they are then trained until they learn the patterns of these inputs with regard to data sets. After that, new patterns are then constructed for the classification stage [124]. The ANN process construction obtained its performance through interconnected processing units called neurons, which are implemented successfully in many applications such as medical science, the automotive industry and electrical power systems [125].

ANN consists of various nodes which are connected together using layers. The connections between these nodes are named neurons, which have weights that play a role in reaching desired targets. ANN is an efficient mathematical technique for the detection, identification and control of complicated processes, due to its non-linear mapping mechanism. The main benefits of employing ANN relate to three factors. First, it can handle random fluctuations operating points through the increase of data. Secondly, ANN accelerates significantly with robust performance in both classification and online processing.

Thirdly, it assists with its non-linear modelling to build functions needed for filtering the system's data [126]. Moreover, other AI techniques such as fuzzy logic systems, expert systems and optimisation techniques can be used in combination with ANN to construct a hybrid intelligent system for the goal of achieving the targeted results.

### 4.4.2 Biological and Artificial Neurons

As the base of processing unit is named 'neuron', it is important to know its background where it refers to the human nervous system [127]. Figure 4-8 shows the main components of the human nervous system, where information signals flow from the left side to the right though neurons. Signal information is transported from the axon to the dendrite, where the synapse is the connector. Such a process in the human brain consists of 10 to 500 billion neurons, the estimated number of processing units [128]. ANNs have gained their concept from the biological neuron.

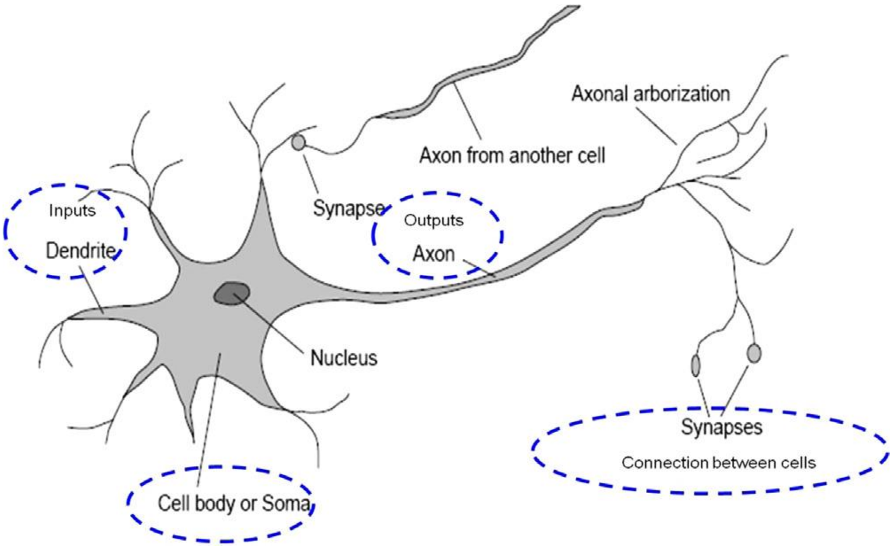


**Figure 4-8 Biological structure of the human neuron [21]**

### 4.4.3 Structure of Artificial Neural Networks

Several publications have described the mechanism of processing information using ANN, as in [129], [130]. Neurons, as the input elements, pass through a series of connectors. Each one of these connections is then associated with weights. These weights represent the magnitude of the connection and the strength. Within the neuron is a non-linear transformation function which is normally called the activation function. This activation function is applied to input neurons to produce output signals. However, neurons are organised into a series of layers, as can be seen from Figure 4-9.

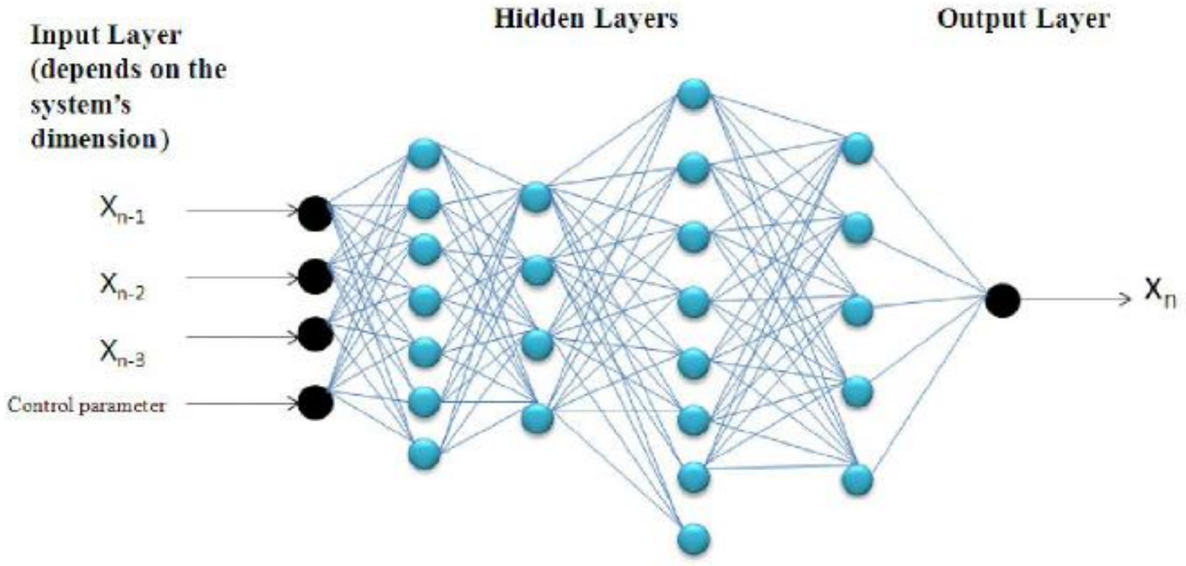


**Figure 4-9 Typical example of Artificial Neural Networks** [131]

An ANN consists of input layers, hidden layers and output layers, with complex connections called neurons. Neurons in ANN system are connected by weights and the learning algorithm, which updates the relation between these weights in the network, as seen in Figure 4-10.

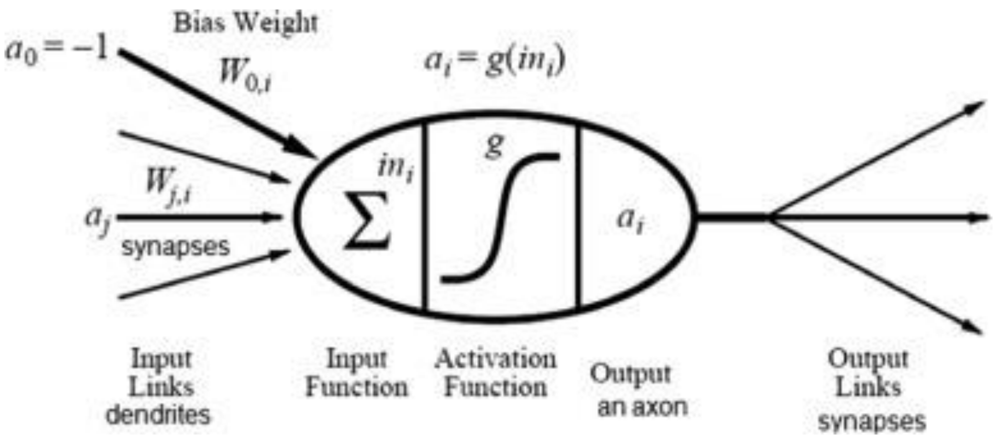


**Figure 4-10 Typical architecture of a neuron** [132]

First, weighted inputs are processed and proceeded to the activation function, which generates outputs. Thereafter, weights and biases are tuned to reduce the error between the generated outputs produced by the activation function and the desired outputs in the network. In this procedure, the output can be defined mathematically as:

$$A_i = g(\sum_{i=0}^{n} W_{ji} * a_j) \tag{4.23}$$

where the output of the network is *Ai*, *Wji* is the network which is connected to a *Jth* neuron, *Ith* is the neuron layers, *aj* is the neuron's inputs, which might involve a single input or many inputs. There are two main procedures in ANNs, and they are named training and testing.

The training stage is the learning part to precisely map the relationship between inputs and outputs. The testing stage investigates and recognises the taught inputs pattern precisely when it generates outputs. Furthermore, if any output in the network does not match the desired one or does not belong to the taught inputs, then the network repeats the training process to address the error in its next run. Such process is continuing until a certain desired value is achieved.

### 4.4.4 Activation Function

The activation function plays an important role in the neural network, where it squeezes the process of weighted inputs to generate outputs. Activation functions come in many shapes or types, such as linear, step, logistic and sigmoid functions, and consequently they vary based on the design of the neural network and nature of the problem. In studies, it is mentioned that the type of activation function might affect the resulting outputs [133]. The activation function also has two stages, which are named the linear combination and transfer function, where the latter transforms the weighted inputs into target units. Transfer functions are selected based on the nature of the problem, as in [134].

### 4.4.5 Types of Artificial Neural Networks

ANN is divided into two main categories, which are feed forward neural networks and recurrent neural networks. In the former type, inputs and connections are propagated, where the information moves from inputs to outputs through planned layers without loops. In the latter type, the network has loops in its processes.

#### 4.4.5.1 Feed Forward Neural Network

Feed Forward Neural Network (FFNN) is a powerful technique with two divisions: single or multi-layer networks between inputs and outputs. In the signal layer division, the connections between inputs and outputs are based on their weights. The sum of the inputs and weights is calculated and applied to the activation function. The resulting function then generates an output that equals either +1 or -1, depending on the input value and if it is less or greater than the threshold value. This procedure is more complex when the multi-layer type is employed, which consists of input layers, output layers and hidden layers, as shown in Figure 4-11 [135]. Information passes from inputs to outputs through hidden layers in a forward direction only. The merit for FFNN is that there is no process impact between hidden layers, where there is no interaction and no loop cycle in this process.

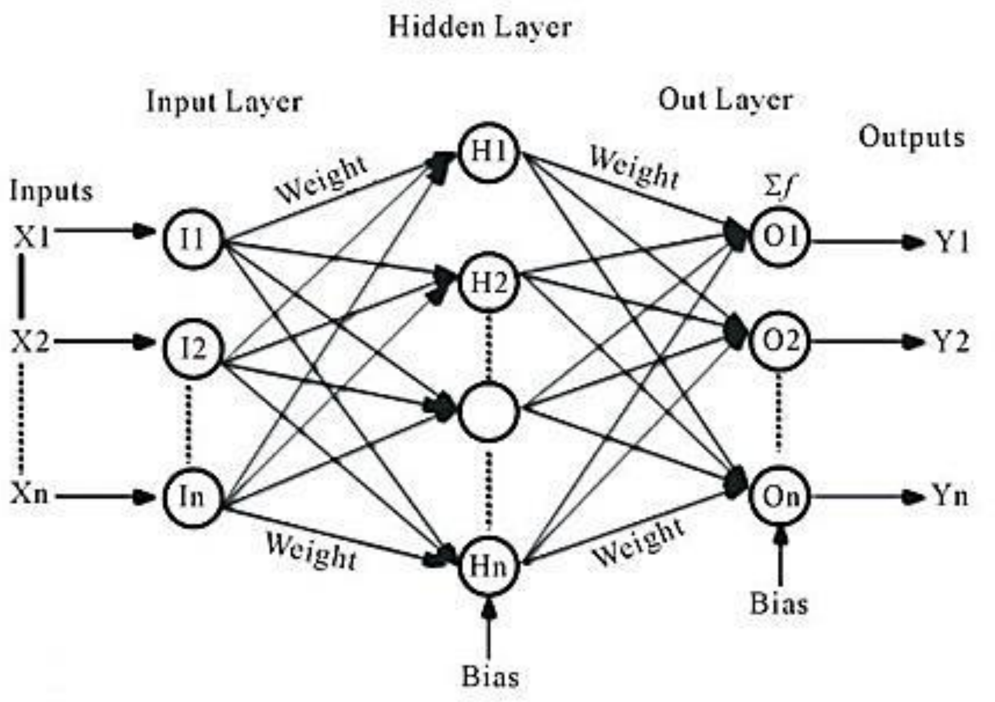


**Figure 4-11 The scheme of feed forward neural networks** [135]

The mathematical equation in FFNN describing each neuron in each layer, as in [136], is given by:

$$y = f(\sum_{i=0}^{I} \omega_i \chi_i + b) \tag{4.24}$$

where $y$ is the output, $\omega_i$ the weights, $\chi_i$ represents inputs, $b$ bias in the network, $f$ represents the activation function, and finally $I$ is the total number of inputs. This equation involves the summation of the multiplying the inputs with the weights of each input in the network, plus a bias.

#### 4.4.5.2 Recurrent Neural Networks

Recurrent Neural Network (RNN) is a technique with linear and non-linear options in terms of the dynamics process. The procedure of RNN is based on a feedback routine from outputs to inputs, as shown in Figure 4-12. Outputs in RNN are functions of time, due to its role when each one of them is rerouted to its particular input. This difference in RNN from the previous technique allows the information to pass in closed loop architecture. Therefore, it is certain that the inputs network is influenced by the outputs network in obtaining the objective function, using back-propagation for the error information. Moreover, RNN has continuous changing dynamic in its nature to accomplish equilibrium. As these changes happen, the network compromises the new state of equilibrium. This type of technique is suitable for time-lagged pattern problems [137].

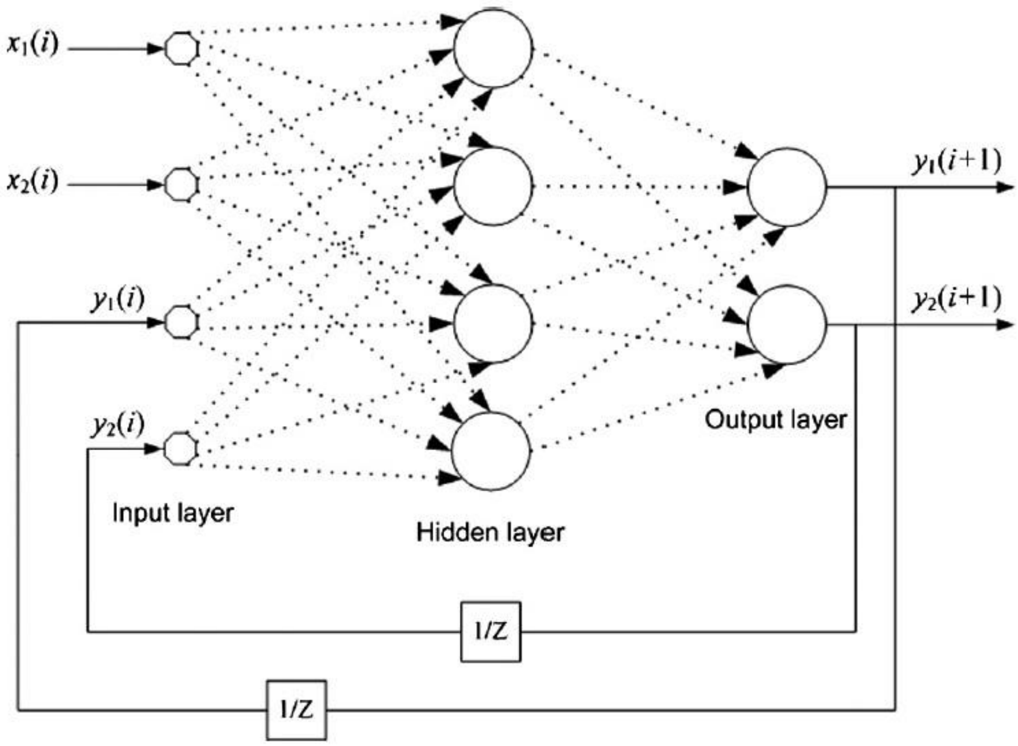


**Figure 4-12 Typical recurrent neural network structure** [138]

### 4.4.6 Learning Methods of Artificial Neural Networks

The main concept in devolving ANN classifier is finding the suitable organisation of learning method to solve and handle classification data in the process. The developed ANN classifier in this study is based on back propagation learning method. Hence, the transfer function of this method is selected to be 'tansig' the hyperbolic tangent which represent the most common transfer function in the classification research.

$$tanh(x) = \frac{2}{1 - e^{-2x}} + 1 \tag{4.25}$$

Nevertheless, learning methods in ANNs are divided into three categories: supervised, unsupervised and reinforced learning.

#### 4.4.6.1 Supervised Learning

Supervised learning depends on an external supervisor to train the network. Furthermore, ANN in supervised learning is training, and expected to gain the desired objectives that are matched and chosen to input motivation. This process has the goal of comparing the resulting outputs to outputs desired, in order to define and calculate the resulting errors. The next stage in this process is using errors found to correct the network's performance by changing and optimising the network's parameters. Supervised learning is also divided into two methods. Firstly, the gradient descent system, which is based on error minimisation using weights of the network and the activation function. The second method is named back-propagation, which offers a simplification of the delta rule. The requirement for this subtype is setting a database with multiple inputs and desired outputs. This method is appropriate when it is utilised for feed forward neural networks [138].

#### 4.4.6.2 Unsupervised Learning

In unsupervised learning method, the process has no specific response plan, with no external supervisor in the network. This method functions based on the principle of self-organising where the network adopts structure features, and as a result the response is based on input patterns [138].

#### 4.4.6.3 Reinforcement Learning

A reinforcement learning method depends on the information provided in building inputs for the network. In this method, the process lacks access to the desired outputs, but it is assisted by the reception stage of reinforcement signals selected for either a true or false choice. Any one of these two choices helps the system to take action, and eventually the outputs are selected based on trial and error, from previous experiences [138].

## 4.5 Experimental Results

### 4.5.1 Detection and Features Extraction Based on the DWT Algorithm

In this stage, a characterisation of a pure sine wave among nine power quality disturbances is conducted. These disturbances are sag, swell, harmonics, interruption, flicker, high frequency transient, low frequency transient, sag with harmonics and swell with harmonics, with precise characterisation and its parameters for each signal, according to the recognised standard IEEE 1159 which is one of the well-known benchmarks in scientific and engineering committees [86]. The strategy used to achieve targets in this research is shown in Figure 4-13.

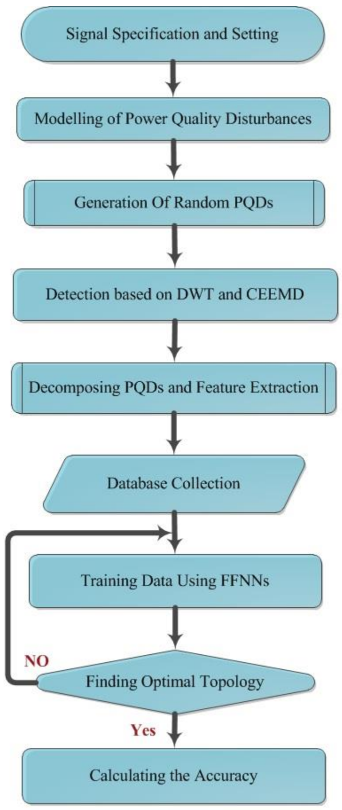


**Figure 4-13 Flowchart of the detection algorithm and classification technique**

To achieve this, it is necessary to design the signal specifications as: Ts (time period) = 0.5 seconds, and f (frequency) = 50 Hz. Modelling of PQDs is generated according to their parametric equations, explained in Chapter 3 and summarised in .

Table 4-1.

**Table 4-1 Signal modelling of power quality disturbances**

| PQ Disturbance | Class Symbol | Mathematical Models | Parameters |
|---|---|---|---|
| **Pure Sine** | C 01 | $f(t) = A\sin(\omega t)$ | $A$=1.0 $f$=50 Hz, $\omega = 2\pi 50$ rad/sec |
| **Sag** | C 02 | $f(t) = A(1-\alpha(u(t-t_1)-u(t-t_2)))\sin(\omega t)$ | $0.1 < \alpha < 0.9$ , $T \leq t2 - t1 \leq 9T$ |
| **Swell** | C 03 | $f(t) = A(1+\alpha(u(t-t_1)-u(t-t_2)))\sin(\omega t)$ | $0.1 < \alpha < 0.8$ , $T \leq t2 - t1 \leq 9T$ |
| **Harmonics** | C 04 | $f(t) = A(\alpha_1\sin(\omega t) + \alpha_3\sin(3\omega t) + \alpha_5\sin(5\omega t)$ | $0.05 \leq \alpha_3, \alpha_5, \alpha_7 \leq 0.15$, $\sum \alpha_i{}^2 = 1$ |
| **Interruption** | C 05 | $f(t) = A(1-\alpha(u(t-t_1)-u(t-t_2)))\sin(\omega t)$ | $0.9 < \alpha < 1.0$ , $T \leq t2 - t1 \leq 9T$ |
| **Flicker** | C 06 | $f(t) = A + \alpha\, f \sin(\omega t)\,(1+\beta\sin(\gamma\omega t))$ | $0.1 < \alpha_f < 0.2$ $0.1 \leq \beta \leq 0.2$ , $0.1 \leq \gamma \leq 0.2$ |
| **High Frequency Transient** | C 07 | $f(t) = A\,(\sin(\omega t) + \alpha e^{-t/\lambda}\sin(b\omega t))$ | $20 \leq b \leq 80$ , $0.1 \leq \lambda \leq 0.2$ , $0.1 \leq \alpha \leq 0.9$ , $T \leq t2 - t1 \leq 3T$, $1500\,Hz < f_n < 2000\,Hz$ |
| **Low Frequency Transient** | C 08 | $f(t) = A\sin(\omega t) + \alpha e^{-t/\lambda}\sin(b\omega t))$ | $5 \leq b \leq 20$ , $0.1 \leq \lambda \leq 0.2$ , $0.1 \leq \alpha \leq 0.9$ , $T \leq t2 - t1 \leq 9T$ , $300\,Hz < f_n < 1000\,Hz$ |
| **Sag with Harmonics** | C 09 | $f(t) = A(1-\alpha(u(t-t_1)-u(t-t_2)))$ $(\sin(\omega t) + \alpha_3\sin(3\omega t) + \alpha_5\sin(5\omega t)))$ | $0.1 < \alpha < 0.9$ , $0.05 < \alpha_3 < 0.15$ , $0.05 < \alpha_5 < 0.15$ , $T \leq t2 - t1 \leq 9T$ , $\sum \alpha_i{}^2 = 1$ |
| **Swell with Harmonics** | C 10 | $f(t) = A(1+\alpha(u(t-t_1)-u(t-t_2)))$ $(\sin(\omega t) + \alpha_3\sin(3\omega t) + \alpha_5\sin(5\omega t)))$ | $0.1 < \alpha < 0.8$ , $0.05 < \alpha_3 < 0.15$ , $0.05 < \alpha_5 < 0.15$ , $T \leq t2 - t1 \leq 9T$ , $\sum \alpha_i{}^2 = 1$ |

In this research, a collection of the most common power quality disturbances is generated and detected based on DWT. The results of this stage are shown in Figure 4-14.

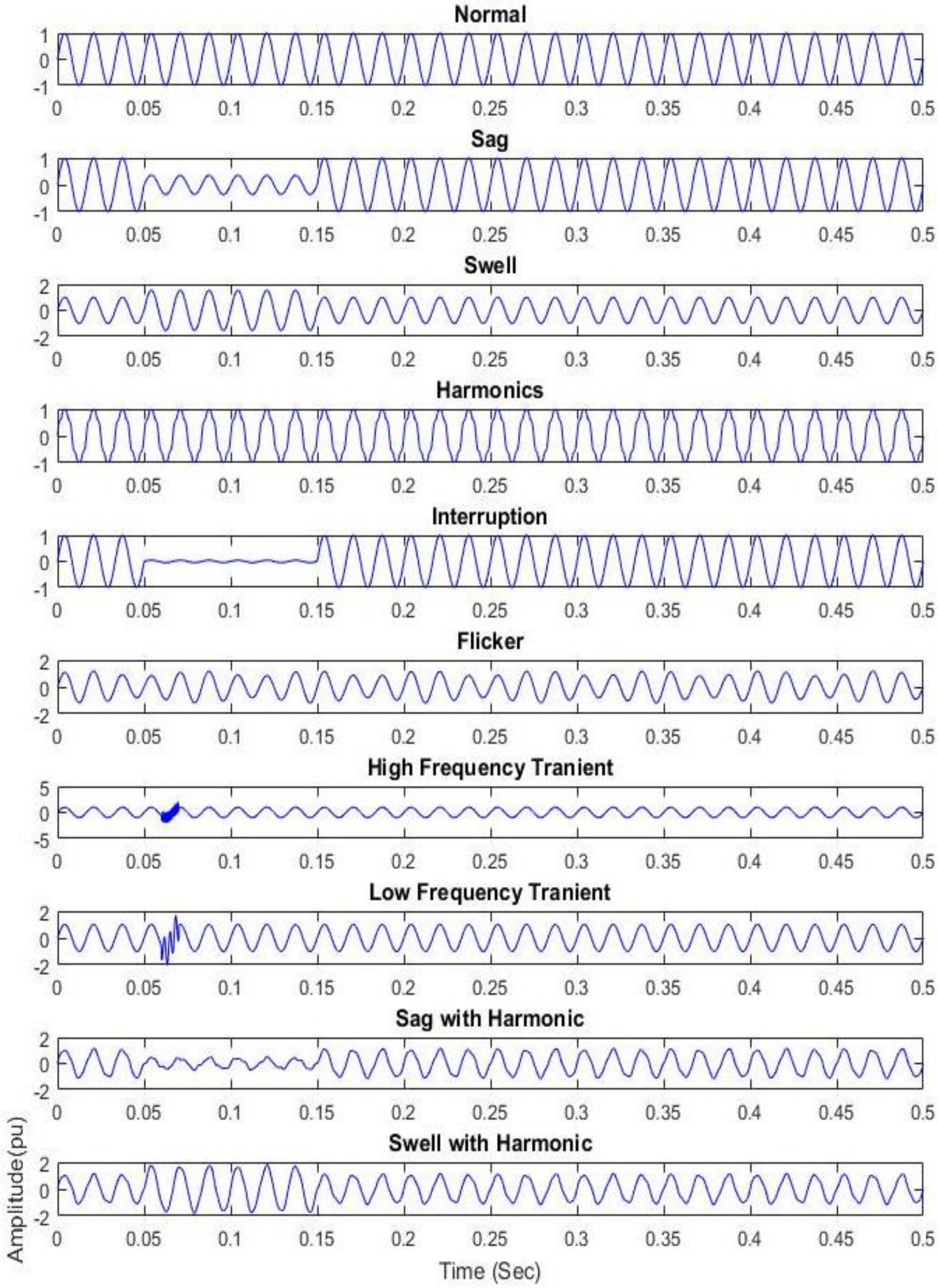


**Figure 4-14 Different PQDs signals**

The goal of decomposition and extraction for each power quality disturbance is to transform the original distorted signal from its time domain into its energy form. In this study, each PQD generated is decomposed into 8 levels using the DWT filter (db8), and the results for selected PQDs are shown from Figure 4-15 to Figure 4-20.

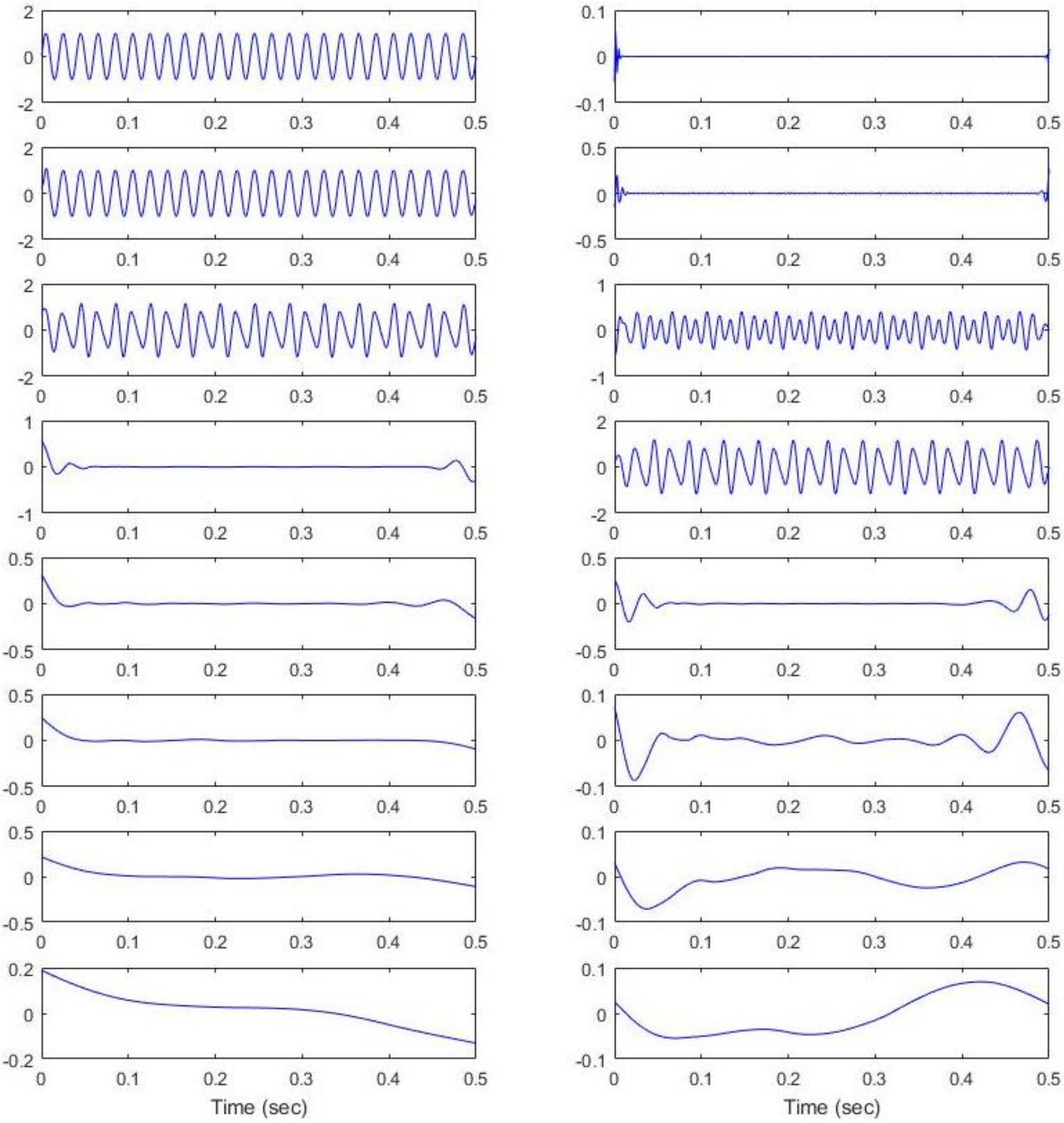


Samples of (a) approximation coefficients

Samples of (d) detailed coefficients

**Figure 4-15 Decomposition and features extracted from pure voltage signal**

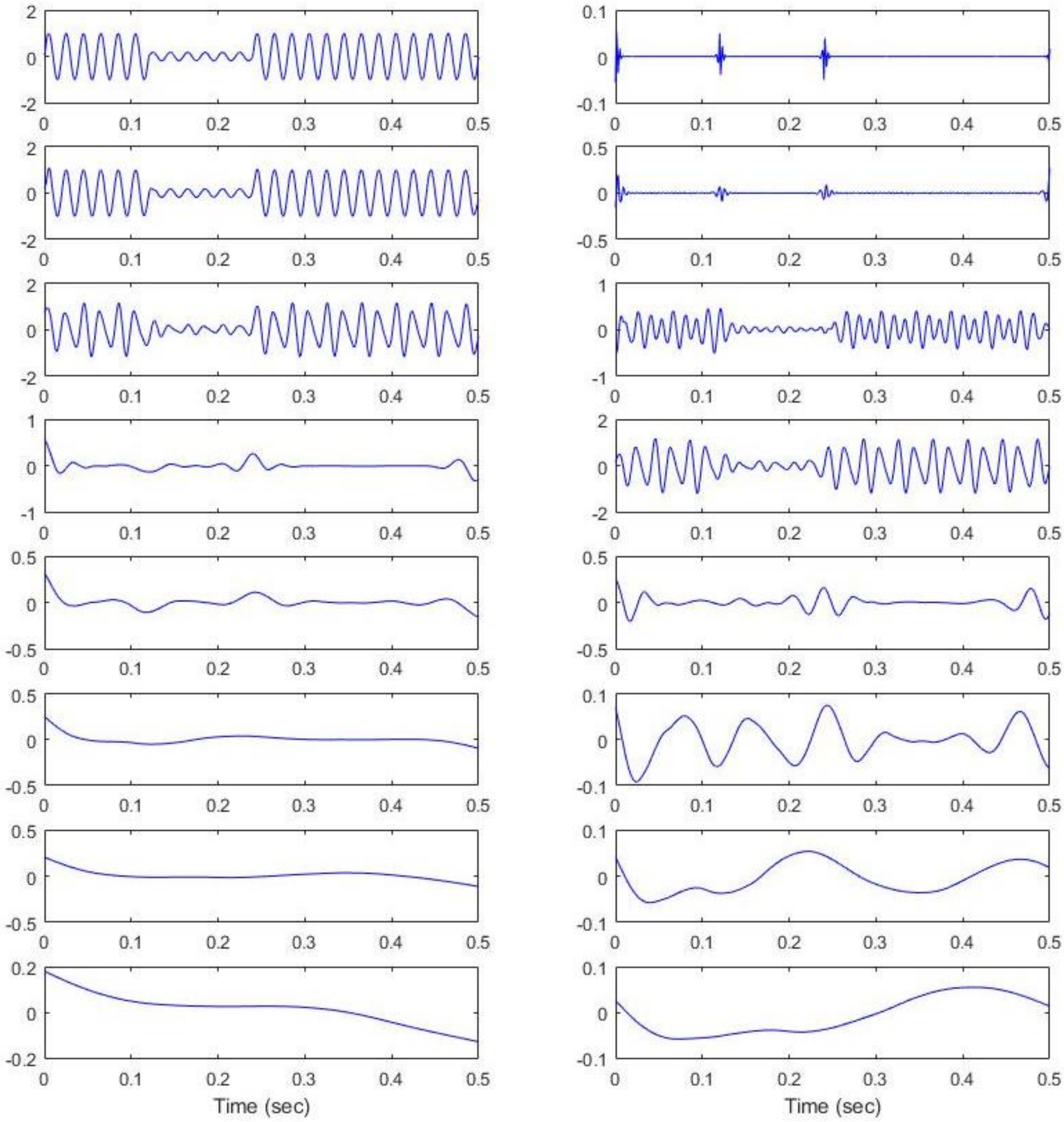


Samples of (a) approximation coefficients          Samples of (d) detailed coefficients

**Figure 4-16 Decomposition and features extracted from voltage sag signal**

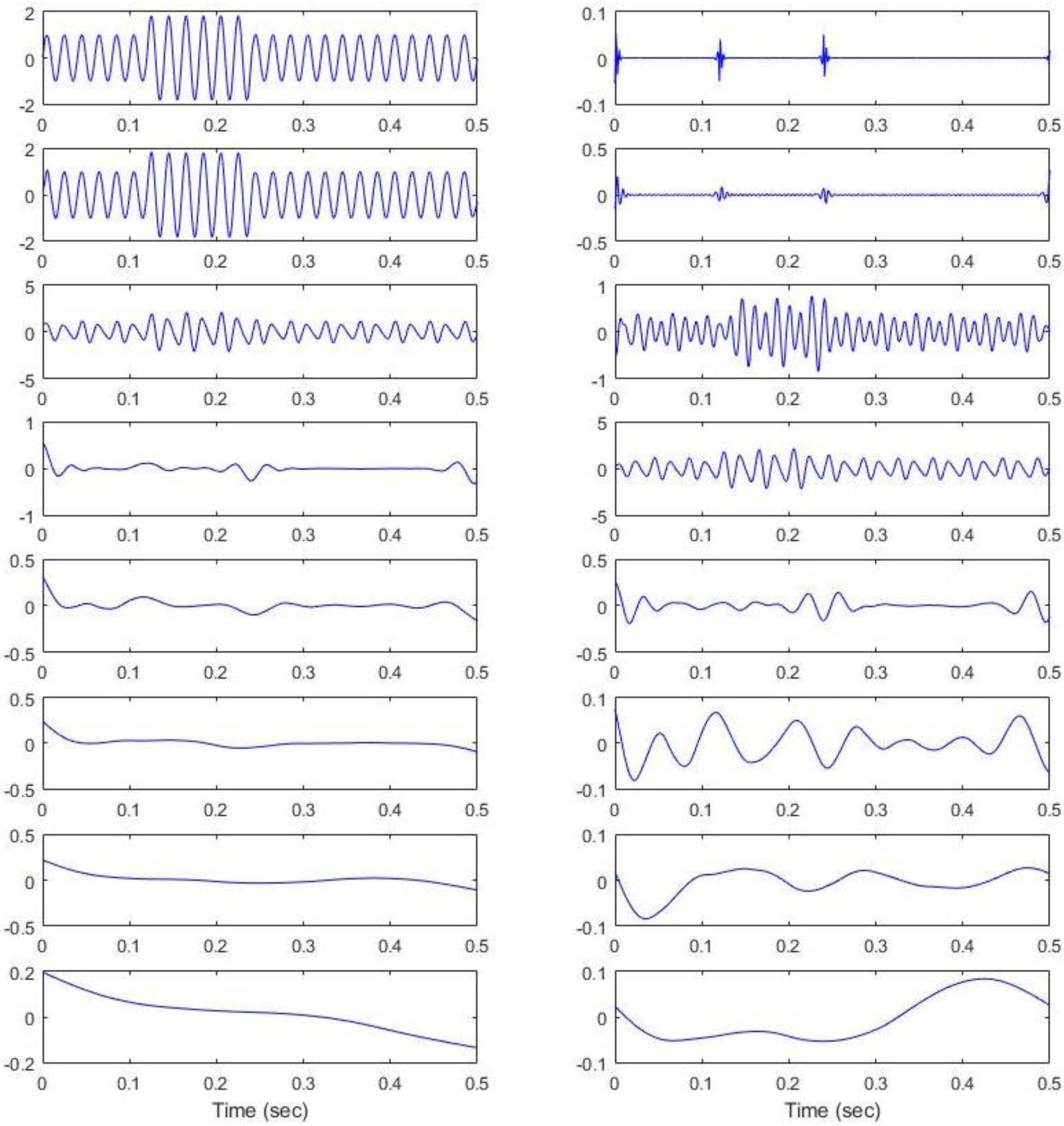


Samples of (a) approximation coefficients

Samples of (d) detailed coefficients

**Figure 4-17 Decomposition and features extracted from voltage swell signal**

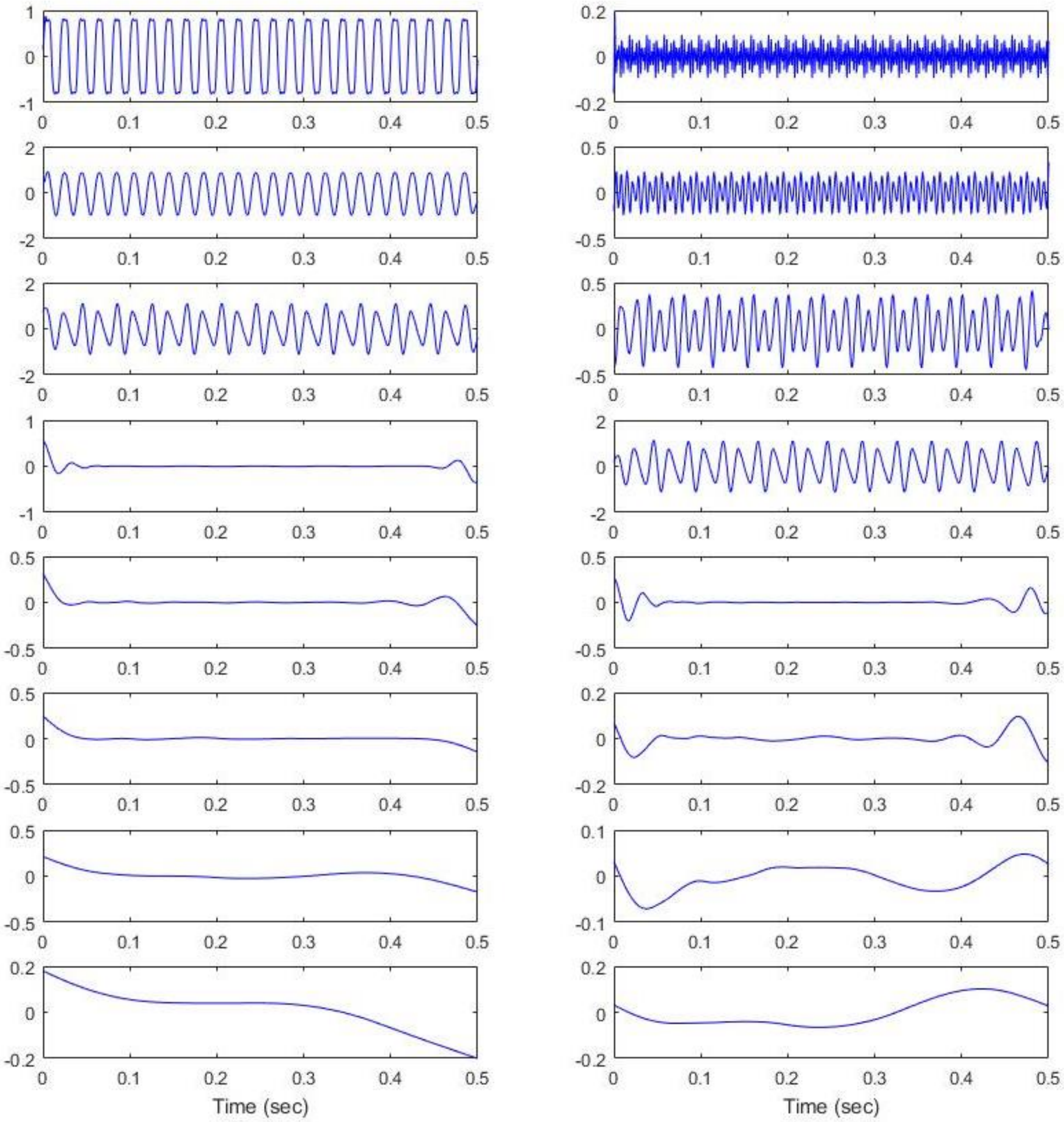


Samples of (a) approximation coefficients Samples of (d) detailed coefficients

**Figure 4-18 Decomposition and features extracted from voltage harmonics signal**

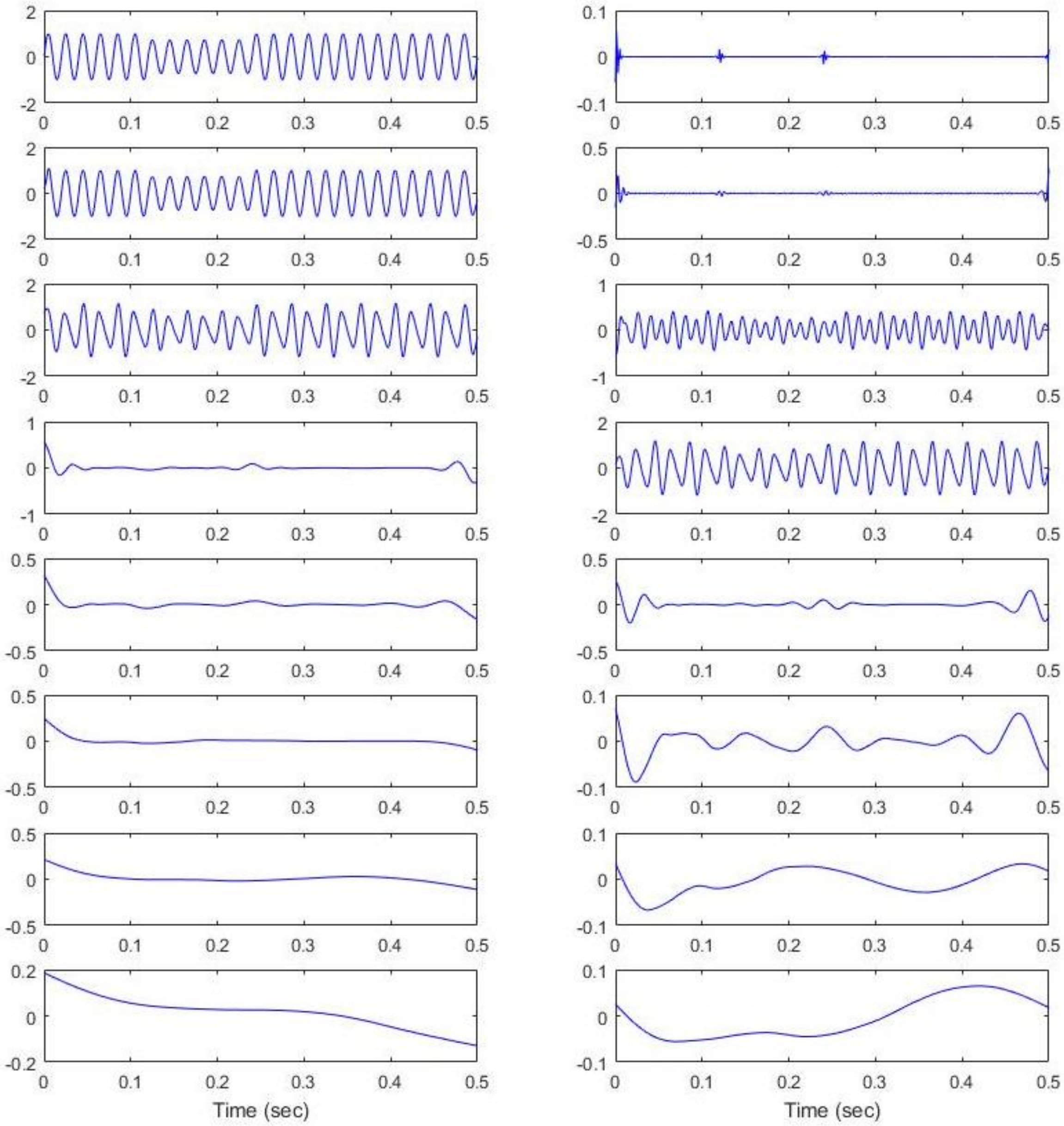


Samples of (a) approximation coefficients Samples of (d) detailed coefficients

**Figure 4-19 Decomposition and features extracted from voltage interruption signal**

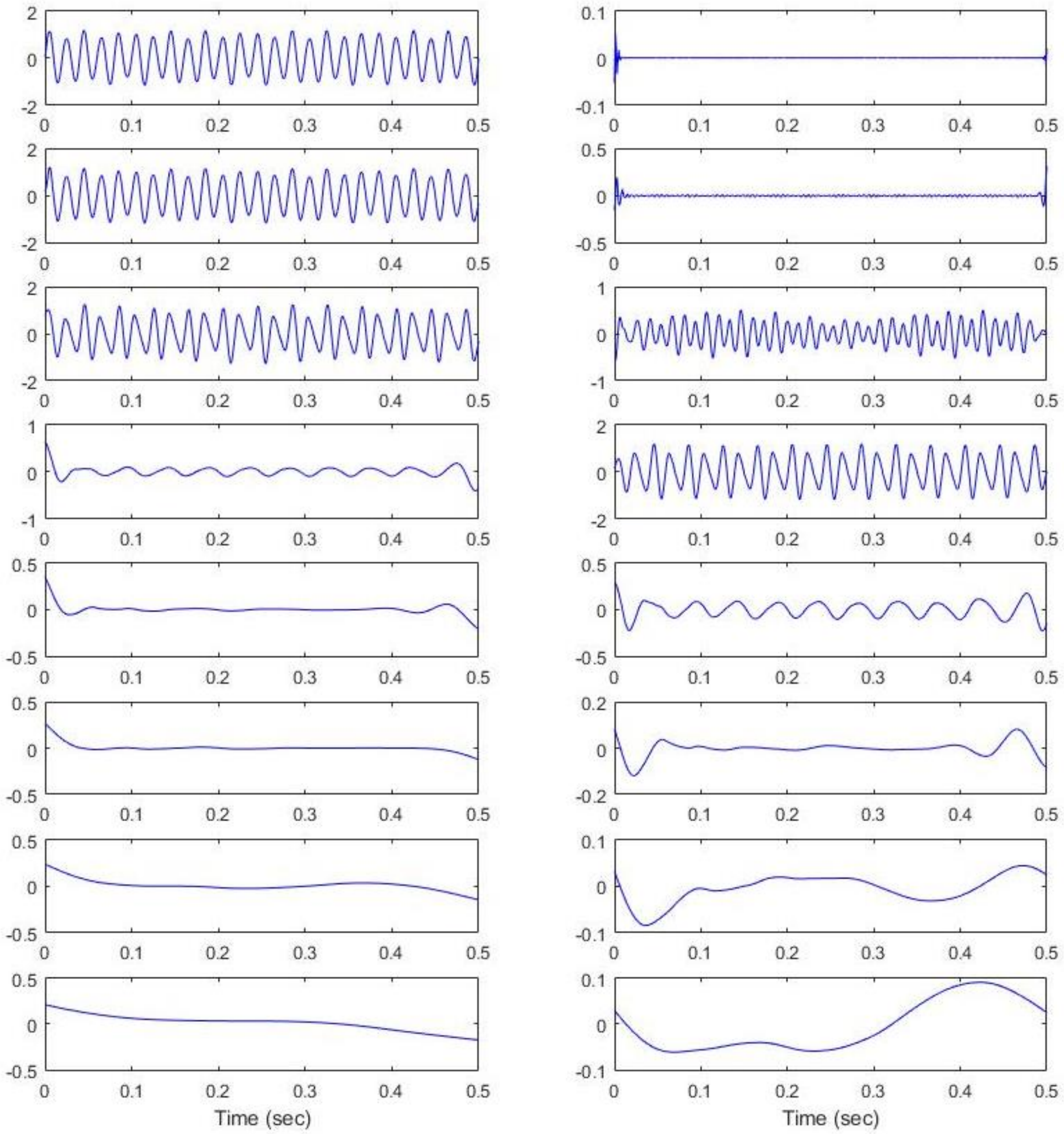


Samples of (a) approximation coefficients          Samples of (d) detailed coefficients

**Figure 4-20 Decomposition and features extracted from voltage flicker signal**

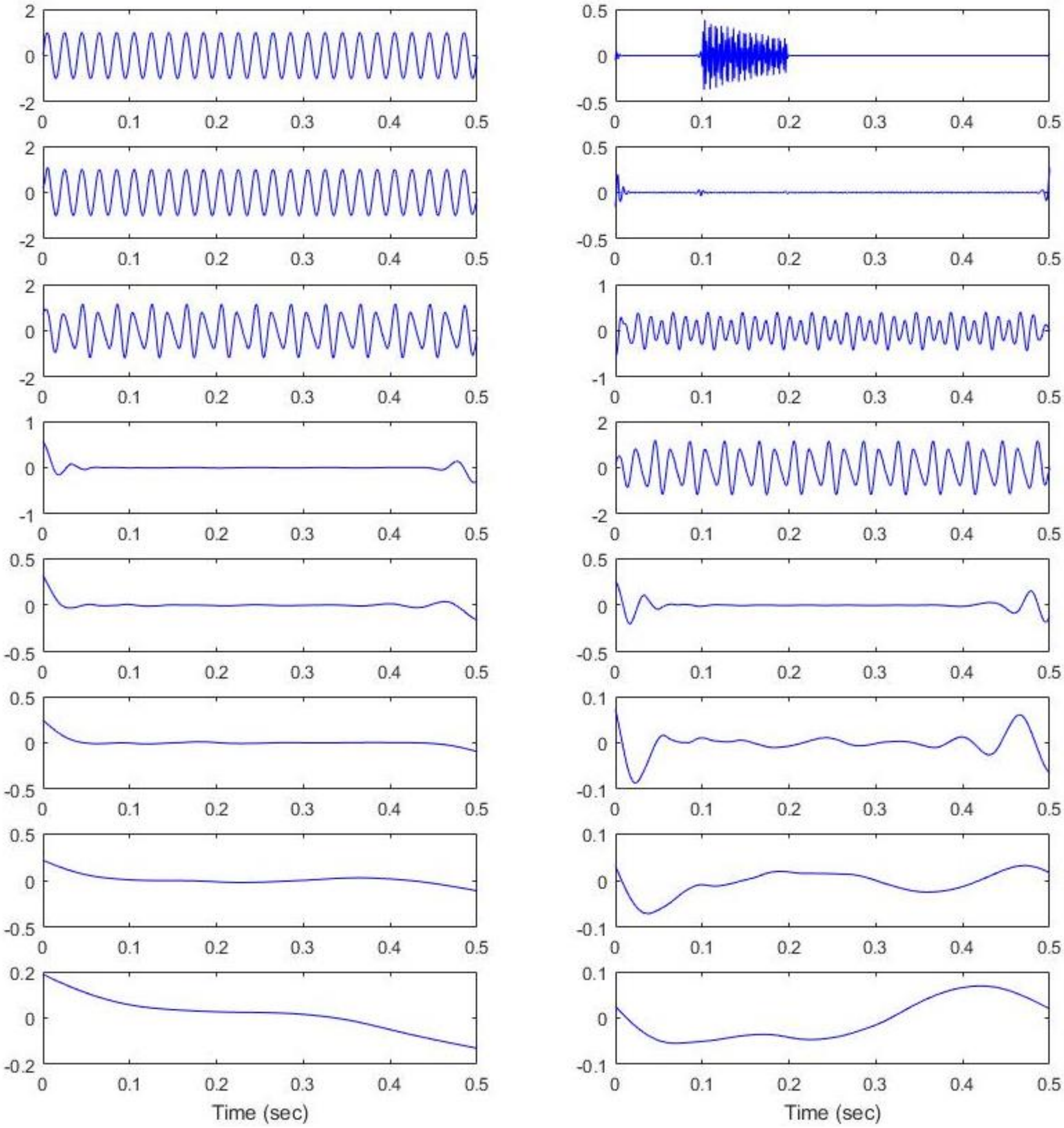


Samples of (a) approximation coefficients

Samples of (d) detailed coefficients

**Figure 4-21 Decomposition and features extracted from voltage high frequency transient**

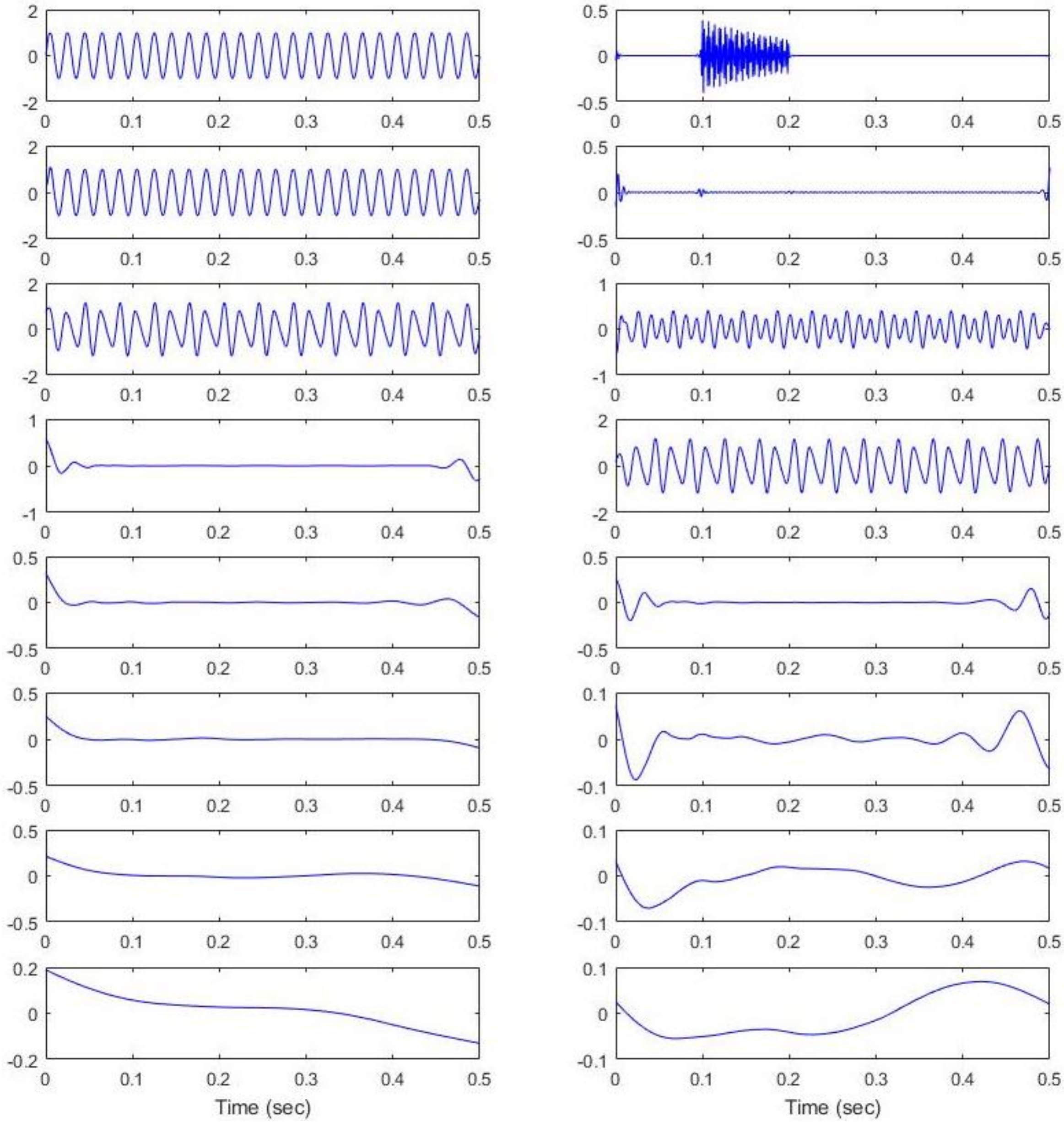


Samples of (a) approximation coefficients

Samples of (d) detailed coefficients

**Figure 4-22 Decomposition and features extracted from voltage low frequency transient**

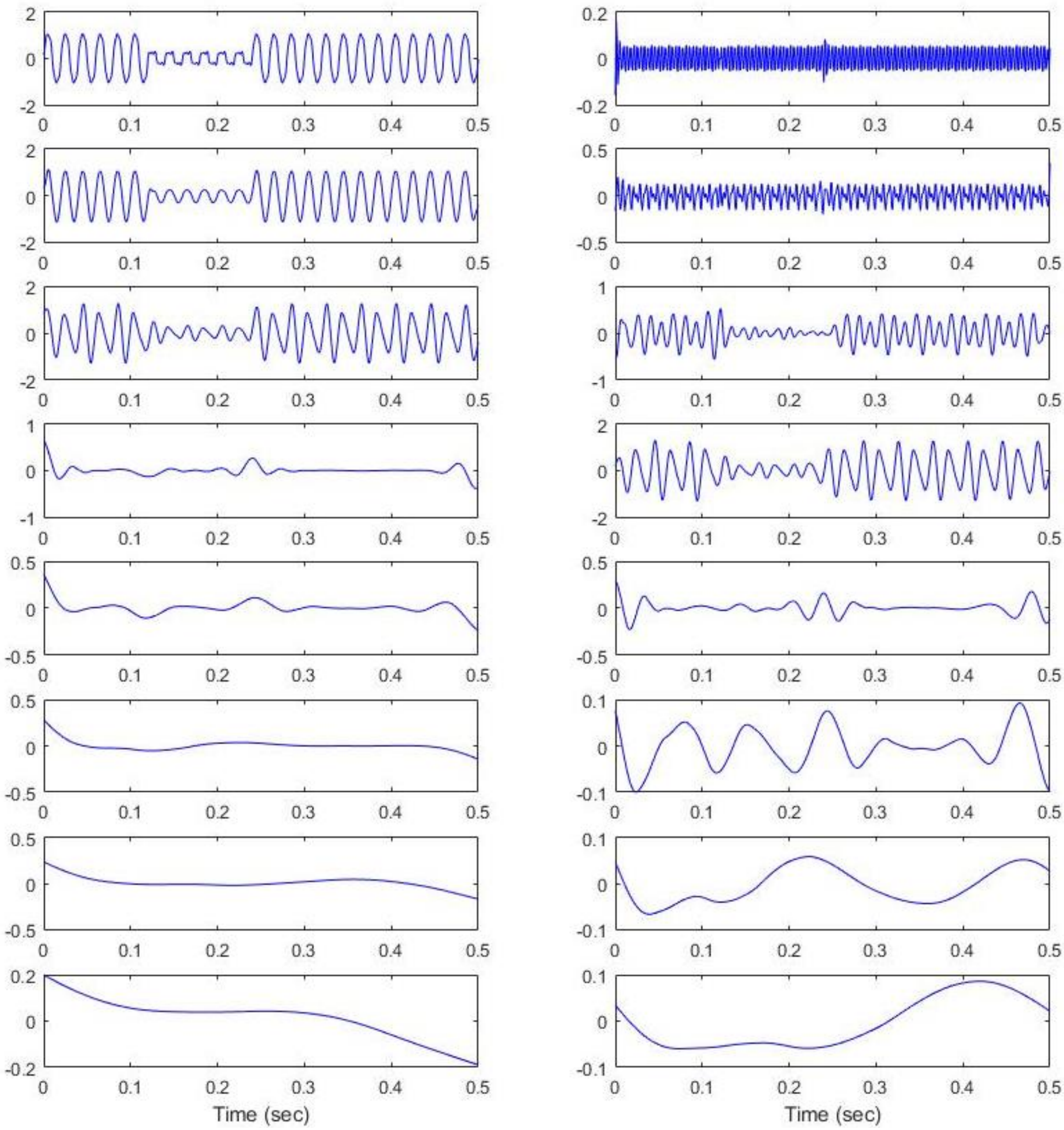


Samples of (a) approximation coefficients

Samples of (d) detailed coefficients

**Figure 4-23 Decomposition and features extracted from voltage sag plus harmonics**

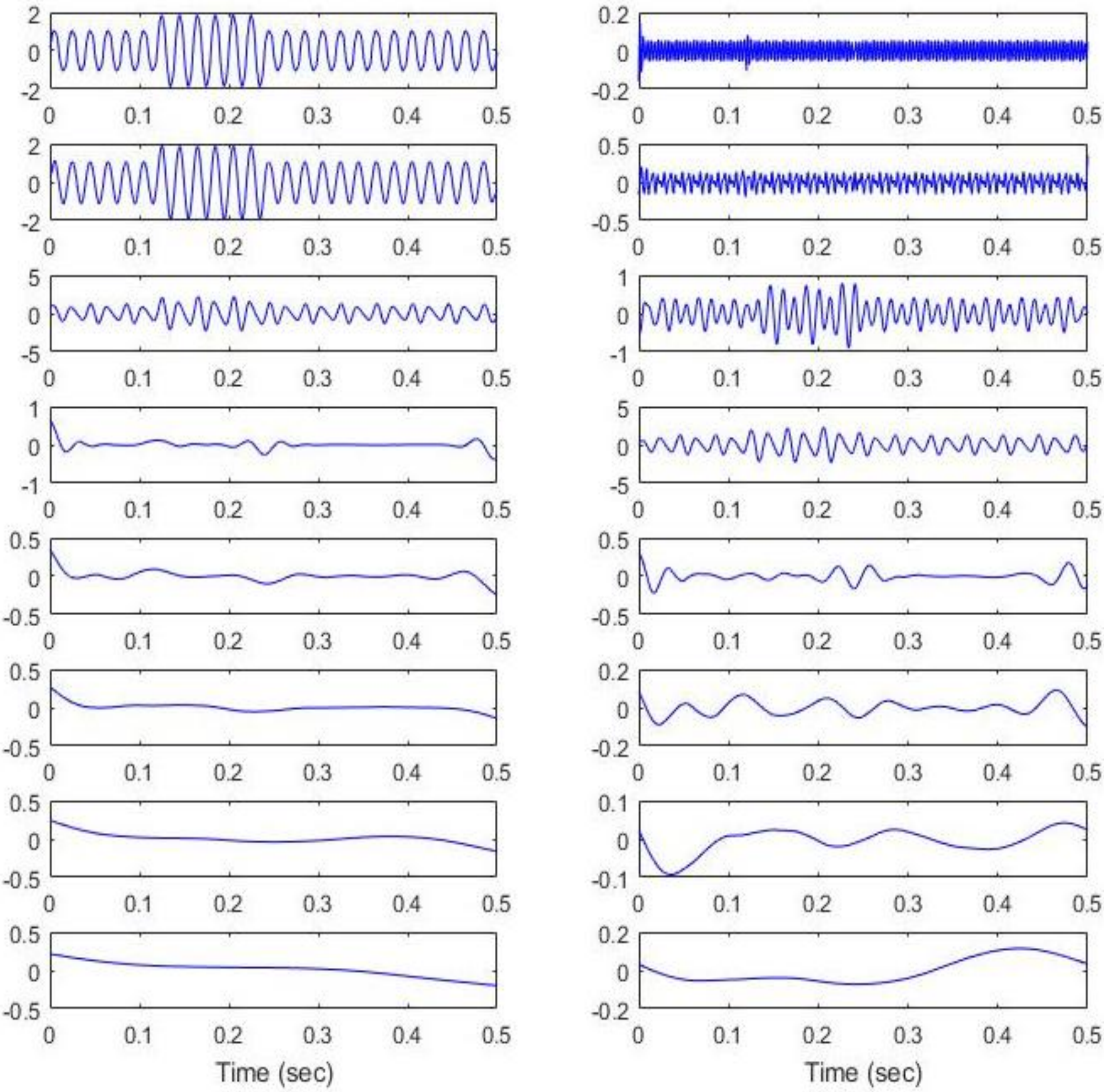


Samples of (a) approximation coefficients

Samples of (d) detailed coefficients

**Figure 4-24 Decomposition and features extracted from voltage swell plus harmonics**

As mathematically explained, results of eight features set are displayed for both DWT coefficients: the approximation coefficient (a) and the detailed coefficient (d) with a total of 16 signals of feature sets for each disturbance. These are categorised and distributed according to their energy, where each higher frequency feature comes first and lower frequency features come last. Feature sets selected to be in the training phase in the classifier are the detailed ones. Thus, 8 × 10 types (1 normal + 9 distorted signals) result in 80 features in each generation step. Each one of these disturbances is modelled to have a random value at every generation based on its numerical parameters.

### 4.5.2 Classification Stage Results

In order to evaluate and examine the performance of the detecting algorithm, a classification system technique is needed. Three phases of training are conducted for data through FFNN. The starting point in this phase is building an inputs database for the classifier. In this study, 40 random generations of power quality disturbances are collected based on the limits of each one, which is mentioned in .

Table 4-1. With each generation step, an 8-level decomposing process provides the database with eight features extracted from each one of these PQDs. The result is a dataset of 3200 samples, founded to move to the learning and training phase. Results of disturbance features extracted are fed to FFNN as inputs.

The second phase is data validation, which is conducted by measuring the network efficiency. FFNN is constructed to measure and classify power quality disturbances, where each one of these disturbances has its own neural. The main advantage of this system is network learning. Thereafter, the learning process is conducted to solve errors attached to data and follow the principle by multiplying inputs with their weights. Then results are calculated with a mathematical process to find the activation function of the neural. The outputs are then calculated by another mathematical model to initiate a structure of rules to classify different new inputs.

The third phase is testing accuracy to ensure the best performance of the network. Furthermore, one, two and three hidden layers from 5 to 50 neurons are used to enhance accuracy and explore the best performance of the classifier. Results of one hidden layer are shown in Table 4-2. The accuracy is detailed for each quality signal and for the overall accuracy and that is applied for one, two and three hidden layers.

**Table 4-2 Classification accuracy of FFNN with hidden layers**

| Case | PQDs | 1 hidden layer [8:20:10] | 2 hidden layers [8:5:15:10] | hidden layers [8:10:15:10:10] |
|---|---|---|---|---|
| **C1** | **Pure Sinusoidal** | 90.786 | 91.271 | 91.128 |
| **C2** | **Sag** | 90.800 | 91.071 | 91.614 |
| **C3** | **Swell** | 90.657 | 90.829 | 91.129 |
| **C4** | **Harmonics** | 91.157 | 91.114 | 90.714 |
| **C5** | **Interruption** | 91.104 | 91.057 | 90.729 |
| **C6** | **Flicker** | 90.786 | 90.771 | 90.742 |
| **C7** | **High Frequency Transient** | 90.714 | 90.414 | 91.114 |
| **C8** | **Low Frequency Transient** | 90.914 | 90.603 | 91.157 |
| **C9** | **Sag with Harmonics** | 90.801 | 90.657 | 91.300 |
| **C10** | **Swell with Harmonics** | 90.314 | 90.671 | 90.729 |
| | **Overall Accuracy** | **90.803** | **90.846** | **91.0356** |

### 4.5.3 Detection and Features Extraction Based on the CEEMD Algorithm

At this stage, it is important to describe power quality disturbances precisely. To achieve this, several standards are implemented to characterise these disturbances, especially the IEEE 1159 standard [86], which describes electromagnetic phenomena, normal operating conditions and variation parameters for voltage, current, power and load supply in electrical power systems. Nevertheless, the European standard EN 50160 specifies the thresholds of RMS measurements for voltages and currents when disturbances occur [93]. Finally, ISO standard IEC 61000-4-30 shows methods of reliability in terms of measuring electrical quantities in power systems [94].

As previously done with the DWT algorithm, ten power quality disturbances are generated according the standards above, especially IEEE 1159. These disturbances are pure sinusoidal sag, swell, harmonics, interruption, flicker, high frequency transient, low frequency transient, sag with harmonics and swell with harmonics. Moreover, the generation stage is implemented successfully for single and multiple events with its parametric limits in .

Table 4-1. The outputs of this stage, shown in are repeated randomly to develop a dataset for the classification stage.

In this section, each waveform of power quality disturbances generated in the detection stage is decomposed into 8 levels of IMFs with the assistance of the CEEMD process. Features extracted from these contain statistical information from each signal such as: standard deviation, energy, amplitude and frequency for each IMF. The key factors at this stage are the instantaneous amplitude and the instantaneous frequency obtained from and calculated for the next classification stage. Figure 4-25 to Figure 4-34 show IMFs of these disturbances in detail, where each disturbance has a unique IMF and they are reflected as a fingerprint to classification process, taking into account that these disturbances are considered as short duration variations. The performance of CEEMD comes from its capability to separate frequencies attached to each power quality disturbance. It starts by finding the cubic spline lines after setting the maxima point of each event as well as envelope limits, and the mean value of these envelopes is zero.

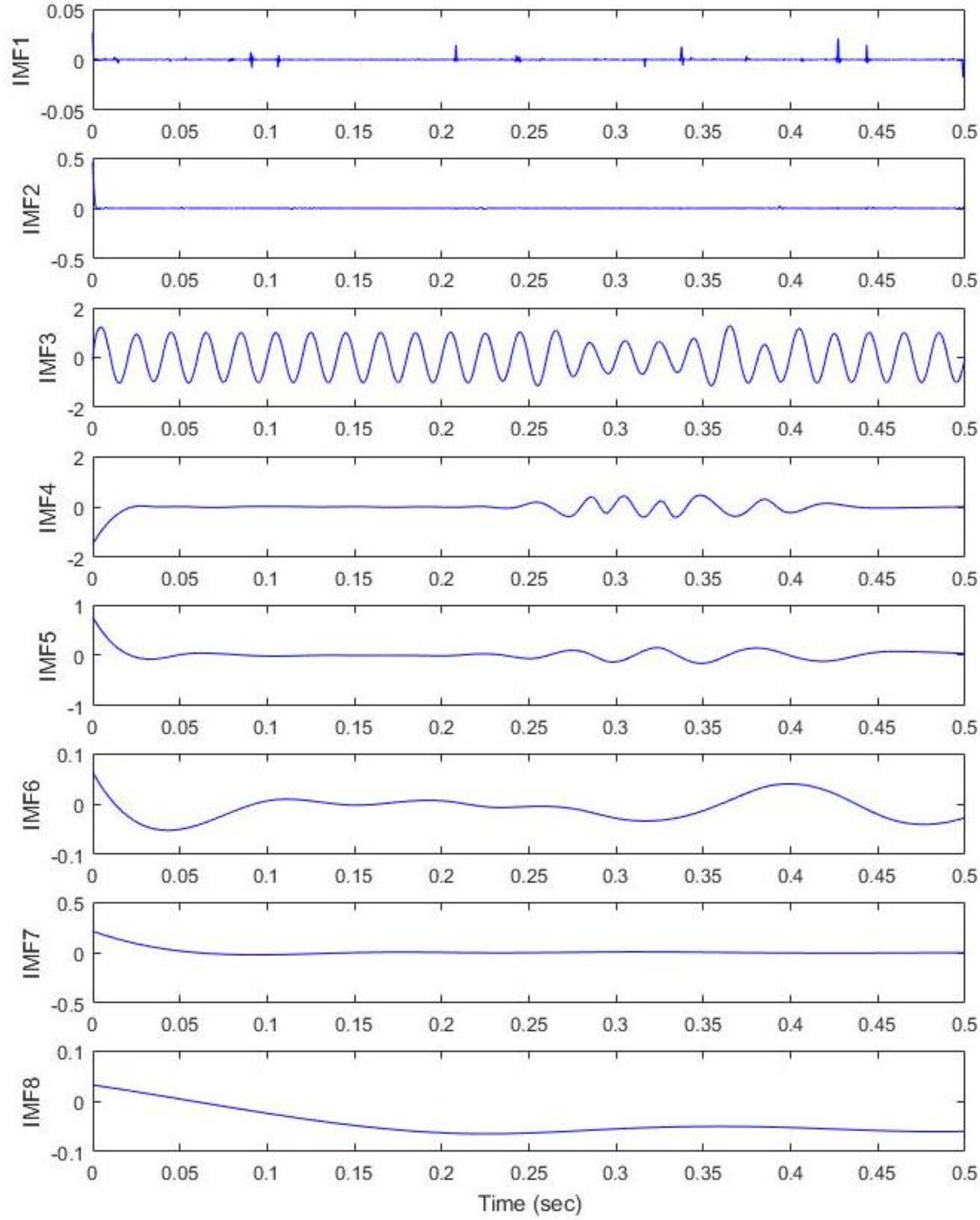


**Figure 4-25 CEEMD IMFs extracted from pure voltage signal**

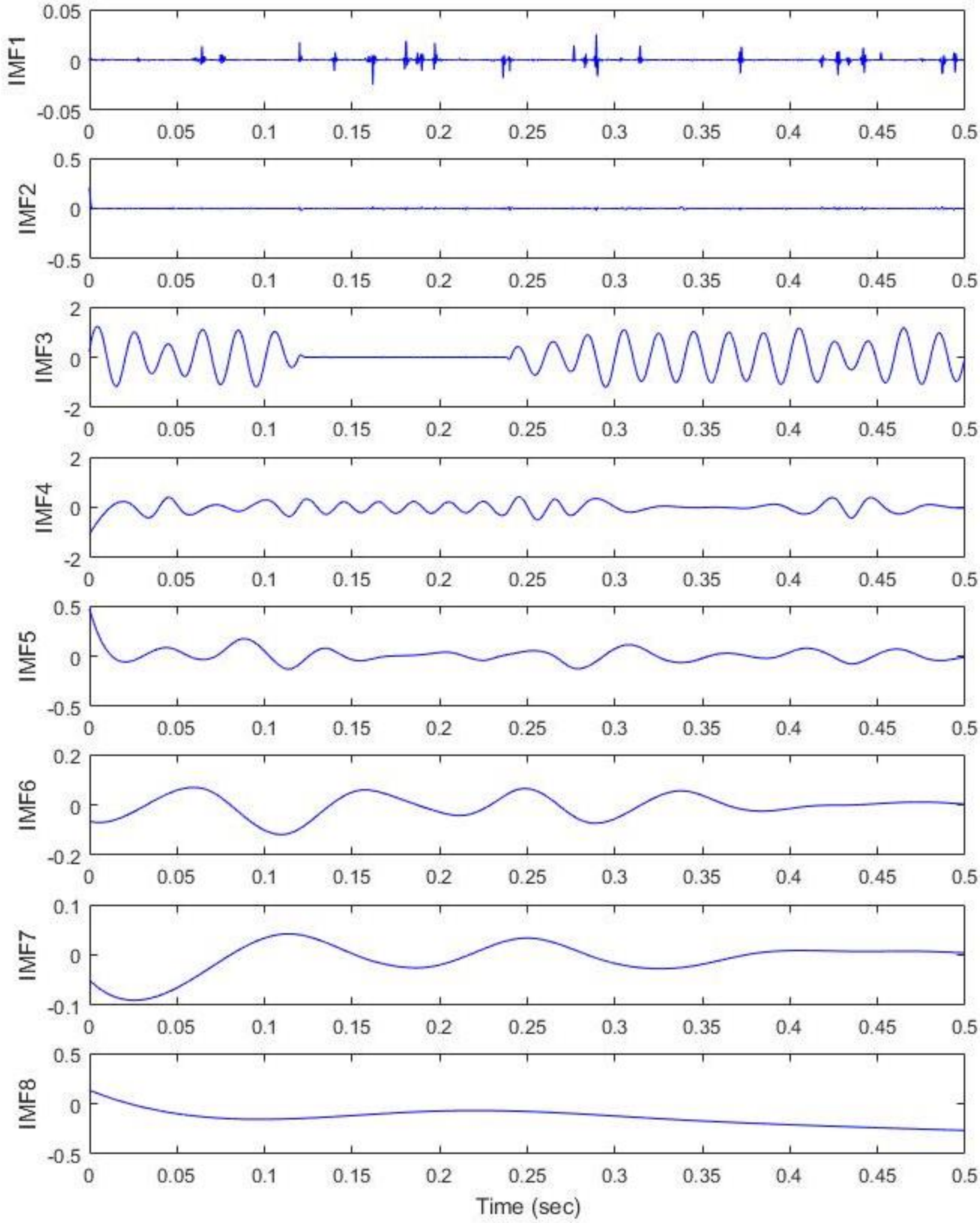


**Figure 4-26 CEEMD IMFs extracted from voltage sag signal**

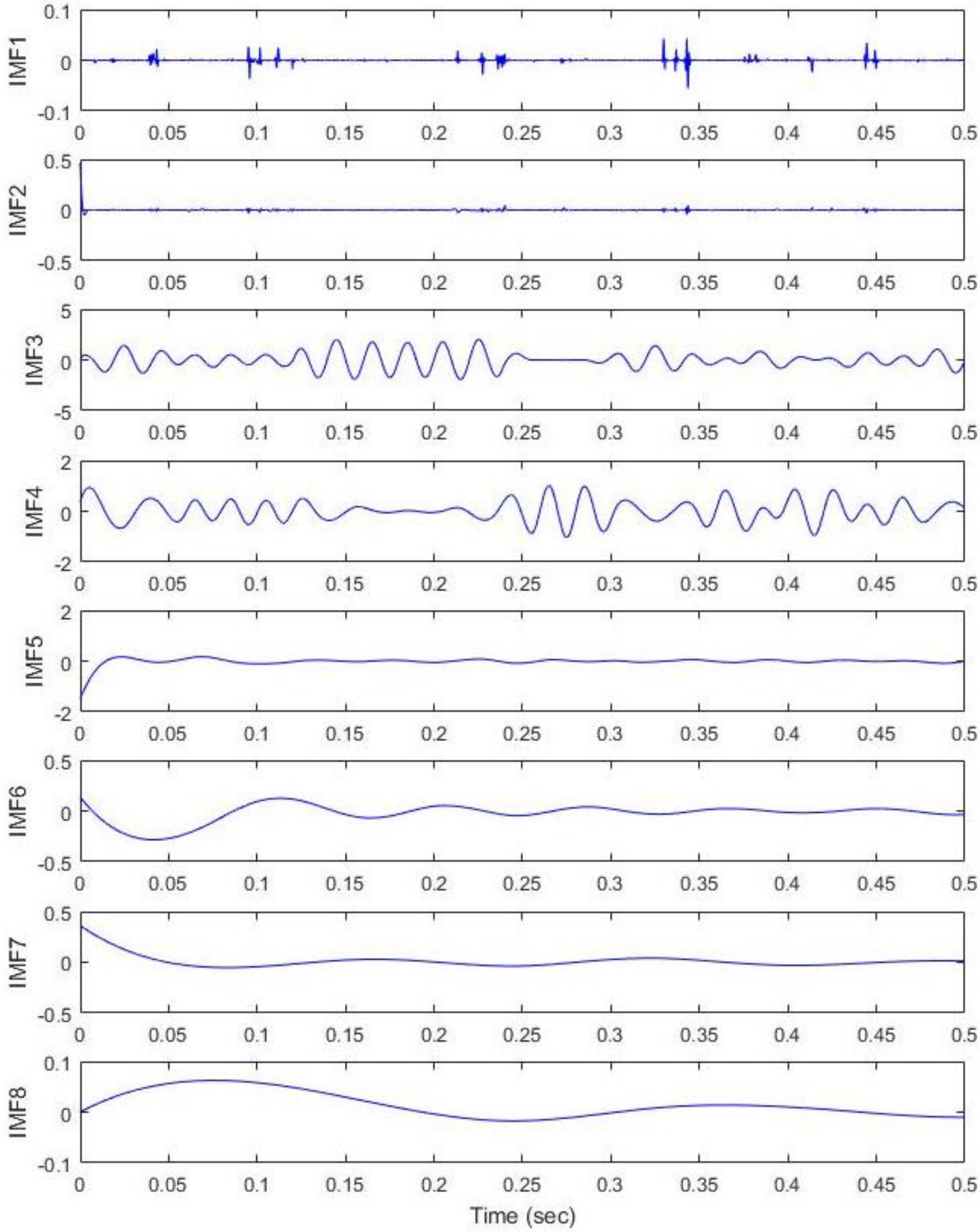


**Figure 4-27 CEEMD IMFs extracted from voltage swell signal**

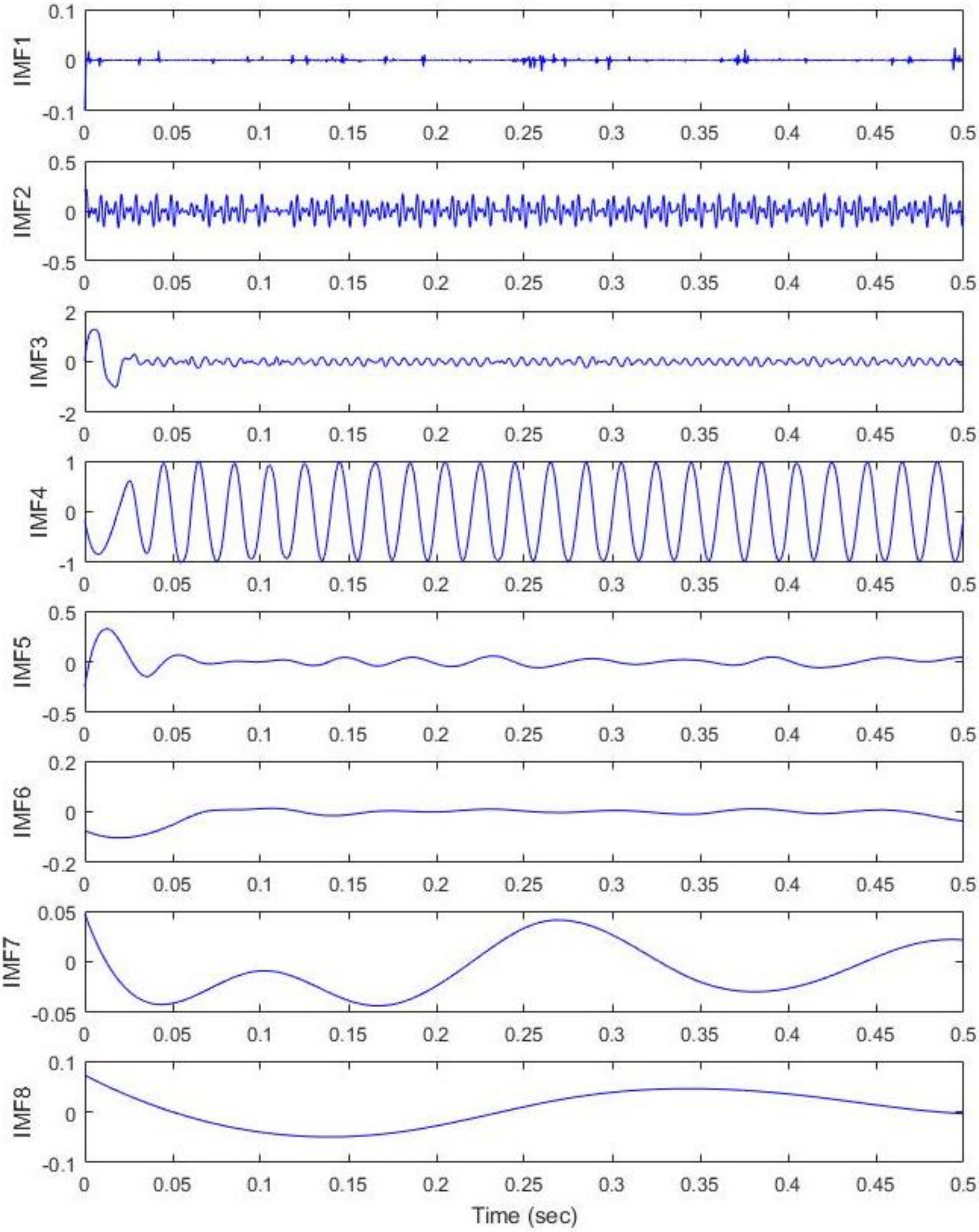


**Figure 4-28 CEEMD IMFs extracted from voltage harmonic signal**

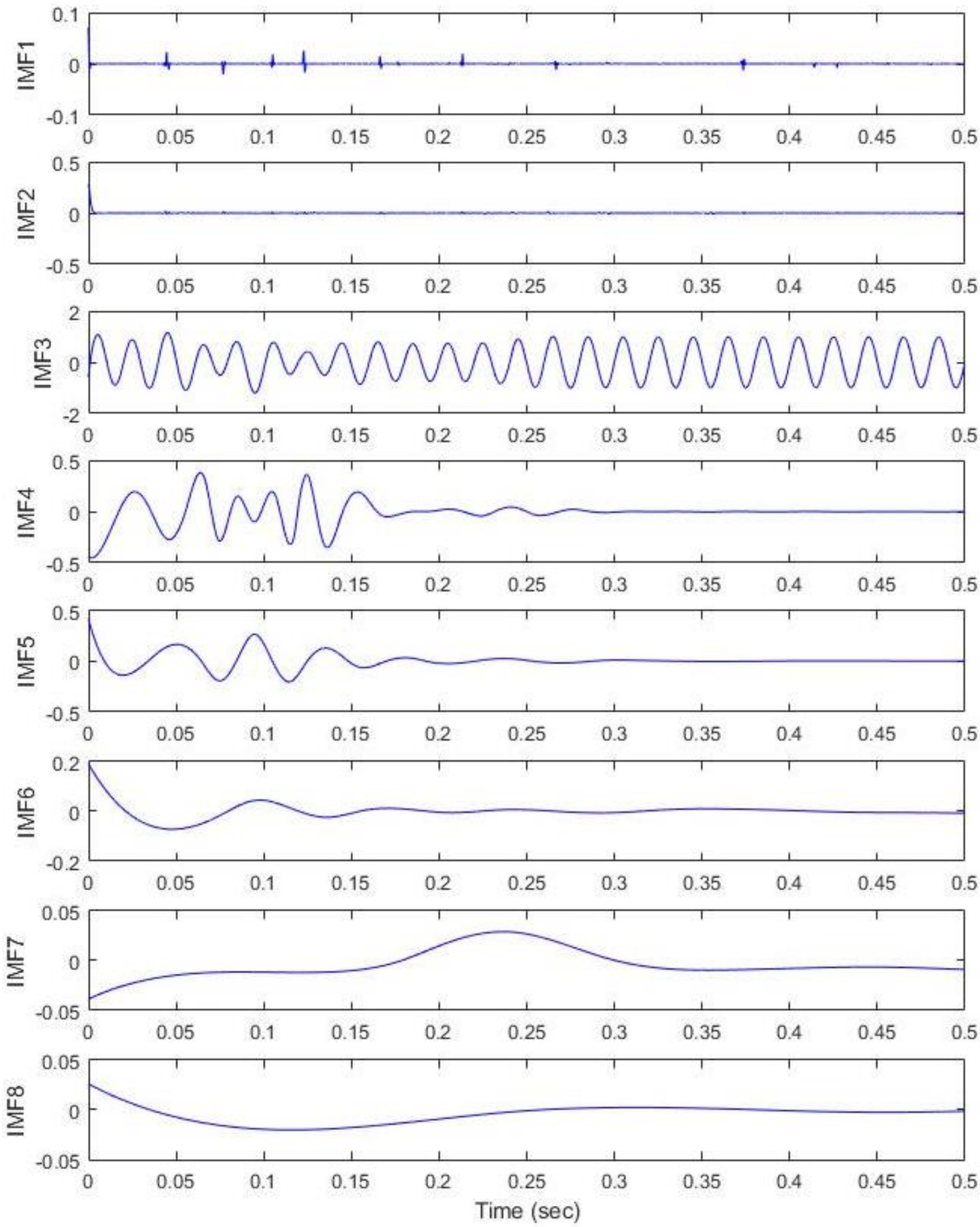


**Figure 4-29 CEEMD IMFs extracted from voltage interruption signal**

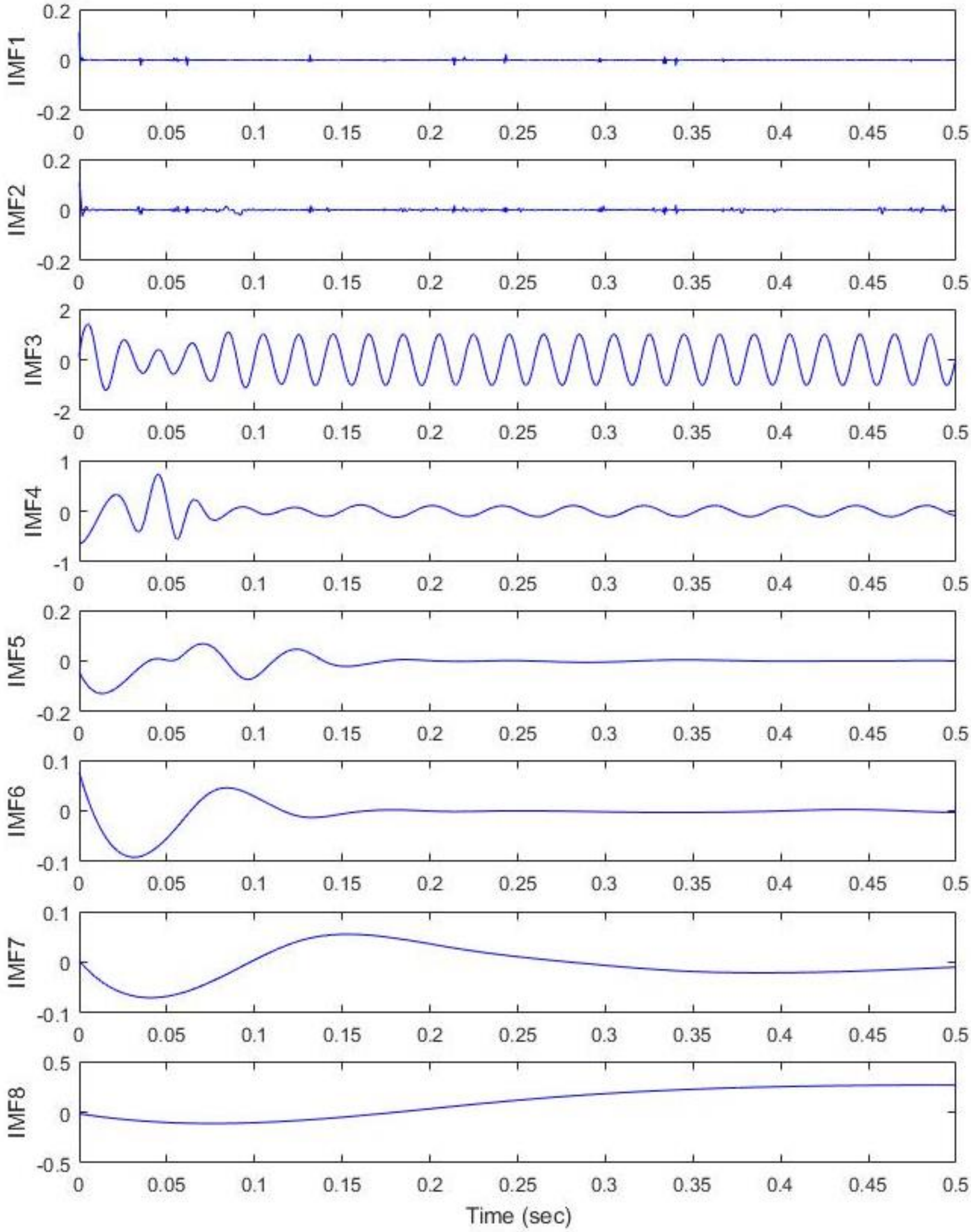


**Figure 4-30 CEEMD IMFs extracted from voltage flicker signal**

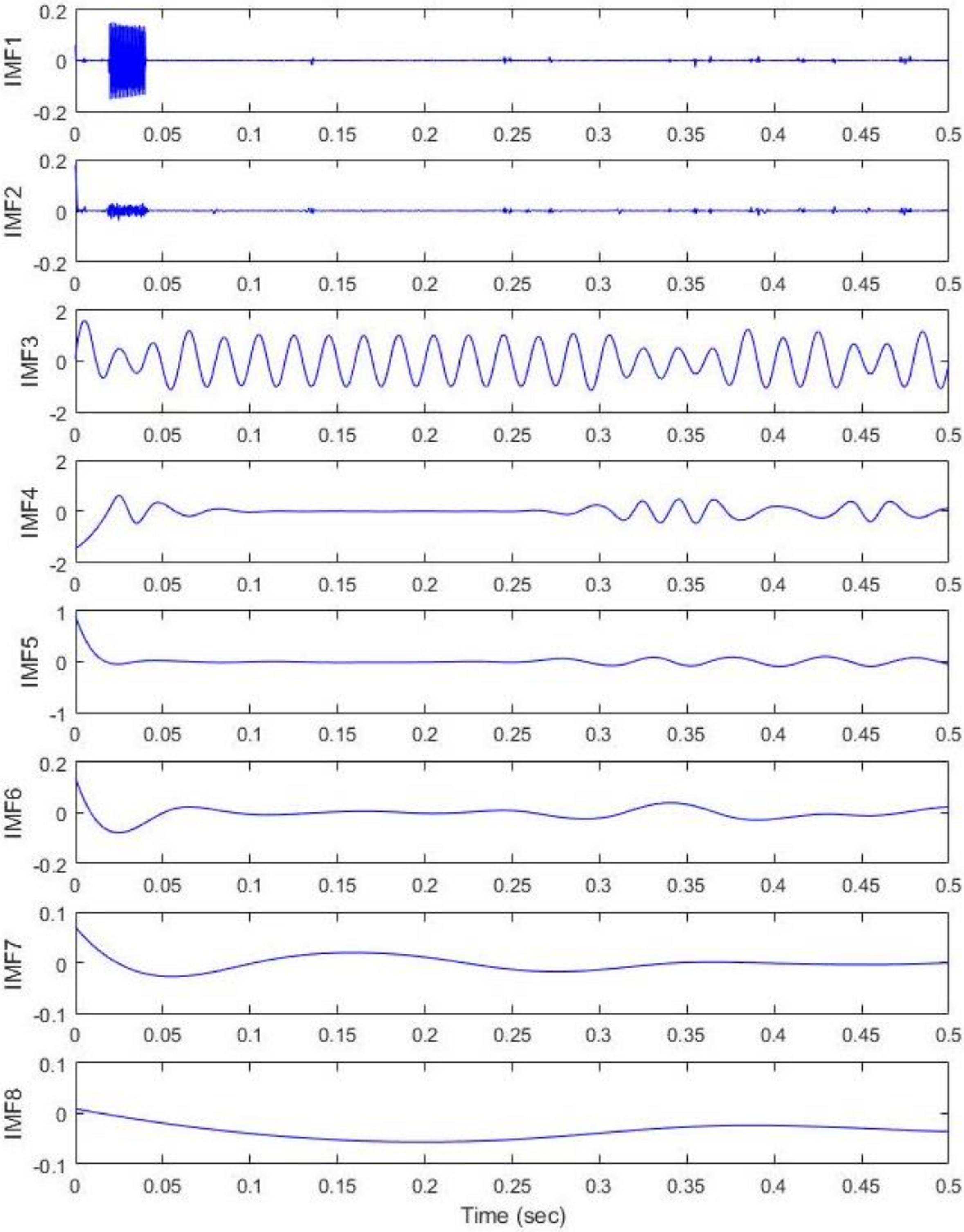


**Figure 4-31 CEEMD IMFs extracted from high frequency transient signal**

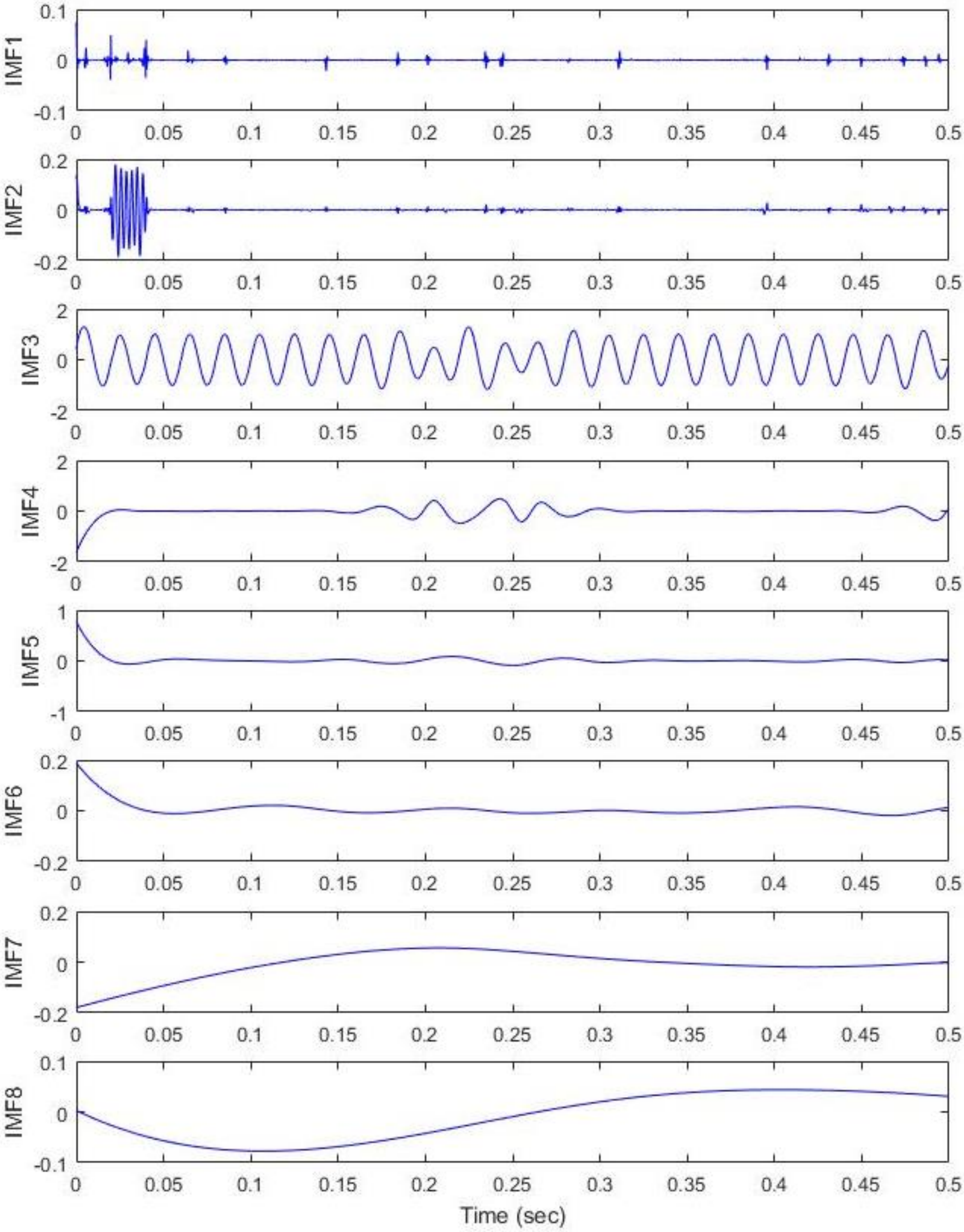


**Figure 4-32 CEEMD IMFs extracted from low frequency transient signal**

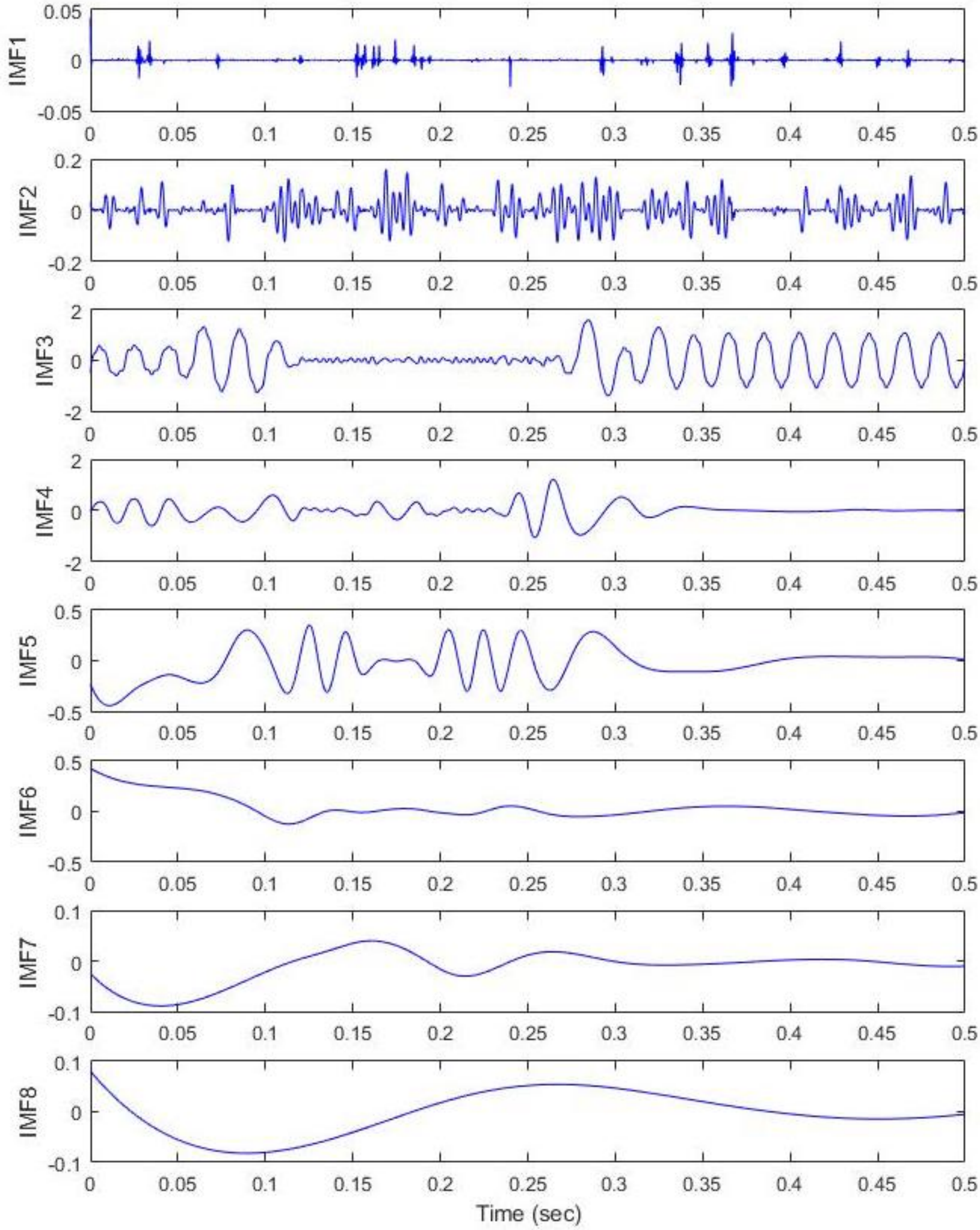


**Figure 4-33 CEEMD IMFs extracted from sag with harmonics signal**

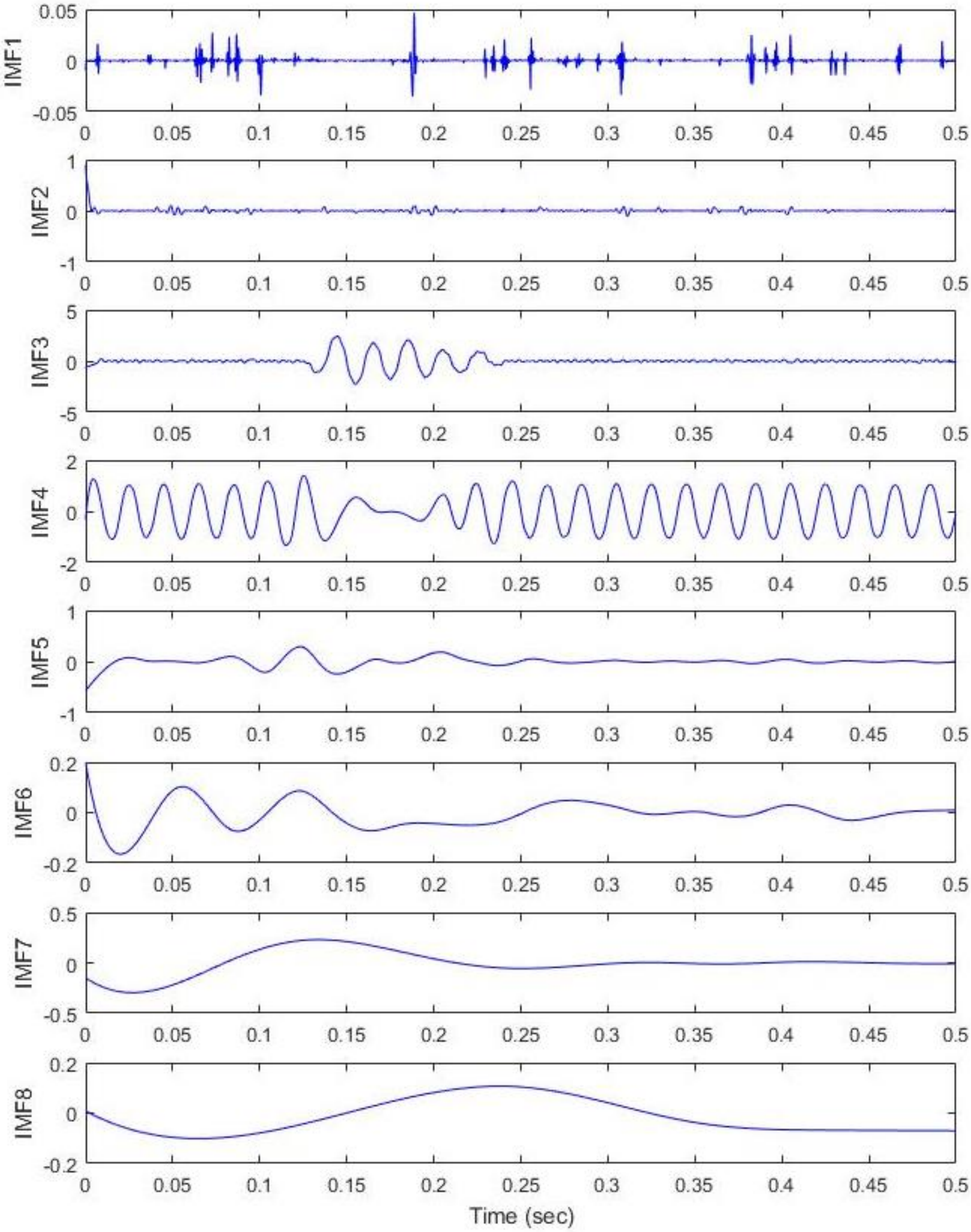


**Figure 4-34 CEEMD IMFs extracted from swell with harmonics signal**

### 4.5.4 Classification Stage Results

In this stage, the classification technique constructed to train and test the data obtained is the FFNN classifier. A dataset of features extracted for ten PQDs is trained, where each one of these disturbances has its own neural.

In this phase, three steps of training processes are involved for data collected. First, features of these disturbances are fed to FFNN as inputs for the training network, according to IMFs. Second is the validations step for trained data network, which is performed by measuring the efficiency. Finally, the step of testing for accuracy to ensure the best performance of the classifier is performed.

Training of FFNN for an inputs database based on extracted features is built up from 40 random input variables of PQDs. Testing of hidden layers of the FFNN classifier is done with one, two and three hidden layers from 5 to 50 neurons to ensure accuracy, and find the best performance of the classifier and better topology in this field. Results of three hidden layers, according to topology [8:15:30:15:10], shows the best accuracy as detailed, as well as the overall accuracy for the FFNN classifier, as shown in Table 4-3.

**Table 4-3 Classification accuracy of FFNN with three hidden layers**

| Neural | Power Quality Disturbances | Accuracy Rate (%) [8:10:15:10:10] |
|---|---|---|
| C 01 | **Pure Sinusoidal** | 99.000 |
| C 02 | **Sag** | 97.642 |
| C 03 | **Swell** | 98.904 |
| C 04 | **Harmonics** | 99.101 |
| C 05 | **Interruption** | 98.402 |
| C 06 | **Flicker** | 100.000 |
| C 07 | **High Frequency Transient** | 98.015 |
| C 08 | **Low Frequency Transient** | 99.012 |
| C 09 | **Sag with Harmonics** | 97.109 |
| C 10 | **Swell with Harmonics** | 97.450 |
| | **Overall Accuracy** | **98.464** |

### 4.5.5 Results Comparison and Analysis

In order to examine the effectiveness and evaluate the feasibility of the proposed detection algorithm and classification technique, a comparison analysis is constructed for the classification technique based on the following factors:

- Both detection algorithms analyse and detect signals in the time-frequency domain and are capable of analysing non-stationary signals.
- The feature extraction process is a function provided by both algorithms, and was 8 features for each disturbance.
- Power quality disturbances are modelled equally for each algorithm, and the same number generation of random values.
- The FFNN classifier was implemented for both algorithms, and searching the best performance by the optimum member of hidden layers has the same strategy where the optimum topology [10:15:30:15:10] is executer to for both methods.

The main factor in the comparison analysis is the accuracy of the classifier, and it can be expressed as shown in Table 4-4.

**Table 4-4 Results comparison of DWT and CEEMD algorithms**

| PQDs | DWT Accuracy Rate (%) | DWT Classification Error (%) | CEEMD Accuracy Rate (%) | CEEMD Classification Error (%) |
|---|---|---|---|---|
| **Pure Sinusoidal** | 91.128 | 8.872 | 99.000 | 1.000 |
| **Sag** | 91.614 | 8.386 | 97.642 | 2.358 |
| **Swell** | 91.129 | 8.871 | 98.904 | 1.096 |
| **Harmonics** | 90.714 | 9.286 | 99.101 | 0.899 |
| **Interruption** | 90.729 | 9.271 | 98.402 | 1.598 |
| **Flicker** | 90.742 | 9.258 | 100.000 | 0.000 |
| **High Frequency Transient** | 91.114 | 8.886 | 98.015 | 1.985 |
| **Low Frequency Transient** | 91.157 | 8.843 | 99.012 | 0.988 |
| **Sag with Harmonics** | 91.300 | 8.700 | 97.109 | 2.891 |
| **Swell with Harmonics** | 90.729 | 9.271 | 97.450 | 2.550 |
| **Overall** | **91.036** | 8.964 | **98.464** | 1.536 |

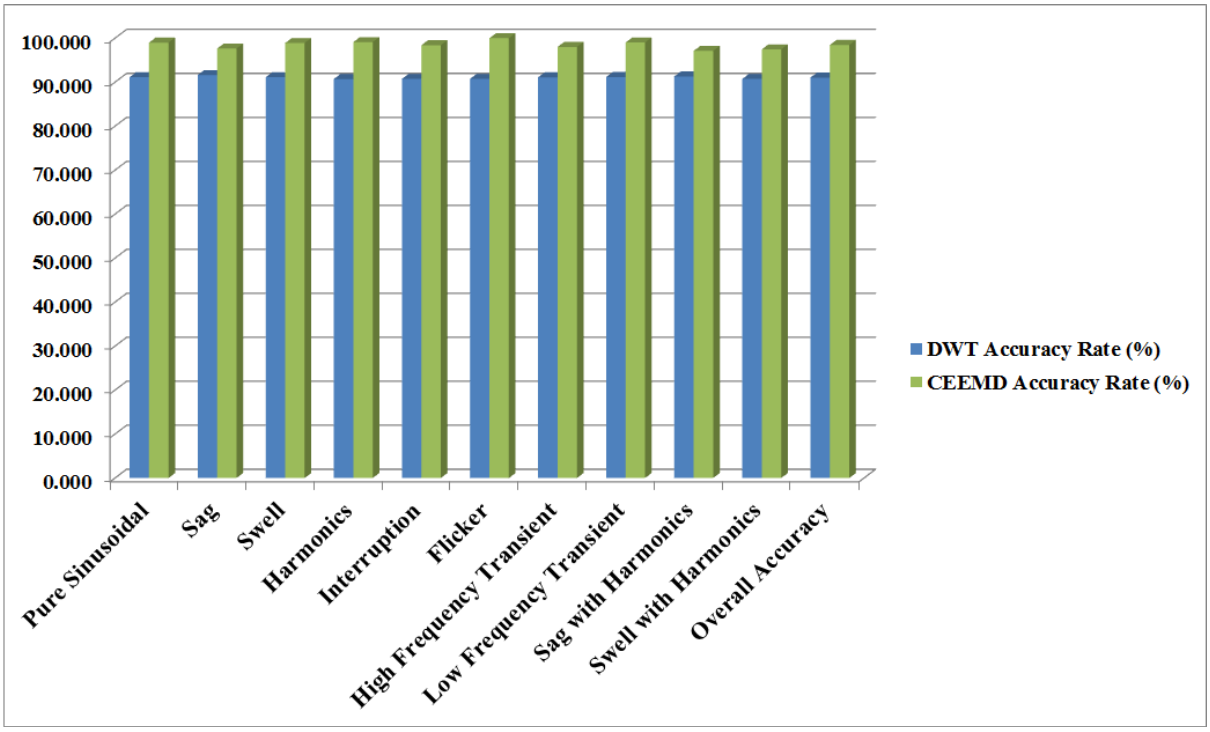


**Figure 4-35 Classification accuracy of DWT and CEEMD algorithms**

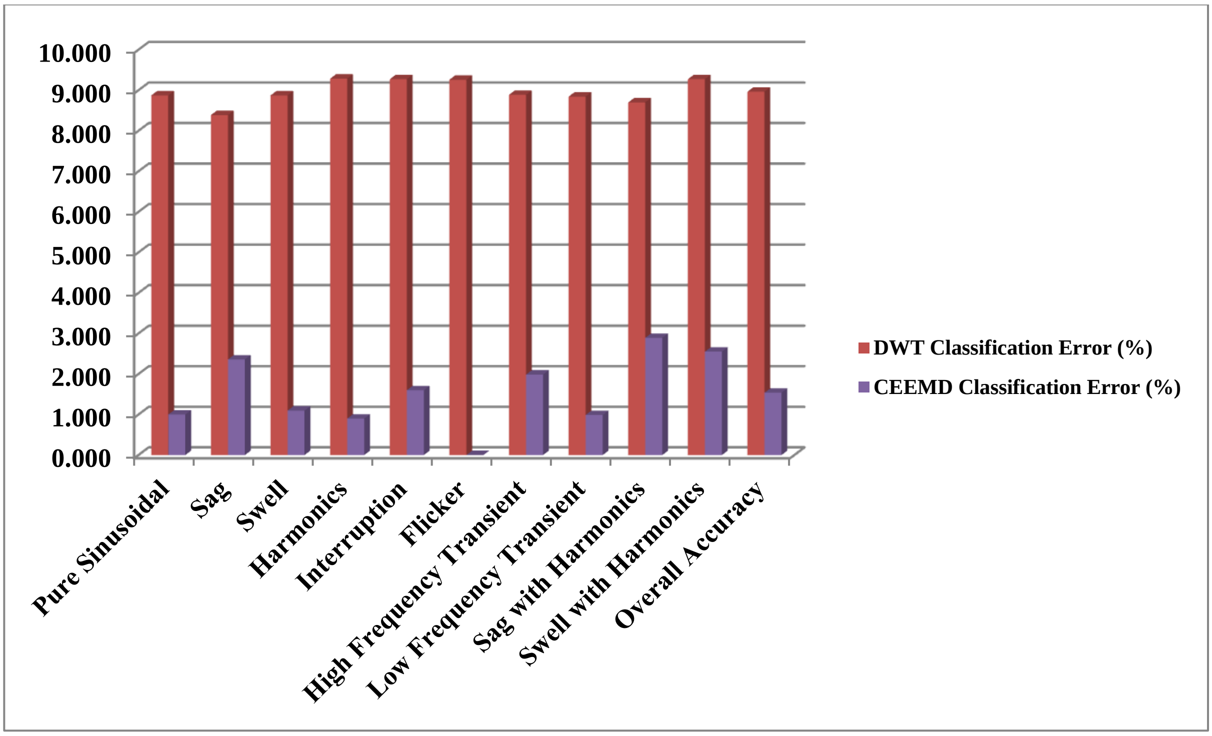


**Figure 4-36 Classification error comparison of DWT and CEEMD algorithms**

From Table 4-4 and Figure 4-35, it can be concluded that when detecting power quality disturbances, discrete wavelet transform is a powerful algorithm of non-stationary analysis for single cases and multiple disturbances, where accuracy was not less than 90% for each disturbance and overall accuracy. However, it is noticeable that WT and consequently DWT suffer from being sensitive to noise in some PQDs, especially disturbances with the appearance of harmonics and flickers. This could also be the reason for the inappropriate results of the classifier accuracy, as proven previously in [34] and [35]. It is also noticed that the computational cost for DWT is still at high level.

Nevertheless, detecting power quality disturbances based on a novel new detection algorithm named Complementary Ensemble Empirical Mode Decomposition (CEEMD) proved the ability to recognise these disturbances and detect them correctly. Moreover, in this analysis, CEEMD presents a significant change in terms of accuracy for each disturbance in the classification technique, where they were no less than 96%. The overall accuracy shows another remarkable change as well, exceeding 98%. Nevertheless, another advantage of the proposed algorithm is the reduction of data size without losing the disturbance characteristics. Therefore, a significant reduction in memory space during operations and a decrease of computation cost result.

## 4.6 Summary

This chapter presents the two main detecting algorithms for power quality disturbances. First, a modelling stage of these disturbances was presented, depending on each disturbance formula, and based on the internationally recognised standards which describe characteristics and limits for each one. Furthermore, DWT was performed as a detection algorithm for power quality disturbances. It was proven in this work that DWT is able to overcome Fourier transform limitations, especially with non-stationary disturbances. Thereafter, features of these PQDs are extracted into 8 levels and a calculation of energy values is conducted for each distorted signal, which is finally used to build the database needed for the classifier.

An FFNN classifier is realised and a database generated with a random sample of 3200 PQDs. Features data of these signals is trained, analysed and tested to discover the accuracy of each disturbance and the overall accuracy. As a result, the accuracy of the classifier of power quality disturbances was more than 90% for each disturbance and for overall accuracy, which shows the success of DWT-FFNNs for power quality disturbances.

On the other hand, the novel approach of the detection algorithm and classification technique for power quality disturbances based on CEEMD and FFNNs for single and multiple situations is also promoted and conducted. In this section, it has been proven that CEEMD is able to overcome other transform limitations such as Fourier transform, with non-stationary waveforms which are detailed in this thesis and, more importantly, sensitivity to noise such as with DWT. Thereafter, the features of these disturbances are extracted to 8 level scenarios of IMFs and based on EMD, and a calculation of energy values is calculated for each disturbance, based on its instantaneous amplitude and instantaneous frequency.

The FFNN classifier is implemented for a database of random PQD generated signals. Results of this data are then analysed, trained and tested to evaluate the accuracy of the detection method and classification technique. As a result, the overall accuracy of the FFNN classifier indicates more than 98% of the performance of HHT and proves the robustness of the classifier.

# Chapter 5 - Experimental Recognition System Based on Online Power Faults

## 5.1 Introduction

In this chapter, comprehensive modelling and analysis are conducted to characterise the real-time power quality disturbances in power grids according to their dynamics. These disturbances appear in reality due to sudden faults that happen unexpectedly in power grids. These faults include line faults, transformer energising, induction motor starting and capacitor bank switching. Modelling of power quality disturbances, which include sag, swell, interruption and oscillatory transients, will be constructed based on various types of models which mainly cover most of the fault types in power systems.

This stage is important to provide researchers and engineers with the exact waveforms and data for these disturbances, which is highly theoretical and has a huge impact on understanding of the phenomena and power system behaviour. Furthermore, it is a proper approach of examination, and supports the hybrid methodology of detecting algorithm and classification technique (CEEMD-FFNN) that were proposed in Chapter 4 by providing more evidence from a different simulation environment and using online power faults.

In this chapter, a model of a power transmission system is introduced with realistic components. Thereafter, a model of each online power fault is constructed, connected to the system and simulated individually. The results for each of these models are analysed and recorded for the recognition stage. At the recognition stage, output waveforms of these faults are fed into the hybrid detection algorithm and classification technique in order to identify the type of disturbance in the transmission system. This chapter concludes with a summary of results achieved in both modelling of power quality disturbances and the recognition process.

**Table 5-1 Summary of causes and impact of power quality disturbances [79]**

| Category | PQD type | Causes | Impacts |
|---|---|---|---|
| **Transients** | Impulsive | Lightning | Transformer failures; Customer equipment damage due to low-side surges |
| | Low Frequency Oscillatory | Capacitor switching. | Tripping of ASDs and other sensitive equipment. Voltage magnification at customer capacitors. |
| | Medium Frequency Oscillatory | Travelling waves from lightning impulses. Capacitor and circuit switching transients. | Failure of customer equipment. |
| | High Frequency Oscillatory | Switching on secondary systems. Lightning-induced ringing. Local ferroresonance | Radiated noise may disrupt sensitive electronic equipment. High rate of rise oscillations may cause low voltage power supplies to fail. |
| **Short Duration Voltage Variations** | Sag | Local and remote faults | Dropouts of sensitive customer equipment |
| | Swell | Single-line-to-ground faults | Equipment overvoltage |
| **Long Duration Voltage Variations** | Overvoltage | Load switching off. Capacitor switching on. System voltage regulation. | Problems with equipment that require constant steady-state voltage |
| | Undervoltage | Load switching on Capacitor. Switching off System voltage regulation. | Problems with equipment that require constant steady-state voltage |
| | Interruptions | Temporary faults. Lightning stroke Tree limb falling across two conductors then dropping clear | Operation interruption, production losses, and revenue losses |
| **Voltage Imbalance** | Voltage Imbalance (Unbalance) | Single phase loads; blown fuses in one phase of a 3-ph capacitor bank | |
| **Waveform Distortion** | DC offset | Disturbance or asymmetry of electric power converters | Additional heating and loss of transformer life. Electrolytic erosion of grounding electrodes. |
| | Harmonics | Nonlinear loads | Misoperation of sensitive equipment. Capacitor failures or fuse blowing. Telephone interference. |
| | Interharmonics | Static frequency converters; Cycloconverter. Induction furnaces; Arcing devices. | Severe resonances on the power system as the varying interharmonic frequency becomes coincident with natural frequencies of the system. |
| | Notching | Normal operation of power electronics equipment | Misoperation of equipment. Equipment failure. |
| | Noise | Improper grounding Normal operation of electronic equipment. Arcing devices. Switching power supplies. | Disturbing electronic devices such as microcomputer and programmable controllers |
| **Voltage Fluctuation** | Flicker | Arc furnaces. Intermitted loads. | Lighting flicker Misoperation of sensitive loads |

## 5.2 Modelling Approach

Recently, architecture and daily lifestyle, along with developments in industry, have led to a huge expansion in power systems. Such expansion is accompanied by more power quality disturbances, which cause supply decline and economic costs. Voltage variation is a serious problem affecting most electronic equipment during operation. To analyse and understand these disturbances, it is necessary to detect power quality disturbances based on their causes. These approaches help decision makers to trace, analyse and devise effective solutions, leading to the safe running of grids, and reduction of oscillation and energy consumption; this works towards the guarantee of normal operational conditions [139].

Several approaches to enhance solutions used in the modern industry were widely introduced by researchers and engineers. These approaches are modelled by many platforms, such as MATLAB [140], which represents power systems with suitable components and faults, and their responses in real life.

Authors presented modelling approaches for simulating power quality disturbances and their waveforms using MATLAB. In their study, basic representation of disturbances was shown using online faults, but not in large-scale transmission or distribution power systems, where the impact of such faults on other components can be seen. Other platforms are also involved in the field of power quality analysis, such as PSCAD, which has the ability to simulate several types of power quality disturbances, as in [141] and [142]. Authors proposed a modified platform named ATP/EMTP [143] for the simulation of these disturbances.

It is clear in these studies that modelling of these disturbances in MATLAB is limited to the basic power system description, and does not take into account the power system concepts such as distance in power lines, generators and other components. Moreover, these scientific research works can represent distorted signals, but not in the same contraction of a power system.

Moreover, the majority of these studies do not take system waveforms in their results, and focus on the phasor representation of system or RMS values only. Therefore, in this section, a detailed model of a real-time power transmission system is developed for this purpose. This model includes two generators, one with a 5000 MW capacity and another with a 1000 MW capacity. These generators are linked to the power grid through high voltage transformers. This model is also provided with a load, bas bars and transmission lines with a distance of 700 km. Moreover, this model is converted into a continuous environment to provide an effective means to analyse distorted waveforms in the system. Each power quality disturbance is implemented using power fault model in the same approach as the system structure, shown in Figure 5-1.

The primary design of the system, as shown in Figure 5-2, is essentially considered mathematically to study transient stability, as in [144]. However, the work in this study was in phasor environment, where it cannot provide sinusoidal waveforms and mainly focused to examine different types of controllers.

One of the main considerations in this model is the representation of power signals as in reality, with a three phase system. It contains generators, transformers, electronic devices, relays and other related devices to analyse results such as scopes and measurement units.

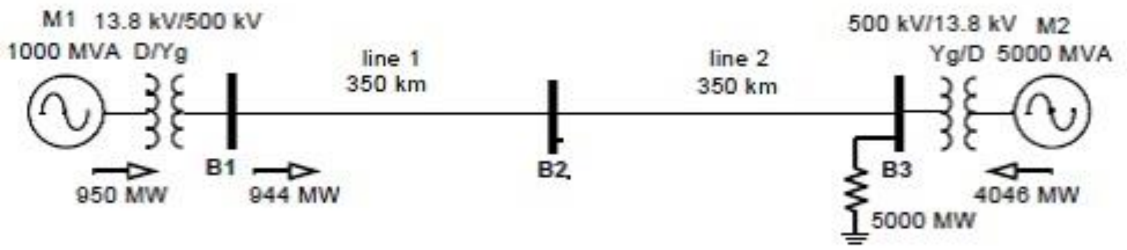


**Figure 5-1 Transmission power system**

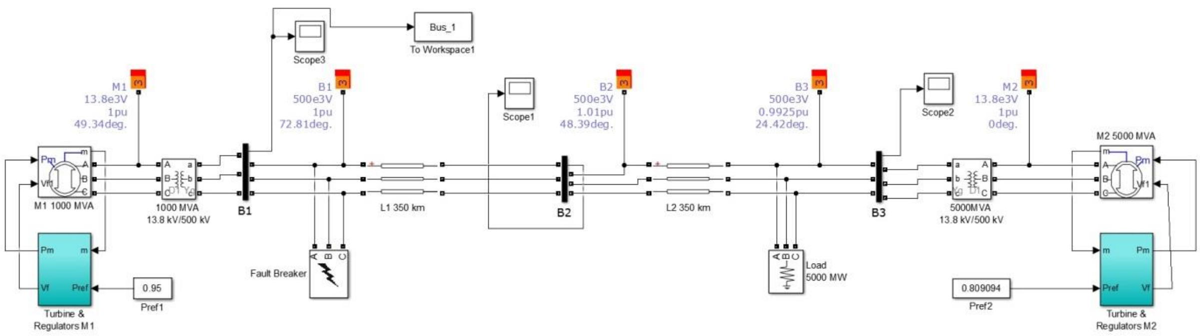


**Figure 5-2 Block diagram of the power system layout in this thesis**

## 5.3 Modelling of Sag Caused by Line Faults

The main reason for the existence of sag disturbances in power transmission and distribution systems is short line faults. The line-to-line fault is applied to the system by adding a fault model next to the bus bar (B1), which has a nominal base voltage of 500 kV, as can be seen in Figure 5-2. The fault block interface provides the ability to make the fault between phase and the other phase in the system.

It can also make the sag based on the fault between single phase and earth or both as shown from its components in Figure 5-5. Additionally, there are multiple possibilities in which sag disturbance can occur: two-phase-to-ground fault or double line-to-ground (LLG), two-phase fault which is also known as a line-to-line fault (LL), and single phase-to-ground fault or single line-to-ground (LG), as detailed in [145] and seen in Figure 5-3.

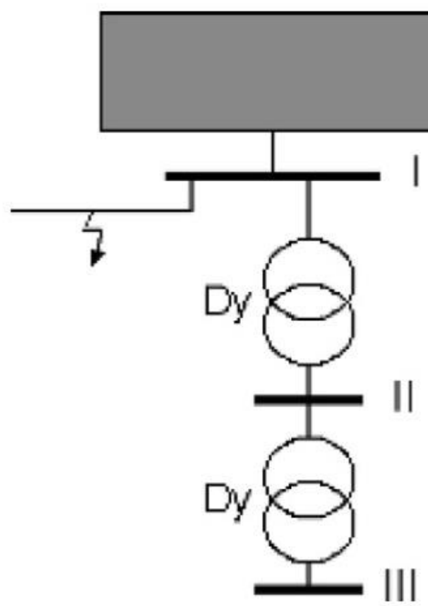


**Figure 5-3 Different voltage sag levels (I, II and III) based on the fault type [145]**

Sag is a short duration decrease in voltage magnitude, typically within 1 second. It is not possible to provide an exact range for the sag duration, but it is broadly accepted that its range in duration is from a half cycle to 1 minute. The voltage during this disturbance, named residual voltage in many scientific publications, has a magnitude below 90% of nominal values.

Mathematically, the case implemented in this study is a phase-to-phase fault between phases (a) and (b) at the bus, which is referred to as *the point of common coupling (between the customer and the fault),* or PCC. These equations are obtained for positive and negative sequence quantities during the sag disturbance (residual voltage) as used by as shown in Equations 5.1 and 5.2:

$$U_1 = \left(1 - \frac{Z_{S1}}{Z_{S1} + Z_{S2} + Z_{F1} + Z_{F2}}\right) E_1 \tag{5.1}$$

$$U_2 = \left(\frac{Z_{S2}}{Z_{S1} + Z_{S2} + Z_{F1} + Z_{F2}}\right) E_1 \tag{5.2}$$

where U1, U2 are the positive and negative sequences of retained voltage at the PCC; E1 is the pre-fault voltage at the PCC; $Z_{F1}$ and $Z_{F2}$ are the positive and negative sequences of the impedance between the PCC and the fault position; and $Z_{S1}$ and $Z_{S2}$ represent the source impedance at the PCC [79].

The sum and difference of positive and negative sequence voltages are used to describe the sag disturbance, as shown in Equations 5.3 and 5.4:

$$U_1 + U_2 = \left(1 - \frac{Z_{S1} - Z_{S2}}{Z_{S1} + Z_{S2} + Z_{F1} + Z_{F2}}\right) E_1 \tag{5.3}$$

$$U_1 - U_2 = \left(\frac{Z_{S1} + Z_{S2}}{Z_{S1} + Z_{S2} + Z_{F1} + Z_{F2}}\right) E_1 \tag{5.4}$$

Equation 5.4 is considered as the characteristic of voltage sag disturbance, as detailed in [146], and therefore the voltage will be as shown in Equation 5.5:

$$V = \left(\frac{Z_{S1} + Z_{S2}}{Z_{S1} + Z_{S2} + Z_{F1} + Z_{F2}}\right) E_1 \tag{5.5}$$

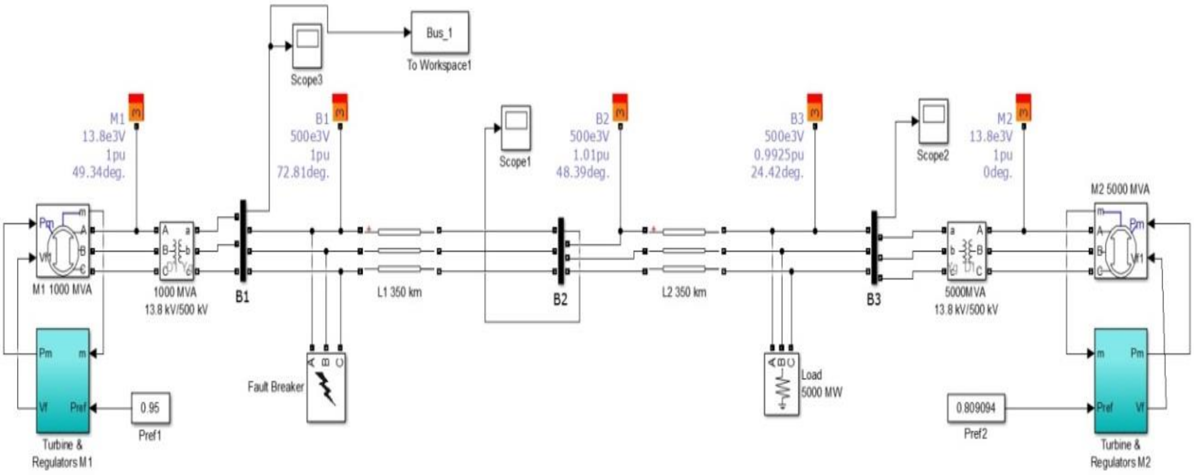


**Figure 5-4 Power system with a line fault causing the sag event**

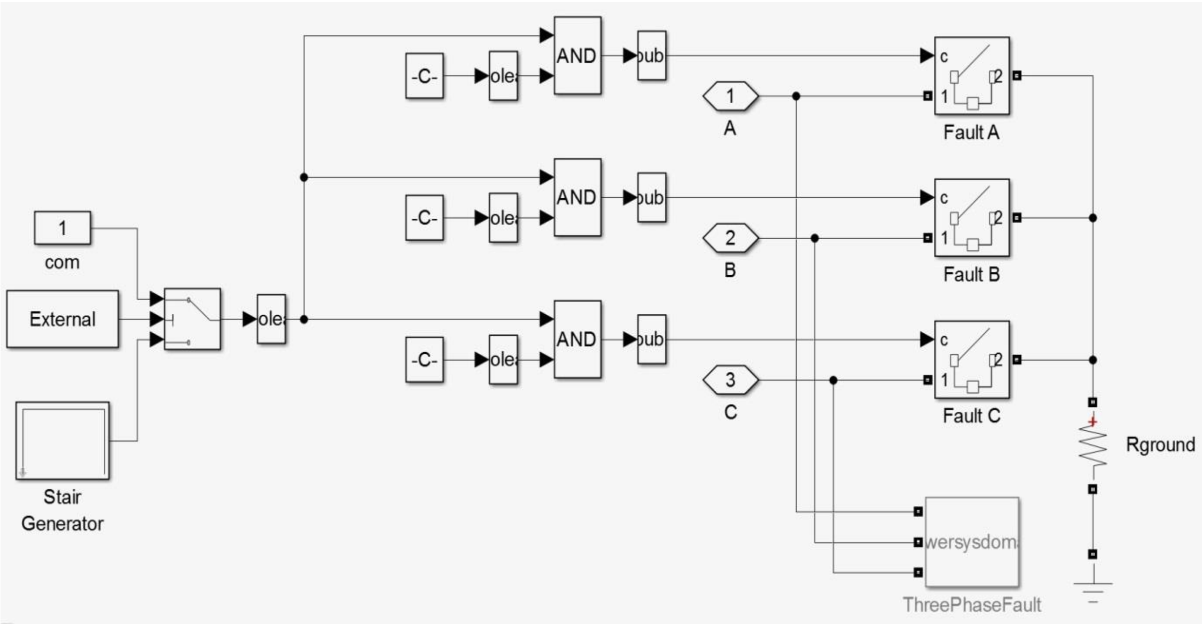


**Figure 5-5 Line fault components**

Inside the configuration of the fault setting block, the parameters are adjusted to reach sag phenomena. First, the fault has occurred between two phases in the system. Thereafter, the time needed to see this waveform is adjusted to be 0.1 second, which starts from t = 1.0 second. Other settings take into account fault resistance and more, as can be seen from Figure 5-6. A display is connected to the bus bar (B1) in the system, and the result of the fault employment for three phase voltages in a continuous environment can be seen in Figure 5-7.

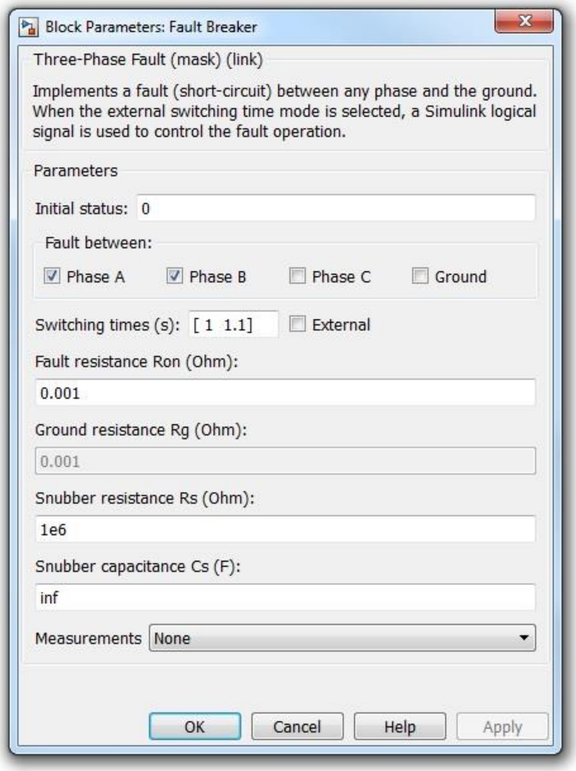


**Figure 5-6 Fault parameter box adjusted for sag phenomena**

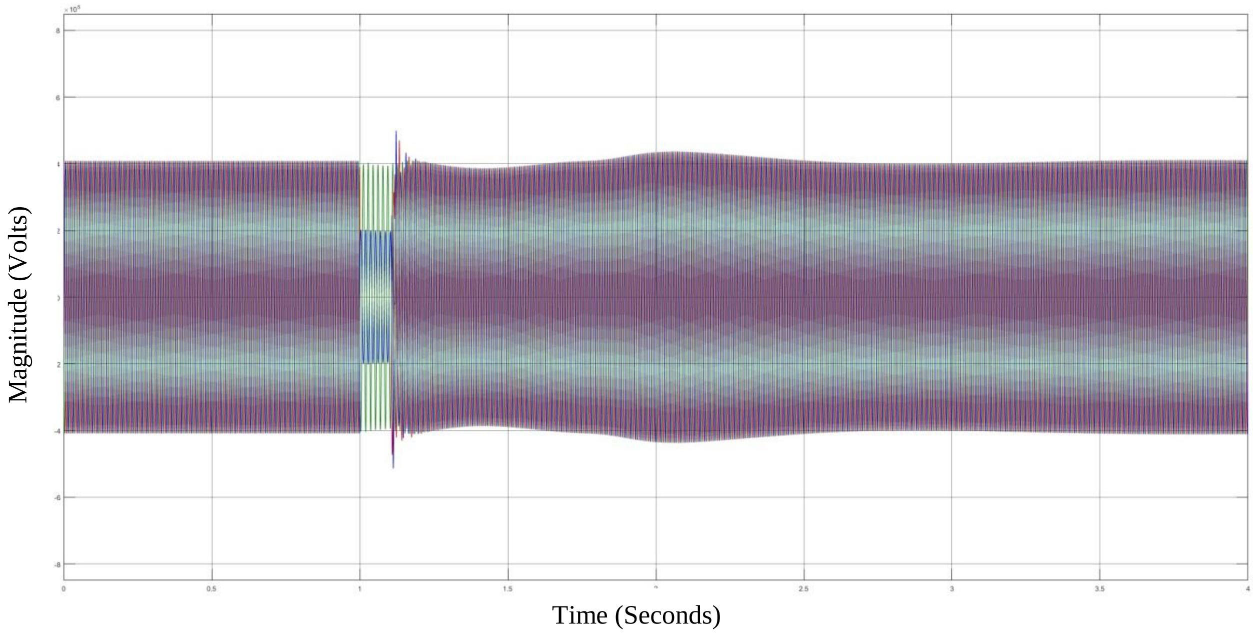


**Figure 5-7 Output results for sag disturbance in the power system**

As can be seen from the system results in Figure 5-7, the bus (B1) experiences the sag disturbance, which is located from 1.0 to 1.1 second. The fault has the blue signal of the phase (A) in the system. Based on the sag definitions described previously in terms of magnitude and duration, a sag disturbance is modelled successfully with a small raise in the other phases' magnitudes, before shortly recovering to their nominal conditions.

## 5.4 Modelling of Swell Caused by Large Load Switching

The main causes behind the presence of swells in power grids include a single line-to-ground fault, energising capacitor banks, and large load switching [110]. Swell can also be associated with circuit faults in a power system, which was described previously. the case employed to analyse swell disturbance in this research is done by implementing a three phase large load switching model, which is developed in the model and localised primarily, as shown in Figure 5-8.

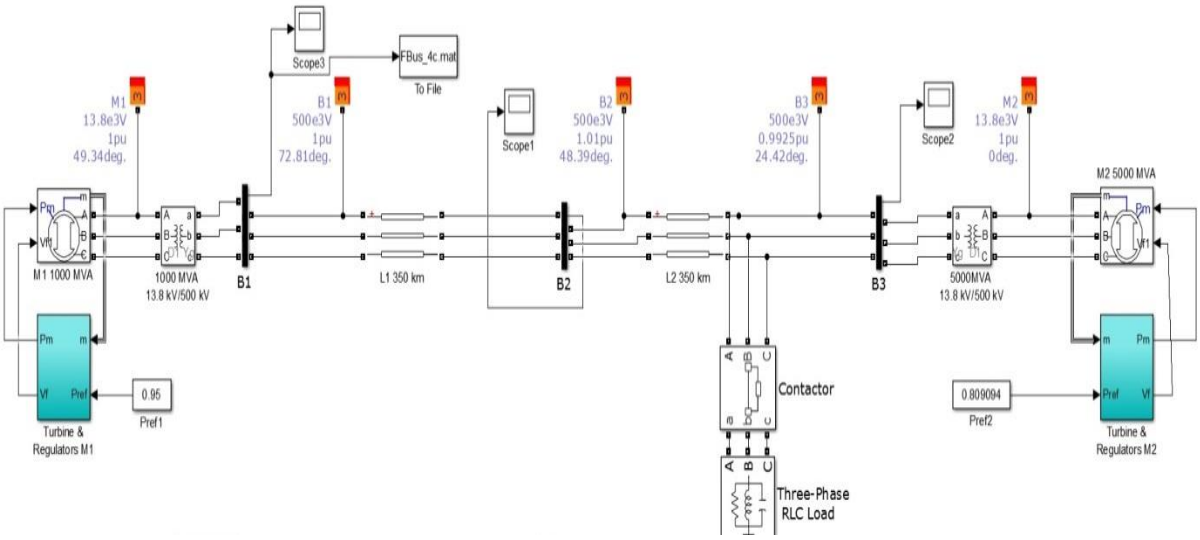


**Figure 5-8 Model with large load switching in the system which shows swell disturbance**

The large load switching blocks are developed on the end of the transmission system, and adjusting parameters are divided into two steps, as shown below in Figure 5-9. First, the switching step is conducted for all three phases with an open circuit at t = 1.0 second. Secondly, the second block is developed for the three phase RLC load configuration. The procedure is started by opening the three phase breaker at t = 1.0 second, causing swell in the system. The result of this stage can be seen in

Figure 5-10, where it is obvious that a swell case is recorded and consequently results in unbalancing the system.

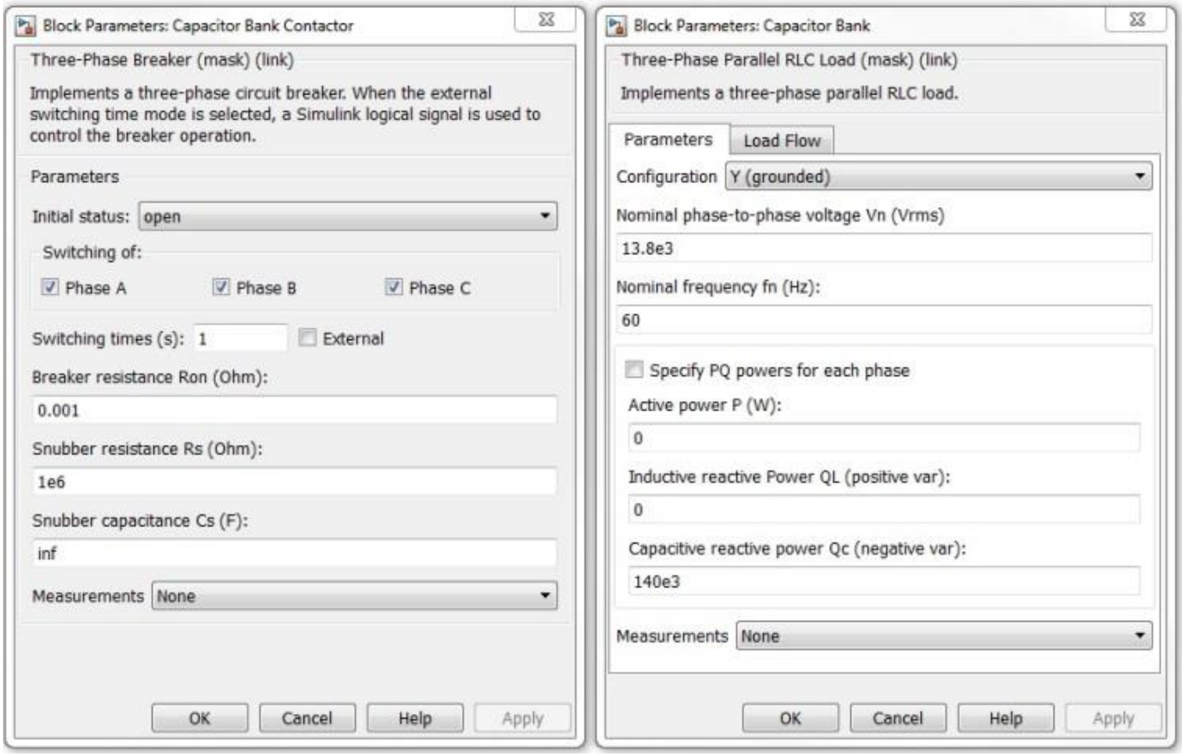


**Figure 5-9 Parameter blocks of large load switching**

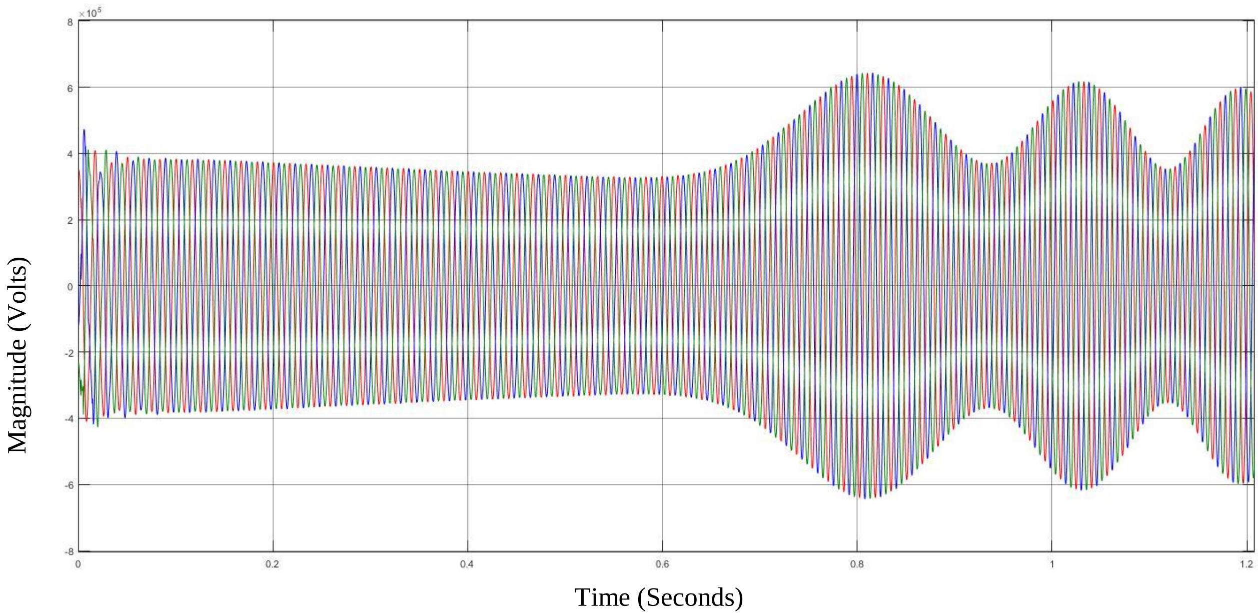


**Figure 5-10 Result of large load switching and the swell phenomenon**

## 5.5 Modelling of Interruption Based on Three Phase-to-Ground Fault

Interruption disturbance, as described previously, is a case where voltage magnitude is close to zero or even zero, which is identified between 1% and 10% of the nominal voltage magnitude. Causes of interruptions include [79]:

- Opening of the circuit breaker in the system or a fuse due to earth fault.
- Accidental operation of electronic devices, which might be the result of a tripping signal generated in the system by a protection relay.
- Disconnecting part of the system or performing maintenance in the grid.

In this section, a three phase fault is developed in the system, as shown in Figure 5-11. This fault is connected to the system with a certain configuration setting to reach interruption phenomena in the transmission system. All three phases are used in this fault and connected to the ground. The voltage decays to zero less than 1 second after the opening of the fault.

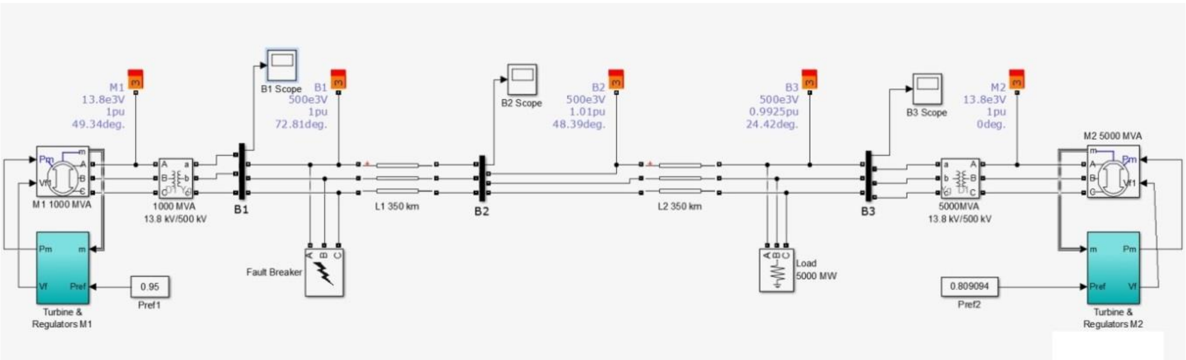


**Figure 5-11 Interruption based on three phase fault**

There were several attempts to adjust the time duration of the interruption in the system. The reason behind this is that introducing the interruption leads to unstable operation in the grid. Moreover, in some cases interruption might cause overvoltage in the system, or even leads to a blackout in many cases. It is concluded that it is difficult to keep the system stable with such a fault. In this case the configuration block is adjusted to be within 0.05 second, as shown in Figure 5-12.

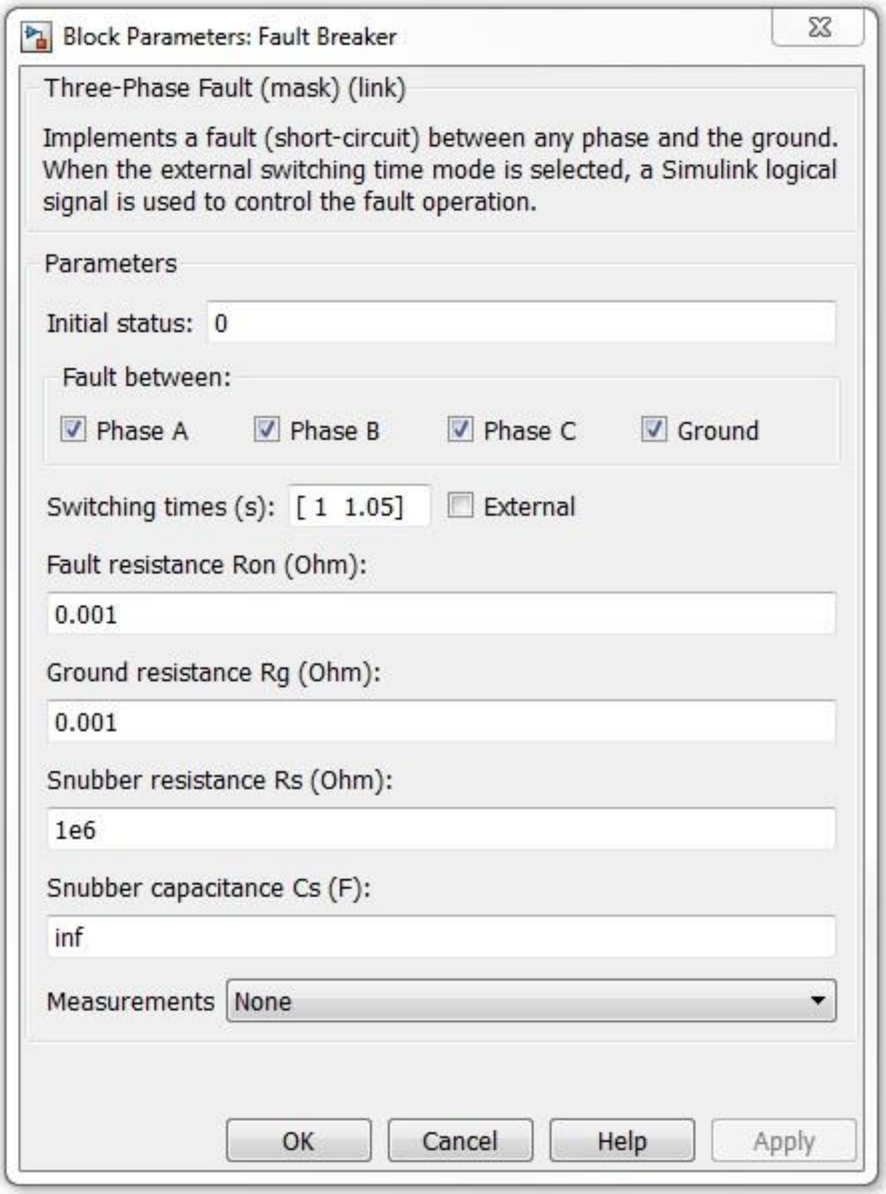


**Figure 5-12 Configuration block for three phase faults which cause interruption**

The result of this fault is an interruption disturbance, as shown in Figure 5-13. As shown in the result obtained, the magnitude of voltage is zero for all phases in the system during the fault time. A sudden rise follows for the three phases, and another slight swell is recorded after that. It is noticeable that, to keep the system stable, the maximum value for time is supposed to be less than 0.1 second in the fault configuration. Furthermore, once the duration setting of time is more than 0.1 second, then the result is unstable performance, as shown in Figure 5-14, where the time of the fault is adjusted in the configuration by 0.1 second.

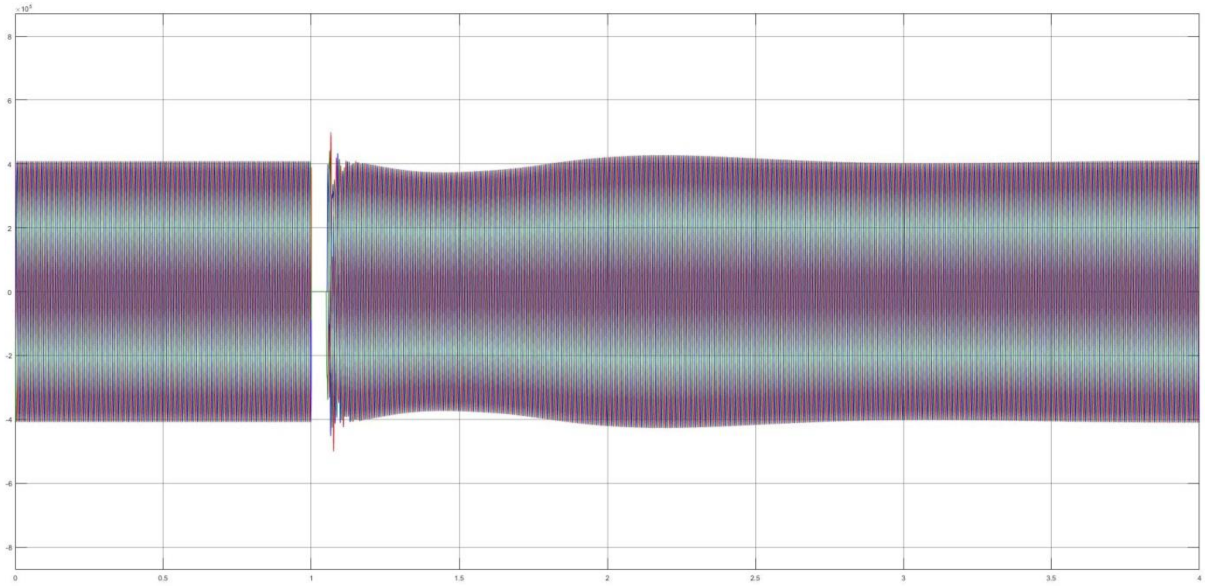


**Figure 5-13 Result of three faults to ground which cause interruption**

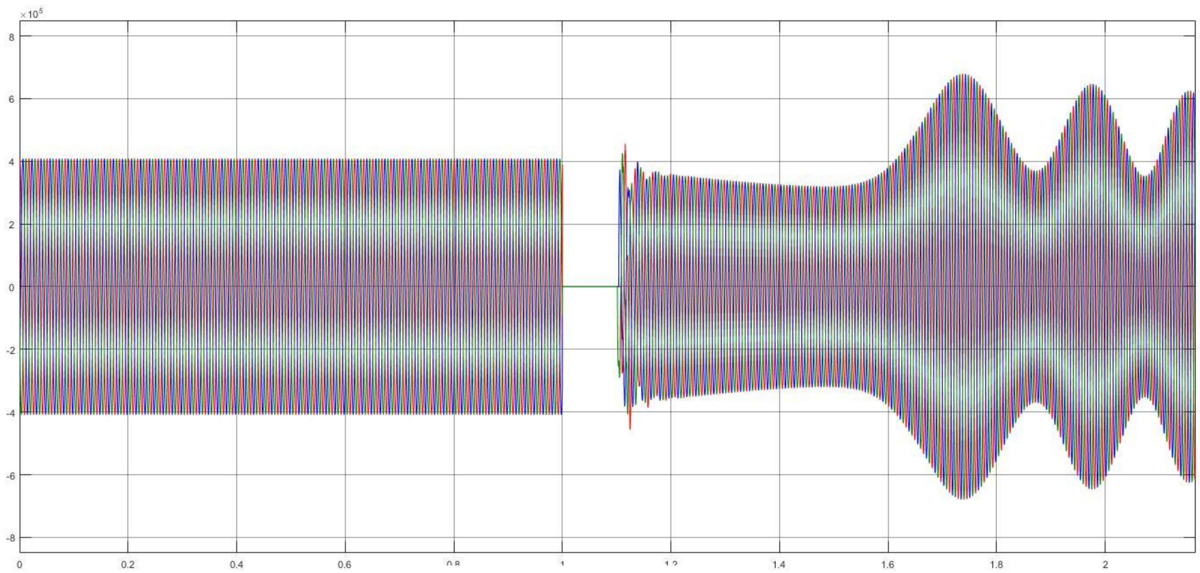


**Figure 5-14 Result of three faults with 0.1 second time**

As shown in Figure**,** the system response to the fault is the interruption in the three phases in the transmission system but the system experienced multiple changes in voltage magnitude when the fault was cleared. First, slight sag resulted immediately after the interruption, and thereafter, multiple swells in the system which led to unstable performance with up-normal operation conditions, and eventually the blackout was recorded just as time t= 2.10 second.

## 5.6 Modelling of Oscillatory Transient Based on Capacitor Bank Energising

Transient disturbance is used generally to describe any voltage change that has a short duration but is considered to be either one half cycle or one cycle as the short duration required, as specified in [147]. Transient can result from transformer inrush current, which lasts for several seconds. It can also occur from lightning strokes in power systems. Moreover, another important reason to identify transient is the switching of capacitors in power grids. Notable switching types [79] are as follows:

- Capacitor energising
- Capacitor de-energising
- Inductor energising
- Inductor de-energising

The most common cause in the power quality field is capacitor energising, which is going to be the case used in this research. It results in immediate changes in the voltage waveform, which reaches zero followed by a frequency oscillation in the signal. This oscillation can be obtained mathematically by drawing the relationship in the circuit shown in Figure 5-15 and Equation 5.6:

$$e(t) = u_L(t) + u_R(t) + u_C(t) = L\frac{di}{dt} + Ri + u(t) \tag{5.6}$$

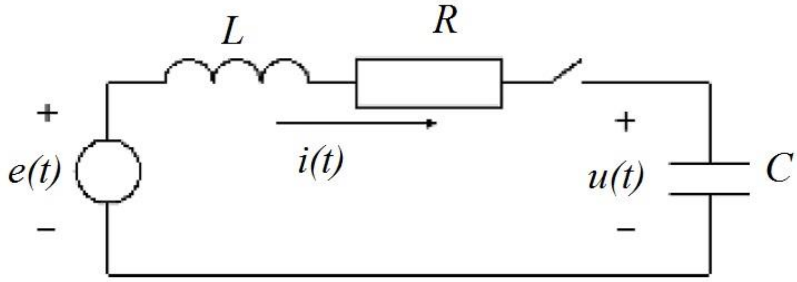


**Figure 5-15 Capacitor-energising circuit [79]**

Thereafter, adding the source voltage results in Equation 5.7:

$$e(t) \ = \sqrt{2}E\ cos\ (\omega_0 t + \phi) \tag{5.7}$$

and consequently, the current in the circuit by adding the capacitor as shown in Equation 5.8:

$$i\ (t)\ =\ C\frac{du}{dt} \tag{5.8}$$

As a result Equation 5.9 describes the voltage:

$$\sqrt{2}E\ cos\ (\omega_0 t + \phi)\ =\ LC(t)\ \frac{d^{2u}}{dt^2} + RC\frac{du}{dt} + u\ (t) \tag{5.9}$$

Thereafter, some factors are eliminated, as detailed in [79], and by introducing the amplitude $A_{tr}$ and phase angle $\phi_{tr}$ of the transient, solutions are gained from initial conditions and the amplitude of the transient will be expressed by Equation 5.10:

$$A_{tr} \approx\ \left| U\sqrt{2}\ |cos\ \ \psi| \right| \tag{5.10}$$

where $\psi$ is the switching angle of the oscillatory transient, which is going to be large for $s\ \ \psi = 1$ .

In this section, a capacitor bank energising model is developed next to the bus bar (B1) in the power transmission system, as shown in Figure 5-16. It is implemented to present the oscillatory transient disturbance as suitable for the grid, as mentioned in [148]. In the capacitor bank configuration block, the switching is adjusted to be for all three phases, when it reaches t = 1.0 second with open status for the circuit, as in Figure 5-17.

The capacitor bank is located next to the bus bar, and the instantaneous waveform scopes are located at the B1 and B2 buses for measurement. The 500 kV capacitor bank at the B1 bus has a capacity of 140 kVAr. Such capability can compensate the power factor for inductive load.

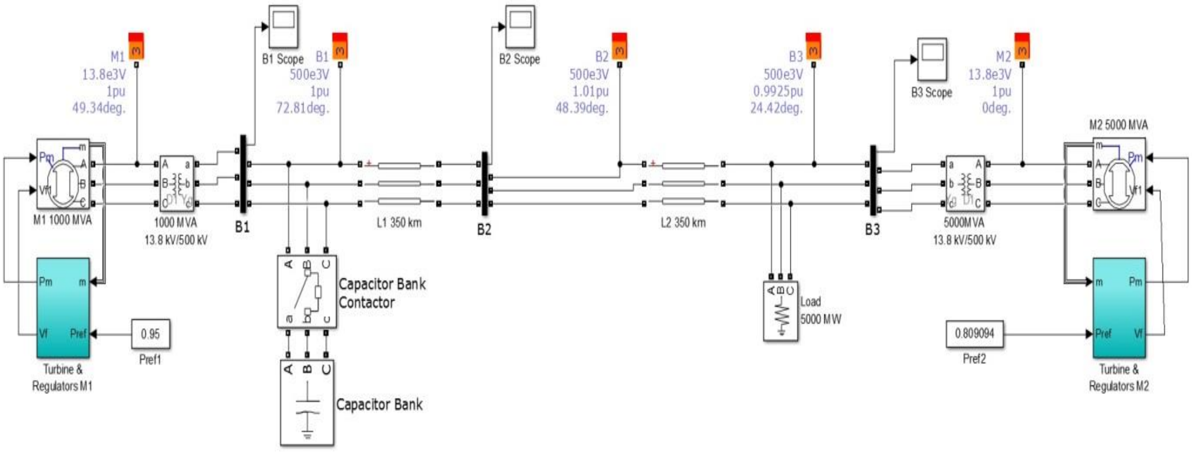


**Figure 5-16 Model for capacitor bank energising causing oscillatory transient**

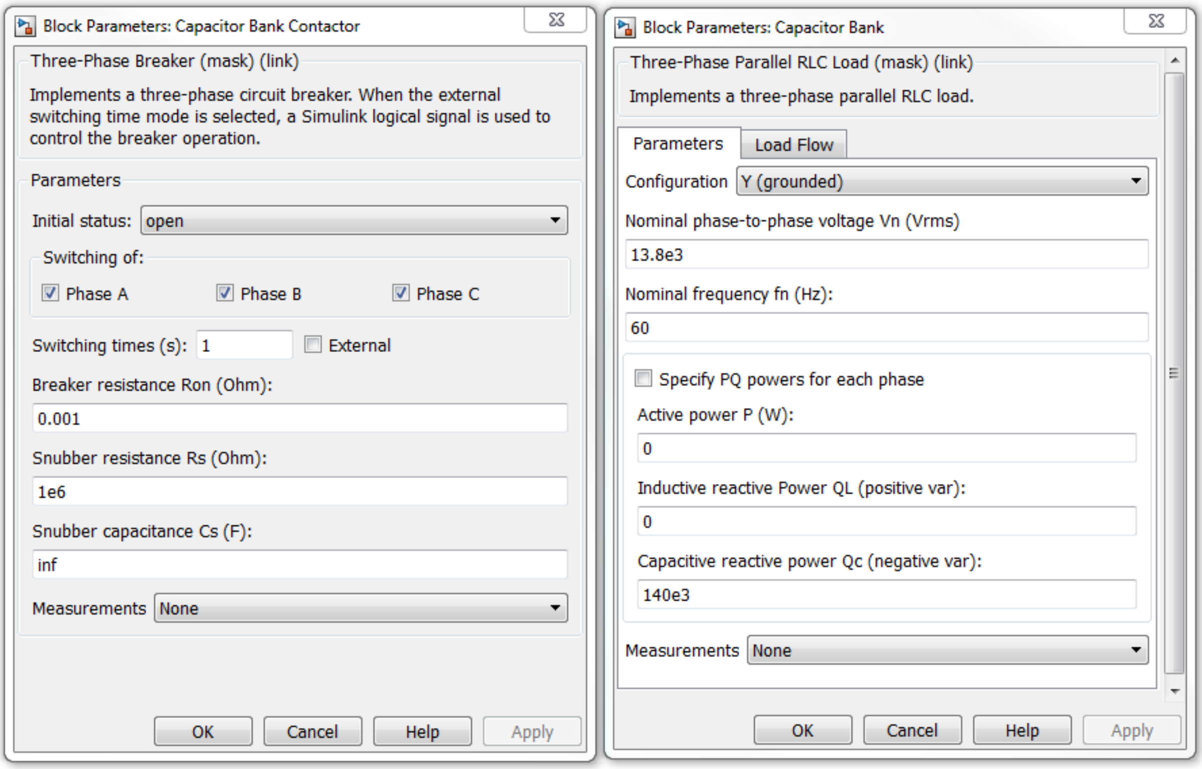


**Figure 5-17 Parameter configuration blocks for the capacitor bank and its contactor**

Results are recorded and presented as shown in Figure 5-18, with the obtained three phase voltage waveforms from bus bar B1. The oscillatory voltage transient can be seen at t = 1.0 second. The transient frequency is controlled by the size capacitor bank, so the oscillation settles down, depending on the size of the real power load.

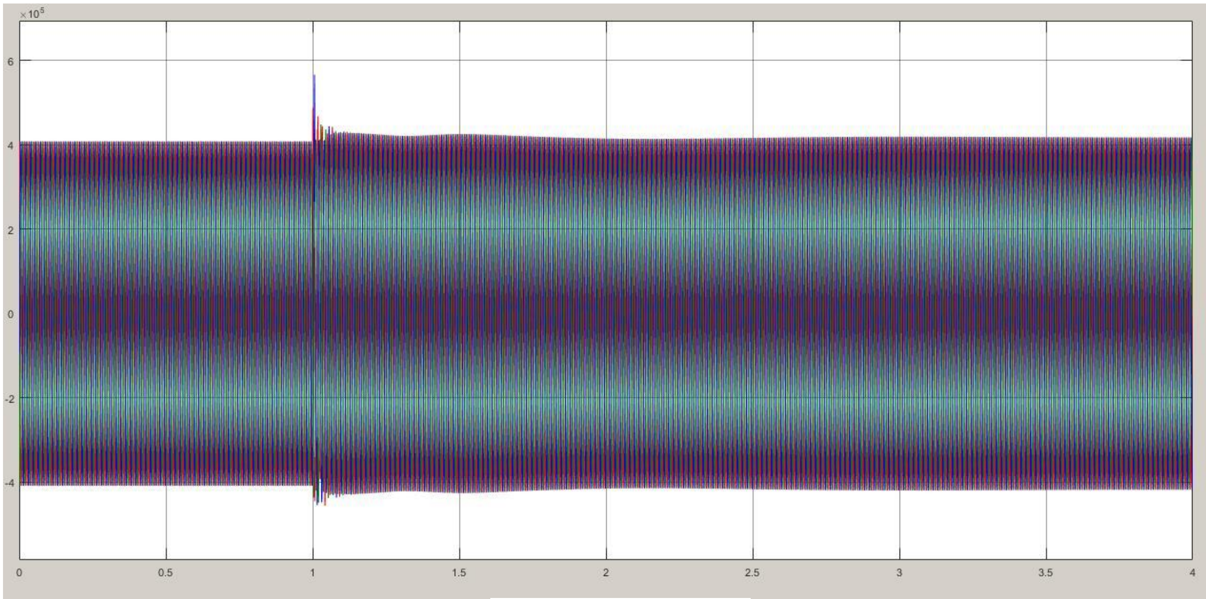


Magnitude (Volts)

Time (Seconds)

**Figure 5-18 Oscillatory transient disturbance caused by capacitor bank energising (full operation)**

Providing additional understanding, a maximising view is conducted, as shown in Figure 5-19. It is obvious that phase (a) (coloured red) crosses zero twice in the same time frame before completing its circle, or, in other words, twice in one cycle of normal operation.

A similar scenario is also observed for the other two phases, as shown in Figure 5-20, where the other phases have suffered from the same cause of the capacitor energising. Three phases of the power system crossed point zero at t = 1.0 second, which resulted in the oscillatory transient disturbance in the whole system.

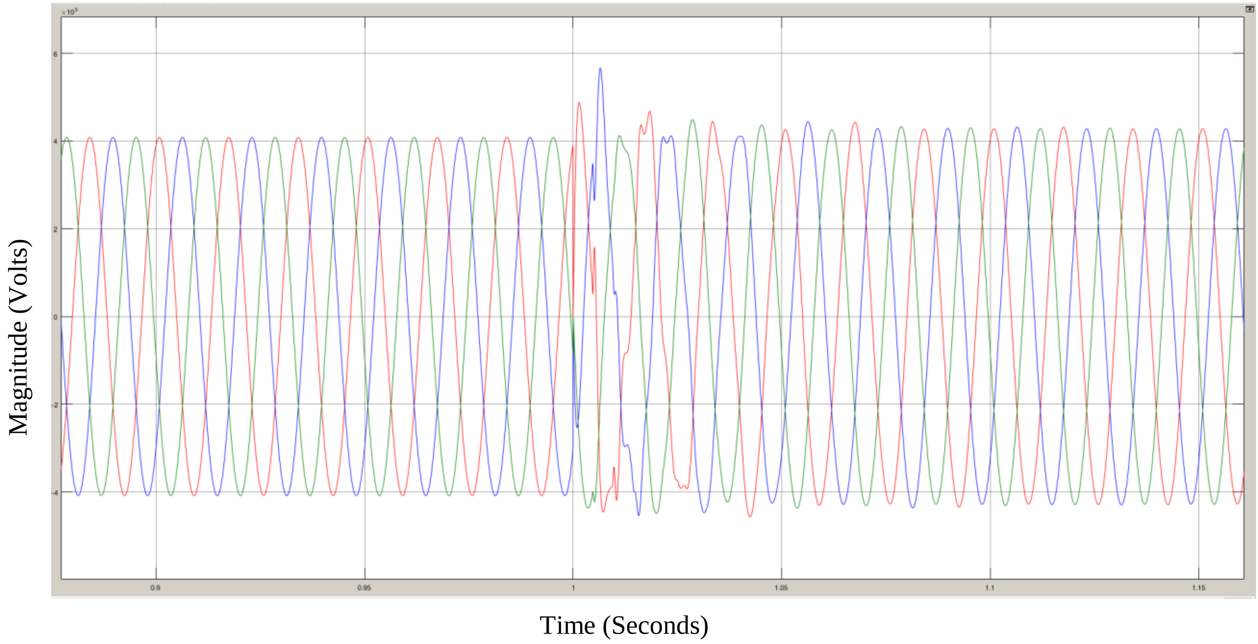


**Figure 5-19 Oscillatory transient disturbance (at Time = 1.0 sec)**

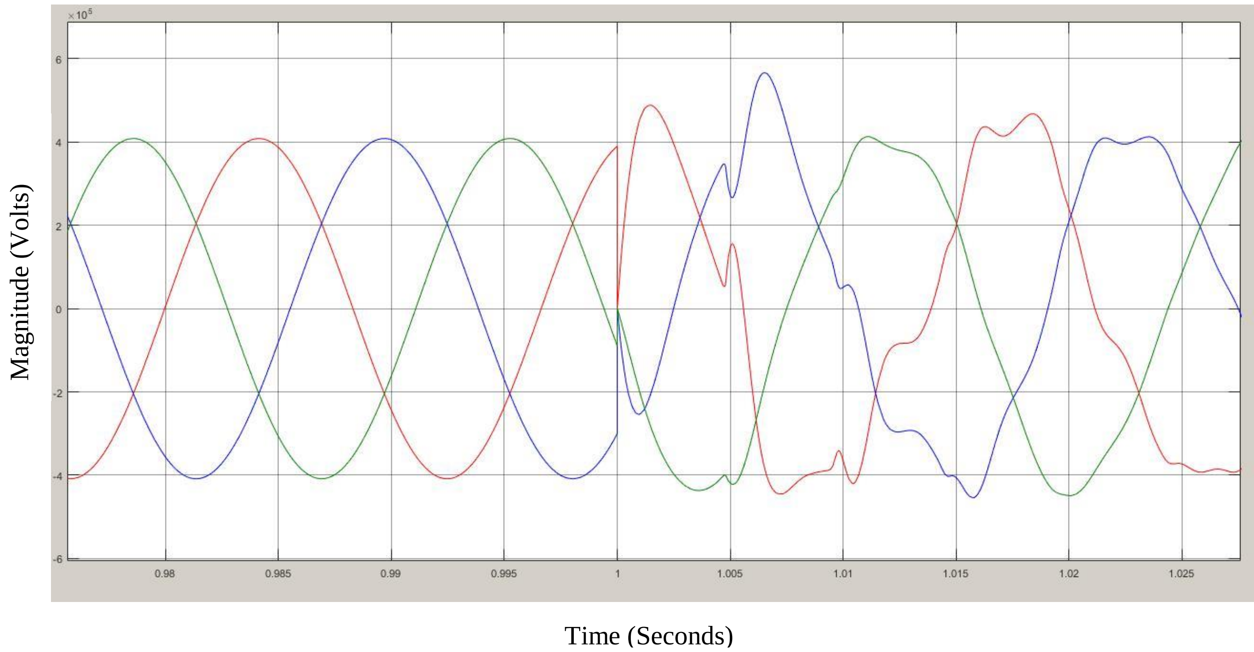


**Figure 5-20 Oscillatory transient disturbance for three phases caused by capacitor bank energising**

## 5.7 An Experimental Recognition System Approach

In this section, results and data of modelled power quality disturbances in power transmission systems due to power faults are collected from measurement scope units in each scenario. Each piece of data selected came after many attempts to reach optimum phenomena for each disturbance. Thereafter, each piece of data is stored and applied through a distinct program script to be analysed by the hybrid detection and classification system (CEEMD-FFNNs).

The goal at this stage is to examine the detection algorithm and classification, and its ability to recognise power quality disturbances in a much wider environment, where there is more than one disturbance, due to many factors in the power transmission system.

Signals data gathered for each system result is fed to a network built by the FFNNs technique. This process has the ability to apply to each of the three phases, where it organises each signal separately. After that, the FFNNs technique shall provide its decision regarding which type of disturbance the signal belongs to.

## 5.8 Results and Discussion

### 5.8.1 Recognition of Sag Disturbance

The system results for the sag disturbance modelling in the power transmission system are collected from the bus bar (B1) and named (FBus_1). Then they are recalled and placed in the program prepared for this step. The code for this process validates the phenomena of each phase against all disturbance characteristics in CEEMD-FFNNs, and the recognition result for sag disturbance is shown below in Figure 5-21.

The results show that CEEMD-FFNNs is able to recognise sag disturbance and its time as well. It also shows the significant appearance of harmonics, which is due to the large load in the transmission system. This means that even if efforts were focused to recognise the sag disturbance which was completely successful, it would also provide recognition of harmonics and consequently non-linear load in the system, which is implemented in the transmission power system.

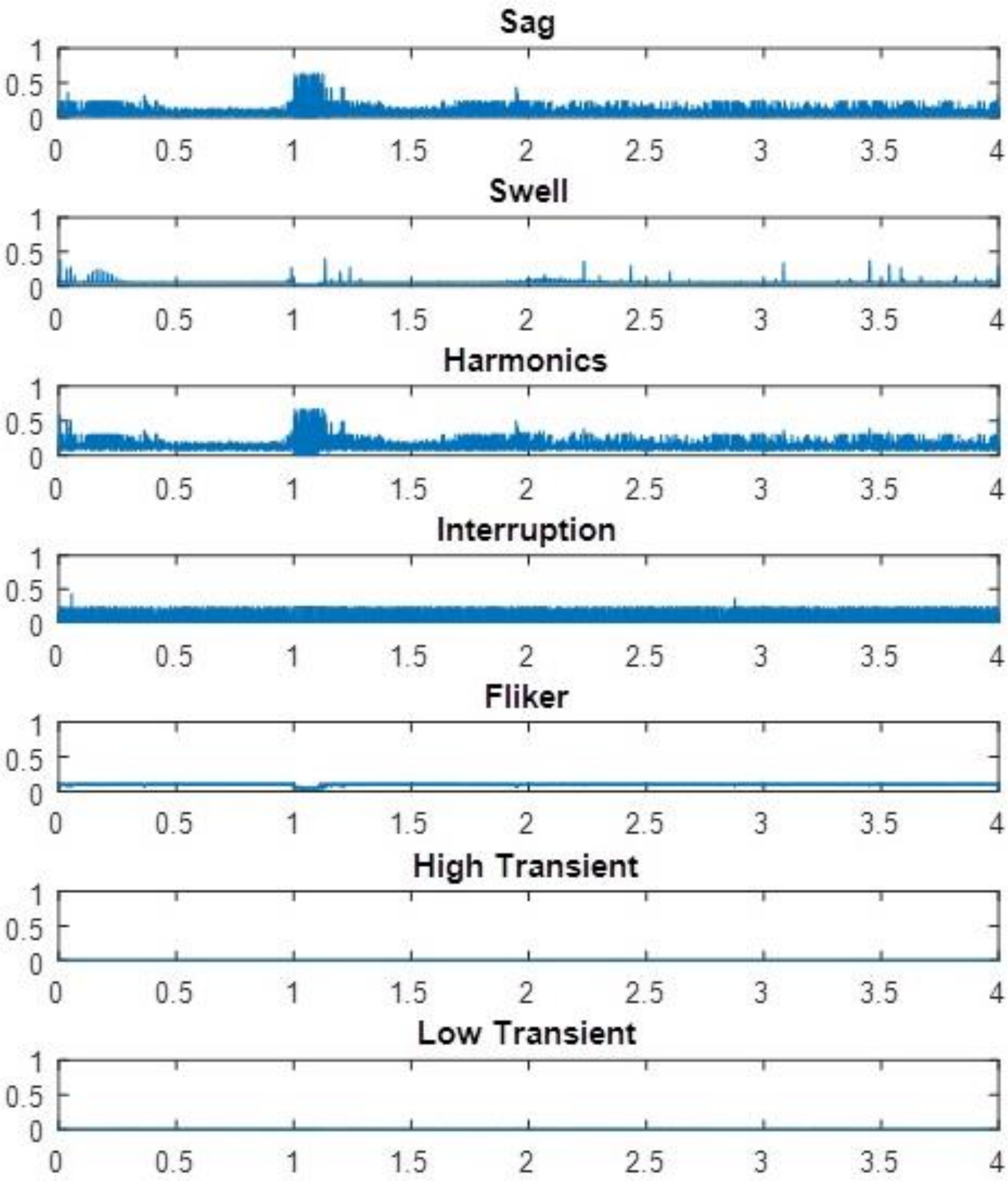


**Figure 5-21 Recognition result for sag disturbance**

### 5.8.2 Recognition of Swell Disturbance

The system results for the swell modelling are collected from the bus bar (B1) and named (FBus_4). This process validates the phenomena through the code prepared for this step for each phase against all disturbances in CEEMD-FFNNs and the recognition result for swell disturbance, as shown below in Figure 5-22. The results show that CEEMD-FFNN has recognised swell disturbance and its time as well. Moreover, it also shows a significant appearance of harmonics, which is due to the large load in the system. This means that even if efforts were focused to recognise swell which were completely successful, it would also provide recognition of harmonics in the system, which is implemented in the transmission power system.

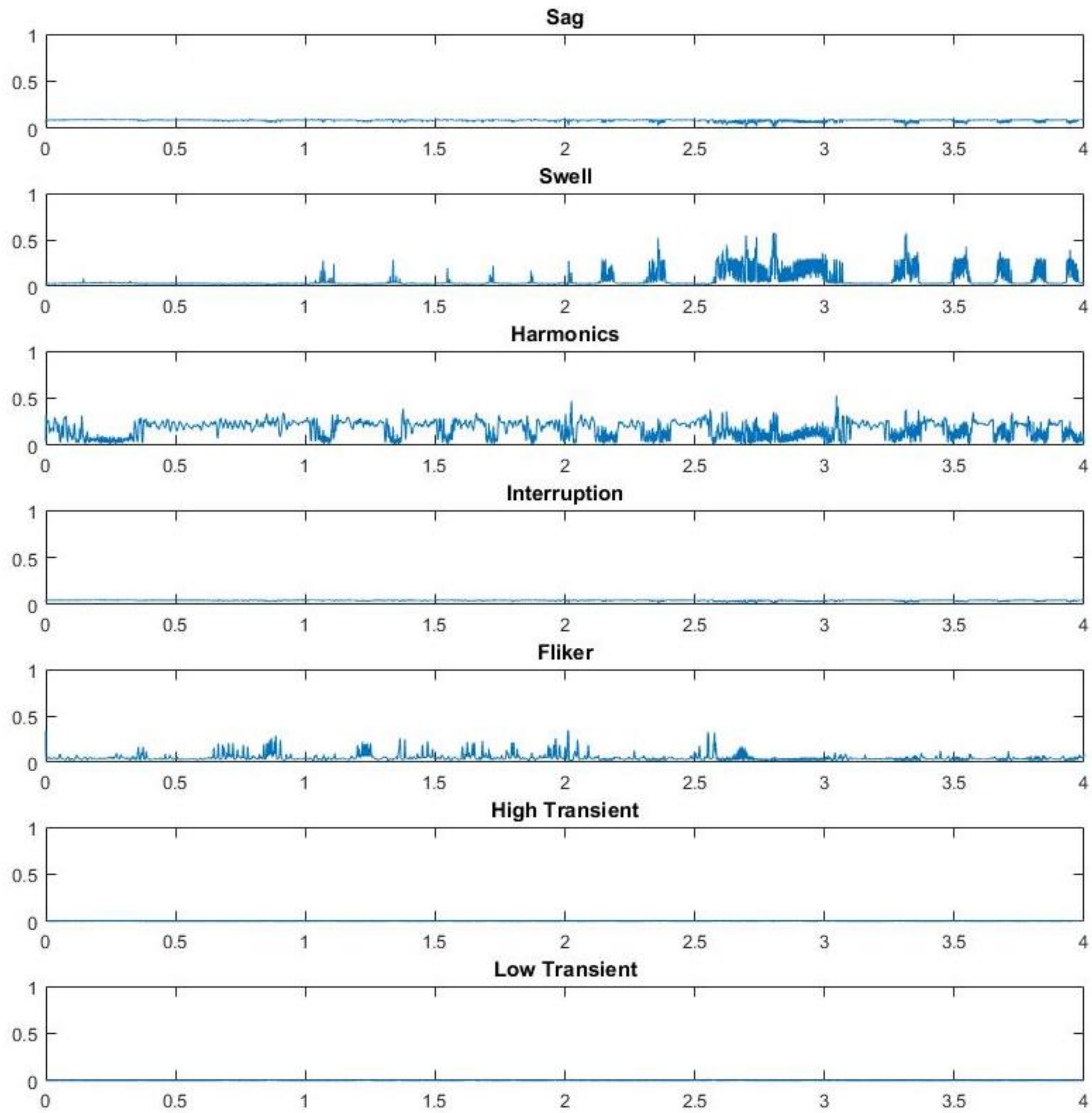


**Figure 5-22 Recognition result for swell disturbance**

### 5.8.3 Recognition of Interruption Disturbance

The system results for the swell modelling are collected from the bus bar (B1) and named (FBus_2). The code for this process validates the interruption phenomena of each phase against all disturbances in CEEMD-FFNNs and the recognition result for interruption disturbance, as shown below in Figure 5-23. The result shows that CEEMD-FFNNs has recognised interruption phenomena and its time as well. However, due to the large load in the system, it also showed the presence of harmonics.

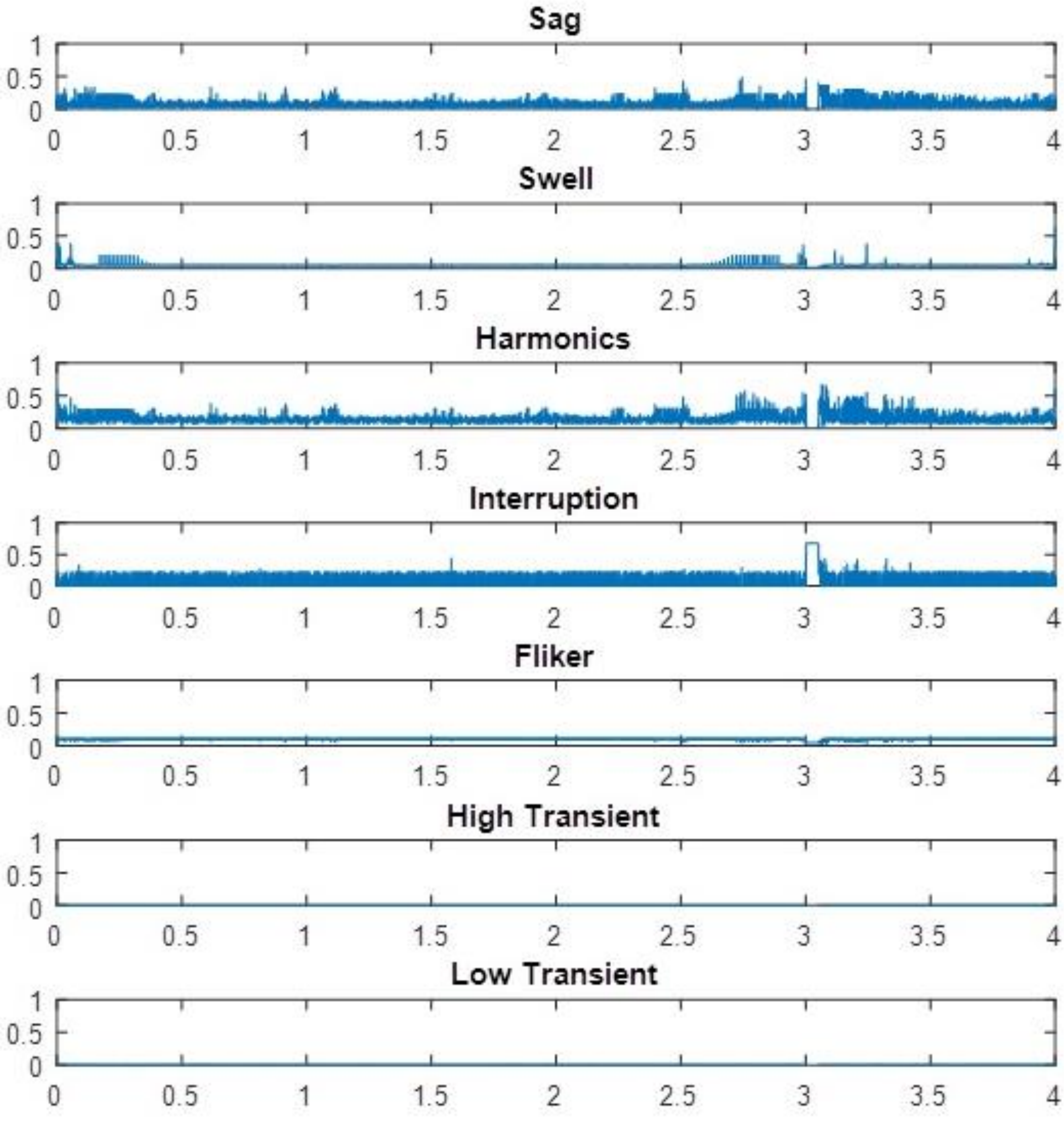


**Figure 5-23 Recognition result for interruption disturbance**

### 5.8.4 Recognition of Oscillatory Transient Disturbance

Results of the transmission system for the oscillatory transient modelling are collected from the bus bar (B1) and named (FBus_3). This process confirms the phenomena of each phase against all power quality disturbances in CEEMD-FFNNs and the recognition result for oscillatory transient, as shown in Figure 5-24**.** The result shows that CEEMD-FFNNs has recognised sag disturbance and its time as well. However, harmonics is also present in this step as well, based on the large load in the transmission system.

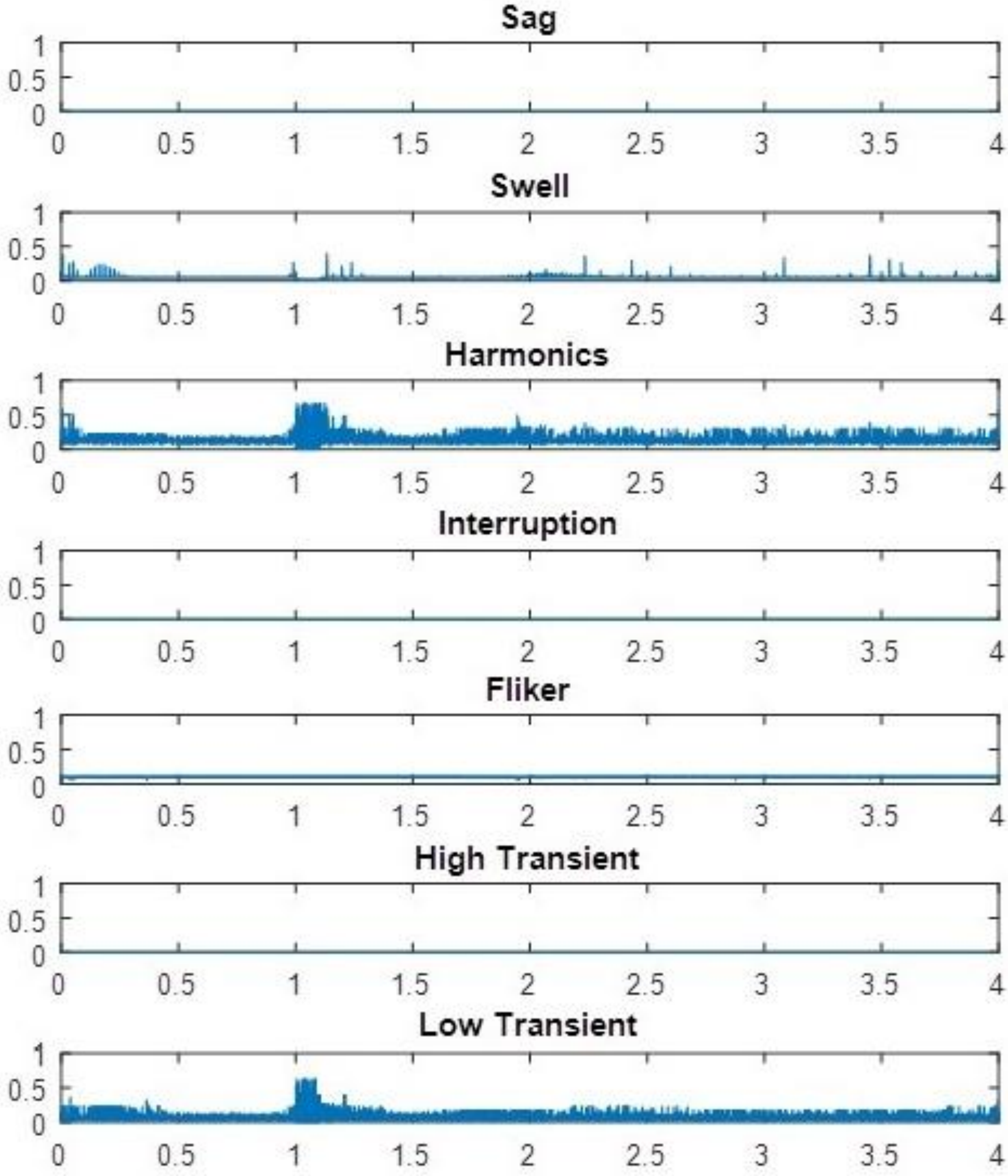


**Figure 5-24 Recognition result for transient disturbance**

## 5.9 Summary

In this chapter, models of short duration power quality disturbances due to faults were developed in a specific system. First, a transmission power system was developed and a power line fault employed. The fault was adjusted to be a line-to-line fault, and the time of this event was set to be 0.1 second. The result of the system response to this change was recorded, and confirmed sag disturbance in the system, according to sag characteristics.

A large load switching model was utilised in the system to represent swell phenomena according to their characteristics. In the configuration blocks, parameters were adjusted next to the bus bar, and results of the system were analysed. The waveforms of the system confirmed swell disturbance in the transmission system. Moreover, the large load switching model was moved and the line fault model retained. The parameters of configuration blocks were adjusted to three phases to ground. The time was also set to be 0.05 seconds. Results confirmed the interruption phenomena in the system precisely for the period from t = 1.00 to 1.05 second. Furthermore, the capacitor bank model was realised in the transmission system. In this step, the capacitor bank energising was built based on the three phases, and switching time was at t = 1.0 second. The result confirmed the oscillatory transient disturbance in the system. As detailed, three phases suffered oscillation and crossed zero twice in one cycle.

Thereafter, an experimental recognition system approach was built based on a special script to identify power quality disturbances, which were achieved with the results discussed. Each one of the system’s waveforms was applied to the code, and the results analysed. This process recognised disturbances occurring in the power transmission system successfully. This process was based on the hybrid detection and classification approach (CEEMD-FFNN) constructed in the previous chapter. To conclude these procedures, this chapter has proven the ability to recognise power quality disturbances in a power transmission system, and shown the robustness of such an algorithm even in other environments.

# Chapter 6 - Power Quality Improvements

## 6.1 Introduction

In this chapter, a comprehensive investigation is conducted into the control of power quality disturbances. Most devices used in controlling power quality disturbances are discussed, along with their limitations. Recent strategies of control are also investigated and discussed. Thereafter, the principle of power system stability is introduced, with its divisions and time durations. Furthermore, a mathematical base of conventional power system stability controllers is explained, as well as the relationship between power generators and these stabilisers. The goal of this stage is to improve system responses when disturbances occur in the system, which are specified in this research as sag, oscillatory transient and harmonics disturbances.

A model of a power transmission system with specific fault (phase-to-phase) is planned to show the sag disturbance in real time, and the harmonics disturbance is a consequence of the non-linear load built in the system. Results of the system are then discussed, investigated and used to instigate improvement in developing more stabilised power system. Furthermore, a proposed set of harmonics filters is then implemented in certain locations in the system. Results of this stage are also presented along with any achievements. Another comparison analysis is conducted in terms of control of the system. In this stage, the controller undergoes tuning and optimisation processes, after adding the harmonics filters bank to the system. Results of the system response are presented, and the power quality improvement achieved is also presented and discussed.

## 6.2 Power Quality Control

The expression ‘power quality control’ comes from the decision-making stage, which is considered the final stage of the quality cycle. It broadly includes processes of maintaining the power delivered at normal conditions. It also includes the controller selection, and design and installation of any supportive hardware equipment or software in the electrical power systems. Furthermore, the control stage involves processes covering all parts of the network, from the generation plant, through the transmission level, to the last customer at the distribution level. The result of this stage is to ensure a clean and efficient electrical power supply [149]. It is known that controllers and equipment have been evolving and becoming more reliable recently. However, it is obvious that power quality disturbances have increased rapidly nowadays, with more complexity, and more importantly, greater economic losses in electrical power systems. Moreover, complex conditioning systems have been installed over traditional resistive heaters, and adjustable speed drives have been broadly used for more control of motors. Modern processors and alternative devices are more sensitive to power quality disturbances, due to their design or the combined communication features. The devices' sensitivity to power quality disturbances is due to the use of semiconductors in their manufacturing, and the growth of microprocessors based in electrical power systems. The revolution in the 90s, regarding the use of computers and other communication tools, also increased the range of interference of several industrial processes. Furthermore, the sensitivity of this equipment to power quality disturbances particularly to short voltage sags and effects caused by its nature of operation, such as harmonics and overheating – has resulted in an increase of attention to controlling power quality.

Deviations in modern power supply concepts have helped to place control of power quality as the focus of concentration. Nowadays, any disruption of production or operation is related to higher financial costs and losses. A key factor regarding the severity of power quality issues is the volume of investments related to this field. Industrial and commercial sectors and companies are very keen to invest capital to improve the quality of the power supply, and decrease the costs of power quality disturbances [8], [150]-[152].

Power utility suppliers including generation, transmission and distribution companies are faced with re-regulation under substantial pressure to improve the quality of the provided service. A failure of power delivery in electrical systems, meaning insufficient quality for customers, is expected to result in financial penalties. The ability to provide the desired quality of power is an extra challenge due to the spread of renewable energy and electronic devices installed in their systems.

New types of generators have a variable output of voltage and power, demanding more advanced control. They are usually connected to the power system through electronic devices, which are more sensitive to power quality disturbances, especially harmonics and its sources. These electronic devices are not only used in the field of controlling renewable generation, but are also implemented as an essential component of other controllers, such as FACTS devices and HVDC. Therefore, it is essential to target improvements towards more effective control applications. Manufacturers and researchers' efforts towards understanding power quality mitigation devices have increased recently in terms of the characterisation and quantification of power quality issues. They need to distinguish and understand the basic characteristics of common power quality disturbances in order to design products to mitigate them, taking into account the costs of mitigation and the capability of the manufacturing platform. Developers of the control software for the microprocessor are also involved in understanding power quality disturbances in order to prevent software disconnections [153]. Industrial automation processes and computers suffer from shut down power quality disturbances, causing more damage to materials than ever before. These disturbances annoy residential consumers, who own a growing array of the electronics products necessary for a modern lifestyle, and find such harm less acceptable in the supply provided.

Regarding the frequency of occurrence of these disturbances and associated costs, voltage sags, harmonics and short interruption are the most detrimental and harmful power quality disturbances in electrical grids [154].

## 6.3 Control Strategies of Power Quality Disturbances

Several options can be implemented and adopted to reduce both the impact on the power system and potential financial losses from voltage disturbances. An effective starting point is reducing the causes of such disturbances. Procedures can be followed by engineers in transmission companies to reduce the occurrence of faults, where the major reasons behind voltage sags are considered. This includes adjusting the transmission tower, installing line arresters and footing resistance with instantaneous protection at the transmission system level. Moreover, regular tree trimming and loop schemes are necessary at the distribution level.

Unfortunately, these preventative procedures cannot completely remove power faults and voltage sags. Thus, further action should be taken to handle remaining faults and ensure the safety of electronic equipment through disturbances. FACTS devices can be used, including static VAR compensator (SVC), STATCOM, Solid State Transfer Switch (SSTS) and dynamic voltage restorer (DVR). However, it is still a problem that these applications are extremely costly and, consequently, only specific devices can be protected, as well as their control system, which can be protected with the installation of superconducting magnetic energy storage (SMES) or UPSs.

Harmonics go through many phases of distraction before they reach the supply source. Harmonic disturbance is considered one of the most common cases in power systems, a naturally occurring phenomenon resulting from different loads. One of the best ways of solving harmonic issues is at the source, by introducing and designing equipment such as pulse width modulation (PWM) and inverter technologies, which lead to a much lower level of distorted voltage waveforms. The harmonic sources in synchronous machines need an appropriate winding pitch, which is able to reduce harmonics in voltage output. An increase in the number of commercial facilities nowadays is also making harmonic problems more complex, due to the neutral conductor currents. Those currents, which are preferably in balanced and not distorted systems, are raised to accidentally high levels, the 3rd harmonic in particular. In these conditions, the neutral conductor should be doubled in size to avoid overheating. Moreover, another solution is installing zig-zag transformers to deliver a low impedance path for the filter of the 3rd current harmonics.

The reduction required in total harmonic distortion (THD) cannot be achieved using one of the above procedures, or even through a combination of them. It is certainly necessary to install passive or active harmonic filters [155]. A beneficial mitigation technique for harmonic currents is installing passive filters in distribution power systems [156]. These filters can also be considered as a source of reactive power. Passive filters are normally located at the centre of a common coupling, so that a harmonic current is kept at the minimum level. However, there are also situations where feeders carry a significant harmonic current, which results in undesirable voltage harmonics at the system buses. This means that filters should be installed at strategic buses of the power grid [157]. In addition, the main factor in designing a harmonic filter is to select a suitable capacitor size, which reflects the desired power factor needed at a fundamental frequency.

The second choice is to install active filters in the system to reduce harmonics, but this is even more expensive. Active filters are connected in shunt, and have the ability to handle lower currents, which are normally the main distorted components. They are a smaller size than passive filters, up to 150 kVA and normally connected close to harmonic sources. Active filters are considered as power electronic devices, which are similar to inverters. The procedure starts by detecting harmonic content in the system load current. Thereafter, a proper signal that cancels the harmonics current is injected with an appropriate switching to the non-linear loads. This signal effectively reduces harmonics when injected into the system network from the load current [158].

## 6.4 Power System Stability

Power system stability studies are important and essential in the planning and operation of power grids. It is considered as the completion of the power quality cycle, taking place in the decision-making stage to maintain stable conditions in the power system. Stable operation conditions are a vital and challenging issue, due to the complexity of modern power architecture.

Power system stability has recently been the focus of attention for researchers and decision makers. It is defined by stability terms and definitions in IEEE as “The ability of an electric power system, for a given initial operating condition, to regain a state operating equilibrium after being subjected to a physical disturbance, with most system variables bounded so that practically the entire system remains intact” [159]. Stability can be categorised into three groups: voltage stability, rotor angle stability and frequency stability [160], as shown in Figure 6-1.

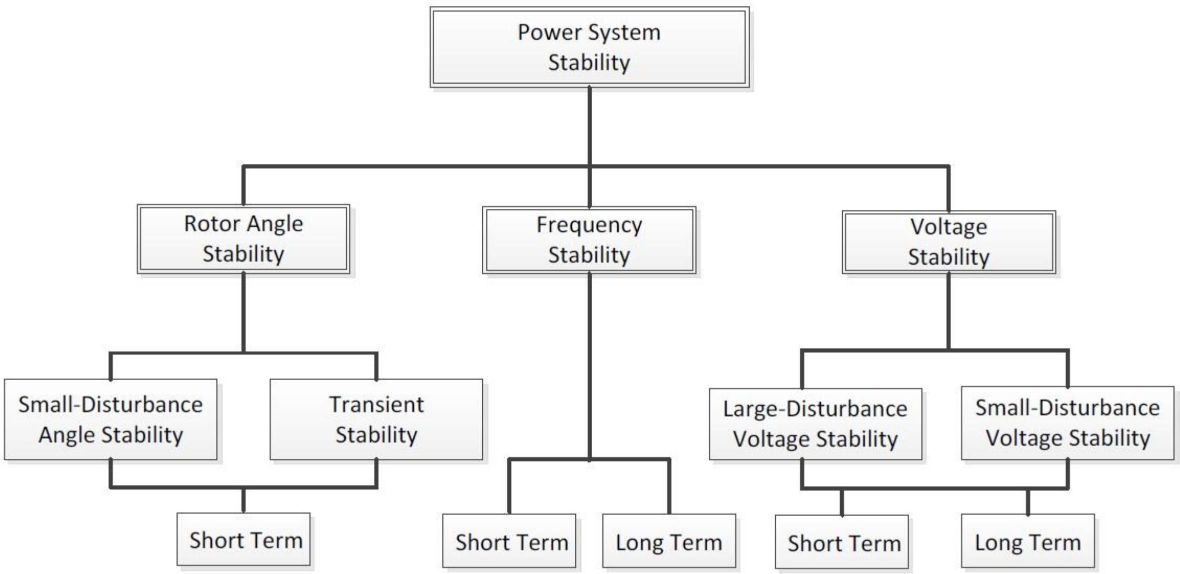


**Figure 6-1 Categories of power system stability [160]**

Voltage stability generally refers to the voltage magnitude, and is defined as: "the ability of power system to maintain steady acceptable voltages at all buses in the network under normal operating conditions or after being subjected to a disturbance" [159]. The main reason for voltage instability in the system is an imbalance between supply and demand. It is a dynamic issue in power networks, and becomes more complicated when it is accompanied by rotor angles running out of order [161]. As a result, voltage instability leads to shut down or low voltage supply in the power system [159].

Rotor angle stability is the capability to maintain the synchronism of power machines after they have been subjected to a disturbance [159]. Rotor angle stability is also categorised into two types: small disturbance angle stability and transient stability [162]. Rotor angle instability is due to the lack of damping or losing synchronising of torques in power systems [163].

Frequency stability is defined as: "the ability of the power system to maintain a steady frequency after a significant imbalance between generation and load has happened due to large disturbance" [159]. Frequency instability leads to a tripping in generating components in the power system or loads.

The dynamics of power systems when a disturbance occurs, in terms of control and stability, are divided into four different groups: wave, electromagnetic, electromechanical and thermodynamic, which are structured based on their physical characteristics [162]. Each of these categories has time duration, as shown in Figure 6-2.

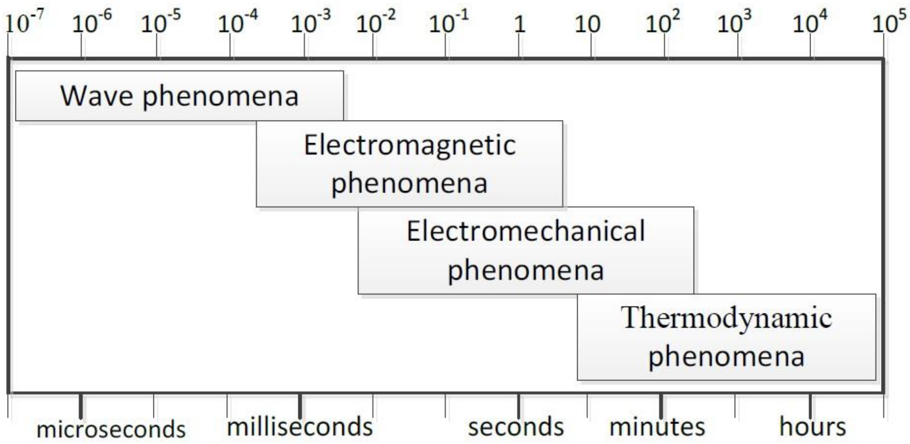


**Figure 6-2 Time duration of the power system dynamic types [162]**

The fastest dynamic phenomena are wave phenomena, which is due to a swell disturbance in the transmission lines. Swell disturbance is associated with the switching operation, or when a lightning strike occurs in the system. the time for such phenomena is between microseconds and millisecond.

The time duration for the second type, electromagnetic phenomena, is between milliseconds and one second. Electromagnetic phenomena are due to the disturbance in machine windings, which leads to changes, especially the relationship between the electrical machines and the protection system. Furthermore, the time duration of electromechanical dynamics is between a second and several seconds, which is due to voltage disturbances. These disturbances occur based on the oscillation in rotating masses in motors and generators.

Finally, the time duration of thermodynamic phenomena is between seconds and hours. Such phenomena result in power grids due to changes in temperature after a boiler change in steam power plants, during the association of a new amount of load. To maintain stability in the electrical power system in stationary conditions of generation, transmission and distribution depends on the disturbance type and the action taken to control the system [162].

## 6.5 Conventional Power Stability Control

Power system controllers are mainly divided into two types: conventional and modern controllers, to handle oscillation problems and voltage variation associated with power signal disturbances. These oscillation problems may sustain to cause a losing synchronism in generators or inadequate damping ratio is available in system [164]. The Power System Stabilizer (PSS) is used effectively to damp frequency oscillations, which is considered conventional and widely implemented in the industry due to its simplicity [165].

The PSS controller is based on a compensation procedure using a tuning process by pole-placement method. With fixed gains values, PSS is designed separately to select dominant modes, and can be tested using the root locus technique. The design of pole-placement is proposed initially to govern the number and size of control stabilisers in multi-machine systems [166], [167]. Therefore, for the damping improvement of the local noises in the system:

$$G_{PSS} = K\left(\frac{s+Z}{s+P}\right) \tag{6.1}$$

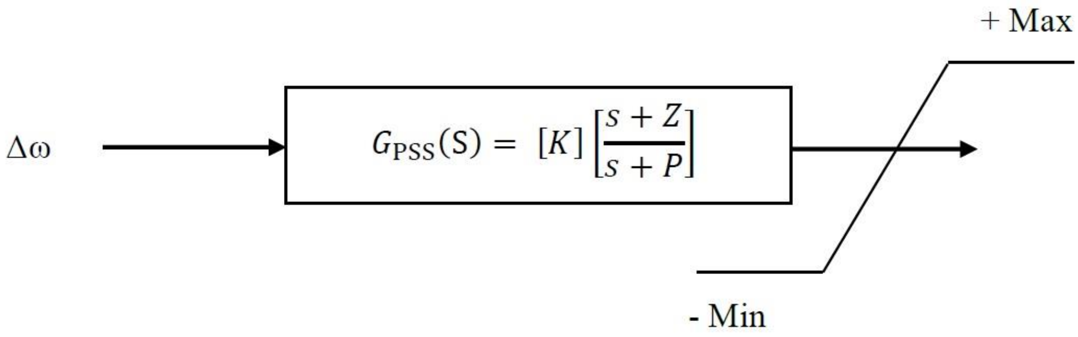


**Figure 6-3 Conventional PSS diagram [21]**

The poles can be modified anywhere in the close loop system using the technique pole placement in the complex plane, and therefore, the result is that the system becomes stable, even after suffering from instability conditions [168].

Moving the complex Eigenvalue ($\lambda$) in the system to the new location ($\lambda_0$) prepared in the s-plane. It should also satisfy the quantified damping ratio as:

$$H(\lambda_0) = \frac{-1}{G(\lambda_0)} \tag{6.2}$$

The equation can be expressed in phase and magnitude terms as follows:

$$|H(\lambda_0)| = \frac{-1}{|G(\lambda_0)|} \tag{6.3}$$

$$arg(H(\lambda_0)) = 180^0 - arg(G(\lambda_0)) \tag{6.4}$$

where $arg(G(\lambda_0))$ represents the phase angle of the residue value ($\lambda_0$)

At the new pole($\lambda_0$), the magnitude and phase of the compensator can be calculated based on Equations 6.2 and 6.3. Whereas the complex frequency response in the system is

$G(\lambda_0)$ and that is after the new pole location $(\lambda_0)$. The compensator $G_c(s)$ contains a lead/lag transfer function and constant gain, which can be expressed in Equation 6.5:

$$G_c(s) = K\frac{sT_w}{1+sT_w}\frac{1+sT_1}{1+sT_2}\dots.\frac{1+sT_{2n-1}}{1+sT_{2n}} \tag{6.5}$$

The main goal of the series compensator is to enhance the damping ratio for the designated oscillation mode. Hence, $\Delta\lambda_0$ should be a real value and with negative polarity to transfer the real part of the Eigenvalue. Moreover, for each compensation component, the phase must be limited to a 60° maximum value. In order to control the displacement direction of the Eigenvalue after the choice of the feedback signal, the parameters of the lead-lag stabiliser, the $i^{th}$ block and the maximum angle $\theta_m$ are determined by Equation 6.6:

$$\theta_m = sin^{-1}\left(\frac{1-\alpha_i}{1+\alpha_i}\right) \tag{6.6}$$

where the maximum angle is given in Equation 6.7:

$$\alpha_i = \frac{T_{2i}}{T_{2i-1}} \tag{6.7}$$

and the frequency is presented by Equation 6.8:

$$\omega_m = \frac{1}{T_{2i-1}\sqrt{\alpha_i}} \tag{6.8}$$

Thus, the theoretical basis of conventional control depends on the root locus and its repetitive values (i.e. gain margins and phase), which direct control devices such as PID and lead/lag. These controllers are used widely, and are still the leading practice for many control devices in controlling and stabilising power systems such as multi-band stabilisers.

The phase and gain margin plays the main role in designing controllers which ensure stability at steady state conditions [169]. Therefore, the compensator delivers phase margins and adequate gain to a specific mode, which should deliver the specification requirements of stability. In general, the lead/lag functions to the required margin. In addition, the first design version has a noticeable effect on the gain and phase margin for other modes which need to be monitored, and solves any problems that might occur (e.g. with a trial and error method).

Eliminating a slight disturbance in a synchronous machine, occurring in the bus, is achievable with a proper control system, taking into consideration the comparison between the synchronisation torque and the damping torque [169].

The frequency response is deeply investigated to analyse stability performance using a special signal, which is derived initially from the rotor speed and has a particular value of rotor angle damping [170]. Using a different signal input as the feedback signal will provide better performance and results. This signal is a combination of the AC bus frequency and accelerating frequency signal in the electrical power system. Frequency response techniques are based mainly on root locus control and Ruth stability, where modern control methods focus on improving damping in the electromechanical oscillation by using the Eigenvalues assessment. The difficulty of modern methods is the calculation of damping from the swing curves when examining the system response. The Eigenvalue technique contributes by defining and easily identifying all modes, which is useful with several oscillation modes. However, many algorithms and techniques are developed to assess and measure the critical Eigenvalues for the analysis of small signal stability [171]. All mentioned techniques with fixed gain of PI placed in the generators, or lead stabilisers phase shift in the system, can give an adequate response to the desired operation conditions, but more effort should be made to enhance the response when these points changes in the system.

## 6.6 Power Generators and Excitation Control

Electric supply in power utilities is still mainly AC as a result of using AC synchronous generators, and voltages provided in the system are controlled by the generator excitation system. Moreover, speed governors in these generators are implemented to control the main movers and maintain the system frequency within acceptable limits in electrical networks. Furthermore, the resulting torque from the interconnected AC generators in the power grid depends on the angular displacement of each individual rotor, which ensures the generators' synchronism or, as named, synchronising torques [172]. The mechanism of this process is achieved by producing an electrical torque to reduce the difference in the increased angular displacement between generators. The purpose of this process is to settle the required power flows in the system. If a large disturbance occurs in the power transmission system, the torque might not be able to recover the generator angles to normal operation conditions or more specifically steady state conditions. Moreover, some generators will miss synchronism and the system will suffer from a transient performance. Alternatively, the synchronising torques maintain the generators nominally in synchronism when the disturbance is small, but an oscillation might occur in the generator relative angles, and an increase in the amplitude.

Transient and oscillations in electrical systems have occurred frequently around the world [173]. This instability appears when the power system is forced to provide additional power, or when the load is suddenly increased on transmission lines, or if the generators are relying on excitation systems to sustain synchronism, as shown in Figure 6-4.

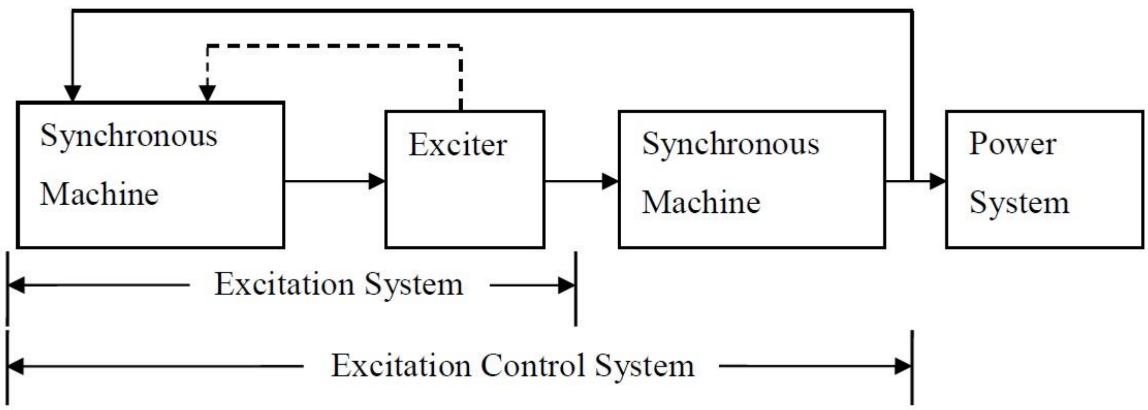


**Figure 6-4 Excitation control system [26]**

To solve this instability, efforts to interconnect electric power systems were introduced. The result is that loads can be exchanged between transmission systems. However, the relationships between neighbours' electrical power systems are still weak [173]. A common issue of oscillatory instability is that power flow can be larger than needed. A slight increase in the power flow over the boundary causes a sudden increase in the power amplitude. The optimum scenario is the system reducing the amplitude of oscillation, stopping it from reaching the limits. Otherwise, the protective relays in the power system are going to suffer from a total or partial collapse in the system [174].

## 6.7 Modelling Platform of Power Quality Control

The system constructed to control power quality was mentioned briefly in previous chapters, but since this chapter is going to investigate mitigation of system response to a power quality disturbance, it is necessary to explore further details of the system.

A power transmission system is implemented with multi-machine generation plants with 700 km transmission lines, as shown in Figure 6-5. The capacities for the hydraulic generators are 1000 MW and 5000 MW. Furthermore, a load is connected to the system with 500 kV, and the system has inertia with 950 MW.

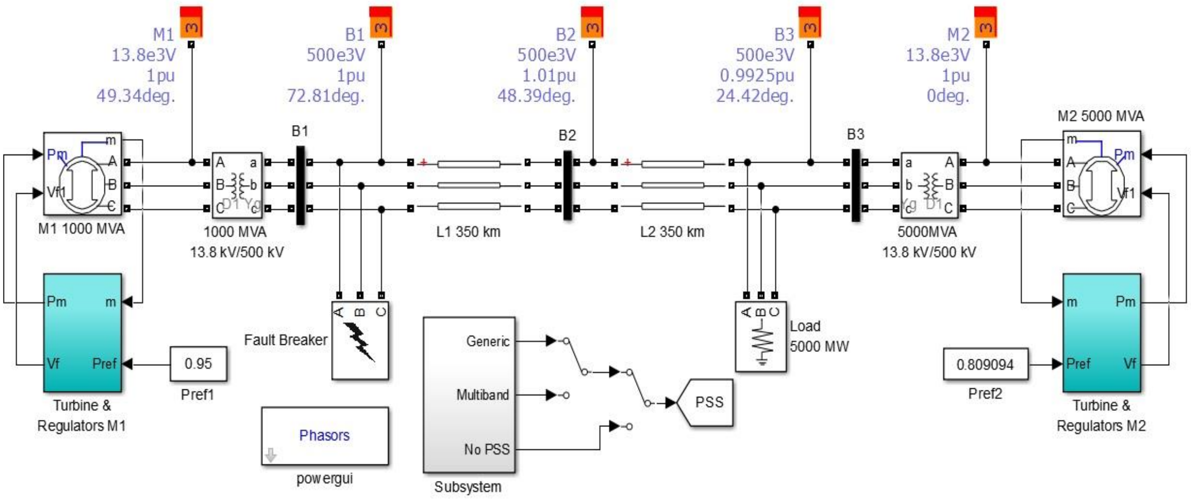


**Figure 6-5 Power transmission system with multi-machine generation plants [175]**

The fault is located in the system next to bus bar B1. The two machines are provided with a hydraulic turbine in the system and a governor (HTG), and an excitation control system. The system is also power system stabiliser (PSS). These models are implemented in two subsystems, named the 'Turbine and Regulator'. The power system stabiliser consists of two types of stabilisers. The first is a generic model which focuses on using the acceleration power (Pa). The acceleration power can be calculated by the difference between the mechanical power (Pm) in the system and output electrical power (Peo). The second stabiliser is the multi-band stabiliser (MB), which focuses on using the speed deviation (dw). The selection of any one of the modelled stabilisers has a specific block in the PSS subsystem.

## 6.8 Multi Band Stabiliser

The latest model type of conventional power system stabilisers was introduced by the Institute of Electrical and Electronic Engineers (IEEE), called the multi-band power system stabiliser (MB) or (PSS4B) [176]. This provides improved performance in comparison to the previous power system stabilisers. MB-PSS consists of three levels of parallel controls, which aim to reduce the damping in oscillation modes and frequency bands in the power systems. The requirements for MB-PSS control start with two input parameters, $\Delta\omega_H$ and $\Delta\omega_{L-I}$, which represent the high frequency and (intermediate with low) frequency, respectively. The parameters in this model type (IEEE PSS4B), as in Figure 6-6, are similar to the parameters in older version types (IEEE PSS2B), where it was integrated to accelerate the power of PSS, when the first practical PSS was introduced in 2005 [176].

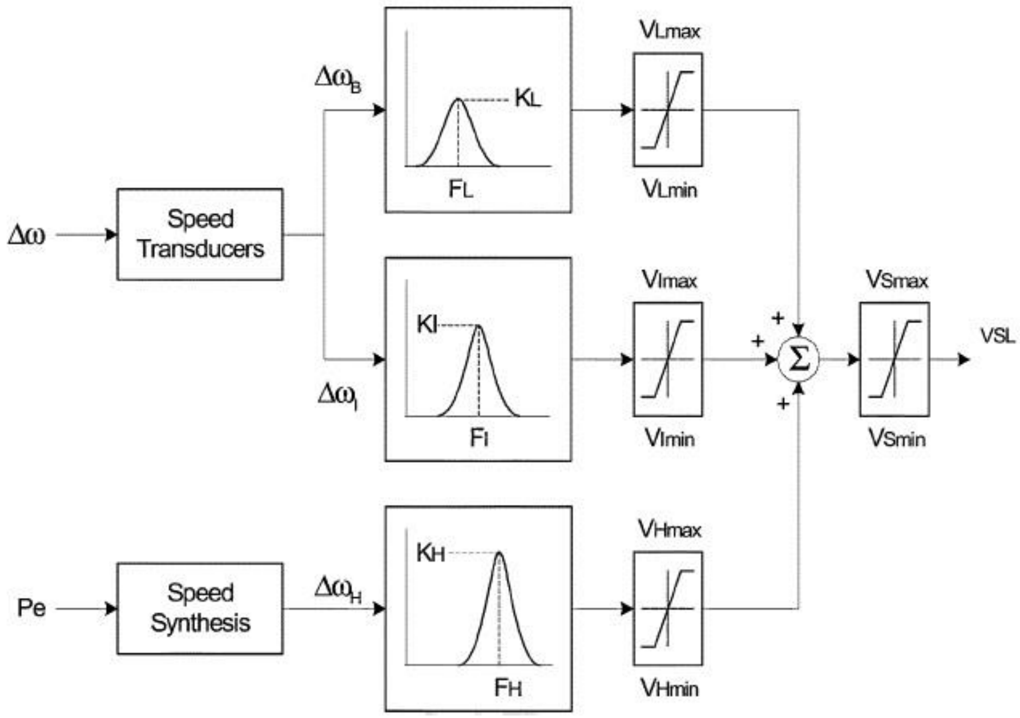


**Figure 6-6 Block diagram of the multi-band PSS (IEEE PSS4B) [176]**

## 6.9 Simulation and Results

To evaluate the robustness and effectiveness of any control system, it must be verified under different conditions covering any disturbance that may occur during normal operation conditions. In this section, investigation of performance following implementation of MB-

PSS is conducted by the model provided, which is based on MATLAB/Simulink software, as shown in Figure 6-7.

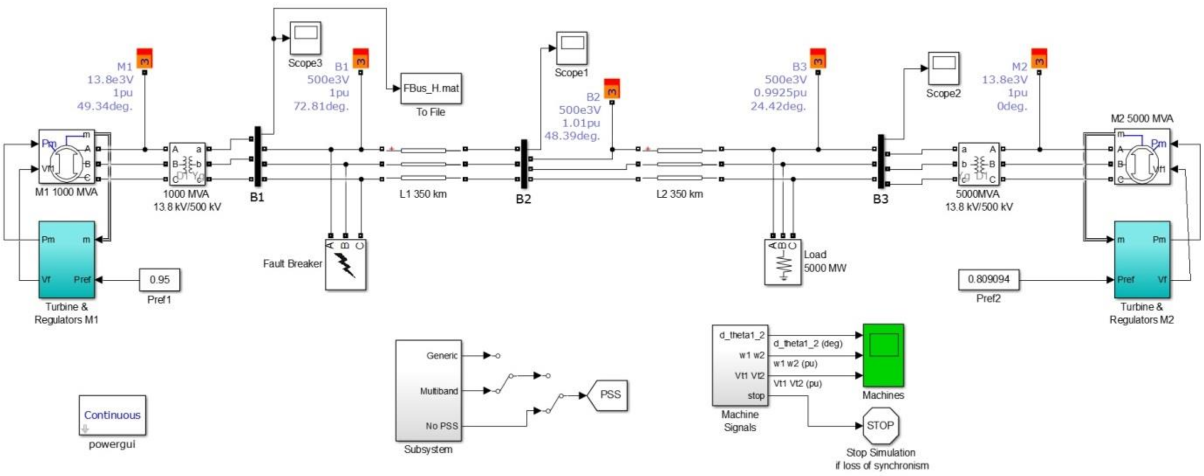


**Figure 6-7 Block diagram of power transmission system with PSSs**

The procedure of the simulation process starts by setting the fault in the system to be a phase-to-phase fault in order to produce the sag disturbance. Moreover, settings of the fault circuit breaker include adjusting time to 0.1 second, which starts from 1.0 to 1.1 second.

The system has been initially modelled to start at steady state conditions. Furthermore, inside the system parameters, synchronous machine blocks M1 and M2 have 1000 MVA and 5000 MVA, respectively. The first generator M1 has a PV type, as shown in the load flow tab, and indicates the active power value with 950 MW and its terminal voltage with 13.8 kV in the Bus named B1, which is connected to the machine terminals. The second generator M2 has the 'swing' type to balance the power with the same terminal voltage, as shown in Figure 6-8.

| | Block type | Bus type | Bus ID | Vbase (kV) | Vref (pu) | Vangle (deg) | P (MW) | Q (Mv... | Qmin (Mvar) | Qmax (Mvar) | V_LF (pu) | Vang |
|---|---|---|---|---|---|---|---|---|---|---|---|---|
| 1 | SM | PV | M1 | 13.80 | 1 | 0.00 | 950.00 | 0.00 | -Inf | Inf | 0 | |
| 2 | SM | swing | M2 | 13.80 | 1 | 0.00 | 0.00 | 0.00 | -Inf | Inf | 0 | |
| 3 | Bus | - | B1 | 500.00 | 1 | 0.00 | 0.00 | 0.00 | 0.00 | 0.00 | 0 | |
| 4 | Bus | - | B2 | 500.00 | 1 | 0.00 | 0.00 | 0.00 | 0.00 | 0.00 | 0 | |
| 5 | RLC load | Z | B3 | 500.00 | 1 | 0.00 | 500... | 0.00 | -Inf | Inf | 0 | |

**Figure 6-8 Load flow block information**

The hydraulic turbine and governor in the system (HTG), along with the excitation control system, are modelled and placed in the two regulator subsystems, where the mechanical power is automatically initialised by the load flow with the field voltage.

The reference voltages and reference mechanical powers for the two machines are placed in the two blocks connected at the inputs of HTG and the excitation system. The variables are set for the first part (M1), with the reference power: Pref1 = 0.95 pu (950 MW), and the reference voltage: Vref1 = 1pu. On the second part (M2) the power: Pref2 = 0.8091 pu (4046 MW), and voltage: Vref2 = 1 pu. In this model, two types of power system stabilisers are implemented – a generic stabiliser, named (PSS2B), with the second controller being a multi-band stabiliser, named (PSS4B) – in order to control each turbine to improve stability performance [174], [177], as shown in Figure 6-9. Its configuration blocks are shown in 6Figure 6-10 and

Figure 6-11.

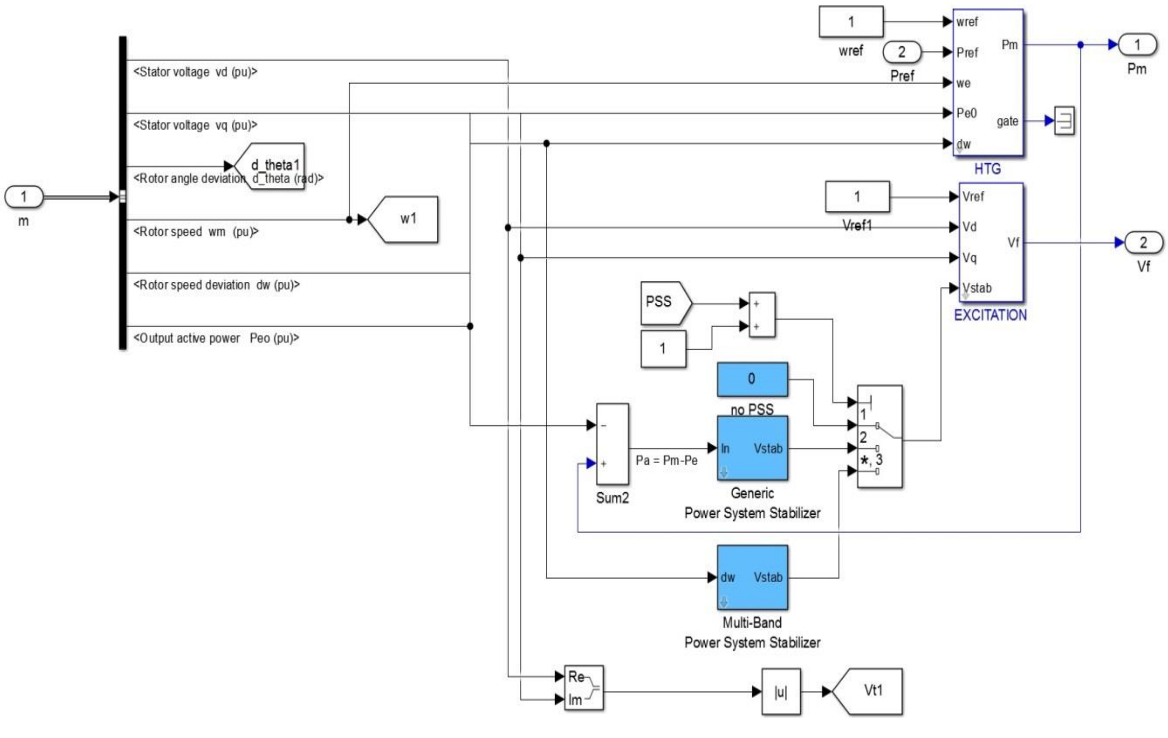


**Figure 6-9 Generic stabiliser (PSS2B) and multi-band stabiliser (PSS4B) controllers in the system**

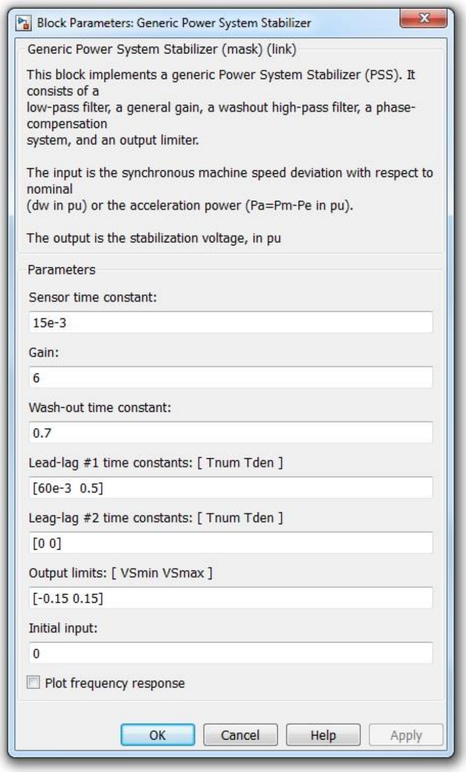


**Figure 6-10 Parameter interface for PSS2B controller**

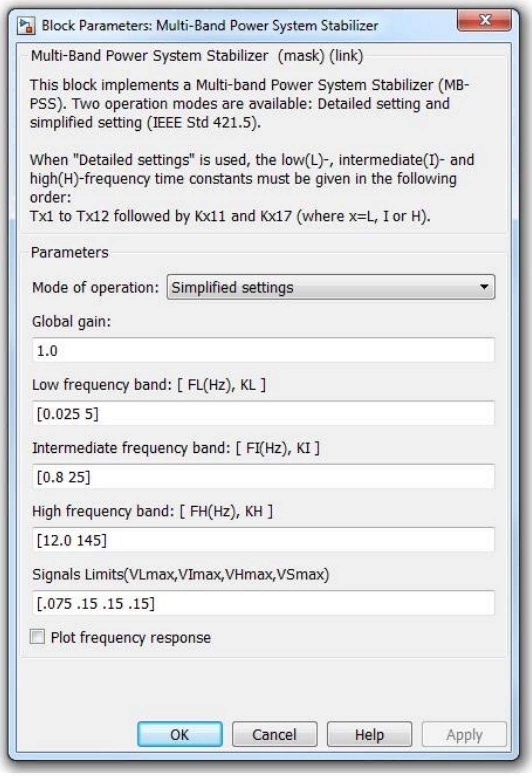


**Figure 6-11 Parameter interface for PSS4B controller**

The system operates for 10 seconds with the phase-to-phase fault for duration of 0.1 second causing a sag disturbance in the system, and the result, without control, was an unstable system, as shown in Figure 6-12.

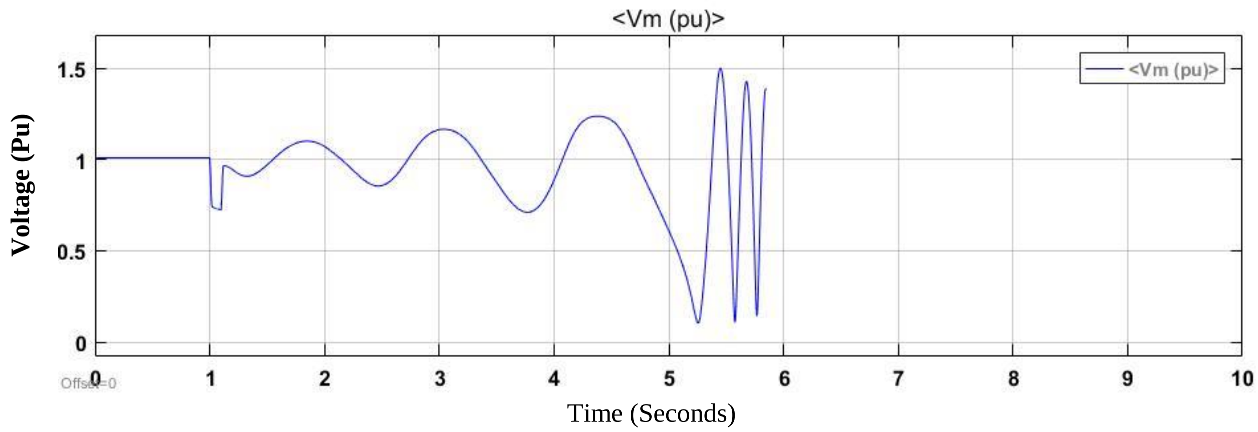


**Figure 6-12 System response without control**

The system was in its normal conditions V=1 pu until it reached the fault between 1.0 to 1.1 second, where the sag occurred. The system started to oscillate immediately after the event. The voltage magnitude continued to oscillate until t = 5.8 seconds, where system shut down and black out was the result.

The power generic stabiliser (PSS2B) is then implemented in the system with the same conditions, same fault and same duration. The result of implementing this was eventually having a stable system, as shown in Figure 6-13. The system suffered sag and oscillated afterwards for the next few seconds. However, the system stabilised when the operation reached 5.3 seconds.

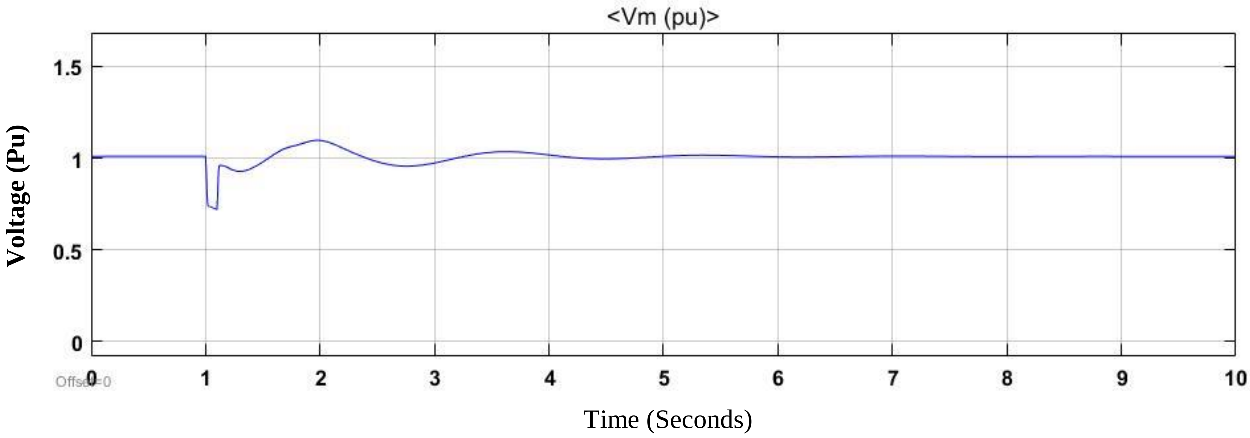


**Figure 6-13 System response with PSS2B control**

The second power system stabiliser MB-PSS, named PSS4B by researchers, is then implemented instead of the older version, PSS2B. The system experienced the sag disturbance with the exact conditions of the two previous cases. The system is, thereafter, stabilised at 4.4 seconds, as shown in Figure 6-14.

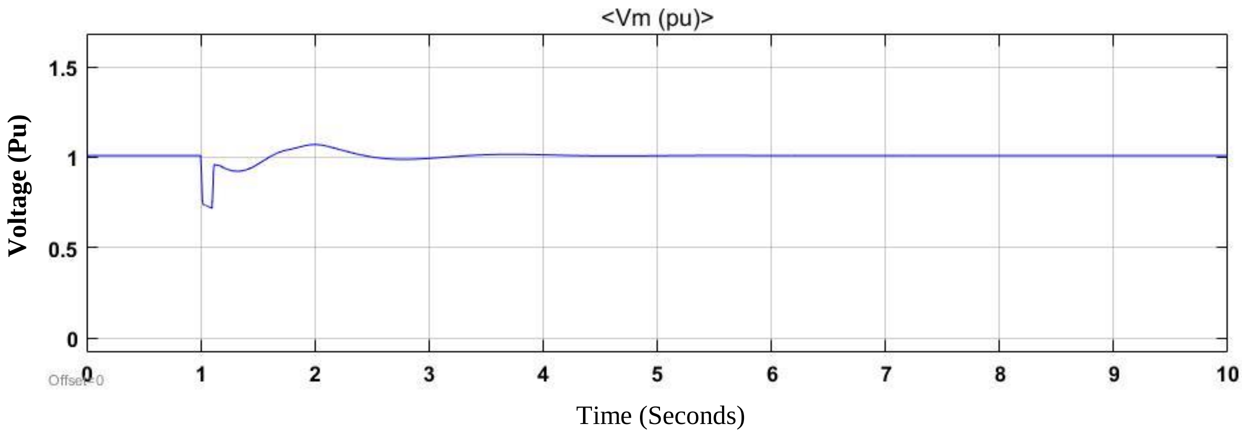


**Figure 6-14 System response with PSS4B control**

## 6.10 The Proposed Optimisation Method of Power Quality Improvement

In this section, the proposed method is introduced to the system, and a comprehensive analysis with compression is conducted. This method is based on adding a bank of passive harmonics filters, placed next to the load. In addition, filters are categorised broadly into two main types; active filters and passive filters. However, this process has the aim to mitigate the harmonics in the system. Adding passive filters is one of the essential methods to mitigate harmonics in steady state conditions, but they vary from according to the system requirement. In Active filters implementation which is used in three phase power systems, the fundamental frequency in the load will be filtered and the rest of residual magnitude and frequency components will be further treat and analysed before the inserting of the current in the system aiming to cancel or eliminate or mitigate individual harmonics.

Passive filters in this approach consist of three main components; the resistance (R), the capacitance (C) and the inductance (L). This type is well known in power systems as (RLC) filter which can be implemented and tuned to reach the mitigation at specific harmonics. Harmonics filters can be derived mathematically generally from Equation 6.9 as:

$$Z_S(\omega) = R_S + j\left(\omega L_S - \frac{1}{\omega C_S}\right) \tag{6.9}$$

where $Z_S$ represent the impedance in the system, $\omega$ is the frequency at the point PCC, $R_S$ the resistance, $L_S$ the inductance and $C_S$ is the capacitance in the model design [79].

The indicator to analyse the effect and the implementation of the harmonics filters is known as Total Harmonic Distortion (THD) on power systems as the signal is decomposed into numbers of harmonics. This signal is categorised by the magnitude and phase of the involved harmonics as the fundamental frequency is 50 or 60 Hz especially for voltage events and more importantly this term is the most used term in harmonics analysis. THD is given mathematically [79] by Equation 6.10:

$$THD = \frac{\sqrt{\sum_{h=2}^{H} V_h^2}}{V_1} \tag{6.10}$$

where THD is normally expressed in percentage value, and the upper value $H = \infty$ and V represent the terminal voltage in the system.

In this model block, a bank of hybrid AC three phase harmonics filters are utilised to decrease harmonic voltages in the power transmission system [79]. The filters subsystem is prepared by four components from the powerlib library as the following:

- A 140 MVAR capacitor bank named (C01) modelled by a RLC load.
- A 140 MVAR high pass filter tuned to the 3rd harmonic (F01).
- A 140 MVAR of double tuned filter 5th/7th harmonic (F02).
- A 140 MVAR high pass filter tuned to the 11th harmonic (F03).

The total value of the filters subsystem is 560 MVAR. A circuit breaker is linked to connect the filters to the bus, as shown in Figure 6-15.

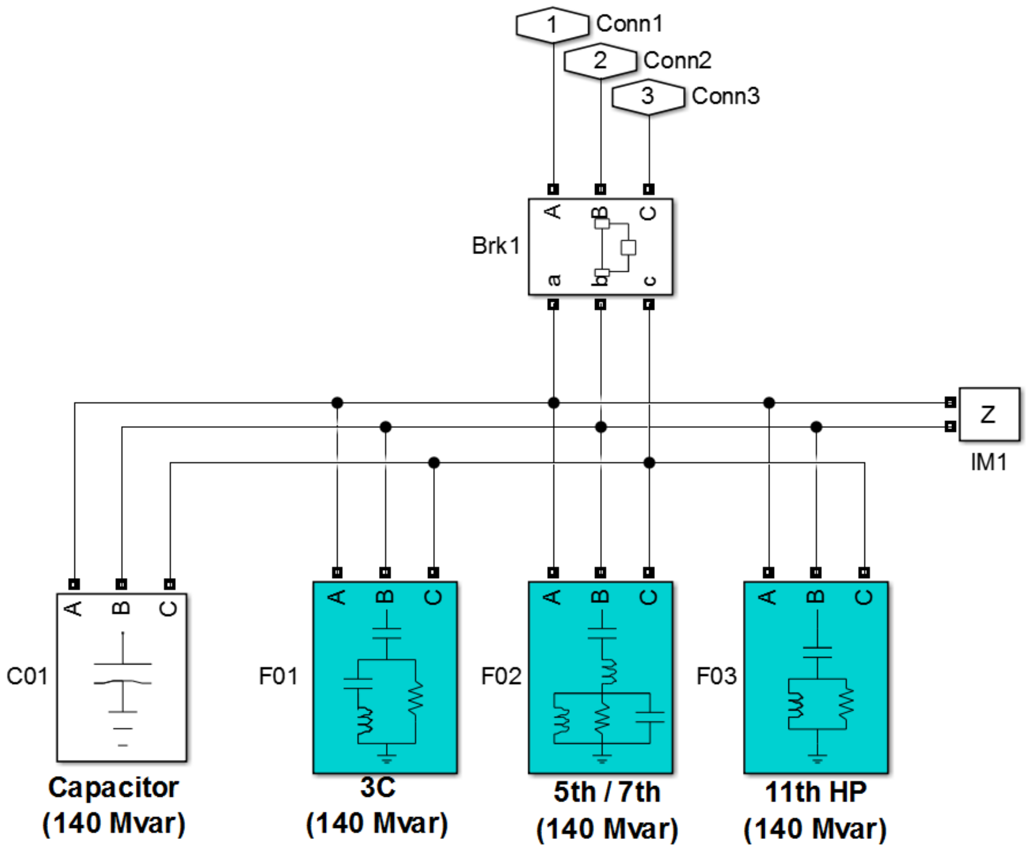


**Figure 6-15 Harmonics filters system [101]**

The bank of harmonics filters is applied in different places in the power transmission system; first it is placed at the beginning of the system, near to M1 and the fault of circuit breaker. The result of this step shows a stable performance in the network, but more value for the first overshot. The system behaviour shows an overshoot in its response, with more than 25%, as shown in Figure 6-16.

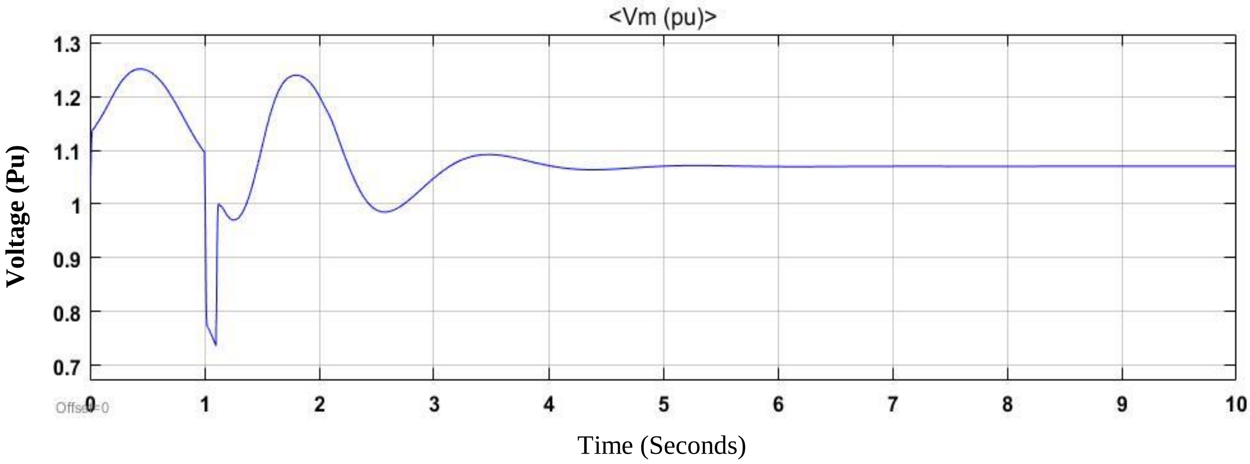


**Figure 6-16 System behaviour with harmonics filters in M1**

The second step is modelling the harmonics filters bank in the middle of the system. The result, shown in Figure 6-17, confirms a stable performance, but unfortunately with more overshot in the system behaviour. Even before the sag disturbance occurred at t = 1.00 second, the system behaviour shows an overshoot in its response by more than 35%.

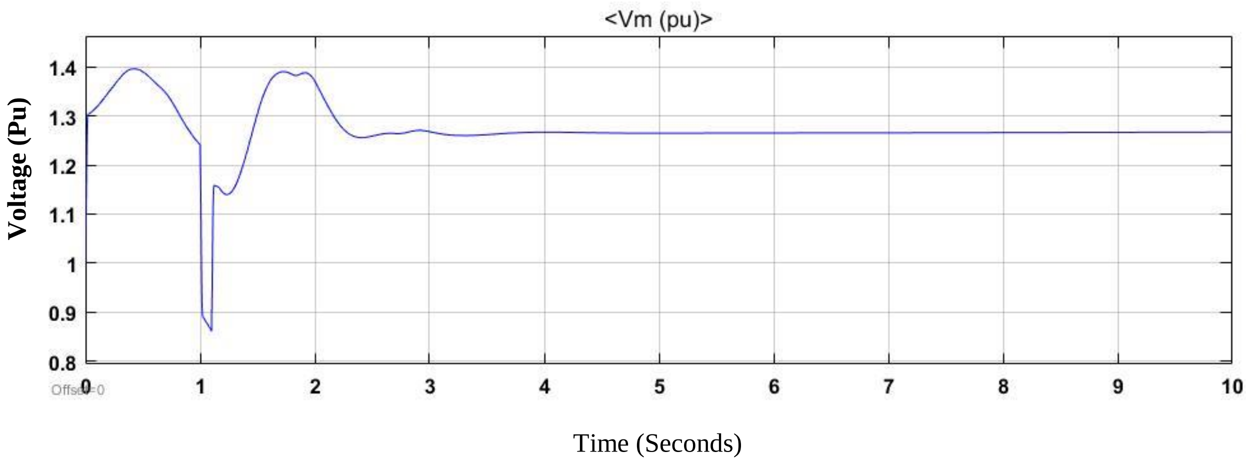


**Figure 6-17 System behaviour with harmonics filters in the middle of the network**

Finally, the third choice is to place the bank of harmonics filters at the end of the system and close to the load, as shown in Figure 6-18. The results of the system behaviour in Figure 6-19 show the system response to the combination of harmonics filters bank and stabiliser PSS4B, where there is a reduction in the signal oscillation, less transient overshoot of the transmission system, and better performance for stability.

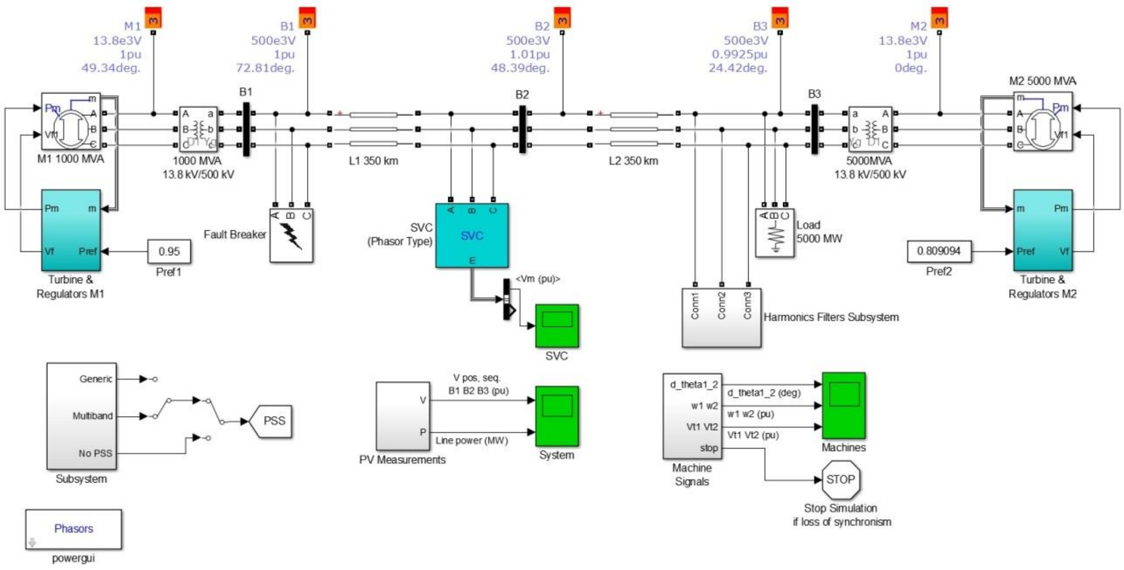


**Figure 6-18 System block diagram with harmonics filters next to the load**

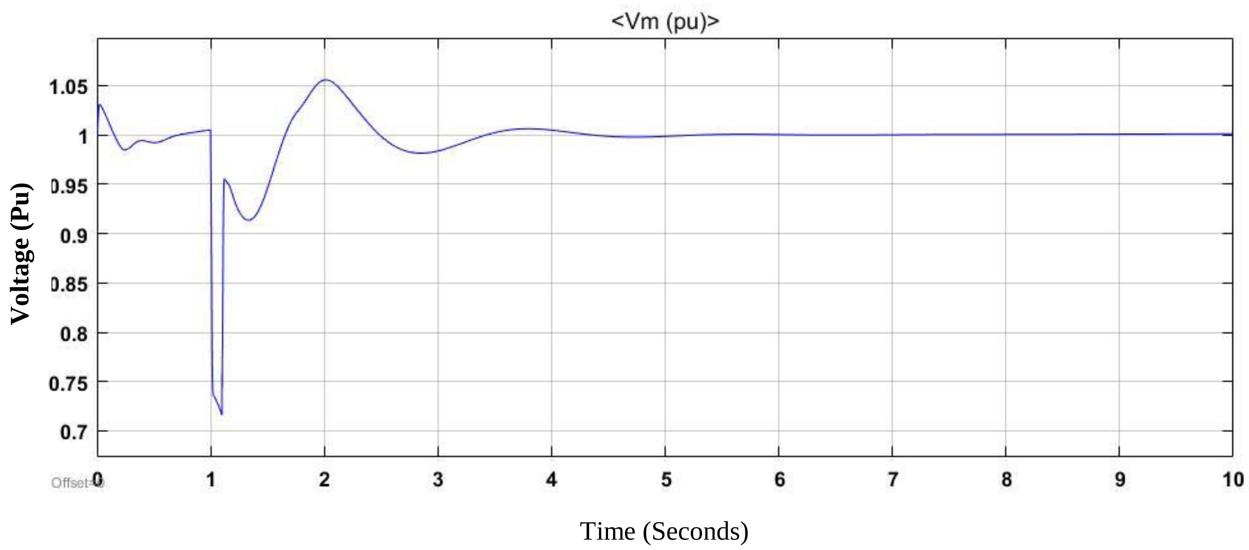


**Figure 6-19 System response with PSS4B control and harmonics filters**

In percentage terms, stabilisation after the above modification has reached 5% less transient. Another important achievement is recorded in the system: a harmonics reduction is accomplished, which has a huge impact in terms of producing a healthy transmission system. Based on the analysis options in the powergui, and precisely the FFT analysis in the tool menu, the original total harmonics distortion (THD) occurring in the system with the PSS4B controller was 80.67%, due mainly to the non-linear load, as shown in Figure 6-20.

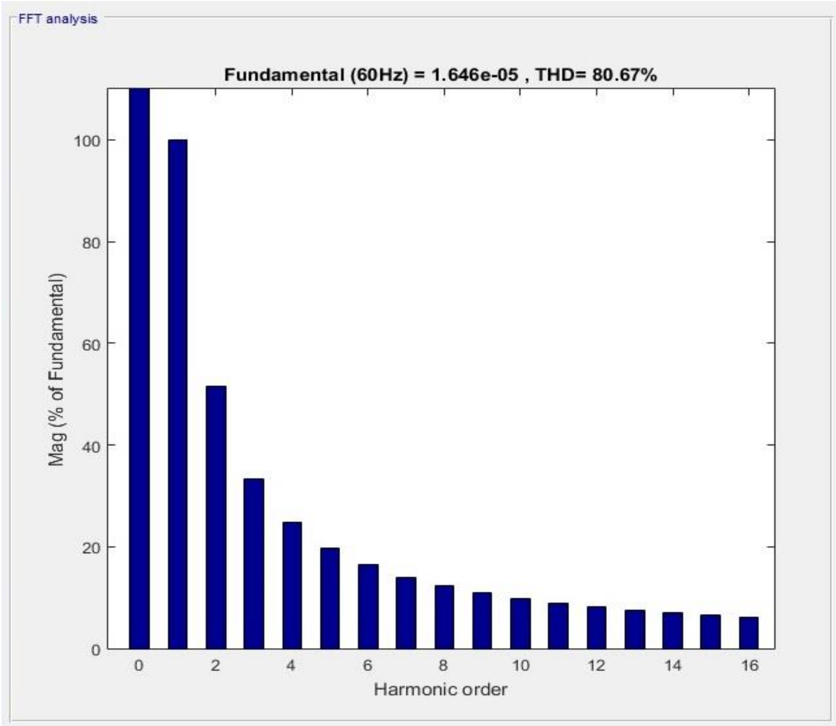


**Figure 6-20 Total harmonics distortion in the system with the PSS4B controller**

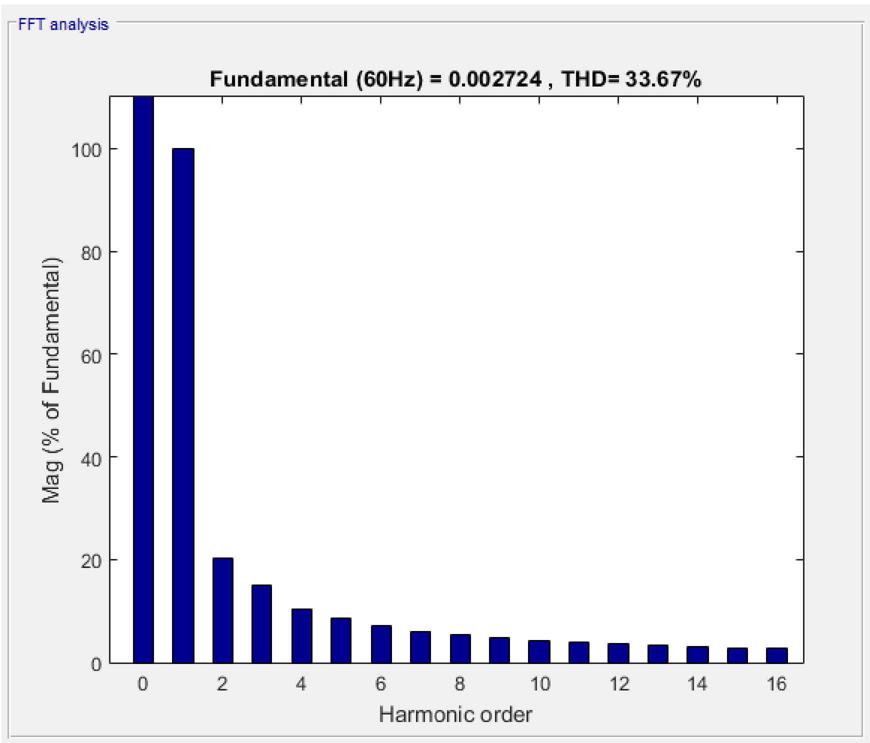


**Figure 6-21 Total harmonics distortion in the system with the PSS4B controller and harmonics filters**

The result of implementing the harmonics filters model in the transmission system was a significant decrease in the total harmonics distortion to 33.67%, which is less than half, as shown in Figure 6-21. Moreover, a comprehensive comparison to all system behaviours due to the same fault, same duration and the exact environment, are tested, investigated as shown in Figure 6-22 and Figure 6-23.

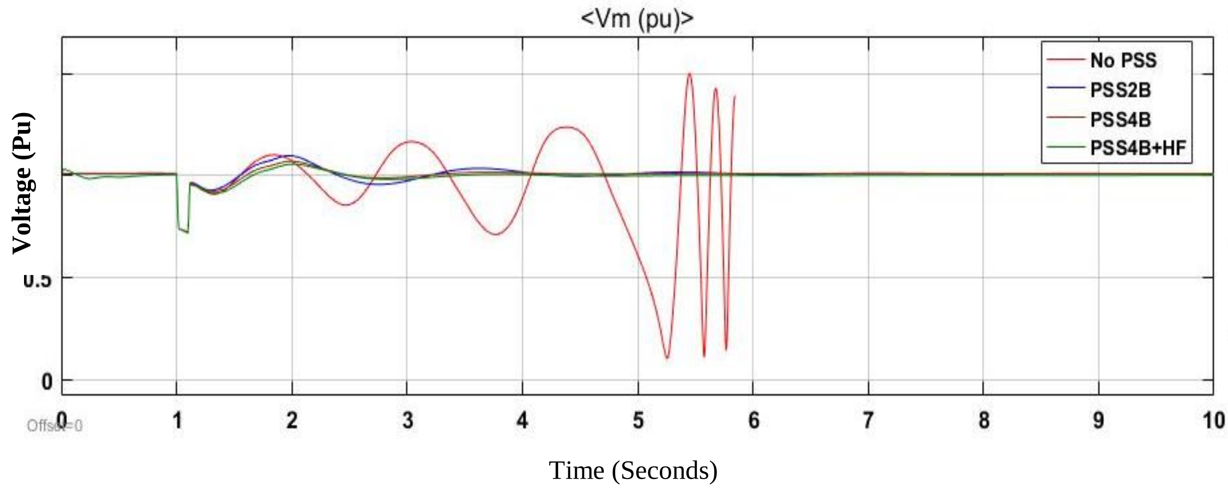


**Figure 6-22 System behaviour during fault with all PSSs types**

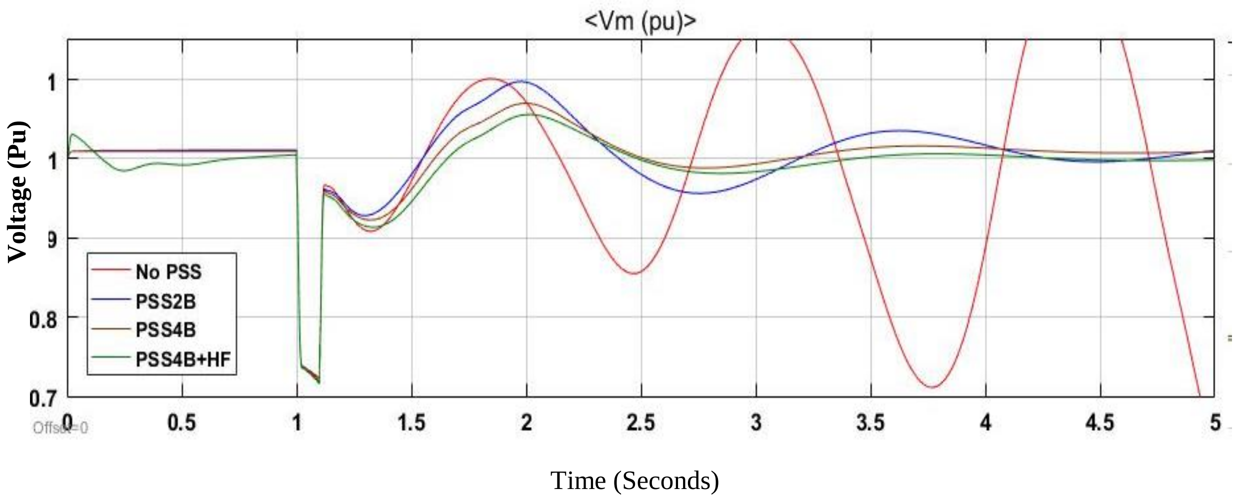


**Figure 6-23 System behaviours during faults with controllers for a shorter time**

As seen from the figures above, the system behaviour varies with each controller used in the power transmission system.

Firstly, the system went unstable without any control, due to the sag disturbance caused by the phase-to-phase fault. Secondly, the system responded to the power system stabiliser PSS2B, the genetic version, and went stable close to time t = 7.4 seconds. Moreover, the system peak was more than 1.1 pu to the voltage in the system, which is considered high and a case of greater impairment. Thirdly, the system behaviour with the PSS4B version of PSSs has more ability to stabilise the system within a shorter time at t = 6.1 seconds.

Finally, the system behaviour with the new modification and improvement of PSS4B is examined, where the model of harmonics filters is added to the transmission system near to the load. With this controller, the system stabilised in a shorter time at t = 4.9 seconds. Furthermore, the peak value of the transient of the system is lower than with any method used before. Moreover, the total harmonics distortion decreases significantly from 80.67% to 34.24%.

## 6.11 Optimising and Tuning of the PI Controller

Power quality improvement in the power transmission system achieved due to the development in this research work leads to further investigation of the PI controller on the grid. Such development needs to be followed with a retuning process to investigate the PI controller robustness. The procedure in this process is studying the effect of the controller, where the proportional gain Kp is set to a specific value = 1.0 and the integral gain Ki is divided into low, intermediate and high frequency bands, which also have specific values of 5, 25 and 145, respectively, as shown in Figure 6-24.

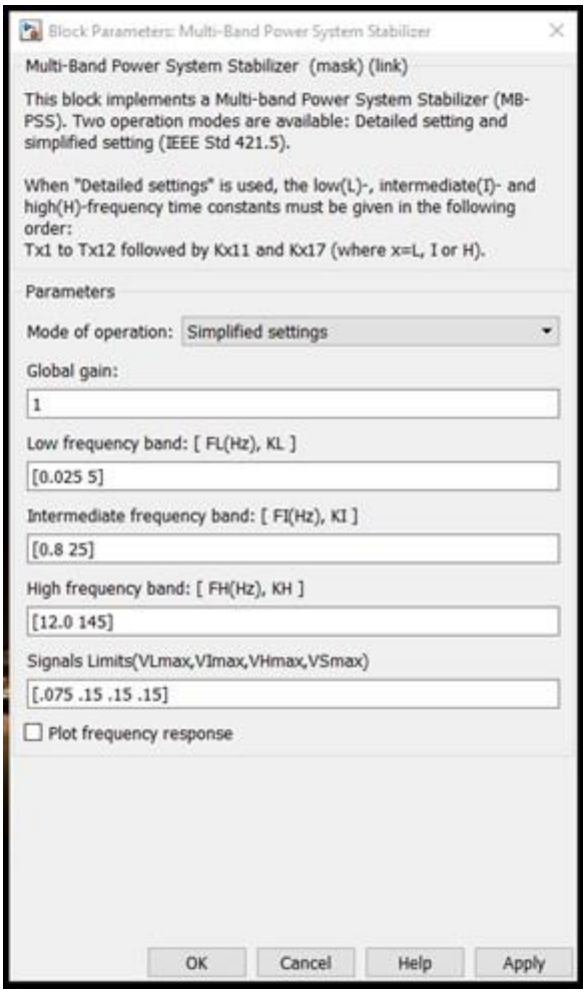


**Figure 6-24 Parameters of multi-band power system stabiliser PSS4B**

The tuning process is conducted separately for each gain. First the proportional gain (Kp) is increased by Kp = n+1 each time as Kp = 2,3,4,5 and results show the gradually increasing value of the transient overshoot. The second step in this process is by decreasing by Kp = n-0.1 as Kp = 0.5 and 0.1, respectively, which also sustains the instability in the system by decreasing the gain value. Moreover, another process is conducted in the integral gain Ki by all of its frequency bands by increasing and decreasing integral gains. The conclusion found is that the effect of integral gains is not beneficial or negligible.

The beneficial results show a positive impact on system stability. Two cases are selected to analyse the optimum value for Kp gain. The first case concerns the proportional gain Kp being applied as Kp = 2.0, where the result of the system behaviour shows reasonable stability conditions, as shown in Figure 6-25**.**

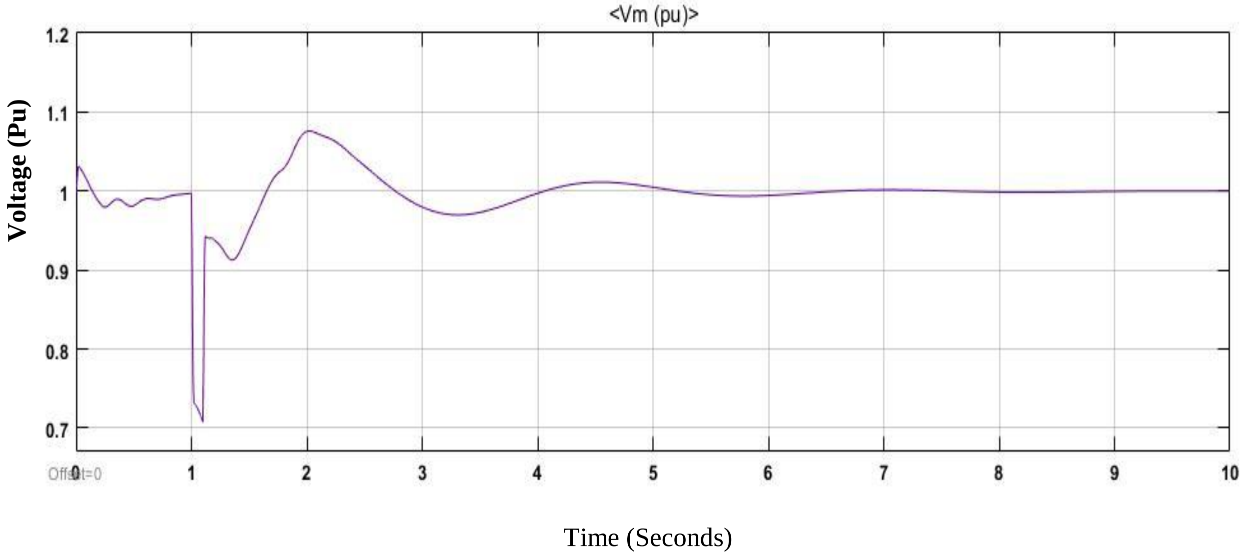


**Figure 6-25 System behaviour with the combination of PSS and HF (Kp = 2)**

The second beneficial case concerns applying the proportional gain as Kp = 0.5, where the result shows a positive impact as well, as shown in Figure 6-26.

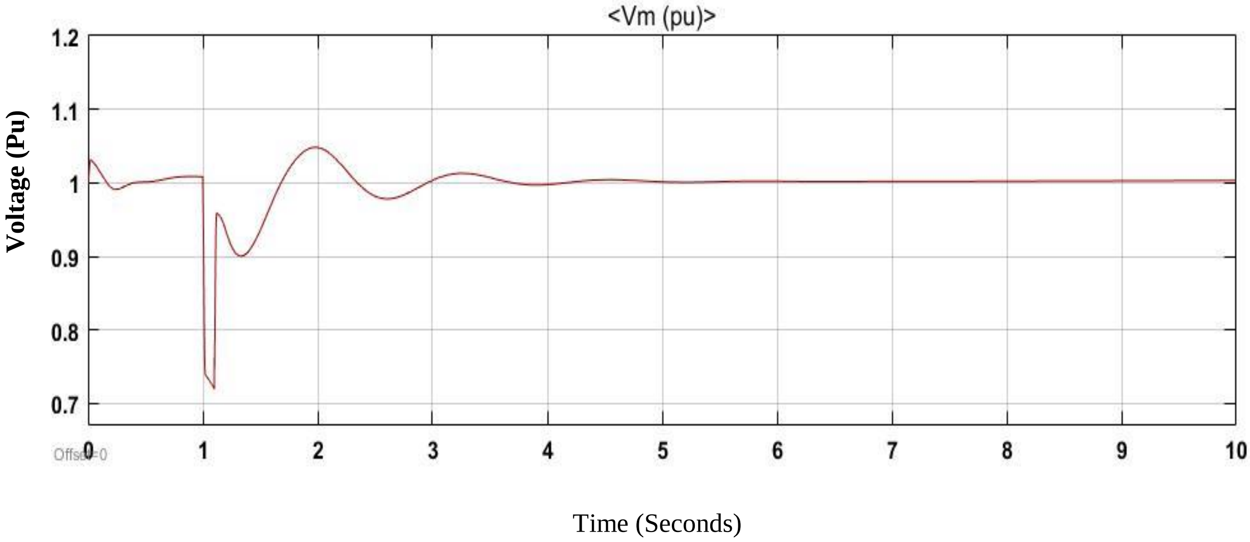


**Figure 6-26 System behaviour with the combination of PSS and HF (Kp = 0.5)**

To conclude the efforts of reaching the optimum controller in the system behaviour suffered from a multiple power quality disturbances, a comparison analysis for the mentioned examination is concluded for both cases, with achieved results gathered by adding the bank of harmonics filters, as shown in Figure 6-27.

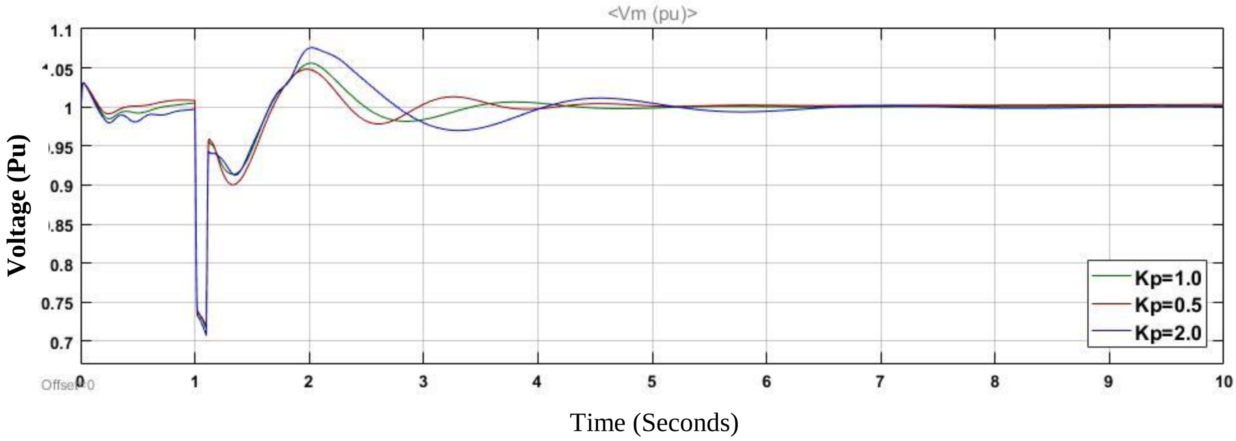


**Figure 6-27 System behaviour with the combination of PSS and HF (Kp = 0.5, 1.0, 2.0)**

Results of all three values of proportional gain show the optimum value found in this study was Kp = 0.5, especially when adding the bank of harmonics filters. The result of this choice was smoother system behaviour at the beginning of the operation of the power system. Moreover, the transient overshoot is less than both Kp = 1.0 and Kp = 2.0. The system performance settled to steady state conditions shorter than ever when t = 4.3 seconds.

## 6.12 Summary

In this chapter, a comprehensive investigation was conducted into control methods and their relation to power quality. Analyses of the methods used in the field of controllers used in the power system were discussed. After that, a power transmission system was introduced with an explanation of its main components. The stabilisation capability for power system stabilisers was then investigated, studied and discussed for PSS2B and PSS4B after adding a specific scenario, with a phase-to-phase fault causing a sag disturbance in the system. Results show that system behaviour showed instability when the sag disturbance accrued, which indicates the necessity of applying power system stabilisers. The PSS4B device has a better performance and a positive impact on the first overshoot, as it is less than with PSS2B.

A bank of three phase harmonics filters was implemented in the system next to the load, and further study was conducted to improve the power quality in the transmission system. There were three options regarding the instalment place: next to the generator M1, or the middle of the transmission system with 350 km, or at the end near to the generator M2 and the system load. Results show the advantage of implanting a modelled bank of harmonics, and its reflection on the system behaviour, as the harmonics disturbances reduced from 80.67% to 34.24% for the total harmonics distortion, with significantly less transient oscillation. Such improvements help the system behaviour in terms of handling multiple power quality disturbances, and enhance stability in the power transmission network.

The next stage in this research is for optimising the PI controller assembled in the power generators. The experiment went through both PI controllers in both generators in the multi-machine power transmission system. This process is conducted by tuning proportional and integral by increasing and decreasing gains. Two of the close cases were then selected for a comparison analysis, as shown above for the optimum values. Results showed that with Kp = 0.5 the behaviour is much smoother at the beginning of the system voltages at rated operation conditions. Moreover, the system behaviour shows less transient overshoot and less oscillation. Furthermore, the system behaviour reaches steady state operation conditions in a shorter time, as proven in this work.

In this chapter, a power quality improvement was achieved regarding power quality disturbances, based on mitigation of the oscillatory transient disturbance and reduction of the harmonics disturbance in the power transmission system at the same time. The system with multi-machine generators had two PI controllers attached to generators, which were also tuned to their optimum values. To conclude these achievements, the outcome is a more reliable system with less transient oscillation and harmonics reduction, and stability enhancement.

# Chapter 7 - Conclusions and Future Work

## 7.1 Conclusions

The main contributions and results of this research are discussed in this chapter. In this thesis, a new detection algorithm and classification technique is proposed for electrical power quality disturbances. Moreover, a validation methodology is conducted based on DWT. Compared with existing algorithms, the proposed methodology showed a better performance based on the accuracy achieved. The novelties of the proposed methodology of the detection algorithm and classification technique can be categorised into four major aspects.

The first stage is characterising power quality disturbances, which is completed by modelling these disturbances according to recognised international standards in the field of power quality. In the characterisation stage, mathematical equations are implemented, considering equation parametrical limits in IEEE 1159 and IEC 61000-4-30. These disturbances include pure sinusoidal, sag, swell, harmonics, interruption, flicker, high frequency transient, low frequency transient, sag with harmonics and swell with harmonics. Chapter 3 shows the phenomena of these events in their single and multiple occasions at the same time.

The second stage is achieved by building the environment to detect and analyse power quality disturbances automatically, based on two powerful signal processing algorithms. At the beginning, power quality disturbances are generated with the requirement mentioned in Chapter 3, as well as the signal specifications needed in this field. Thereafter, DWT is performed to detected and identify distorted power signals.  DWT proved its capability to detect and identify non-stationary disturbances and to overcome Fourier Transform limitations in this issue on the time-frequency domain. Thereafter, features of these disturbances are extracted into 8 levels of the decomposition process. After generating power quality disturbances 40 times, 3200 samples of features in the database are realised to investigate and study the reliability of the detection algorithm.

In the classification stage, FFNN classifier is employed as one of the most powerful artificial intelligence techniques. The database of features extracted is fed into the classifier where they are trained, validated, and tested to find the accuracy of each one of these disturbances and the overall accuracy. The classification stage resulted in an accuracy of over 90% for detecting each power quality disturbance, and 91% for the overall accuracy for the hybrid system based on DWT-FFNN.

In this thesis, a new detecting algorithm is proposed based on complementary ensemble empirical mode decomposition (CEEMD). The exact number of power quality disturbances is generated, which include single and multiple non-stationary disturbances in power systems. Each waveform of these disturbances is decomposed using CEEMD into 8 levels of intrinsic mode functions (IMFs). These IMFs are considered to be a fingerprint for each waveform due to the information that is included such as standard deviation and energy, and more importantly, the instantaneous amplitude and the instantaneous frequency.

The obtained results are then calculated and fed into FFNN at the classification stage. As mathematically conducted with DWT, the database of IMFs is trained, validated and tested. In the classification stage, the accuracy of detecting power quality disturbances was more than 97% for each one of these disturbances and more than 98% for the overall accuracy for the hybrid system based on CEEMD-FFNN. This achievement indicated the efficiency and robustness of the detection algorithm and classification technique with the best topology achieved [8:15:30:15:10] with three hidden layers.

The third aspect in this thesis, a recognition system approach, is constructed using on-line power faults implemented in a specific model of a power transmission system, which represents real-time scenarios. Firstly, the system is built – this consists of a multi-generator principle as mentioned in Chapter 5. Thereafter, a sag disturbance is modelled by implementing the phase-to-phase fault in the system (line-to-line fault) at a specified time. The system then experiences the sag disturbance in the system and results of the three-phase system are introduced in Chapter 5. Thereafter, the sag model is removed from the power transmission system and the large load switching model is employed in the system. After adjusting parameters in the model and running the system, the swell disturbance occurring in the system is recorded in the transmission system. Nevertheless, the interruption disturbance is modelled by employing the phase-to-ground (L-G) fault in the power system. The results show the interruption phenomenon for less than 0.1 second and its effect on the system.

Furthermore, the oscillatory transient disturbance is explained theoretically and mathematically in the power system. The oscillatory transient waveform is implemented by the capacitor bank energizing the transmission system. The parameters are adjusted in terms of time, frequency and phases switching and as a result the oscillatory transient disturbance that occurred in the system is analysed.

For additional reliability of the proposed algorithm and the classification technique, the next stage went further by applying the data of these phenomena in the three-phase power transmission system to the hybrid approach of CEEMD-FFNN. The phenomena applied to the hybrid system were unknown and undefined. The results showed that CEEMD-FFNN is capable of recognising these disturbances effectively. Moreover, in this experimental recognition system, CEEMD-FFNN showed that it can identify more than one case at the same time, which proved the robustness of such an algorithm.

The fourth aspect was the control and optimisation part of this thesis, in which the target was to achieve power quality improvement and to mitigate transient response in magnitude and duration after any disturbance in the system that was sag. First, the principle of quality control is discussed and investigated. Thereafter, modern strategies of power systems control are analysed and highlighted. Thereafter, power system stability is explained and discussed. Conventional power system controllers are mathematically investigated with their impact on power systems. In order to improve system stability in the transmission power system, both controllers, Genetic (PSS-2B) and multiband controller (PSS-4B), are analysed and examined to determine which has the best performance. The result of this evaluation was that (PSS-4B) has a better performance in the system.

A bank of harmonics filters are connected to the transmission system with 140 MVAr to each branch of the subsystem. The location of the model implemented was another challenge; the best location was found to be next to the load, with improvement in terms of both transient analysis and harmonics reduction. The results of this process showed less transient magnitude with a reduction of more than half in the system. The total harmonics distortion in the system reduced from 80.67% to 33.67% because of this implementation. Thereafter, several attempts were conducted to investigate the optimum value of the controller gains in the system. In this model, there are four options to handle the system behaviour and retune the gains (Kp, Kl, Ki and Kh).

The optimum value was achieved effectively by reducing the proportional gain to 0.5 in the system. This resulted in a smoother response to the disturbance and less transient magnitude due to the sag event in the system. In addition, the impact of implementing a harmonics filter bank was a stable system within a shorter time, which indicates the reliability of the filter back implemented and the power quality improvement achieved.

## 7.2 Future Work

- The main contributions in this thesis have focused on the most common power quality disturbances. These disturbances are benchmarks in most of the investigations and researchers in this field, as discussed in the literature review. However, this thesis did not include all power quality disturbances in power systems due to their negligible effect or to the lower percentage of their appearance in power systems.

- The statistical information on the importance of research in this field are still limited. It should also be conducted in many areas in the world to enhance the research communities with handling such financial loss.

- Power quality disturbances are mentioned in international standards such IEEE 1159 and IEC 61000-4-30 in precise and mathematical which helps researched and engineers to recognise and classify them. However, these standards need to unified measurement units based on international systems of units (SI units).

- In this thesis, the characterisations of power quality disturbances are based on their mathematical equations described by scientific communities, published as international standards and recognised by most of standardisation bodies all over the world. However, it might be beneficial to include real events data. This milestone could be promising future work based on the achievements in this thesis and building a comparison analysis.

- In this thesis, it was essential to use the identical classification technique based on artificial neural networks due to necessity of comparison analysis factors. However, It might be useful to develop other classifier suing one of the Artificial intelligence techniques in the field of power quality.

- In terms of control and stability, although the achieved reduction in harmonics and the lower transient magnitude in the system are sufficient, it might be beneficial to involve artificial intelligence in the control efforts, especially in the larger scale of power grids.

# References

[1] A. Thapar, T. K. Saha and Z. Y. Dong, "Investigation of power quality categorisation and simulating it's impact on sensitive electronic equipment," in *Power Engineering Society General Meeting, 2004. IEEE,* 2004, pp. 528-533.

[2] R. C. Dugan, M. F. McGranaghan and H. W. Beaty, "Electrical power systems quality," *New York, NY: McGraw-Hill,| c1996,* 1996.

[3] P. K. Ray, S. R. Mohanty and N. Kishor, "Classification of power quality disturbances due to environmental characteristics in distributed generation system," *IEEE Transactions on Sustainable Energy,* vol. 4, *(2),* pp. 302-313, 2013.

[4] H. He, X. Shen and J. A. Starzyk, "Power quality disturbances analysis based on EDMRA method," *International Journal of Electrical Power & Energy Systems,* vol. 31, *(6),* pp. 258-268, 2009.

[5] D. Chapman, "Costs–The Cost of Poor Power Quality," *Power Quality Application Guide, Version 0b,* 2001.

[6] K. Darrow *et al*, "The role of distributed generation in power quality and reliability," *New York State Energy Research and Development Authority,* 2005.

[7] K. H. LaCommare and J. H. Eto, "Understanding the cost of power interruptions to US electricity consumers," *Lawrence Berkeley National Laboratory,* 2004.

[8] D. Lineweber and S. McNulty, "The cost of power disturbances to industrial & digital economy companies," *Madison, WI: Primen,* 2001.

[9] H. Math Bollen, "Understanding Power quality problems voltage sags and interruptions," 2001.

[10] M. Zhang, K. Li and Y. Hu, "A real-time classification method of power quality disturbances," *Electr. Power Syst. Res.,* vol. 81, *(2),* pp. 660-666, 2011.

[11] E. Styvaktakis, I. Y. Gu and M. H. Bollen, "Voltage dip detection and power system transients," in *Power Engineering Society Summer Meeting, 2001,* 2001, pp. 683-688.

[12] T. Zhu, S. Tso and K. Lo, "Wavelet-based fuzzy reasoning approach to power-quality disturbance recognition," *IEEE Trans. Power Del.,* vol. 19, *(4),* pp. 1928-1935, 2004.

[13] T. Cease and P. Johnston, "A magneto-optic current transducer," *IEEE Trans. Power Del.,* vol. 5, *(2),* pp. 548-555, 1990.

[14] IEEE 1459-2010, “1459-2010 Power System Instrumentation and Measurements of the IEEE Power & Energy Society," 2010.

[15] E. Fuchs *et al*, "Comparison of wavelet and fourier analysis in power quality," in *Electric Power Quality and Supply Reliability Conference (PQ), 2012,* 2012, pp. 1-7.

[16] P. G. Axelberg, I. Y. Gu and M. H. Bollen, "Support vector machine for classification of voltage disturbances," *IEEE Trans. Power Del.,* vol. 22, *(3),* pp. 1297-1303, 2007.

[17] J. R. Macias and A. G. Exposito, "Efficient moving-window DFT algorithms," *IEEE Trans. Circuits Syst. II Analog Digital Signal Process.,* vol. 45, *(2),* pp. 256-260, 1998.

[18] D. Granados-Lieberman *et al*, "Techniques and methodologies for power quality analysis and disturbances classification in power systems: a review," *Generation, Transmission & Distribution, IET,* vol. 5, *(4),* pp. 519-529, 2011.

[19] P. Dash *et al*, "Power quality disturbance data compression, detection, and classification using integrated spline wavelet and S-transform," *IEEE Trans. Power Del.,* vol. 18, *(2),* pp. 595-600, 2003.

[20] Y. H. Gu and M. H. Bollen, "Time-frequency and time-scale domain analysis of voltage disturbances," *IEEE Trans. Power Del.,* vol. 15, *(4),* pp. 1279-1284, 2000.

[21] S. Huang, C. Hsieh and C. Huang, "Application of Morlet wavelets to supervise power system disturbances," *IEEE Trans. Power Del.,* vol. 14, *(1),* pp. 235-243, 1999.

[22] F. Zhang, Z. Geng and W. Yuan, "The algorithm of interpolating windowed FFT for harmonic analysis of electric power system," *Power Delivery, IEEE Transactions On,* vol. 16, *(2),* pp. 160-164, 2001.

[23] H. Qian, R. Zhao and T. Chen, "Interharmonics analysis based on interpolating windowed FFT algorithm," *IEEE Trans. Power Del.,* vol. 22, *(2),* pp. 1064-1069, 2007.

[24] P. O'Shea, "A high-resolution spectral analysis algorithm for power-system disturbance monitoring," *IEEE Trans. Power Syst.,* vol. 17, *(3),* pp. 676-680, 2002.

[25] S. Santoso, E. J. Powers and W. Grady, "Power quality disturbance data compression using wavelet transform methods," *Power Delivery, IEEE Transactions On,* vol. 12, *(3),* pp. 1250-1257, 1997.

[26] S. Nath, P. Sinha and S. K. Goswami, "A wavelet based novel method for the detection of harmonic sources in power systems," *International Journal of Electrical Power & Energy Systems,* vol. 40, *(1),* pp. 54-61, 2012.

[27] S. Huang, C. Hsieh and C. Huang, "Application of wavelets to classify power system disturbances," *Electr. Power Syst. Res.,* vol. 47, *(2),* pp. 87-93, 1998.

[28] P. Pillay and A. Bhattacharjee, "Application of wavelets to model short-term power system disturbances," *IEEE Trans. Power Syst.,* vol. 11, *(4),* pp. 2031-2037, 1996.

[29] L. Angrisani *et al*, "A measurement method based on the wavelet transform for power quality analysis," *Power Delivery, IEEE Transactions On,* vol. 13, *(4),* pp. 990-998, 1998.

[30] A. Gaouda *et al*, "Power quality detection and classification using wavelet-multiresolution signal decomposition," *IEEE Trans. Power Del.,* vol. 14, *(4),* pp. 1469-1476, 1999.

[31] L. Angrisani *et al*, "A measurement method based on the wavelet transform for power quality analysis," *Power Delivery, IEEE Transactions On,* vol. 13, *(4),* pp. 990-998, 1998.

[32] Ö Gencer, S. Öztürk and T. Erfidan, "A new approach to voltage sag detection based on wavelet transform," *International Journal of Electrical Power & Energy Systems,* vol. 32, *(2),* pp. 133-140, 2010.

[33] S. Deokar and L. Waghmare, "Integrated DWT–FFT approach for detection and classification of power quality disturbances," *International Journal of Electrical Power & Energy Systems,* vol. 61, pp. 594-605, 2014.

[34] S. Alshahrani *et al*, "Evaluation and classification of power quality disturbances based on discrete wavelet transform and artificial neural networks," in *Power Engineering Conference (UPEC), 2015 50th International Universities,* 2015, pp. 1-5.

[35] E. Y. Hamid and Z. Kawasaki, "Wavelet-based data compression of power system disturbances using the minimum description length criterion," *IEEE Trans. Power Del.,* vol. 17, *(2),* pp. 460-466, 2002.

[36] W. G. Morsi and M. El-Hawary, "Wavelet packet transform-based power quality indices for balanced and unbalanced three-phase systems under stationary or nonstationary operating conditions," *Power Delivery, IEEE Transactions On,* vol. 24, *(4),* pp. 2300-2310, 2009.

[37] W. G. Morsi and M. El-Hawary, "A new perspective for the IEEE Standard 1459-2000 via stationary wavelet transform in the presence of nonstationary power quality disturbance," *Power Delivery, IEEE Transactions On,* vol. 23, *(4),* pp. 2356-2365, 2008.

[38] R. G. Stockwell, L. Mansinha and R. Lowe, "Localization of the complex spectrum: the S transform," *IEEE Transactions on Signal Processing,* vol. 44, *(4),* pp. 998-1001, 1996.

[39] P. Dash, B. Panigrahi and G. Panda, "Power quality analysis using S-transform," *IEEE Trans. Power Del.,* vol. 18, *(2),* pp. 406-411, 2003.

[40] R. Naidoo and P. Pillay, "A new method of voltage sag and swell detection," *IEEE Trans. Power Del.,* vol. 22, *(2),* pp. 1056-1063, 2007.

[41] S. Mishra, C. Bhende and B. Panigrahi, "Detection and classification of power quality disturbances using S-transform and probabilistic neural network," *IEEE Trans. Power Del.,* vol. 23, *(1),* pp. 280-287, 2008.

[42] S. He, K. Li and M. Zhang, "A real-time power quality disturbances classification using hybrid method based on S-transform and dynamics," *IEEE Transactions on Instrumentation and Measurement,* vol. 62, *(9),* pp. 2465-2475, 2013.

[43] R. Yokeeswaran and A. Vetrivel, "Measurement and Comparison of Power Quality Disturbances using Discrete Wavelet Transform (DWT) and Discrete Orthogonal S-Transform (DOST)," *Measurement,* vol. 2, *(3),* pp. 808-813, 2012.

[44] M. Chilukuri and P. Dash, "Multiresolution S-transform-based fuzzy recognition system for power quality events," *IEEE Trans. Power Del.,* vol. 19, *(1),* pp. 323-330, 2004.

[45] N. E. Huang *et al*, "The empirical mode decomposition and the hilbert spectrum for nonlinear and non-stationary time series analysis," in *Proceedings of the Royal Society of London A: Mathematical, Physical and Engineering Sciences,* 1998, pp. 903-995.

[46] N. E. Huang *et al*, "A confidence limit for the empirical mode decomposition and hilbert spectral analysis," in *Proceedings of the Royal Society of London A: Mathematical, Physical and Engineering Sciences,* 2003, pp. 2317-2345.

[47] G. Rilling, P. Flandrin and P. Goncalves, "On empirical mode decomposition and its algorithms," in *IEEE-EURASIP Workshop on Nonlinear Signal and Image Processing,* 2003, pp. 8-11.

[48] L. Yang, J. Yu and Y. Lai, "Disturbance source identification of voltage sags based on hilbert-huang transform," in *2010 Asia-Pacific Power and Energy Engineering Conference,* 2010, pp. 1-4.

[49] S. Shukla, S. Mishra and B. Singh, "Empirical-Mode Decomposition With Hilbert Transform for Power-Quality Assessment," *IEEE Trans. Power Del.,* vol. 24, *(4),* pp. 2159 <last_page> 2165, 2009.

[50] C. Norman *et al*, "Hybrid wavelet and Hilbert transform with frequency-shifting decomposition for power quality analysis," *IEEE Transactions on Instrumentation and Measurement,* vol. 61, *(12),* pp. 3225-3233, 2012.

[51] F. Hafiz, A. H. Chowdhury and C. Shahnaz, "An approach for classification of power quality disturbances based on hilbert huang transform and relevance vector machine," in *Electrical & Computer Engineering (ICECE), 2012 7th International Conference On,* 2012, pp. 201-204.

[52] J. Yeh, J. Shieh and N. E. Huang, "Complementary ensemble empirical mode decomposition: A novel noise enhanced data analysis method," *Advances in Adaptive Data Analysis,* vol. 2, *(02),* pp. 135-156, 2010.

[53] W. R. A. Ibrahim and M. M. Morcos, "Artificial intelligence and advanced mathematical tools for power quality applications: A survey," *Power Delivery, IEEE Transactions On,* vol. 17, *(2),* pp. 668-673, 2002.

[54] M. Uyar, S. Yildirim and M. T. Gencoglu, "An effective wavelet-based feature extraction method for classification of power quality disturbance signals," *Electr. Power Syst. Res.,* vol. 78, *(10),* pp. 1747-1755, 2008.

[55] A. K. Ghosh and D. L. Lubkeman, "The classification of power system disturbance waveforms using a neural network approach," *Power Delivery, IEEE Transactions On,* vol. 10, *(1),* pp. 109-115, 1995.

[56] D. Srinivasan, W. Ng and A. Liew, "Neural-network-based signature recognition for harmonic source identification," *Power Delivery, IEEE Transactions On,* vol. 21, *(1),* pp. 398-405, 2006.

[57] K. Silva, B. Souza and N. Brito, "Fault detection and classification in transmission lines based on wavelet transform and ANN," *Power Delivery, IEEE Transactions On,* vol. 21, *(4),* pp. 2058-2063, 2006.

[58] S. Alshahrani, M. Abbod and B. Alamri, "Detection and classification of power quality events based on wavelet transform and artificial neural networks for smart grids," in *2015 Saudi Arabia Smart Grid (SASG),* 2015, pp. 1-6.

[59] I. Monedero *et al*, "Classification of electrical disturbances in real time using neural networks," *Power Delivery, IEEE Transactions On,* vol. 22, *(3),* pp. 1288-1296, 2007.

[60] V. N. Vapnik, "The Nature of Statistical Learning Theory," 1995.

[61] G. Lv *et al*, "PQ disturbances identification based on SVMs classifier," in *Neural Networks and Brain, 2005. ICNN&B'05. International Conference On,* 2005, pp. 222-226.

[62] C. A. Naik and P. Kundu, "Power quality disturbance classification employing S-transform and three-module artificial neural network," *International Transactions on Electrical Energy Systems,* vol. 24, *(9),* pp. 1301-1322, 2014.

[63] A. S. Cerqueira *et al*, "Power quality events recognition using a SVM-based method," *Electr. Power Syst. Res.,* vol. 78, *(9),* pp. 1546-1552, 2008.

[64] S. Ekici, "Classification of power system disturbances using support vector machines," *Expert Syst. Appl.,* vol. 36, *(6),* pp. 9859-9868, 2009.

[65] J. Yen and R. Langari, *Fuzzy Logic: Intelligence, Control, and Information.* Prentice Hall Upper Saddle River, 1999*1*.

[66] P. Dash *et al*, "Classification of power system disturbances using a fuzzy expert system and a Fourier linear combiner," *IEEE Trans. Power Del.,* vol. 15, *(2),* pp. 472-477, 2000.

[67] S. Farghal, M. Kandil and A. Elmitwally, "Quantifying electric power quality via fuzzy modelling and analytic hierarchy processing," *IEE Proceedings-Generation, Transmission and Distribution,* vol. 149, *(1),* pp. 44-49, 2002.

[68] Y. Liao and J. Lee, "A fuzzy-expert system for classifying power quality disturbances," *International Journal of Electrical Power & Energy Systems,* vol. 26, *(3),* pp. 199-205, 2004.

[69] S. K. Meher and A. K. Pradhan, "Fuzzy classifiers for power quality events analysis," *Electr. Power Syst. Res.,* vol. 80, *(1),* pp. 71-76, 2010.

[70] J. Huang, M. Negnevitsky and D. T. Nguyen, "A neural-fuzzy classifier for recognition of power quality disturbances," *IEEE Trans. Power Del.,* vol. 17, *(2),* pp. 609-616, 2002.

[71] V. F. Pires, T. G. Amaral and J. Martins, "Power quality disturbances classification using the 3-D space representation and PCA based neuro-fuzzy approach," *Expert Syst. Appl.,* vol. 38, *(9),* pp. 11911-11917, 2011.

[72] J. Holland and D. Goldberg, "Genetic Algorithms in Search, Optimization and Machine Learning," 1989.

[73] A. El-Zonkoly, "Power system model validation for power quality assessment applications using genetic algorithm," *Expert Syst. Appl.,* vol. 29, *(4),* pp. 941-944, 2005.

[74] M. Wang and Y. Tseng, "A novel analytic method of power quality using extension genetic algorithm and wavelet transform," *Expert Syst. Appl.,* vol. 38, *(10),* pp. 12491-12496, 2011.

[75] P. G. Axelberg, I. Y. Gu and M. H. Bollen, "Support vector machine for classification of voltage disturbances," *Power Delivery, IEEE Transactions On,* vol. 22, *(3),* pp. 1297-1303, 2007.

[76] Y. H. Gu and M. H. Bollen, "Time-frequency and time-scale domain analysis of voltage disturbances," *Power Delivery, IEEE Transactions On,* vol. 15, *(4),* pp. 1279-1284, 2000.

[77] P. F. Ribeiro, "Wavelet transform: An advanced tool for analyzing non-stationary harmonic distortions in power systems," in *Proceedings IEEE ICHPS VI,* 1994, pp. 365-369.

[78] B. H. Chowdhury, "Power quality," *IEEE Potentials,* vol. 20, *(2),* pp. 5-11, 2001.

[79] M. H. Bollen and I. Gu, *Signal Processing of Power Quality Disturbances.* John Wiley & Sons, 2006*30*.

[80] E. F. Fuchs and M. A. S. Masoum, *Power Quality in Power Systems and Electrical Machines.* Amsterdam ; Boston: Academic Press/Elsevier, 2008.

[81] R. Chouhy Leborgne, "Voltage sags characterisation and estimation," 2005.

[82] B. Franken *et al*, "Regulation of voltage quality," in *9th International Conference" Electric Power, Quality and Utilisation", Barcelona,* 2007, .

[83] J. Schlabbach, D. Blume and T. Stephanblome, "Voltage Quality in Electrical Power Systems," pp. 252, 2001.

[84] J. Arrillaga, M. H. Bollen and N. R. Watson, "Power quality following deregulation," *Proc IEEE,* vol. 88, *(2),* pp. 246-261, 2000.

[85] B. Singh, V. Verma and J. Solanki, "Neural network-based selective compensation of current quality problems in distribution system," *IEEE Trans. Ind. Electron.,* vol. 54, *(1),* pp. 53-60, 2007.

[86] IEEE Standards Association, "1159-2009. IEEE Recommended Practice for Monitoring Electric Power Quality Industrial and Commercial Applications," 2009.

[87] K. Schipman and F. Delincé, "The importance of good power quality," *ABB Power Qual.Prod., Charleroi, Belgium, ABB Review,* 2010.

[88] C. Sankaran, *Power Quality.* CRC press, 2001.

[89] P. Q. A. Guide, "Voltage Disturbances," *Standard EN,* vol. 50160, 2004.

[90] I. Std, "61000-4-15; citation_journal_title= Electromagnetic Compatibility (EMC)," *Part4: Testing and Measurement Techniques.Section,* vol. 15, .

[91] J. C. Smith, G. Hensley and L. Ray, "IEEE Recommended Practice for Monitoring Electric Power Quality," *IEEE Std,* pp. 1159-1995, 1995.

[92] R. Langella and A. Testa, "IEEE Standard Definitions for the Measurement of Electric Power Quantities Under Sinusoidal, Nonsinusoidal, Balanced, or Unbalanced Conditions," 2010.

[93] B. EN, "50160: 2010 Voltage characteristics of electricity supplied by public electricity networks,"," *British Standards Institution,* 2011.

[94] International Electrotechnical Commission, "IEC 61000-4-30: testing and measurement techniques," *Power Quality Measurement Methods,* 2008.

[95] IEEE Standards Association, "1159-2009. IEEE Recommended Practice for Monitoring Electric Power Quality Industrial and Commercial Applications," 2009.

[96] International Electrotechnical Commission, "IEC 61000-4-30: testing and measurement techniques," *Power Quality Measurement Methods,* 2008.

[97] A. E. Turner and E. Collins, "The performance of AC contactors during voltage sags," in *Proceedings of 7'Th Int. Conf. on Harmonics and Quality of Power,* 1996, pp. 589-595.

[98] B. M. Instruments, "Handbook of Power Signatures," 1993.

[99] IEEE Std C62. 41, "IEEE Recommended Practice on Characterization of Surges in Low-Voltage (1000 V and Less) AC Power Circuits," *IEEE Std C62. 41. 2-2002,* pp. 0_1, 2003.

[100] IEEE Std 519-2014, "IEEE Recommended Practice and Requirements for Harmonic Control in Electric Power Systems - Redline," *IEEE Std 519-2014 (Revision of IEEE Std 519-1992) - Redline,* pp. 1-213, 2014.

[101] IEEE Std 519-2014, "IEEE Recommended Practice and Requirements for Harmonic Control in Electric Power Systems," *IEEE Std 519-2014 (Revision of IEEE Std 519-1992),* pp. 1-29, 2014.

[102] A. Std, "C84. 1-2006," *For Electric Power Systems and Equipment-Voltage Ratings (60 Hz),* 2006.

[103] Z. Hanzelka and A. Bien, "Voltage Disturbances-Flicker," *Copper; Development Association-Institution of Engineering and Technology Endorsed Training Provider,* 2006.

[104] IEEE Std 1159-2009, "IEEE Recommended Practice for Monitoring Electric Power Quality," *IEEE Std 1159-2009 (Revision of IEEE Std 1159-1995),* pp. c1-81, 2009.

[105] E. Compatibility, "Part 3-3: Limits—Limitation of Voltage Changes, Voltage Fluctuations and Flicker in Public Low-Voltage Supply Systems, for Equipment With Rated Current≤ 16 A per Phase and Not Subject to Conditional Connection," *IEC Standard,* pp. 61000-61003, 2005.

[106] IEEE Std 1453-2015, "IEEE Recommended Practice for the Analysis of Fluctuating Installations on Power Systems," *IEEE Std 1453-2015 (Revision of IEEE Std 1453-2011),* pp. 1-74, 2015.

[107] I. Std, "61000-4-15," *IEC Flicker Meter–Functional and Design Specification,* 1997.

[108] IEEE Std 141-1993, "IEEE Recommended Practice for Electric Power Distribution for Industrial Plants," *IEEE Std 141-1993,* pp. 1-768, 1994.

[109] IEEE Std 100-2000, "The Authoritative Dictionary of IEEE Standards Terms, Seventh Edition," *IEEE Std 100-2000,* pp. 1-1362, 2000.

[110] M. H. Bollen, *Understanding Power Quality Problems.* IEEE press New York, 2000*3*.

[111] S. Mallat, *A Wavelet Tour of Signal Processing.* Academic press, 1999.

[112] J. Morlet *et al*, "Wave propagation and sampling theory—Part I: Complex signal and scattering in multilayered media," *Geophysics,* vol. 47, *(2),* pp. 203-221, 1982.

[113] A. Bruce, D. Donoho and H. Gao, "Wavelet analysis [for signal processing]," *IEEE Spectrum,* vol. 33, *(10),* pp. 26-35, 1996.

[114] A. Graps, "An introduction to wavelets," *IEEE Computational Science and Engineering,* vol. 2, *(2),* pp. 50-61, 1995.

[115] de Castro Fernández, Rosa Ma and H. N. D. Rojas, "An overview of wavelet transforms application in power systems," *Proc.14th PSCC, Sevilla, Session,* vol. 1, pp. 1-8, 2002.

[116] S. Chen and H. Y. Zhu, "Wavelet transform for processing power quality disturbances," *EURASIP Journal on Advances in Signal Processing,* vol. 2007, *(1),* pp. 047695, 2007.

[117] I. Daubechies, *Ten Lectures on Wavelets.* SIAM, 1992*61.*

[118] G. Heydt and A. Galli, "Transient power quality problems analyzed using wavelets," *Power Delivery, IEEE Transactions On,* vol. 12, *(2),* pp. 908-915, 1997.

[119] N. E. Huang *et al*, "A confidence limit for the empirical mode decomposition and hilbert spectral analysis," in *Proceedings of the Royal Society of London A: Mathematical, Physical and Engineering Sciences,* 2003, pp. 2317-2345.

[120] R. Kumar, B. Singh and D. T. Shahani, "Recognition of single-stage and multiple power quality events using Hilbert–Huang transform and probabilistic neural network," *Electric Power Components and Systems,* vol. 43, *(6),* pp. 607-619, 2015.

[121] N. E. Huang *et al*, "On instantaneous frequency," *Advances in Adaptive Data Analysis,* vol. 1, *(02),* pp. 177-229, 2009.

[122] M. Z. Lubis and M. Si, "SIGNAL PROCESSING FOR POWER SPECTRAL DENSITY (PSD)," .

[123] J. Yeh, J. Shieh and N. E. Huang, "Complementary ensemble empirical mode decomposition: A novel noise enhanced data analysis method," *Advances in Adaptive Data Analysis,* vol. 2, *(02),* pp. 135-156, 2010.

[124] S. A. Kalogirou, "Artificial neural networks in renewable energy systems applications: a review," *Renewable and Sustainable Energy Reviews,* vol. 5, *(4),* pp. 373-401, 2001.

[125] L. L. Lai, *Intelligent System Applications in Power Engineering: Evolutionary Programming and Neural Networks.* John Wiley & Sons, Inc., 1998.

[126] M. T. Haque and A. Kashtiban, "Application of Neural Networks in Power Systems; A Review," *World Academy of Science, Engineering and Technology, International Journal of Electrical, Computer, Energetic, Electronic and Communication Engineering,* vol. 1, *(6),* pp. 889-893, 2007.

[127] J. C. Principe, N. R. Euliano and W. C. Lefebvre, *Neural and Adaptive Systems: Fundamentals through Simulations.* Wiley New York, 2000*672*.

[128] D. Rumelhart, "E., and McClelland, JL," Parallel Distributed Processing", Vols. 1 & 2," 1986.

[129] R. J. Schalkoff, *Artificial Neural Networks.* McGraw-Hill Higher Education, 1997.

[130] B. Bhattacharya, A. Lobbrecht and D. Solomatine, "Neural Networks and Reinforcement Learning in Control of Water System," 2003.

[131] R. Falahian *et al*, "Artificial neural network-based modeling of brain response to flicker light," *Nonlinear Dyn.,* vol. 81, *(4),* pp. 1951-1967, 2015.

[132] M. Q. Raza and A. Khosravi, "A review on artificial intelligence based load demand forecasting techniques for smart grid and buildings," *Renewable and Sustainable Energy Reviews,* vol. 50, pp. 1352-1372, 2015.

[133] G. Zhang, B. Eddy Patuwo and M. Y. Hu, "Forecasting with artificial neural networks:: The state of the art," *Int. J. Forecast.,* vol. 14, *(1),* pp. 35-62, 3/1, 1998.

[134] A. Mellit and S. A. Kalogirou, "Artificial intelligence techniques for photovoltaic applications: A review," *Progress in Energy and Combustion Science,* vol. 34, *(5),* pp. 574-632, 10, 2008.

[135] N. Michael, "Artificial intelligence a guide to intelligent systems," 2005.

[136] M. Valtierra-Rodriguez *et al*, "Detection and classification of single and combined power quality disturbances using neural networks," *IEEE Trans. Ind. Electron.,* vol. 61, *(5),* pp. 2473-2482, 2014.

[137] H. Hahn, S. Meyer-Nieberg and S. Pickl, "Electric load forecasting methods: Tools for decision making," *Eur. J. Oper. Res.,* vol. 199, *(3),* pp. 902-907, 12/16, 2009.

[138] L. H. Hassan *et al*, "Current state of neural networks applications in power system monitoring and control," *International Journal of Electrical Power & Energy Systems,* vol. 51, pp. 134-144, 2013.

[139] M. F. McGranaghan and S. Santoso, "Challenges and trends in analyses of electric power quality measurement data," *EURASIP Journal on Applied Signal Processing,* vol. 2007, *(1),* pp. 171-171, 2007.

[140] B. Yuan, J. Chen and W. Zhang, "Power transmission lines shorting analysis based on Matlab," *Science Technology and Engineering,* vol. 8, *(15),* pp. 4319-4320, 2008.

[141] A. Rodríguez *et al*, "Rule-based classification of power quality disturbances using S-transform," *Electr. Power Syst. Res.,* vol. 86, pp. 113-121, 2012.

[142] H. Zhengyou *et al*, "Study of a new method for power system transients classification based on wavelet entropy and neural network," *International Journal of Electrical Power & Energy Systems,* vol. 33, *(3),* pp. 402-410, 2011.

[143] H. Erişti and Y. Demir, "A new algorithm for automatic classification of power quality events based on wavelet transform and SVM," *Expert Syst. Appl.,* vol. 37, *(6),* pp. 4094-4102, 2010.

[144] D. Jovcic and G. Pillai, "Analytical modeling of TCSC dynamics," *IEEE Trans. Power Del.,* vol. 20, *(2),* pp. 1097-1104, 2005.

[145] M. H. Bollen and L. Zhang, "Different methods for classification of three-phase unbalanced voltage dips due to faults," *Electr. Power Syst. Res.,* vol. 66, *(1),* pp. 59-69, 2003.

[146] L. Zhan and M. H. Bollen, "Characteristic of voltage dips (sags) in power systems," *IEEE Trans. Power Del.,* vol. 15, *(2),* pp. 827-832, 2000.

[147] *IEEE Std 100-2000* "IEEE Recommended Practice for Powering and Grounding Electronic Equipment," *IEEE Std 100-2000 (Revision of IEEE Std 1100-1999),* pp. 1-703, 2006.

[148] M. H. Bollen, E. Styvaktakis and I. Y. Gu, "Categorization and analysis of power system transients," *IEEE Trans. Power Del.,* vol. 20, *(3),* pp. 2298-2306, 2005.

[149] A. E. Emanuel, "Harmonics in the early years of electrical engineering: A brief review of events, people and documents," in *Harmonics and Quality of Power, 2000. Proceedings. Ninth International Conference On,* 2000, pp. 1-7.

[150] M. Marchand, "The seven services which EDF provides to small and medium-sized companies," 1997.

[151] J. Javerzac, "Contracting the quality of electricity: The french experience," in *Harmonics and Quality of Power, 2000. Proceedings. Ninth International Conference On,* 2000, pp. 431-437.

[152] F. C. Pereira *et al*, "An analysis of costs related to the loss of power quality," in *Harmonics and Quality of Power Proceedings, 1998. Proceedings. 8th International Conference On,* 1998, pp. 777-782.

[153] B. Fortenbury and E. C. E. Solutions, "High performance buildings: Data centers uninterruptible power supplies (UPS)," 2005.

[154] V. E. Wagner, A. A. Andreshak and J. P. Staniak, "Power quality and factory automation," *IEEE Transactions on Industry Applications,* vol. 26, *(4),* pp. 620-626, 1990.

[155] G. J. Wakileh, *Power Systems Harmonics: Fundamentals, Analysis and Filter Design.* Springer Science & Business Media, 2001.

[156] G. W. Chang, S. Chu and H. Wang, "Sensitivity-based approach for passive harmonic filter planning in a power system," in *Power Engineering Society Winter Meeting, 2002. IEEE,* 2002, pp. 937-940.

[157] E. B. Makram *et al*, "Harmonic filter design using actual recorded data," *IEEE Trans. Ind. Appl.,* vol. 29, *(6),* pp. 1176-1183, 1993.

[158] Z. Hanzelka and J. V. Milanović, "Principles of electrical power control," *Power Electronics in Smart Electrical Energy Networks,* pp. 13-53, 2008.

[159] P. Kundur *et al*, "Definition and classification of power system stability IEEE/CIGRE joint task force on stability terms and definitions," *IEEE Trans. Power Syst.*, vol. 19, *(3),* pp. 1387-1401, 2004.

[160] M. Eremia and M. Shahidehpour, *Handbook of Electrical Power System Dynamics: Modeling, Stability, and Control.* John Wiley & Sons, 20139*2.*

[161] P. M. Anderson and A. A. Fouad, *Power System Control and Stability.* John Wiley & Sons, 2008.

[162] S. K. Nallagalva, M. K. Kirar and G. Agnihotri, "Transient stability analysis of the IEEE 9-bus electric power system," *International Journal of Scientific Engineering and Technology,* vol. 1, *(3),* pp. 161-166, 2012.

[163] P. Kundur, N. J. Balu and M. G. Lauby, *Power System Stability and Control.* McGraw-hill New York, 1994*7.*

[164] M. Abido and Y. Abdel-Magid, "Coordinated design of a PSS and an SVC-based controller to enhance power system stability," *International Journal of Electrical Power & Energy Systems,* vol. 25, *(9),* pp. 695-704, 2003.

[165] A. Phiri and K. A. Folly, "Application of breeder GA to power system controller design," in *Swarm Intelligence Symposium, 2008. SIS 2008. IEEE,* 2008, pp. 1-5.

[166] M. Klein *et al*, "H/sub/spl infin damping controller design in large power systems," *IEEE Trans. Power Syst.,* vol. 10, *(1),* pp. 158-166, 1995.

[167] P. Pivoňka *et al*, "The short sampling period in adaptive control," in *Proceedings of the World Congress on Engineering and Computer Science,* 2009, .

[168] Q. Li, D. Zhao and Y. Yu, "A new pole-placement method for excitation control design to damp SSR of a nonidentical two-machine system," *IEEE Trans. Power Syst.,* vol. 4, *(3),* pp. 1176-1181, 1989.

[169] F. P. Demello and C. Concordia, "Concepts of synchronous machine stability as affected by excitation control," *IEEE Transactions on Power Apparatus and Systems,* vol. 88, *(4),* pp. 316-329, 1969.

[170] E. Larsen and D. Swann, "Applying power system stabilizers Part III: Practical considerations," *IEEE Transactions on Power Apparatus and Systems, (6),* pp. 3034-3046, 1981.

[171] R. V. de Oliveira, R. A. Ramos and N. G. Bretas, "A mixed procedure based on classical and modern control to design robust damping controllers," *IEEE Trans. Power Syst.,* vol. 22, *(3),* pp. 1231-1239, 2007.

[172] U. Bakshi and M. Bakshi, *Generation, Transmission and Distribution.* Technical Publications, 2009.

[173] G. Rogers, "Demystifying power system oscillations," *IEEE Comput. Appl. Power,* vol. 9, *(3),* pp. 30-35, 1996.

[174] A. Feliachi and X. Yang, "Identification and control of inter-area modes," in *Decision and Control, 1994., Proceedings of the 33rd IEEE Conference On,* 1994, pp. 4061-4066.

[175] E. Larsen and D. Swann, "Applying power system stabilizers Part III: Practical considerations," *IEEE Transactions on Power Apparatus and Systems, (6),* pp. 3034-3046, 1981.

[176] I. Kamwa, R. Grondin and G. Trudel, "IEEE PSS2B versus PSS4B: the limits of performance of modern power system stabilizers," *IEEE Trans. Power Syst.,* vol. 20, *(2),* pp. 903-915, 2005.

[177] H. Inamdar and R. Hasabe, "It based energy management through demand side in the industrial sector," in *Control, Automation, Communication and Energy Conservation, 2009. INCACEC 2009. 2009 International Conference On,* 2009, pp. 1-7.